Stony Brook University

A culture-independent study of dominant sulfur-utilizing chemoautotrophs within the Cariaco Basin's redoxcline

A Dissertation Presented

by

Agnieszka Podlaska

to

The Graduate School

in Partial Fulfillment of the

Requirements

for the Degree of

Doctor of Philosophy

in

Marine and Atmospheric Science

Stony Brook University

December 2013

Stony Brook University

The Graduate School

Agnieszka Podlaska

We, the dissertation committee for the above candidate for the

Doctor of Philosophy degree, hereby recommend

acceptance of this dissertation.

Gordon T. Taylor
Dissertation Advisor
Professor, School of Marine and Atmospheric Sciences

Jackie L. Collier
Chairperson of Defense
Associate Professor, School of Marine and Atmospheric Sciences

Mary I. Scranton
Professor, School of Marine and Atmospheric Sciences

Robert C. Aller
Distinguished Professor, School of Marine and Atmospheric Sciences

Lee J. Kerkhof
Professor, School of Environmental and Biological Sciences,
Institute of Marine and Coastal Sciences, Rutgers University

This dissertation is accepted by the Graduate School

Charles Taber
Interim Dean of the Graduate School

Abstract of the Dissertation

A culture-independent study of dominant sulfur-utilizing chemoautotrophs within the Cariaco Basin's redoxcline

by

Agnieszka Podlaska

Doctor of Philosophy

in

Marine and Atmospheric Science

Stony Brook University

2013

As in many other stratified bodies of water, microbial chemoautotrophic productivity in the anoxic Cariaco Basin is a major source of fixed carbon across the oxic-anoxic boundary yet the identity of the chemoautotrophic microbes and what fuels their metabolism are poorly understood. In this work, multiple techniques were used to investigate the distribution, abundance, and activity of major proteobacterial and archaeal clades during nine cruises from 2006 to 2010 in order to identify the dominant chemoautotrophs.

Among seven clades examined in this study by fluorescence in situ hybridization (FISH), ε-proteobacteria and β-proteobacteria were the prevalent clades and on average accounted for about 15 and 10 % of the total prokaryotic community in the redoxcline, respectively. Other bacterial clades (γ-proteobacteria, α-proteobacteria, and sulfate-reducing δ-proteobacteria) on average accounted for 4-6 % and archaeal clades (Thaumarchaeota and Euryarchaeota) for 4-8 % of the total community in the redoxcline, depending on location. Non-parametric permutational multivariate analysis of abundances of all clades showed significant variability in the prokaryotic community distributions among cruises. Abundances of ε-proteobacteria, γ-proteobacteria, and β-proteobacteria exhibited strongest covariations with intermediate sulfur species (thiosulfate,

sulfite, elemental sulfur). Distributions of thiosulfate alone accounted for 13-55 % of variance in distributions of ε-proteobacteria and 15 % in β-proteobacteria. Distributions of sulfite alone accounted for 21 and 35 % of variance in distributions of γ-proteobacteria and β-proteobacteria, respectively. Distributions of elemental sulfur alone accounted for 20 % of variance in distributions of γ-proteobacteria. These results suggest that members of these clades are mostly thiotrophic. Findings from this study also suggest that the Cariaco Basin's redoxcline is a site of dynamic geochemistry and prokaryotic community.

A study of the effect of bacterivory and excess of selected sulfur substrates on the activity of the clades showed preferential grazing on α-proteobacteria while abundances of other clades increased regardless of the presence or absence of the bacterivorous grazers. Addition of H_2S/NO_3^- stimulated growth of ε-proteobacteria and Thaumarchaeota while addition of H_2S/Mn(IV) stimulated growth of Thaumarchaeota in the presence or absence of predators. Growth of other clades either did not change significantly compared to unamended samples or was inhibited by these additions.

Microautoradiography combined with FISH showed active uptake of ^{14}C-bicarbonate by up to 26 % of the total prokaryotic community in the upper anoxic layer. In samples amended with just ^{14}C-bicarbonate, γ-proteobacteria accounted for 44-50 % of all γ-proteobacterial cells. In samples amended with H_2S/Fe(III), ε-proteobacteria, γ-proteobacteria, and Thaumarchaeota accounted for 91, 14, and 80 % of all probe-positive cells, respectively. In samples amended with $S_2O_3^{2-}/NO_3^-$, ε-proteobacteria accounted for up to 25 % of all ε-proteobacterial cells. These findings signify that these prokaryotes are chemoautotrophs with thiotrophic metabolism.

^{13}C/^{15}N-DNA stable isotope probing combined with terminal restriction fragment length polymorphism (TRFLP) and cloning and sequencing of bacterial 16S rRNA genes resulted in identification of ε-proteobacteria closely related to the genus *Sulfurovum* and a demonstration of their chemoautotrophic activities with H_2S and $S_2O_3^{2-}$ as energy substrates and NO_3^-, Fe(III), or Mn(IV) as oxidants.

In summary, this work has shown that ε-proteobacteria closely related to the genus *Sulfurovum* might represent the dominant chemoautotrophs in the Cariaco Basin's redoxcline and yet unidentified representatives of chemoautotrophic γ-proteobacteria and Thaumarchaeota are active in this system as well. These chemoautotrophs are capable of obtaining energy from reduced sulfur species and use nitrate or metal oxides as electron acceptors.

This work is dedicated to my Family and Friends in Poland.

Special dedication is to my Mom Jadwiga and my Uncle Ziutek.

Table of contents

List of Figures

List of Tables

Acknowledgments

I am very grateful and thankful to my advisor Prof. Gordon T. Taylor for giving me the opportunity to work on this project, for supporting me financially and emotionally, for not giving up on me at difficult times, and for endless patience during writing of this dissertation.

I thank my committee members: Profs. Mary I. Scranton, Jackie L. Collier, Robert C. Aller, and Lee J. Kerhof for very helpful suggestions and comments on how to improve this work, and for their patience.

I especially thank Prof. Lee J. Kerkhof and Lora McGuiness from Rutgers University for welcoming me to their lab and helping me with processing samples from my DNA-SIP study. Without their help, that study would not have been completed.

I thank Prof. Kamazima Lwiza for being my mentor and friend, for helping me to adapt to the graduate life here at SoMAS, for always willing to listen and for helping me with studying for the comprehensive exam.

I thank Prof. Josephine Y. Aller for supporting me emotionally, for caring and always wanting to help.

I thank Prof. Robert M. Cerrato for helping me with statistical and NMS analyses and Prof. Anne E. McElroy for helping me with personal matters and making sure I had funding.

I thank Carol Dovi and Christina Fink for keeping me on track and helping with administrative issues.

I thank Prof. Marvin O'Neal III and Deborah A. Spikes from the Undergraduate Biology at Stony Brook University for giving me the opportunity to teach two undergraduate biology courses. It has been a great experience.

I thank Prof. Ramon Varela, Yrene Astor, and staff of EDIMAR-FLASA in Venezuela for their field and laboratory help during cruises. I also thank the captain and crew of *B/O Hermano Gines* for their help at sea.

I am indebted to the following undergraduate students who helped me with microscopy analyses: Cassandra Bauer, Robyn Bell, Katie Kennedy, Eugenia Leonidou, Jennifer Kim, Tai-Ling Moya, Greg Smith, and Nicole Adrion.

I am grateful to Ying Xu, Mariela Lopez-Gasca and Xiaona Li for collecting samples for me during three cruises.

I thank my great friend and labmate Mariela Lopez-Gasca for her friendship, support, and fun times during my time at Stony Brook. I also thank my SoMAS friends Zosia Baumann, Paula Rose, and Jeronimo Pan for their support in difficult times and fun times in between.

I thank my labmates Michael Finiguerra, Sara Cernadas Martin, and Liz Suter for their help and support.

I am grateful and thankful to my friends Julika Wocial, Rosemary Auld, Janet Sacklow, Joseph and Cynthia Mitchells for their support and encouragement throughout the years. My life with you in it has been so enjoyable.

And last, but not least, I thank my family and friends in Poland for their never-ending support and encouragement to pursue my dream, even though it meant not seeing them for long periods of time. Thank you for patiently waiting for me to come back home.

This work was supported by NSF grants OCE0326175 and MCB0347811 awarded to M. I. Scranton and G. T. Taylor.

Chapter 1

Introduction

Some stratified pelagic realms provide oxic, micro-oxic, micro-anoxic and anoxic environments. These environments are characterized by steep gradients in physico-chemical conditions and foster the proliferation of microbial communities collectively capable of carrying out diverse biogeochemical transformations. A common feature of permanently anoxic pelagic systems is a transition zone between shallower oxic and deeper anoxic layers called the redoxcline. It is characterized by gradients in chemical and microbial processes and has been described for many locations, including the Cariaco Basin (Tuttle and Jannasch, 1979; Taylor et al., 2001), Black Sea (Jorgensen et al., 1991; Yilmaz et al., 2006), Baltic Deeps (Labrentz et al., 2005; Jost et al., 2008) and some fjords (Zopfi et al., 2001; Strauss, 2006). Compared to marine sediments, the relatively attenuated slopes of pelagic redoxclines are advantageous for studying microbiota within biogeochemical gradients because environmental transitions here extend over meters rather than millimeters to centimeters. Geochemical studies carried out across oxic-anoxic boundaries in sediments and water columns have mainly focused on availability, concentrations and transformations of different electron donors and acceptors. The majority of microbiological studies have focused on identification of microbiological function in cycling of these electron donors and acceptors. Both geochemists and microbiologists try to establish the link between chemical and biological processes.

Physical and chemical setting of the Cariaco Basin

The Cariaco Basin is the second largest permanently anoxic aquatic system, and the largest truly marine anoxic system in the world. It has long been known to be devoid of oxygen below a depth of 250-300 m (Richards, 1975). The Basin is located on the continental shelf off the northern coast of central Venezuela and is separated from the Caribbean Sea by a sill varying in depth from 90 to 150 m (Richards, 1975). A saddle rising to a depth of 900 m divides the 1400 m deep basin into two sub-basins (Richards, 1975). Above the sill, water exchange with the open

sea is restricted, largely moving through two narrow channels on the northern and western margins (Richards, 1975; Astor et al., 2003).

Seasonal upwelling usually starts in January and lasts until May and secondary upwelling can occur in July-August in response to seasonal intensification of Trade Winds controlled by the intertropical convergence zone (ITCZ) position (Richards, 1975; Muller-Karger et al., 2004). Temperature, salinity and density of the water column below 200-250 m are almost homogeneous (Richards, 1975; Scranton et al., 1987; Holmen and Rooth, 1990). Temperature of deep water is >17° C, which is at least 12-13° C warmer than outside the basin and most of the world ocean at comparable depths (Scranton et al., 1987; Astor et al., 2003). Limited water exchange facilitates stability of the water column and combined with absence of benthic macrofauna allows good preservation of undisturbed sediments (Black et al., 1999, 2004).

Chemical gradients of electron donors such as H_2S, NH_4^+, CH_4, Mn^{2+}, Fe^{2+} and sulfur intermediates ($S_2O_3^{2-}$, SO_3^{2-}, and S^0), and electron acceptors such as O_2, NO_3^-, NO_2^-, MnO_2, Fe_2O_3 in the Cariaco's redoxcline are pronounced (Hayes et al., 2006; Li et al., 2008; Percy et al., 2008) and similar to those in marine sediments (Burdige, 1993). Intrusions of oxygenated water from the Caribbean Sea (Scranton et al., 2001, Astor et al., 2003) may supply enough oxygen for oxidation of Mn(II) and Fe(II), which then could be a source of oxidants to prokaryotes proliferating within the redoxcline. Fluvial inputs and runoff of terrestrial materials after rain events (Lorenzoni, 2005) may also be important sources of these metals. Since the concentrations of sulfur intermediates and metals are elevated within the redoxcline, this appears to be an active layer for microorganisms that depend on chemical gradients.

Microbial ecology of the Cariaco Basin

For the purposes of my microbiological and geochemical studies, I divide the water column of the Cariaco Basin into four basic layers: photic zone (< 100 m), oxycline from 100 to about 250 m, suboxic zone where $O_2 \leq 2$ μM and $H_2S < 1$ μM, and anoxic zone below 250 - 300 m where concentrations of H_2S, NH_4^+ and CH_4 increase with depth. When a clear O_2/H_2S interface is present, its depth varies temporally and spatially within the Basin and has varied between 250 and 310 m (Richards, 1975; Scranton et al., 2001; Astor et al., 2003; Percy et al., 2008). The thickness of the suboxic zone also fluctuates temporally and spatially from nonexistent to 100 m (Scranton et al., 2001; Ho et al., 2004; Percy et al., 2008). There is evidence that the thickness of

the suboxic zone is mainly influenced by the hydrography (upwelling and river input) of the Basin as well as by lateral intrusions of oxygenated waters over the sills and through the channels (Astor et al., 2003; Scranton et al., 2006).

The relatively shallow photic zone over the Cariaco Basin (< 80 m) is a site of high primary production with carbon fixation rates of up to 1.6 g C m^{-2} d^{-1} and averaging 550 g C m^{-2} yr^{-1} (Goñi et al., 2003; Muller-Karger et al., 2004). In the global ocean, sinking flux of organic carbon resulting from primary production usually decreases as a power function of depth as organic carbon is decomposed and on average about 1% of organic carbon produced in the surface water reaches the deep ocean's bottom (Martin et al., 1987; Berger et al., 1988). In the Cariaco Basin, fluxes of organic matter to the 475 m sediment trap below the oxic-anoxic interface exceeded those to the shallower one at 275 m on many occasions (Thunell et al., 1999, 2000; Taylor et al., 2001). Molecular (n-alkanes and n-alcohols) and isotopic signatures ($\delta^{13}C_{org}$) of the organic matter collected in the sediment traps show that it is mostly of marine origin, but suggest sources other than surface primary production (Thunell et al., 1999).

The source(s) of elevated mid-water organic matter fluxes remains an open question. Vertical migration of metazoans (zooplankton and fish), lateral advection of organic carbon from more productive areas and *in situ* microbial production all have been hypothesized to produce anomalously high fluxes at depth (Taylor et al., 2001, 2006). There is considerable evidence for midwater microbial production. Transmissometer profiles reveal a deep light scattering layer and a particle maximum is typically observed within the redoxcline and at first appearance of sulfide (Taylor et al., 2001). Peaks in abundances of viral like particles (VLPs) and protozoans (ciliates and flagellates) coincide with the particle peaks suggesting active prokaryotic communities supporting proliferation of viruses and grazers (Taylor et al., 2003, 2006). Dark inorganic carbon assimilation measurements show elevated chemoautotrophic production in the redoxcline which can vary between 10 and 333% of surface primary production (Taylor et al., 2001).

Plausible chemoautotrophic metabolic pathways

A number of studies (e.g. Tuttle and Jannasch, 1977; Morris et al., 1985; Nealson et al., 1991) have shown that dark carbon assimilation is greatest across the O_2/H_2S interface and can be stimulated both *in situ* and in laboratory experiments by additions of thiosulfate, sulfite, elemental sulfur, or Mn and Fe oxides. Concentrations of dissolved Mn and Fe in the Cariaco are

high in the vicinity of elevated dark carbon assimilation suggesting possible importance of metal-reducing sulfide-oxidizing organisms in chemoautotrophic production in addition to reduced sulfur species and nitrogen substrates (Taylor et al., 2001). Burdige and Nealson (1986) suggested the manganese/iron shuttle as a way of cycling of these metals and redox couples in sedimentary systems. Soluble reduced dissolved Mn and Fe diffuse upward from anoxic pore waters to oxic water where they are oxidized to particulate Mn and Fe. Oxidized insoluble particulate Mn and Fe sink back to the anoxic zone where they are chemically reduced by sulfide or biologically reduced by microbes (Burdige and Nealson, 1986). In sediments, manganese oxides are more efficient in sulfide oxidation than iron oxides but the latter are usually more abundant and may enhance sulfur disproportionation by sulfide scavenging (Jorgensen and Nelson, 2004). However, in the Cariaco Basin both metal oxides are measured at comparable concentrations (Li et al., 2008). The following stoichiometries are obtained:

$$3S^0 + 2FeOOH \rightarrow SO_4^{2-} + 2FeS + 2H^+ \qquad \Delta G^0 = -34.4 \text{ kJ/mol} \qquad (1)$$

$$S^0 + 3MnO_2 + 2H_2O \rightarrow SO_4^{2-} + 3Mn^{2+} + 4OH^- \qquad \Delta G^0 = -733 \text{ kJ/mol} \qquad (2)$$

In addition to sulfide, ammonium and reduced metals, intermediate oxidation state sulfur species may be potential energy sources in the anoxic Cariaco Basin. Complete sulfide oxidation to sulfate in anoxic environments may comprise a series of chemical and biological reactions involving manganese and iron oxides producing FeS, FeS_2, and intermediate oxidation state sulfur species (Perry et al., 1993; Zopfi et al., 2004). In sediments, FeS can be oxidized to S^0 by MnO_2 (reaction 3) and FeS_2 is first chemically oxidized to $S_2O_3^{2-}$ and then biologically to SO_4^{2-} by MnO_2 reducing bacteria (reaction 4) (Aller and Rude, 1988; Zopfi et al., 2004).

$$FeS + 1.5\ MnO_2 + 3H^+ \rightarrow Fe(OH)_3 + S^0 + 1.5\ Mn^{2+} \qquad (3)$$

$$FeS_2 + 7.5\ MnO_2 + 11H^+ \rightarrow Fe(OH)_3 + 2SO_4^{2-} + 7.5\ Mn^{2+} + 4H_2O \qquad (4)$$

Intermediate oxidation state sulfur species can be reduced, oxidized or disproportionated by different groups of bacteria (Jorgensen, 1990; Fossing et al., 1992). Disproportionation of $S_2O_3^{2-}$, SO_3^{2-} and S^0 is an inorganic fermentation reaction in which oxidation of sulfur species occurs without external oxidants (Bak and Cypionka, 1987; Bak and Pfennig, 1987). For example, during thiosulfate disproportionation, the oxidation state changes from +5 in $S_2O_3^{2-}$ to +6 in

SO_4^{2-} in the inner sulfur atom and from -1 in $S_2O_3^{2-}$ to -2 in H_2S in the outer sulfur atom (Jorgensen and Nelson, 2004). According to Jorgensen (1990), disproportionation of thiosulfate seems to be more important in the sedimentary sulfur cycle than its complete reduction or oxidation. He stressed that a "thiosulfate shunt" (disproportionation) seems to be essential in the coupling of thiosulfate reduction and oxidation processes in the sulfur cycle. In 1998, Cypionka et al. proposed a combined pathway of $S_2O_3^{2-}$, SO_3^{2-}, and S^0 disproportionation in the following reaction steps:

$$S_2O_3^{2-} + 2H^+ \rightarrow H_2S + SO_3^{2-} \qquad \Delta G^0 = -21.9 \text{ kJ mol}^{-1}\ S_2O_3^{2-} \qquad (5)$$

$$SO_3^{2-} + H_2O \rightarrow SO_4^{2-} + 2H^+ \qquad \Delta G^0 = -58.9 \text{ kJ mol}^{-1}\ SO_3^{2-} \qquad (6)$$

$$S^0 + 4H_2O \rightarrow SO_4^{2-} + 3HS^- + 5H^+ \qquad \Delta G^0 = +10.2 \text{ kJ mol}^{-1}\ S^0 \qquad (7)$$

The last reaction (7) becomes energetically favorable when free hydrogen sulfide concentration falls below 10 mM and oxidized metals are used as sulfide scavengers (Thamdrup et al., 1993; Finster, 2008). Based on specific geochemical conditions found in the Cariaco Basin's redoxcline, Li et al. (2008) calculated the following stochiometries and energy yields for the three above reactions:

$$S_2O_3^{2-} + H_2O \rightarrow SO_4^{2-} + HS^- + H^+ \qquad \Delta G^0 = -72.8 \text{ kJ mol}^{-1}\ S_2O_3^{2-} \qquad (8)$$

$$4SO_3^{2-} + H^+ \rightarrow 3SO_4^{2-} + HS^- \qquad \Delta G^0 = -29.6 \text{ kJ mol}^{-1}\ SO_3^{2-} \qquad (9)$$

$$4S^0 + 4H_2O \rightarrow SO_4^{2-} + 3HS^- + 5H^+ \qquad \Delta G^0 = -70.2 \text{ kJ mol}^{-1}\ S^0 \qquad (10)$$

All three reactions with intermediate oxidation state sulfur species are thermodynamically favorable and can be potentially carried out by prokaryotes residing in the Cariaco Basin. Concentrations of intermediate oxidation state sulfur species in the Cariaco's suboxic zone are elevated relative to waters above and below (Hayes et al., 2006; Percy et al., 2008; Li et al., 2008). Chemical gradients of other electron donors such as H_2S or NH_4^+, and electron acceptors, such as NO_3^-, Mn(IV), Fe(III) in the redoxcline potentially can sustain activities of chemoautotrophic prokaryotes and result in elevated rates of dark carbon assimilation. In fact, in the Cariaco Basin, Morris et al. (1985) stimulated dark carbon assimilation by thiosulfate addition and the maximum rate was observed below the oxic-anoxic interface. Also Madrid

(2000) used enrichment cultures to demonstrate the presence of thiosulfate-oxidizing nitrate reducing and thiosulfate-oxidizing manganese-reducing bacteria. Taylor et al. (2001, 2006) found that thiosulfate, sulfite, and elemental sulfur amendments (50 μM final concentration) stimulated dark carbon assimilation by more than 2-fold and even as high as 100-fold. Based on these findings, possible dominant reaction pathways involved in the cycling of carbon, sulfur, nitrogen, and metals in the anoxic environments, such as the Cariaco Basin, are illustrated in Fig. 1.1.

Mechanisms controlling prokaryotic community structure in the redoxcline

Biological oxidation of sulfide and sulfur is carried out by phylogenetically and physiologically diverse microorganisms belonging to the domains *Bacteria* and *Archaea* (Fredrich et al., 2005). Members of α-proteobacteria (e.g., *Paracoccus pantotrophus, Rhodobacteraceae)*, β-proteobacteria (e.g., *Thiobacillus denitrificans),* and γ-proteobacteria (e.g., *Acidithiobacillus ferrooxidans)* (reviewed in Fredrich et al., 2005; Cytryn et al., 2005) as well as members of Archaea of order *Sulfolobales* (Kletzin et al., 2004) have been identified as sulfide/sulfur-oxidizers. In the Cariaco's redoxcline ε-proteobacteria (enumerated by fluorescence in situ hybridization, FISH) can account for ~ 30% of total prokaryotic inventories (Lin et al., 2006) and a majority of sequences obtained from a 16S rDNA library of the 320-m microbial community (below the first appearance of H_2S) belonged to close relatives of chemoautotrophic ε-proteobacteria found in hydrothermal vents (Madrid et al., 2001). These findings suggest that this clade might be important in chemoautotrophic production in the Cariaco Basin. Distributions of plausible chemoautotrophic clades in the redoxcline and their relationship with energy substrates and oxidants can provide hints about metabolic potential of these prokaryotes as well as factors controlling their growth. On the other hand, bacterivory can have a significant effect on the composition of the prokaryotic community in the Cariaco Basin (Lin et al., 2007). Elevated numbers of flagellates, ciliates, and viral-like particles coincide with elevated activities of prokaryotes indicating an active microbial food web (Taylor et al., 2003, 2006). How the balance between these two controlling factors affects the prokaryotic community is poorly known in the Cariaco.

Advances in molecular approaches – DNA-stable isotope probing (SIP)

The culture-independent stable isotope probing (SIP) technique has considerable potential for identifying microorganisms responsible for specific metabolic processes in marine environments (Boschker et al., 1998; Radajewski et al., 2000; Manefield et al., 2002a, 2002b; Lueders et al., 2004a, 2004b). SIP involves incorporation of stable isotopes such as ^{13}C and ^{15}N from labeled substrates into macromolecules such as DNA, RNA and lipids. DNA-SIP permits analysis of 16S rRNA and functional genes derived from organisms utilizing specific substrates. For example, analyses of FAMEs (fatty acid methyl esters) in the Cariaco Basin and the Baltic Deeps showed enrichments in ^{13}C-labeled fatty acids derived from sulfur-oxidizing bacteria across the oxic-anoxic interface indicating that reduced sulfur substrates can be very important to metabolism of thiotrophic ε-proteobacteria and γ-proteobacteria (Glaubitz et al., 2009; Wakeham et al., 2010).

Objectives

The goal of this project is to provide insights into the functioning of highly stratified microaerophilic and anaerobic chemoautotrophic prokaryotic communities of the Cariaco Basin's redoxcline and to identify key chemoautotrophs responding to strong electron donor and acceptor gradients. In addition, I evaluate the importance of grazing pressure and substrate enrichments on abundances and growth of major prokaryotic clades.

The following objectives guided this dissertation research:

1) Compare variations in prokaryotic community structure with environmental variables to infer primary bottom-up drivers of prokaryotic community composition.
2) Identify dominant prokaryotic groups responsive to grazing pressure and selected reductants and oxidants using size exclusion incubations and FISH.
3) Visualize and document variations in redoxcline chemoautotrophic community structure in response to enrichments with H_2S, MnO_2 and NO_3^- using microautoradiography-FISH (MAR-FISH) with specific oligonucleotide probes for bacterial and archaeal clades and ^{14}C-bicarbonate as a metabolic tracer.
4) Identify chemoautotrophic clades from stimulation experiments with selected energy substrates and electron acceptors in redoxcline samples using $^{13}C/^{15}N$-DNA stable isotope

probing combined with terminal restriction fragment length polymorphism (TRFLP), cloning and sequencing of 16S rRNA genes.

Based on previous studies and my preliminary results, I hypothesize that ε-proteobacteria, β-proteobacteria, γ-proteobacteria, and Thaumarchaeota are the chemoautotrophic microorganisms responsible for most of the dark carbon fixation within Cariaco Basin's redoxcline. Further, I predict that selected reductants, such as H_2S and $S_2O_3^{2-}$ and oxidants, such as NO_3^-, Mn and Fe oxides support metabolic demands of these plausible chemoautotrophs.

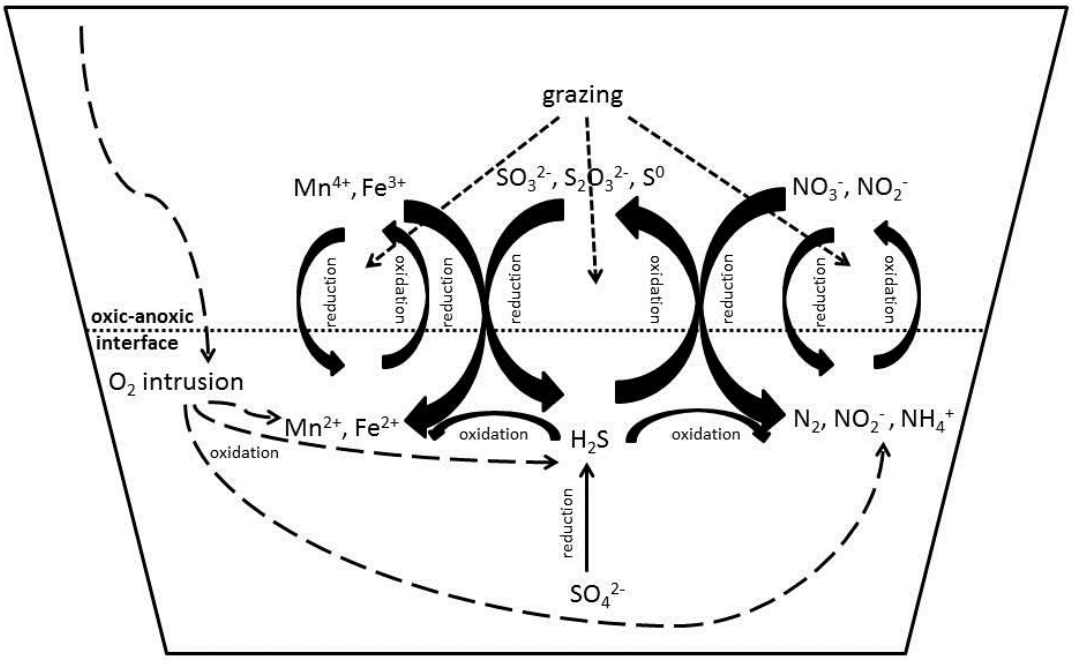

Figure 1.1. Schematic illustration of major biogeochemical processes in the Cariaco Basin's redoxcline.

Chapter 2

Temporal and spatial variations in prokaryotic community structure and environmental conditions in the Cariaco Basin's redoxcline

1. Abstract

Prokaryotic community structure of the Cariaco Basin was investigated during nine cruises from 2006 to 2010 at three stations. Distribution and abundance of five major bacterial and two archaeal clades were assessed using fluorescence in situ hybridization (FISH). Results revealed prevalence of ε-proteobacteria and β-proteobacteria which on average accounted for up to 15 and 10 % of the total community in the redoxcline, respectively. Other bacterial clades on average accounted for 4-6 % of the total community and archaeal clades on average accounted for 4-8 % of the total community in the redoxcline. Permutational multivariate analysis of variance of all seven clades showed significant differences in their distributions among cruises and covariations of individual clades with at least one out of eight environmental variables examined. Distributions of intermediate sulfur species (sulfite, thiosulfate, elemental sulfur) accounted for the highest percentage of variation in distributions of ε-proteobacteria, β-proteobacteria, γ-proteobacteria, and nitrogen species (ammonium, nitrate) in distributions of ε-proteobacteria, β-proteobacteria, and Thaumarchaeota. Covariations among environmental variables and individual clades suggest that plausible chemoautotrophic functional groups represented by ε-proteobacteria, β-proteobacteria, γ-proteobacteria and Thaumarchaeota might include sulfur-substrate oxidizers, nitrite and nitrate reducers as well as ammonium and nitrite oxidizers.

2. Introduction

The Cariaco Basin's prokaryotic community structure (distribution and abundance) and productivity have been shown to fluctuate seasonally and spatially in response to physico-chemical parameters (Taylor et al., 2001; Lin et al., 2006). Fluctuations in oxygen, nutrients, and other chemical resources can affect the growth of prokaryotes by either promoting "blooms" if a

specific nutrient/resource becomes available in concentrations higher than usual or intensify competition if resources become scarce. In the Cariaco Basin, in addition to the shifts in environmental conditions due to upwelling and non-upwelling conditions, prokaryotic community may experience transient but more dramatic changes due to episodic lateral intrusions of oxygenated waters below 200 m and downward mixing of surface waters to the redoxcline (Astor et al., 2003). These intrusions from the Caribbean Sea may also supply enough oxygen for oxidation of dissolved metals to particulate Mn(IV) and Fe(III), which then could be a source of oxidants to prokaryotes proliferating within the redoxcline (Scranton et al., 2001; Astor et al., 2003). In the oxygen depleted redoxcline of the Cariaco Basin sulfur species are believed to be the main source of chemical energy to microbes carrying out microaerobic and anaerobic processes of remineralization (Taylor et al., 2001, 2006; Li et al., 2008). Chemical gradients of electron donors such as H_2S, NH_4^+, CH_4, Mn^{2+}, Fe^{2+} and sulfur intermediates ($S_2O_3^{2-}$, SO_3^{2-}, and S^0), and electron acceptors such as O_2, NO_3^-, NO_2^-, MnO_2, and Fe_2O_3 in the Cariaco's redoxcline are pronounced and similar to those in the sediments (Burdige, 1993; Hayes et al., 2006; Percy et al., 2008; Li et al., 2008).

Thiotrophic (sulfur-utilizing) microbial taxa were previously detected in the Cariaco Basin's redoxcline and sediments (Tuttle and Jannasch, 1972, 1973; Madrid et al., 2001) and representatives of sulfite- and thiosulfate-oxidizers belonging to both β- and γ-proteobacteria have been identified in diverse environments, such as hot springs, acid mines, hydrothermal vents (Vesteinsdottir et al., 2011; Bhowlal and Chakraorty, 2011; Crespo-Medina et al., 2009). Presence of these clades was also documented in the water column of the Black and Baltic Seas which contain suboxic and anoxic conditions similar to those in the Cariaco Basin (Vetriani et al., 2003; Jost et al, 2008; Glaubitz et al., 2010, 2013). Previous studies in the Cariaco Basin showed enhanced numbers of ε-proteobacteria in the redoxcline (Lin et al., 2006) as has been documented in other anoxic/sulfidic marine environments where members of this clade are thought to be responsible for chemoautotrophic sulfide removal (Labrenz et al., 2005; Campbell et al., 2001; Lavik et al., 2009). Among chemoautotrophic microorganisms utilizing nitrogen substrates ammonia-oxidizing β- and γ-proteobacteria are well known to be major players in the nitrogen cycle (Kowalchuk and Stephen, 2001) in oxygen minimum zones (Stevens and Ulloa, 2008; Lam et al., 2009; Podlaska et al., 2012) as well as in the suboxic waters of the Black Sea (Lam et al., 2007).

The goal of this study was to survey major proteobacterial and archaeal clades in the Cariaco Basin's water column with a special emphasis on the redoxcline community structure during nine cruises staged in both upwelling and non-upwelling conditions. Data from the survey were used to determine relationships between the major clades and environmental variables, thereby shaping prokaryotic community composition. I hypothesize that the availability of substrates essential to prokaryotic metabolism, such as reduced sulfur species, significantly affect major clade distributions in the water column. I predict that the prokaryotic community in the redoxcline covaries with concentrations of selected chemical species indicating that these environmental factors are important for prokaryotic growth. To test this hypothesis, I used the fluorescence in situ hybridization (FISH) method to detect and enumerate major bacterial and archaeal clades in the Cariaco Basin's water column. Then, I compared temporal and spatial variability in the prokaryotic community structure (abundance and distribution) and eight environmental variables among cruises using a non-parametric permutational multivariate analysis of variance. A distance-based multivariate analysis for a linear model with a forward selection was used to determine how much the fluctuations in environmental variables affected the variations in the prokaryotic community structure in the redoxcline.

3. Materials and methods

3.1. Study site

The study area (Fig. 2.1) is located off the northern coast of Venezuela and samples were collected during the CARIACO (CArbon Retention In A Colored Ocean) Ocean Time Series project. One to three stations depending on cruise (station A, maximum depth ~1400 m, 10°30'N 64°40'W, station B, max. depth ~650 m, 10°40'N 64°45'W, and station D, max. depth ~500 m, 10°43'N 64°32'W) were sampled for microbiological and chemical analyses during upwelling and non-upwelling seasons between 2006 and 2010 (Table 2.1).

3.2. Sampling

Hydrographic data were obtained using an SBE-25 CTD system mounted on a SeaBird rosette equipped with 12 8-liter Teflon-lined Niskin bottles, a SBE43 oxygen probe for continuous O_2 measurements, ECO fluorometer (Wetlabs) for chlorophyll-a (Chl-a) measurements, and a C-Star transmissometer (660 nm, Wetlabs) for beam attenuation measurements. Seawater samples from 18 depths (station A) and 12 depths (stations B and D) spanning oxic ($[O_2] > 2$ µM), suboxic ($[O_2] \leq 2$ µM, $[H_2S] < 1$ µM), and anoxic/sulfidic ($[H_2S] > 1$ µM) layers were carefully withdrawn from the Niskin bottles under N_2 or Ar pressure to prevent aeration. Samples for individual dissolved oxygen measurements were withdrawn into duplicate glass stoppered bottles and processed using Winkler method as described in Astor et al. (2003). Samples for nutrients analyses (NH_4^+, NO_2^-, NO_3^-) were withdrawn into 250 mL polyethylene bottles, then subsamples were filtered through Nuclepore Track-Etched membranes into 30 mL HDPE bottles, and samples were analyzed following Gordon et al. (1993) protocols by K. Fanning from the University of South Florida. Triplicate samples for sulfide, thiosulfate, and sulfite measurements were collected with a gas-tight syringe as described in Li et al. (2008). Sulfide samples were analyzed using a modified method of Cline (1969); thiosulfate and sulfite samples were analyzed by X. N. Li (Li et al., 2008) using the DTNP method of Valravamurthy and Mopper (1990) as modified by Hayes et al. (2006). Samples for particulate elemental sulfur measurements were collected in duplicates by gravity filtering and analyzed as described by Li et al. (2008) and references therein. Details of all analyses can be found at the CARIACO project Web site (http://www.imars.usf.edu/CAR/). I provide brief descriptions of these measurements as background. Environmental data are courtesy of M.I. Scranton, X.N. Li, Y. Astor, and K. Fanning.

3.3. Total prokaryotic community abundance

At each depth, 200 mL of whole water was preserved with 2 % borate-buffered formaldehyde (final concentration) and stored at 4ºC. In the home laboratory, standard acridine orange-stained (AO) slides were prepared for total bacterial enumeration by epifluorescence microscopy (Hobbie et al., 1977).

3.4. Fluorescence in situ hybridization (FISH) for prokaryotic community

For analyses of prokaryotic community structure at the time of sampling 90 mL water samples were collected from each depth, preserved with 2 % ([v/v] final concentration) borate-buffered formaldehyde, and frozen at -20° C for about 24 h to increase cell membrane permeability before further processing. After thawing, cells were captured on Millipore Isopore® Membrane filters (47 mm diameter, 0.2 µm pore size, GTTP type), rinsed with 10 mL of distilled water, dried, and stored in Petrislides® at -20˚C.

All samples to investigate community structure were processed using oligo-FISH (for the domain Bacteria) and CARD-FISH (catalyzed reporter deposition-FISH) (for Archaea) techniques as described in Pernthaler et al. (2001a) and Lin et al. (2006), respectively. Cy3-monolabeled rRNA oligonucleotide probes were used to detect clades within the domain Bacteria, and horseradish peroxidase (HRP)-labeled probes (ThermoFisher Scientific, Ulm, Germany) were used to detect Thaumarchaeota and Euryarchaeota (Table 2.2). Previous evaluations of both oligo-FISH and CARD-FISH methods employed in the detection of Cariaco's prokaryotic community showed that only application of CARD-FISH was necessary for enumeration of Thaumarchaeota and Euryarchaeota. Detection of bacterial clades with oligo-FISH was not demonstrably different from parallel CARD-FISH preparations (Lin et al., 2006). Individual filters were cut into 12-16 wedges and single or multiple (where applicable) probes were applied to hybridize with specific clades of microorganisms. Additionally, DAPI (4'6-diamidino-2-phenylindole) staining on the same filter wedges was performed to quantify total prokaryotic abundances. Depending on sample, between 10 grids and 30 fields or at least 300 DAPI-positive cells were counted using epifluorescence microscope to obtain the coefficient of variation below 20 % (Pernthaler et al., 2001a). Specific clade probe-positive cell counts are reported as percentages of total DAPI-positive inventory (% of prokaryotic community) and as absolute cell concentrations (cells L^{-1}). Probe-positive cell counts were compared to DAPI-positive cell counts from the same filter wedges to derive fraction of total community. Ambient abundances of each clade were calculated from their fractional contribution times AO-derived total community size.

3.5. Statistical analyses

Non-parametric multivariate multiple regression analysis of variance (PERMANOVA) was used to test for significant differences in the multivariate biological data (Anderson, 2005) among eight cruises at station A, three cruises at station B, and two cruises at station D. Data from cruise CAR163 were excluded from the statistical analyses due to an incomplete data set. Seven consecutive depths within the redoxcline were chosen to obtain a balanced design (equal number of samples for every cruise) required for the Permanova test. Depth of first appearance of hydrogen sulfide ($H_2S > 1$ µM) was chosen as a reference depth to identify the oxic-anoxic interface in the analysis. Because prokaryotic productivities in the Cariaco Basin usually peak at or below the interface (Fig. 2.2), two depths above and four depths below the reference depth were chosen in each cruise to span the suboxic and upper anoxic layers within the redoxcline. Permanova analyses were constrained to the redoxcline layer at depths between 215 and 400 m at station A, 180 and 450 m at station B, and 240 and 450 m at station D. Oxic and deep anoxic layers were excluded from statistical analyses to balance design and focus on similar geochemical gradients. Biological data (proteobacterial and archaeal clades abundances as cell concentrations L^{-1}) from seven depths within the redoxcline from eight cruises were checked for normality with Shapiro-Wilk normality test (failed at $p < 0.001$) and then transformed logarithmically using the following equation:

$y' = \log (x_{ij} + d) - c,$

where y' is the transformed value, x_{ij} is the original value being transformed,

$d = \log^{-1}(c),$

$c = \log (\min(x_{ij})),$

where d is a decimal constant which preserves the order of magnitude in the original value, c is the order of magnitude constant which truncates x_{ij} to an integer and drops the digits after the decimal place, and $min(x_{ij})$ is a minimal non-zero value among the values being tested (McCune and Mefford, 2006).

In addition to Permanova analyses of clade distributions, eight environmental variables (oxygen (Winkler method), sulfide, sulfite, thiosulfate, ammonium, nitrite, and nitrate concentrations) thought to be biologically important to investigated clades were tested as covariables to determine which one was significantly influencing community structure

(distribution and abundance). Net (downward and upward) fluxes of these variables at each depth were also calculated assuming a vertical eddy diffusivity model and used in Permanova analyses but they explained little variability in the clade data. Details of those analyses are provided in Appendix A. Thus simple concentrations were used in Permanova analyses because they explained more variability in clade data. Concentrations of environmental variables were standardized to obtain z-scores by subtracting the mean from the original value and dividing it by its standard deviation (McCune and Mefford, 2006). Permanova analyses were done using 9999 unrestricted permutations (for clades) or 9999 permutations of residuals under the reduced model (for covariables) at a significance level $\alpha < 0.01$and were based on Bray-Curtis similarities calculated from the transformed clades data (Anderson, 2001). Bray-Curtis similarity is a measure of distance between two groups on a scale of 0 to 100 %, where 'zero' means no difference (perfect similarity) and 100 % means biggest difference (perfect dissimilarity) between two groups (Anderson, 2001; 2005). Unconstrained non-parametric multidimensional scaling (NMS) ordination was used to visualize the patterns in the multivariate clade data (McCune and Mefford, 2006). NMS analyses were based on Bray-Curtis similarities of transformed clade data. Joint plots were used to project the distribution of environmental variables within the total community for all eight cruises. All NMS analyses and plots were done using PC-ORD software Version 5.10 (MjM Software, Gleneden Beach, Oregon, USA). Because NMS ordination is unconstrained, joint plots do not illustrate correlations between data but rather distribution of ranked distances and interpretation of graphs should be approached with caution.

A distance-based multivariate analysis for a linear model using forward selection (DISTLM_*forward*) was applied to determine how much of the variability in the clade data was represented by each environmental variable (Anderson, 2003). These analyses could not be completed for individual cruises due to small sample sizes. Therefore, data from all cruises were combined for each station and transformed logarithmically as described above. Similarly, data sets for environmental variables (concentrations standardized to z-scores) were created. All analyses were done using 9999 permutations of residuals (type I errors) under a reduced model at a significance level $\alpha < 0.01$and were based on Bray-Curtis similarities calculated from the transformed clade data as described above (Anderson, 2003). Because the environmental variables can correlate with each other, their variance with clade data was tested sequentially

(conditionally) - each consecutive variable was fitted into the model based on the significance of the preceding variable (Anderson, 2003).

4. Results

4.1. Physico-chemical conditions

Oxygen concentrations decreased from about 200 µM at the surface to less than 2 µM at depths between 215 m and 280 m depending on the cruise and station. I operationally defined the upper boundary of the suboxic layer as the depth where oxygen concentrations fell below 2 µM mark. Hydrogen sulfide concentrations above 1 µM were measured at depths between 245 and 300 m depending on the cruise and station, and mark the lower boundary of the suboxic layer as well as the depth of the oxic-anoxic interface. Hydrogen sulfide concentrations increased to > 50 µM in the deep anoxic layer. The suboxic layer thickness varied between 15 and 40 m at station A, 15 and 30 m at station B, and 10 and 20 m at station D, depending on the cruise.

Elemental sulfur concentrations were consistently low (< 0.6 µM) throughout the water column but exhibited peaks of up to 1.2 µM in the lower suboxic layer in close proximity to the oxic-anoxic interface where O_2 and H_2S were < 2 µM. Sulfite and thiosulfate concentrations were highest during CAR122 (up to about 3 µM within the redoxcline) and lower during other cruises by 2-3-fold, although sulfite concentrations were consistently higher than concentrations of thiosulfate. Peaks in sulfite and thiosulfate concentrations were observed within the redoxcline as well as in upper anoxic layers.

Ammonium concentrations increased with depth to above 20 µM in the anoxic layer at stations A and B, and to about 10 µM at station D. In the redoxcline, ammonium concentrations varied between 2.4 and 3.2 µM, depending on station. Nitrite concentrations were consistently low (< 0.2 µM) throughout the water column during all cruises at three stations but exhibited small maxima up to 3.8 µM in the redoxcline during CAR122 at station A. Nitrate concentrations were highest (up to 10 µM) in the oxic layer and were diminished to between 0.8 and 2.3 in the redoxcline before totally disappearing in anoxic waters.

4.2. Abundance and distribution of total prokaryotic community

Total prokaryotic community cell concentrations (based on AO counts) varied considerably among cruises and stations. At station A, among nine cruises the total prokaryotic community abundances varied between 0.6 and $9.2x10^8$ cells L^{-1} in the oxic layer, between 0.5 and $6.6x10^8$ cells L^{-1} in the redoxcline (200-400 m) and between 0.4 and $4.8x10^8$ cells L^{-1} in the deep anoxic layer (Fig. 2.3). At station B, abundances of the total prokaryotic community varied between 0.5 and $5.3x10^8$ cells L^{-1} in the oxic layer, between 1.7 and $6.0x10^8$ cells L^{-1} in the redoxcline, and between 2.0 and $3.0x10^8$ cells L^{-1} in the anoxic layer (Fig. 2.4). At station D, abundances of the total prokaryotic community varied between 2.9 and $5.4x10^8$ cells L^{-1} in the oxic layer, between 1.5 and $4.9x10^8$ cells L^{-1} in the redoxcline, and between 1.4 and $3.1x10^8$ cells L^{-1} in the anoxic layer (Fig. 2.5). Distinct peaks in abundances of the total prokaryotic community were observed across the oxic-anoxic interface during each cruise.

4.3. Vertical distributions of Bacteria and Archaea in the water column

Twelve oligonucleotide rRNA-targeted probes were used to enumerate specific groups of *Bacteria* and *Archaea* throughout the water column during nine cruises using FISH method. Clade-specific probes were chosen based on previous studies applying them in the Cariaco Basin as well as coverage of individual target groups. In general, highest abundances of α-proteobacteria were observed in surface waters (up to $10.2x10^7$ cells L^{-1}) but on occasion elevated numbers were observed across the oxic-anoxic interface and in the deeper anoxic layer (Tables B.1, B.2, B.3). On average this clade accounted for 3.2-6.6 % of the total prokaryotic community in the redoxcline at all stations (Figs. 2.3, 2.4, 2.5). β-proteobacteria abundances at station A were generally highest in the redoxcline reaching up to $9.8x10^7$ cells L^{-1} and on average this clade accounted for 10.0 % of the total community (Table B.1, Fig. 2.3). Occasional peaks up to $5.5x10^7$ L^{-1} were observed in the surface waters (Table B.1). At stations B and D, peaks in abundances of β-proteobacteria were observed across the oxic-anoxic interface (Tables B.1, B.2, Figs. 2.4, 2.5) and on average this clade accounted for 7.1 and 10.2 % of the total community in the redoxcline, respectively. Abundances of γ-proteobacteria were highest in the oxygenated waters at stations A and D, and reached maxima of up to $5.6x10^7$ and $4.9x10^7$ cells L^{-}

^{1}, respectively (Tables B.1, B.3) while at station B abundances of this clade were generally highest in the redoxcline. Single peaks (up to $5.4x10^{7}$ cells L^{-1}) in abundances of this clade were also observed across the oxic-anoxic interface at station A. In the redoxcline, average contribution of this clade to the total community varied between 2.6 % at station D, 3.8 % at station B and 5.4 % at station A.

Sulfate-reducing δ-proteobacteria (SRB) distributions varied the most between cruises at station A with no particular pattern. Elevated abundances of this clade were observed across the oxic-anoxic interface as well as in the oxygenated and anoxic layers (Table B.1, Fig. 2.3). At stations B and D, elevated abundances of this clade (between $6.0x10^{7}$ and $8.7x10^{7}$ cells L^{-1}) were observed in oxygenated waters and across the oxic-anoxic interface while generally lowest abundances were observed in the anoxic layer (below $2.0x10^{7}$ cells L^{-1}) (Tables B.2, B.3). At station A, average contribution of this clade in the redoxcline (5.3 %) was similar to that of γ-proteobacteria while at stations B and D, SRB accounted for 6.7 and 5.3 % of the total community, respectively.

Distributions of ε-proteobacteria varied considerably throughout the water column at station A among all cruises but in general elevated abundances (up to $30.7x10^{7}$ cells L^{-1}) were observed within the redoxcline (Table B.1). At station B, peaks in abundances of this clade were observed above the oxic-anoxic interface ($5.9x10^{7}$ cells L^{-1}) and in the deeper anoxic waters ($10.3x10^{7}$ cells L^{-1}) while at station D elevated abundances of ε-proteobacteria were observed across the interface and varied between $2.1x10^{7}$ and $4.7x10^{7}$ cells L^{-1}) (Tables B.2, B.3). Average contributions of this clade to the total prokaryotic community in the redoxcline varied between 8.9 % at station B, 10.3 % at station D, and 15.3 % at station A.

At station A, distributions of Thaumarchaeota and Euryarchaeota were elevated in the redoxcline as well as exhibiting peaks in the surface and deep anoxic waters during cruises CAR122, CAR128, and CAR132 (Fig. 2.3). During these cruises, maximal abundances of Thaumarchaeota varied between $3.5x10^{7}$ and $9.7x10^{7}$ cells L^{-1} (Table B.1) and Euryarchaeota varied between $1.6x10^{7}$ and $11.6x10^{7}$ cells L^{-1} throughout the water column (Table B.1). During remaining cruises abundances of these clades were an order of magnitude lower and mostly uniformly distributed throughout the water column but single peaks in abundances were observed within the redoxcline or in deep anoxic layer. At stations B and D, only during CAR122 elevated abundances of Thaumarchaeota ($5.5\text{-}12.8x10^{7}$ cells L^{-1}) and Euryarchaeota

(4.4-8.4x10^7 cells L^{-1}) were observed across the oxic-anoxic interface while during remaining cruises these abundances of these clades were much lower (Tables B.2, B.3). In the redoxcline at station A, both clades on average accounted for ~ 4.0 % of the total community (Fig. 2.3). In the redoxcline at stations B and D, Thaumarchaeota accounted for 7.9 and 8.3 % of the total community, respectively while Euryarchaeota contributed on average 4.4 and 8.6 %, respectively.

Fraction of the total community that was either not targeted or did not hybridize with selected probes was operationally called undefined. At station A, undefined fraction varied between 7.2 and 85.6 % of the total community in the oxic layer, between 0.9 and 92.3 % in the redoxcline, and between 5.9 and 86.9 % in the deep anoxic layer depending on cruise (Fig. 2.3). At station B, undefined fraction varied between 33.9 and 88.2 % of the total community in the oxic layer, between 2.4 and 91.1 % in the redoxcline, and between 24.7 and 86.5 % in the anoxic layer (Fig. 2.4). At station D, undefined fraction accounted for 23.8 to 88.4 % of the total community in the oxic layer, 4.3 to 88.8 % in the redoxcline, and 59.3 to 82.9 % in the anoxic layer (Fig. 2.5).

4.4. Variability in prokaryotic community structure and its relationship to environmental variables

Permutational multivariate analysis of variance (PERMANOVA) based on Bray-Curtis dissimilarities was used to test for significant differences in clade distributions among eight cruises at station A, three cruises at station B, and two at station D. The unconstrained NMS ordination was used to illustrate the results from Permanova analyses.

Station A. Temporal differences in total clade distribution (all seven clades) were statistically significant ($p < 0.001$, $n = 56$) for all eight cruises tested altogether. However, pair-wise *a posteriori* comparison of clade distributions among individual cruises revealed no differences between cruises CAR139 and CAR145, and between CAR145 and CAR153 (Table 2.3). Distributions of all clades were most similar during CAR128 and CAR139 (12 % similarity) while the biggest differences were observed between cruises CAR132 and CAR169 (38 % dissimilarity). Generally, distributions of α-proteobacteria, β-proteobacteria, ε-proteobacteria, and Thaumarchaeota covaried significantly with concentrations of sulfide, sulfite, thiosulfate, and ammonium (Table 2.4). Distributions of β-proteobacteria additionally covaried with

distributions of elemental sulfur, nitrate, and oxygen. Distributions of γ-proteobacteria covaried significantly with distributions of sulfite and thiosulfate while distributions of sulfate-reducing δ-proteobacteria covaried only with distributions of elemental sulfur. Distributions of Euryarchaeota covaried significantly only with sulfide and ammonium concentrations (Table 2.3).

NMS ordination illustrated that cruises CAR139, CAR145, and CAR153 were very tightly clustered together while other cruises had a more pronounced dispersion. Cruises CAR132 and CAR169 were farthest from each (highest dissimilarity) which is in agreement with the results obtained from Permanova analysis (Fig. 2.6). The environmental variables most associated with the NMS axes were elemental sulfide, sulfite, thiosulfate, and ammonium. Clade distributions in CAR122 and CAR128 were mostly associated with sulfite and thiosulfate concentrations while in other cruises, clade distributions did not show specific associations with concentrations of other variables. Clade distributions in CAR132, CAR153, and CAR169 did not show strong associations with any particular environmental variables (Fig. 2.6). The NMS analysis 2-dimensional solution showed that 44.6 % of variance in clade distributions were associated with axis 1 and 49 % were associated with axis 2.

Station B. Temporal differences in total clade distributions at this station were statistically significant ($p < 0.001$, $n = 21$). Pair-wise *a posteriori* comparison of clade distributions between individual cruises also showed significant differences ($p < 0.05$) (Table 2.3). Clade distributions in CAR122 and CAR128 were more similar to each other than to those in CAR132. However, clade distributions in CAR132 were less dissimilar to those in CAR128 (37 % dissimilarity) then to those in CAR122 (45 % dissimilarity). Distributions of α-proteobacteria and Euryarchaeota covaried significantly only with distributions of elemental sulfur and those of Thaumarchaeota covaried with distributions of sulfide and thiosulfate (Table 2.4). Distributions of γ-proteobacteria and sulfate-reducing δ-proteobacteria significantly covaried with distributions of sulfide and nitrite while distributions of β-proteobacteria covaried with nitrite and ammonium (Table 2.4). Distributions of ε-proteobacteria did not covary significantly with any of the tested environmental factors. The NMS ordination of clade distributions did not show any clustering which illustrates the significant differences between cruises (Fig. 2.7). The NMS analysis 3-dimensional solution showed that almost 44 % of variance in clade distributions was associated with axis 1, about 31 % was associated with axis 2, and 23 % of variance was associated with

axis 3. A 3-dimensional solution with two axes that explained the most variance is shown in Fig. 2.7.

Station D. Temporal differences in total clade distributions at this station were statistically significant ($p < 0.005$, $n = 14$). Pair-wise *a posteriori* comparison of clade distributions between individual cruises also showed significant differences ($p < 0.05$) (Table 2.3). Among individual clade, distributions of β-proteobacteria significantly covaried with distributions of elemental sulfur while distributions of SRB covaried with sulfide and thiosulfate (Table 2.4).Distributions of other bacterial clades did not significantly covary with any environmental factors tested. Distributions of Thaumarchaeota covaried with distributions of ammonium and nitrite while distributions of Euryarchaeota covaried with distributions of sulfide and ammonium (Table 2.4). The 2-dimensional NMS ordination illustrated no clustering of samples, 77.5 % of variance in clade distributions was associated with axis 1 and 18.8 % with axis 2 (Fig. 2.8).

4.5. Relationship of environmental variables to individual clade distributions (DISTLM_*forward* analyses)

To determine how much variability in clade distributions could be explained by distributions of environmental variables, a distance-based multivariate analysis for a linear model with a forward selection was applied in statistical analysis (Anderson 2003).

Station A. Among all eight environmental variables, distributions of thiosulfate and sulfide concentrations explained 11.9 and 5.8 % of variance in total clade distributions, respectively ($p < 0.05$, $n = 56$, Table 2.5). Variations in distributions of several environmental variables explained significant portions of the variations in individual clade distributions. For example, distributions of sulfide accounted for 5.3 and 16.4 % of variance in distributions of Thaumarchaeota and Euryarchaeota, respectively. Distributions of sulfite accounted for 7.9 and 20.7 % of variance in distributions of α-proteobacteria and γ-proteobacteria, respectively, while distributions of thiosulfate concentration represented between 7.0 and 15.0 % of variance in distributions of β-proteobacteria, ε-proteobacteria and Thaumarchaeota. Distributions of ammonium accounted for 7-8 % of variance in distributions of β-proteobacteria and ε-proteobacteria. Distributions of nitrate and elemental sulfur concentrations were only significant to distributions of SRB and

Thaumarchaeota and accounted for 5.1 and 12.6 % of variance, respectively. Nitrite distributions did not account for any of variance in any clade distribution tested (Table 2.5).

Station B. Among all environmental variables combined, distributions of sulfite and thiosulfate concentrations accounted for 23.0 and 15.4 % of variance in the total clade distributions, respectively ($p < 0.05$, $n = 21$, Table 2.5). Analyses of individual clade distributions in relation to distributions of environmental variables showed that distributions of sulfite concentrations accounted for the highest percentage of variance in distributions of α-proteobacteria (31.4 % of variance), β-proteobacteria (35.4 % of variance), and Euryarchaeota (17.1 % of variance). Additionally, distributions of α-proteobacteria were represented by 19.4 and 10.8 % of variance in distributions of thiosulfate and sulfide, respectively, while distributions of β-proteobacteria were represented by 15.0 and 9.6 % of variance in thiosulfate and oxygen, respectively. Distributions of elemental sulfur accounted for 20.4 % of variance in distributions of only γ-proteobacteria while nitrate accounted for 25.2 % of variance in distributions of only ε-proteobacteria. SRB clade and Thaumarchaeota distributions were not explained by distributions of any environmental factors tested (Table 2.5).

Station D. Among eight environmental variables, four accounted for 69.7 % of variance in distributions of all clades ($p < 0.05$, $n = 14$, Table 2.5). Distributions of thiosulfate concentrations accounted for the highest percentage of variance in distributions of α-proteobacteria (29.2 %) and ε-proteobacteria (55.2 %). Distributions of elemental sulfur accounted for 28.7 and 24.4 % of variance in archaeal clades only (Thaumarchaeota and Euryarchaeota, respectively). Distributions of ammonium concentration accounted for 35.9 and 28.3 % of variance in distributions of β-proteobacteria and Euryarchaeota, while oxygen for 23.9 % of variance in distributions of SRB clade. Distributions of sulfide, sulfite, nitrite, and nitrate did not account for any variance in distributions of any clade at this station. Furthermore, distributions of γ-proteobacteria did not relate to any of the environmental factors tested at this station (Table 2.5).

5. Discussion

5.1. Predominant bacterial and archaeal clades

FISH analyses of the prokaryotic community structure in the Cariaco's water column revealed predominance of ε- and β-proteobacteria in the redoxcline which on average accounted for up to 15 and 10 % of the total DAPI counts, respectively. Other bacterial clades (α-, γ-proteobacteria, and SRB) were consistently detected in lower numbers but occasional peaks in their abundances were also observed in the redoxcline. Thaumarchaeota and Euryarchaeota contributed much less to the total community than bacterial clades but their abundances exhibited occasional peaks up to 8 % in the redoxcline as well. These findings are consistent with previous FISH surveys conducted by Lin et al. (2006) in the Cariaco Basin. ε-proteobacteria, γ-proteobacteria, β-proteobacteria and Thaumarchaeota are the major clades consistently recognized or postulated to be the most important chemoautotrophs responsible for enhanced dark carbon assimilation in suboxic and anoxic marine pelagic redoxclines (Taylor et al., 2001; Lin et al., 2006; Lam et al., 2007; Labrenz et al., 2007; Grote et al., 2008; Glaubitz et al., 2009; Walsh et al., 2009; Zaikova et al., 2010). ε-proteobacteria and γ-proteobacteria have been shown to be the major chemoautotrophs in the redoxcline of the Baltic Sea (Labrenz et al., 2007; Grote et al., 2008; Glaubitz et al., 2009). Recent findings in the Baltic Sea point to γ-proteobacteria SUP05 subgroup (Glaubitz et al., 2013) and ε-proteobacteria related to genus *Sulfurimonas* (Jost et al., 2010) as the major sulfur-oxidizing chemoautotrophs. ε-proteobacteria related to genus *Sulfurimonas* were previously detected in 16S rRNA gene libraries of the Cariaco Basin (Madrid et al., 2001) and of the Black Sea (Vetriani et al., 2003). In the Black Sea, in addition to anaerobic sulfur oxidation, nitrification by γ-proteobacteria and β-proteobacteria (Lam et al., 2007) and anaerobic ammonium oxidation (anammox) (Kuypers et al., 2003) are believed to be important chemoautotrophic processes in the redoxcline. Recent studies by Wakeham et al. (2012) and Cernadas-Martin (2012) present evidence for anammox activity and nitrification by γ-proteobacteria and β-proteobacteria in the Cariaco Basin as well. The consistent presence of ε-proteobacteria and β-proteobacteria in enhanced numbers and occasional peaks in abundance of γ-proteobacteria and Thaumarchaeota in the redoxcline indicate that these clades are important components of the redoxcline prokaryotic community of the Cariaco Basin. Thus, the questions to be asked are what environmental factors affect the numbers and distributions of the major clades in the Cariaco Basin and what are the links and/or correlations between the clades and the environmental factors.

5.2. Chemoautotrophic functional groups

Distributions of all clades varied significantly between investigated cruises at all three stations in this study. Distributions of the majority of individual clades covaried significantly with the distributions of at least one out of eight environmental variables considered important to prokaryotic metabolism. Variability in distributions of clades and covariation with environmental variables is most likely influenced by fluctuations in concentrations of oxygen in the upper redoxcline layer which determines the width of the suboxic layer and specific gradients of other substrates. Stations B and D are located north of station A and closer to La Tortuga Channel which connects the Cariaco Basin with the Caribbean Sea. Therefore, the redoxcline communities at stations B and D are potentially experiencing more frequent episodic lateral intrusions of oxygenated waters from the Caribbean Sea than those at station A (Astor et al. 2003, Scranton et al. 2006). At station A, distributions of thiosulfate and ammonium concentrations accounted for ~ 21 % of variance in distribution of ε-proteobacteria while at stations B and D, distributions of nitrate and thiosulfate accounted for ~ 25 and 55 % of variance in distribution of ε-proteobacteria, respectively. Such considerable influence of distributions of these variables on distribution of ε-proteobacteria suggests their great importance to the metabolism of this clade. Plausible representatives of ε-proteobacteria with thiotrophic metabolism might include relatives of genus *Sulfurimonas* which have been shown to utilize a variety of inorganic sulfur substrates as electron donors and nitrate or nitrite as electron acceptors (Brettar et al., 2006). Recently, ε-proteobacterium *Sulfurimonas gotlandica* sp. has been identified as an important chemoautotroph in the suboxic waters of the Baltic Sea (Grote et al., 2007, 2008, 2011; Labrenz et al., 2013). Sequences of ε-proteobacteria related to genus *Sulfurimonas* (previously identified as *Thiomicrospira denitrificans*-like ε-proteobacteria) have been detected in the Cariaco Basin (Madrid et al., 2001) as well as in other oxygen-deficient environments, such as hydrothermal sediments in the Mid-Okinawa Trough, southwest African shelf, and oxygen minimum zone off Chile (Inagaki et al., 2003, 2004; Lavik et al., 2009; Canfield et al., 2010).

β-proteobacteria distributions were most affected by distributions of thiosulfate and ammonium concentrations (~ 22.5 % variance) at station A, thiosulfate and sulfite concentrations (~ 50 % of variance) at station B, and by ammonium concentrations (~ 36 % of variance) at

station D. These results indicate that this clade might be represented by anaerobic chemoautotrophs utilizing sulfite or thiosulfate as electron donors and nitrite or nitrate as electron acceptors (Kelly and Wood, 2000; Beller, 2006) such as representatives of *Thiobacillus* spp., e.g., *Thiobacillus denitrificans*. These prokaryotes have been found in the suboxic waters of the central Baltic Sea (Brettar and Rheinheimer, 1991). Additionally, this clade might be represented by nitrifying β-proteobacteria which have been suggested to be important in the nitrogen cycle in the suboxic waters of the Black Sea and oxygen minimum zone off Peru (Lam et al., 2007; Lam et al., 2009). A quantitative PCR-based survey of ammonia-oxidizing functional genes provided evidence for presence of β-nitrifying bacteria in the Cariaco Basin as well (Cernadas-Martin, 2012).

Distributions of γ-proteobacteria were affected by distributions of sulfite concentrations (~ 21 % of variance) at station A, and elemental sulfur (~ 20 %) at station D. These results indicate that this clade might harbor chemoautotrophic representatives using sulfide, thiosulfate, or elemental sulfur as electron donors and oxygen or nitrate as electron acceptor in their metabolism. Representatives of this metabolic group might belong to SUP05 group whose presence has been documented in the hydrothermal plumes (Sunamura et al., 2004), oxygen-deficient waters of Saanich Inlet and eastern tropical South Pacific (Walsh et al., 2009; Canfield et al., 2010) as well as in the suboxic waters of the Black Sea and Baltic Deeps (Fuchsman et al., 2012; Glaubitz et al., 2013). Additionally, sequences of thiotrophic γ-proteobacteria representatives distantly related (90 % identity) to *Thiomicrospira* spp. and *Thioprofundum* spp. which are usually found in the hydrothermal vents (Jannasch 1985, Scott et al. 2006, Takai et al. 2009, Mori et al. 2011) were also retrieved from the Cariaco Basin (Rodriguez Mora, 2012; Rodriguez Mora et al., 2013). Another metabolic group might be represented by nitrifying γ-proteobacteria which convert ammonium to nitrite and subsequently to nitrate. This speculation is supported by significant relationships between distributions of γ-proteobacteria and distributions of nitrite concentrations in my study as well as by recent quantitative PCR-based survey of ammonia-oxidation functional genes by Cernadas-Martin (2012) which revealed presence of γ-proteobacterial nitrifying bacteria in the Cariaco Basin. Similar findings were described for γ-proteobacterial nitrifiers in the suboxic waters of the Black Sea (Lam et al., 2007).

Thaumarchaeota distributions covaried with distributions of ammonium and nitrite concentrations at stations A and D. These findings indicate presence of chemoautotrophic

nitrifying Thaumarchaeota which, in fact, have also been recently identified in the Cariaco Basin (Cernadas-Martin, 2012) and have been shown to be important players in the nitrogen cycle of the suboxic waters of the Black Sea (Lam et al., 2007), the oxygen minimum zone off Peru (Lam et al., 2009) as well as other marine environments (Konneke et al., 2005; Wuchter et al. 2006).

5.3. Other functional groups

Distributions of elemental sulfur concentrations accounted for ~ 13 % of variance in distributions of SRB. These results indicate that SRB in the Cariaco Basin most probably are represented by classic sulfate-reducing bacteria which are ubiquitous in anoxic waters and sediments but are also found in association with particle aggregates where local oxygen depletions lead to production of sulfide from sulfur reduction (Woebken et al., 2007). SRB in aggregates might also be accompanied by nitrate-reducing, sulfide-oxidizing bacteria (Greene et al., 2003).

Distributions of sulfite concentrations accounted for 8-31 % of variance in distribution of α-proteobacteria at stations A and B while distributions of thiosulfate concentrations accounted for 19-29 % of variance in distributions of α-proteobacteria at stations B and D. Additionally, distributions of α-proteobacteria covaried with distributions of ammonium concentrations. These results indicate that α-proteobacteria might be represented by obligately heterotrophs capable of oxidation of sulfide or elemental sulfur to sulfate via sulfite or thiosulfate (Sorokin, 2003) and by nitrate reducers (Friedrich et al., 2000; Urios et al., 2008).

Distributions of sulfide, sulfite, and elemental sulfur concentrations accounted for ~ 17-24 % of variance in distributions of Euryarchaeota, depending on station. Additionally, distributions of ammonium concentrations accounted for ~ 28 % of variance in distribution of Euryarchaeota at station D. This clade might be represented here by species capable of ammonium oxidation under sulfidic conditions (La Cono et al., 2013). Distributions of sulfide (~ 5 % of variance), thiosulfate (~ 7 % of variance), and elemental sulfur (~ 29 % of variance) concentrations in addition to nitrogen species accounted for considerable variance in distributions of Thaumarchaeota. These findings suggest that this clade might be represented by mixotrophic sulfur-utilizing archaea (Fiala et al., 1986; Zillig et al., 1983, 1990) beside chemoautotrophic nitrifiers described above.

6. Conclusions

This study showed that there are statistically significant temporal variations in major bacterial and archaeal clade distributions at three geographically separated locations in the Cariaco Basin's redoxcline. Distributions of specific clades significantly covaried with distributions of selected energy substrates and oxidants. Distributions of intermediate sulfur species and nitrogen species accounted for significant proportions of variations in the distributions of major clades suggesting strong relationships between abiotic and biotic factors as well as importance of the environmental factors examined in this study to prokaryotic metabolism. Unexplained variation in all clade distributions suggest that factors other than those examined in this study e.g., metal oxides, mortality, might be important to these prokaryotes. Variations in undefined fraction of the total prokaryotic community suggest that some members of specific clades might not be targeted with the suite of probes applied in this study and that some portion of the community might not be active, hence not detectable by FISH. In general, findings from this study suggest that the geochemistry and microbial ecology in the Cariaco Basin and in other marine anoxic environments might be as dynamic as in oxic ones.

Table 2.1. Summary of cruises during which samples were collected.

Cruise number/Station	Date	Season
CAR122A, CAR122B, CAR122D	May 19-20, 2006	upwelling
CAR128A, CAR128B	Nov 10-12, 2006	non-upwelling
CAR132A, CAR132B, CAR132D	Apr 11-13, 2007	upwelling
CAR139A	Nov 30-Dec 1, 2007	non-upwelling
CAR145A	May 6-7, 2008	upwelling
CAR153A	Jan 19-20, 2009	upwelling
CAR157A	May 16-17, 2009	upwelling
CAR163A	Nov 5-6, 2009	non-upwelling
CAR169A	May 6-7, 2010	upwelling

Table 2.2. Oligonucleotide probes used in this study.

Probe name	Target	Sequence (5' to 3')	F* (%)	Reference
NONEUB	Nonsense probe	ACTCCTACGGGAGGCAGC	35	Wallner et al., 1993
ALF968	α-proteobacteria	GGTAAGGTTCTGCGCGTT	20	Neef, 1997
BET42a	β-proteobacteria	GCCTTCCCACTTCGTTT	35	Manz et al., 1992
BONE23A	β-proteobacteria	GAATTCCATCCCCCTCT	35	Amann et al., 1996
GAM42a	γ-proteobacteria	GCCTTCCCACATCGTTT	35	Manz et al., 1992
GAM42a_T1038	γ-proteobacteria	GCCTTTCCACATCGTTT	35	Siyambalapitiya and Blackall, 2004
GAM42a_T1038_G1031	γ-proteobacteria	GCCTTTCCACATGGTTT	35	Siyambalapitiya and Blackall, 2004
EPS682	ε-proteobacteria	CGGATTTTACCCCTACAC	35	Lin et al., 2008
SRB385	Most sulfate reducers (δ-proteobacteria)	CGGCGTCGCTGCGTCAGG	35	Amann et al., 1990
CREN537	Thaumarchaeota	TGACCACTTGAGGTGCTG	20	Teira et al., 2004
EURY806	Euryarchaeota	CACAGCGTTTACACCTAG	20	Teira et al., 2004

*Formamide

Table 2.3. Non-parametric permutational multivariate analysis of variance in clade distributions at stations A, B, and D based on Bray-Curtis dissimilarity measure and pair-wise a posteriori comparisons of clade distributions among cruises; p value obtained from 9999 permutations.

Cruise/St. A	**p**	**Cruise/St. A**	**p**
(C122, C128)	0.0008	(C132, C145)	0.0014
(C122, C132)	0.0013	(C132, C153)	0.0009
(C122, C139)	0.0010	(C132, C157)	0.0003
(C122, C145)	0.0003	(C132, C169)	0.0007
(C122, C153)	0.0004	(C139, C145)	0.2432
(C122, C157)	0.0029	(C139, C153)	0.0047
(C122, C169)	0.0004	(C139, C157)	0.0006
(C128, C132)	0.0004	(C139, C169)	0.0007
(C128, C139)	0.0005	(C145, C153)	0.3797
(C128, C145)	0.0009	(C145, C157)	0.0050
(C128, C153)	0.0006	(C145, C169)	0.0231
(C128, C157)	0.0005	(C153, C157)	0.0094
(C128, C169)	0.0003	(C153, C169)	0.0002
(C132, C139)	0.0009	(C157, C169)	0.0014

Cruise/St. B	**p**
(C122, C128)	0.0014
(C122, C132)	0.0004
(C128, C132)	0.0042

Cruise/St. D	**p**
(C122, C132)	0.0032

Table 2.4. Non-parametric permutational multivariate analysis of variance in individual clade distributions at stations A, B, and D with each environmental factor as covariable based on Bray-Curtis dissimilarity measure ; x for $p < 0.05$; p value obtained from 9999 permutations.

Station A	ALF	BET	GAM	SRB	EPS	THAUM	EURY
Sulfide	x	x			x	x	x
Sulfite	x	x	x		x	x	
Thiosulfate	x	x	x		x	x	
Sulfur		x		x			
Ammonium	x	x			x	x	x
Nitrite							
Nitrate		x	x				
Oxygen		x					
Station B	ALF	BET	GAM	SRB	EPS	THAUM	EURY
Sulfide			x	x		x	
Sulfite							
Thiosulfate						x	
Sulfur	x						x
Ammonium		x					
Nitrite		x	x	x			
Nitrate							
Oxygen							
Station D	ALF	BET	GAM	SRB	EPS	THAUM	EURY
Sulfide				x			x
Sulfite							
Thiosulfate				x			
Sulfur		x					
Ammonium						x	x
Nitrite						x	
Nitrate							
Oxygen							

Table 2.5. Bray-Curtis distance-based analysis of variance in clade distribution for a linear model using forward selection of individual environmental factors fitted into a model sequentially (DISTLM_*forward*). Values represent percentage of variance in clade distributions explained by variance in environmental factors at $p < 0.05$ (based on 9999 permutations).

Station A	ALF	BET	GAM	SRB	EPS	THAUM	EURY	All Clades
Sulfide						5.3	16.4	5.8
Sulfite	7.9		20.7					
Thiosulfate		15.2			12.7	7.2		11.9
Sulfur				12.6				
Ammonium		7.4			8.1			
Nitrite								
Nitrate						5.1		
Oxygen								
% cumulative	**7.9**	**22.6**	**20.7**	**12.6**	**20.8**	**17.6**	**16.4**	**17.7**
Station B	ALF	BET	GAM	SRB	EPS	THAUM	EURY	All Clades
Sulfide	10.8							
Sulfite	31.4	35.4					17.1	23.0
Thiosulfate	19.4	15.0						15.4
Sulfur			20.4					
Ammonium								
Nitrite								
Nitrate					25.2			
Oxygen		9.6						
% cumulative	**61.6**	**60.0**	**20.4**	**0.0**	**25.2**	**0.0**	**17.1**	**38.4**
Station D	ALF	BET	GAM	SRB	EPS	THAUM	EURY	All Clades
Sulfide		30.4						24.5
Sulfite								
Thiosulfate	29.2				55.2			10.1
Sulfur						28.7	24.4	19.6
Ammonium							28.3	
Nitrite		35.9						15.6
Nitrate								
Oxygen				23.9				
% cumulative	**29.2**	**66.3**	**0.0**	**23.9**	**55.2**	**28.7**	**52.7**	**69.7**

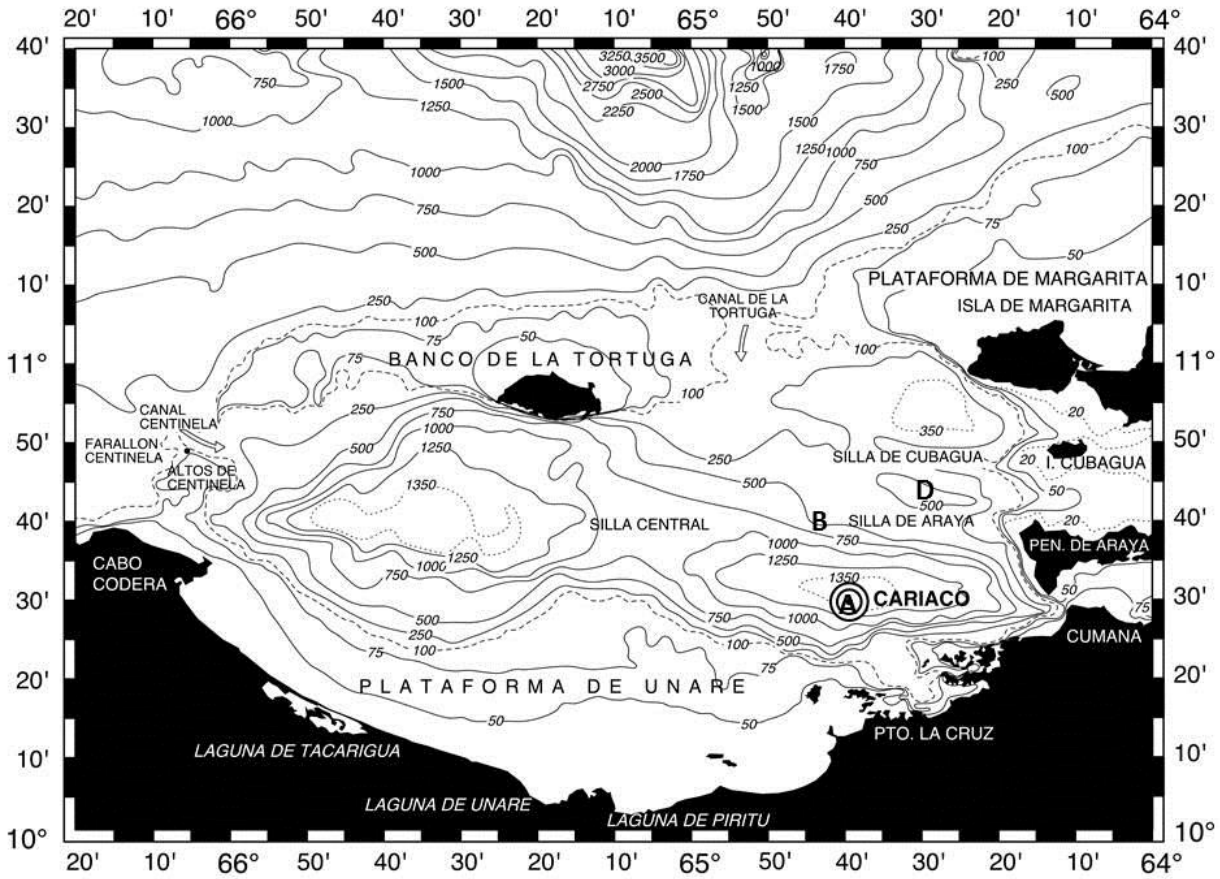

Figure 2.1. Map of the Cariaco Basin. Labels A, B, D mark the positions of corresponding stations investigated in this study.

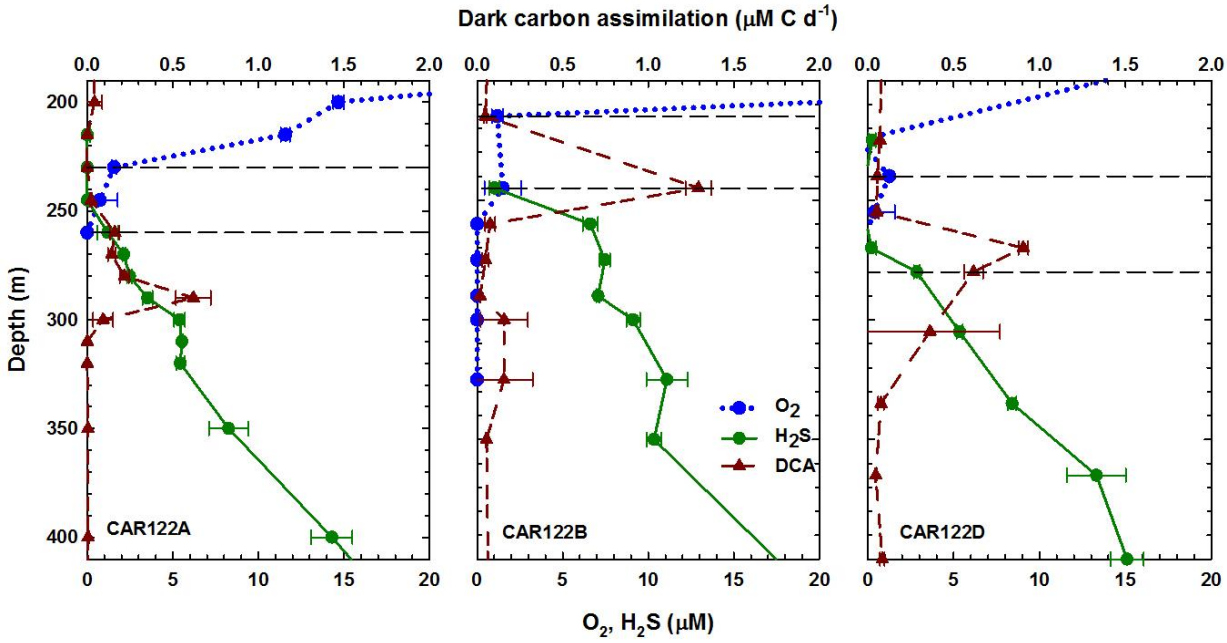

Figure 2.2. Vertical distributions of oxygen, hydrogen sulfide, and chemoautotrophic productivity (measured as dark inorganic carbon assimilation, DCA). Dashed lines represent upper and lower boundary of the suboxic layer (O_2 < 2 μM, H_2S < 1 μM). Error bars represent one standard deviation. Data published in Li et al., 2008.

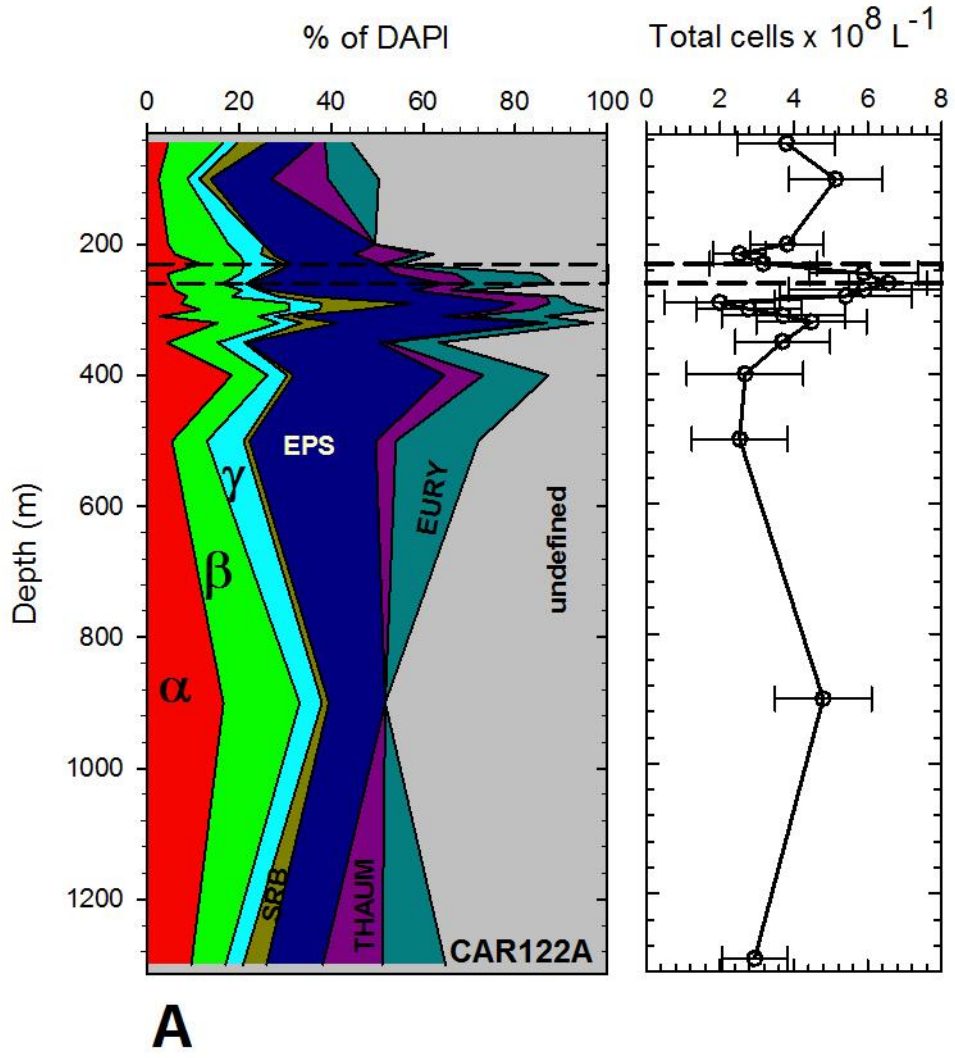

Figure 2.3. A-I. Vertical distributions of Bacteria and Archaea (left panel) and total prokaryotic community (right panel) abundances at station A during nine cruises. Abundances of clades are presented as percentages of the total prokaryotic community based on coincident DAPI-positive cell counts. Dotted lines depict upper and lower boundary of the suboxic layer (O_2 < 2 µM). Bacteria: α-proteobacteria, β-proteobacteria, γ-proteobacteria, ε-proteobacteria, sulfate-reducing bacteria (SRB) as representatives of δ-proteobacteria. Archaea: Thaumarchaeota and Euryarchaeota. Undefined fraction represents fraction of the prokaryotic community not captured by suite of selected probes. Error bars represent one standard deviation.

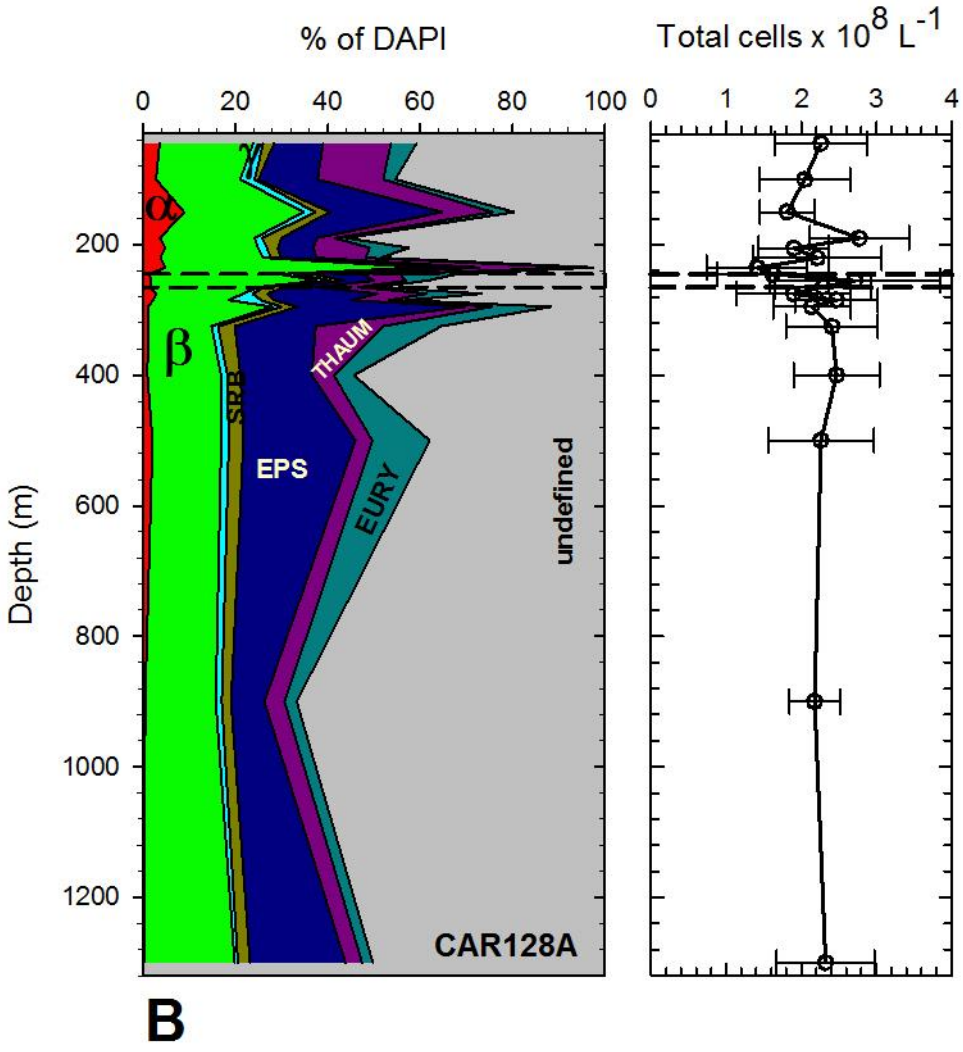
% of DAPI
Total cells x 10^8 L^-1
0
20
40
60
80
100
0
1
2
3
4
Depth (m)
200
400
600
800
1000
1200
α
β
γ
SRB
EPS
THAUM
EURY
undefined
CAR128A

B

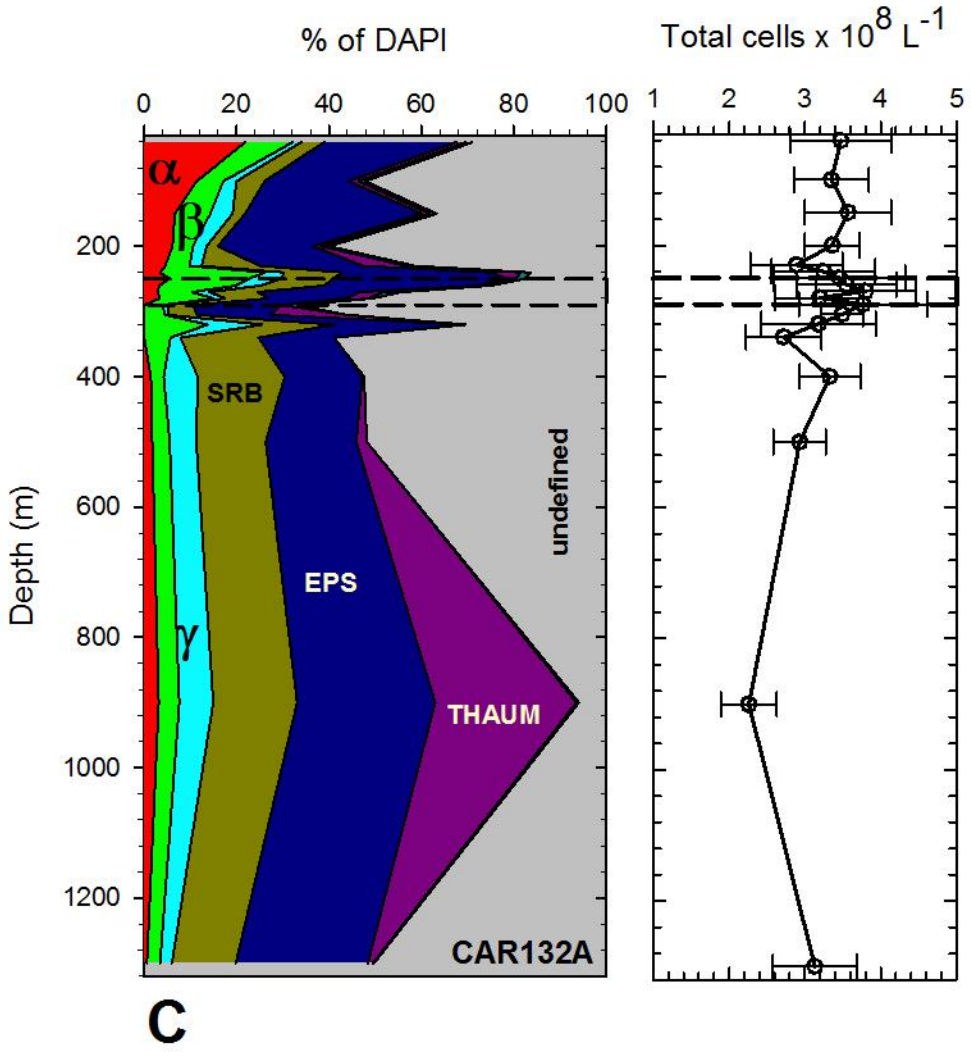
% of DAPI
Total cells x 10^8 L^-1
0
20
40
60
80
100
1
2
3
4
5
Depth (m)
200
400
600
800
1000
1200
α
β
γ
SRB
EPS
THAUM
undefined
CAR132A
C

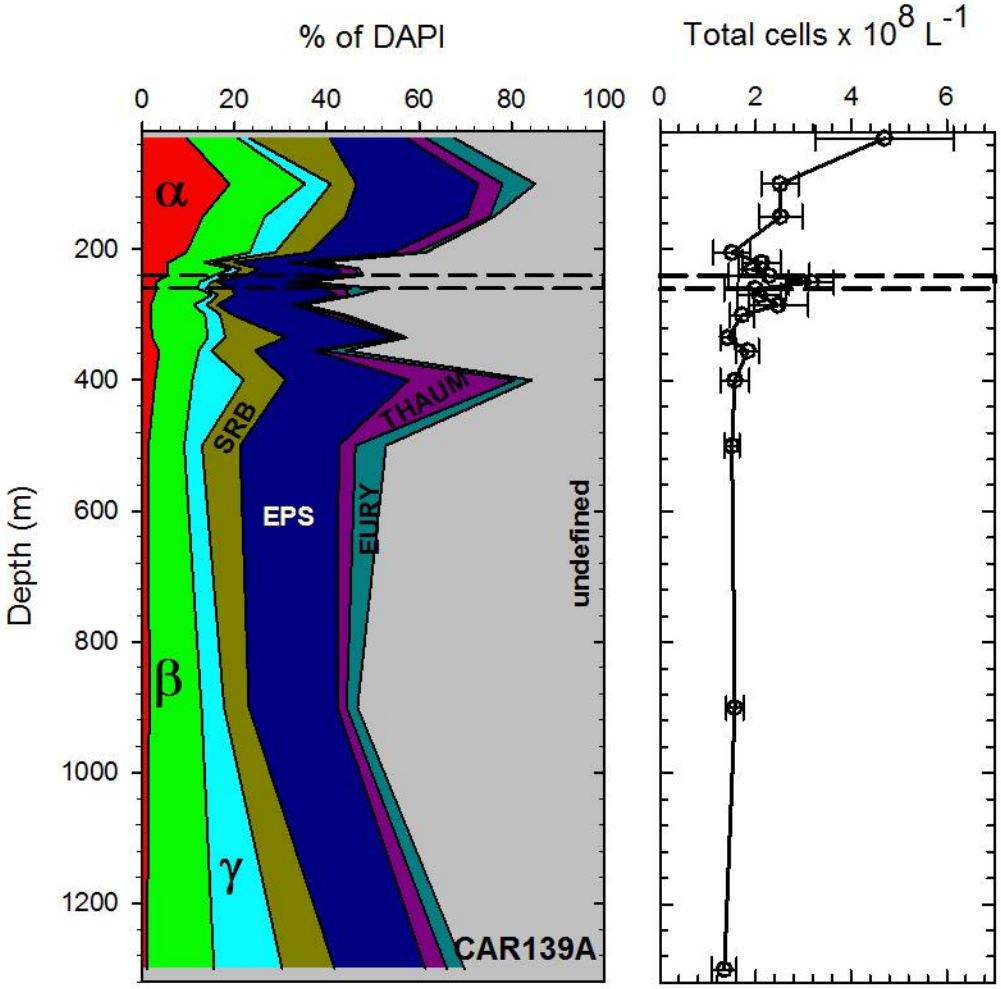
% of DAPI
Total cells x 10^8 L^-1
0
20
40
60
80
100
0
2
4
6
200
400
600
800
1000
1200
Depth (m)
α
β
γ
SRB
EPS
EURY
THAUM
undefined
CAR139A

D

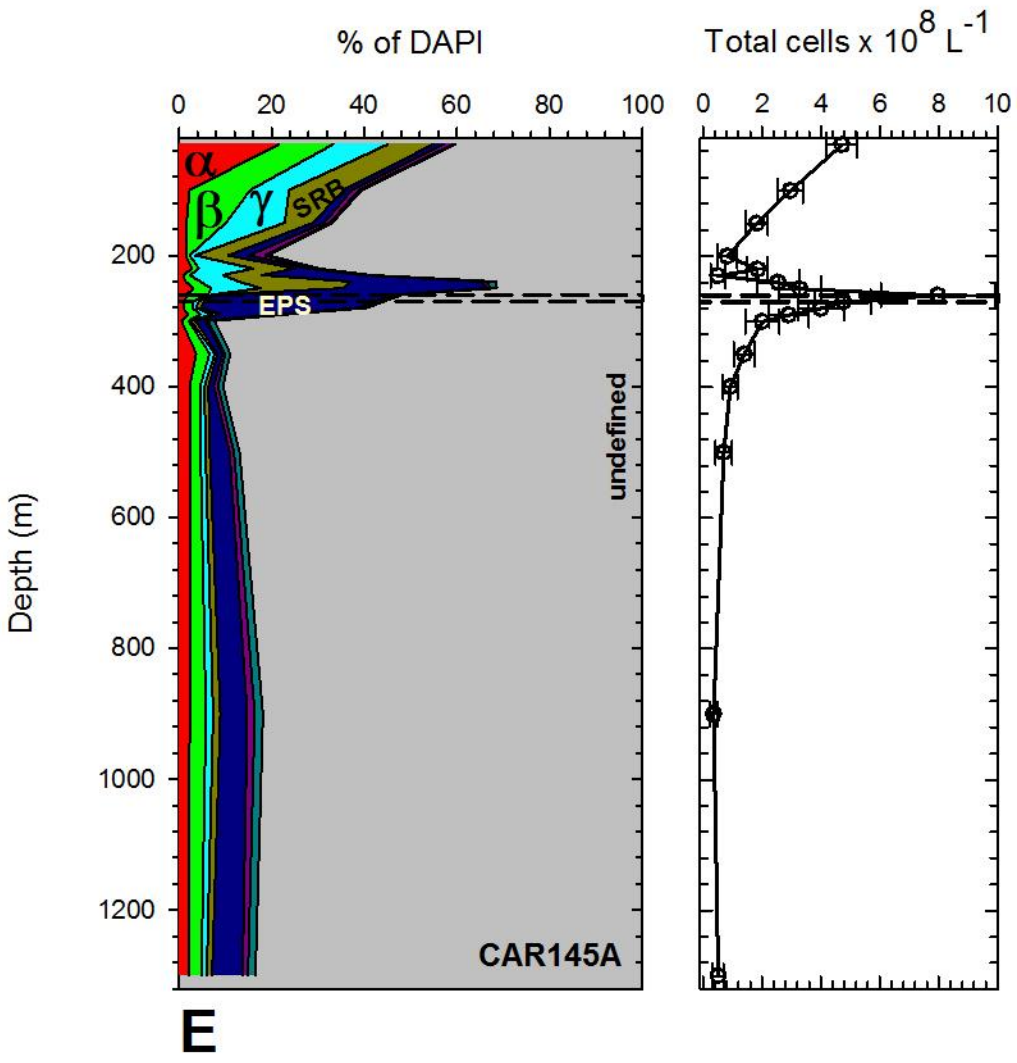
% of DAPI
Total cells x 10^8 L^-1
0
20
40
60
80
100
0
2
4
6
8
10
α
β
γ
SRB
EPS
undefined
CAR145A
Depth (m)
200
400
600
800
1000
1200
E

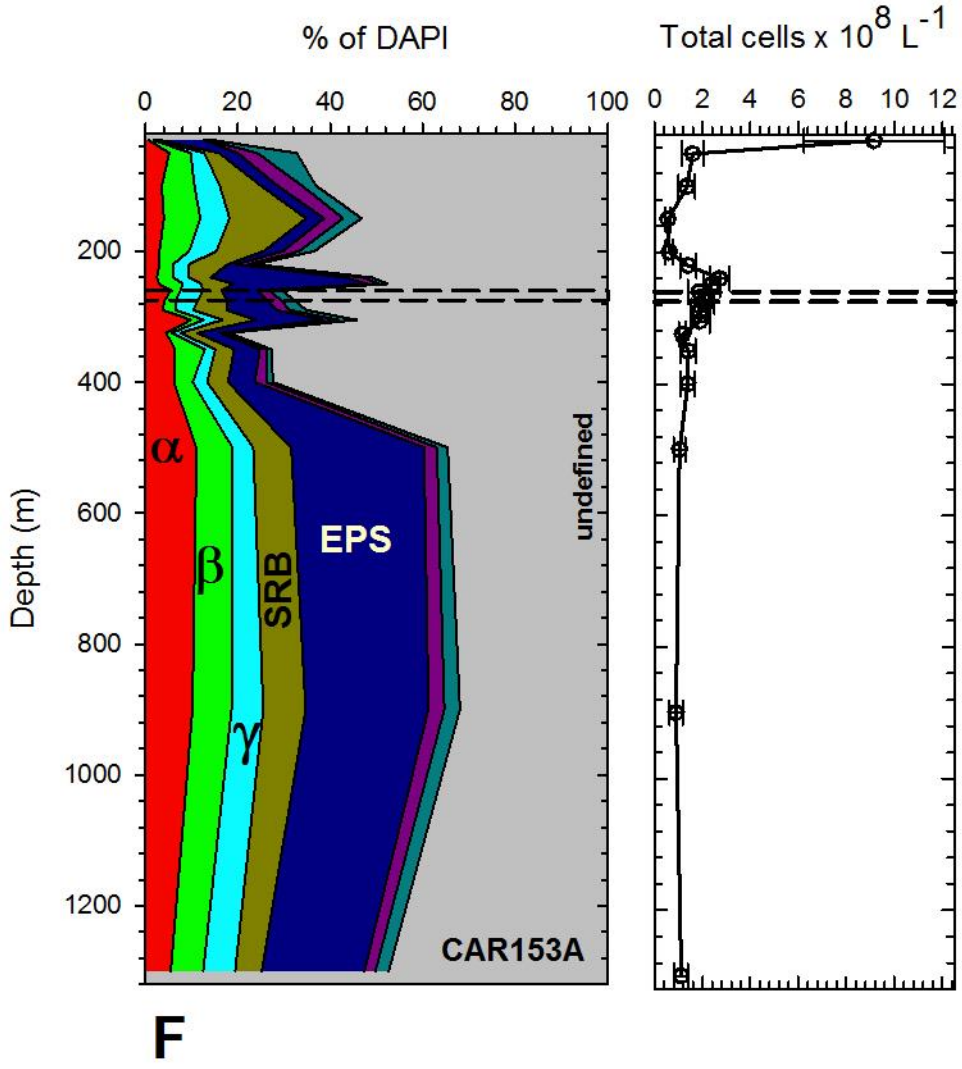
% of DAPI
Total cells x 10^8 L^-1
0
20
40
60
80
100
0
2
4
6
8
10
12
200
400
600
800
1000
1200
Depth (m)
α
β
γ
SRB
EPS
undefined
CAR153A
F

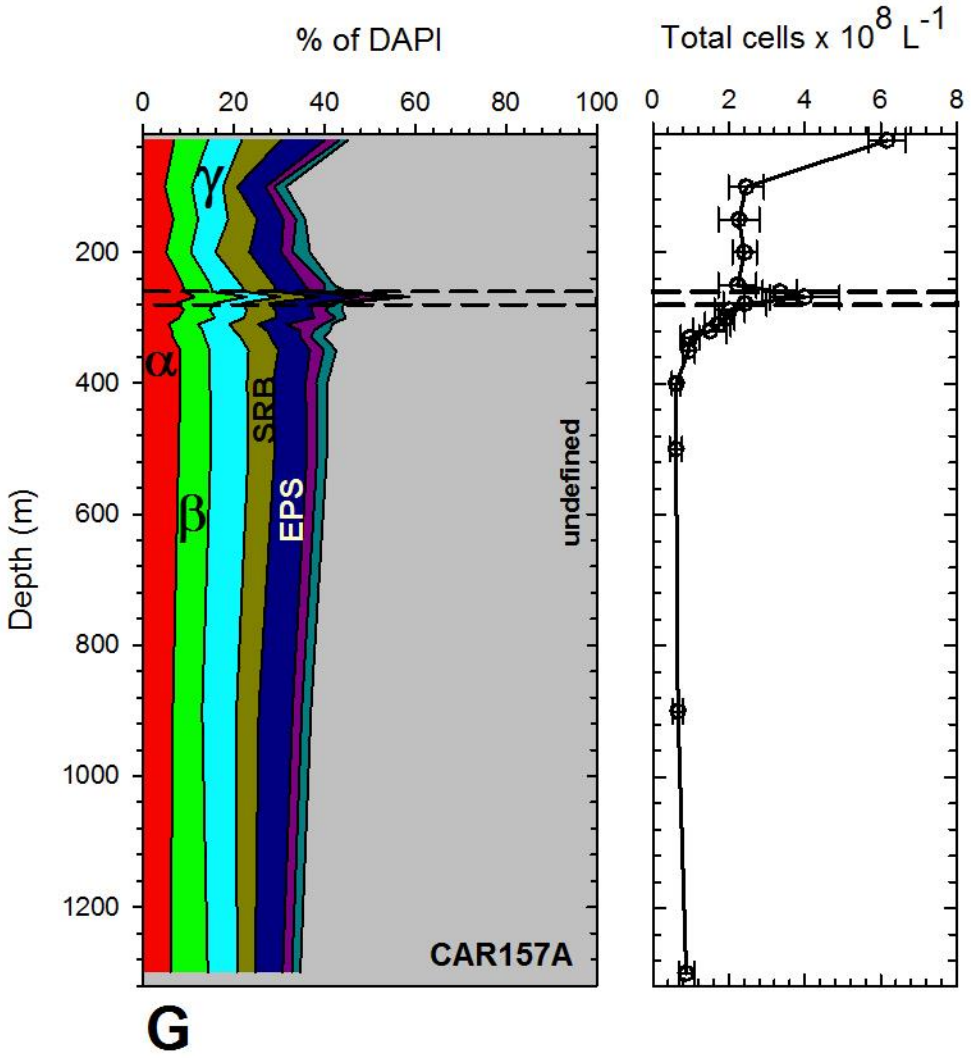
% of DAPI
Total cells x 10^8 L^-1
0
20
40
60
80
100
0
2
4
6
8
Depth (m)
200
400
600
800
1000
1200
α
β
γ
SRB
EPS
undefined
CAR157A
G

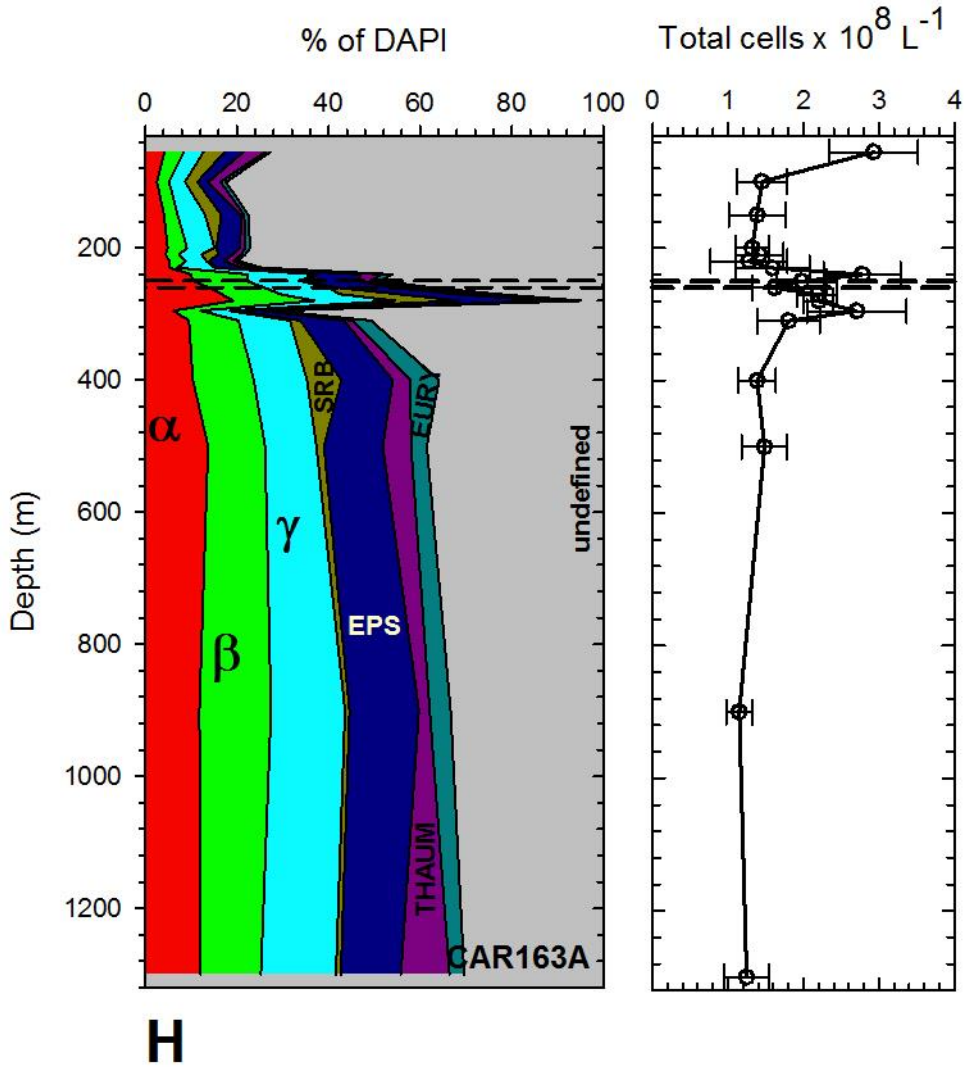
% of DAPI
Total cells x 10^8 L^-1
0
20
40
60
80
100
0
1
2
3
4
200
400
600
800
1000
1200
Depth (m)
α
β
γ
SRB
EUK
EPS
THAUM
undefined
CAR163A

H

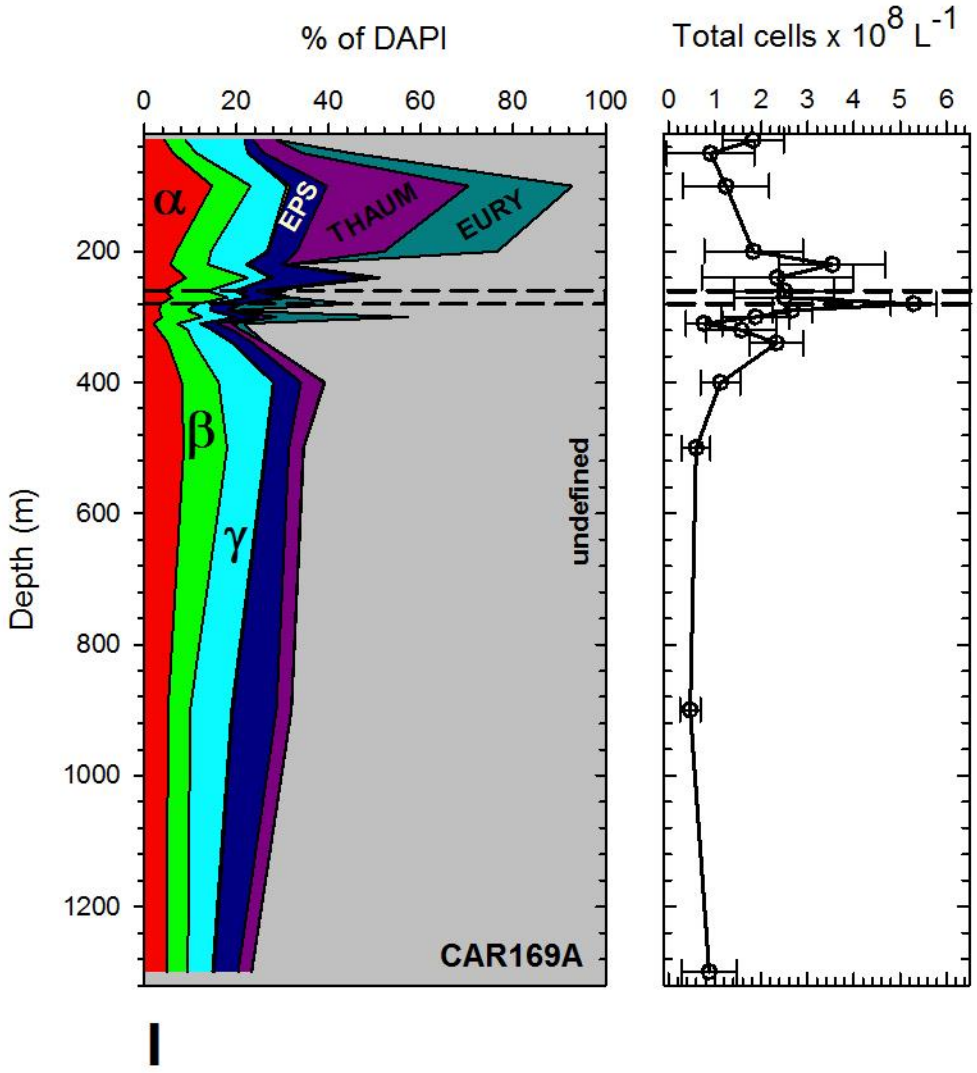
% of DAPI
Total cells x 10^8 L^-1
0
20
40
60
80
100
0
1
2
3
4
5
6
Depth (m)
200
400
600
800
1000
1200
α
β
γ
EPS
THAUM
EURY
undefined
CAR169A

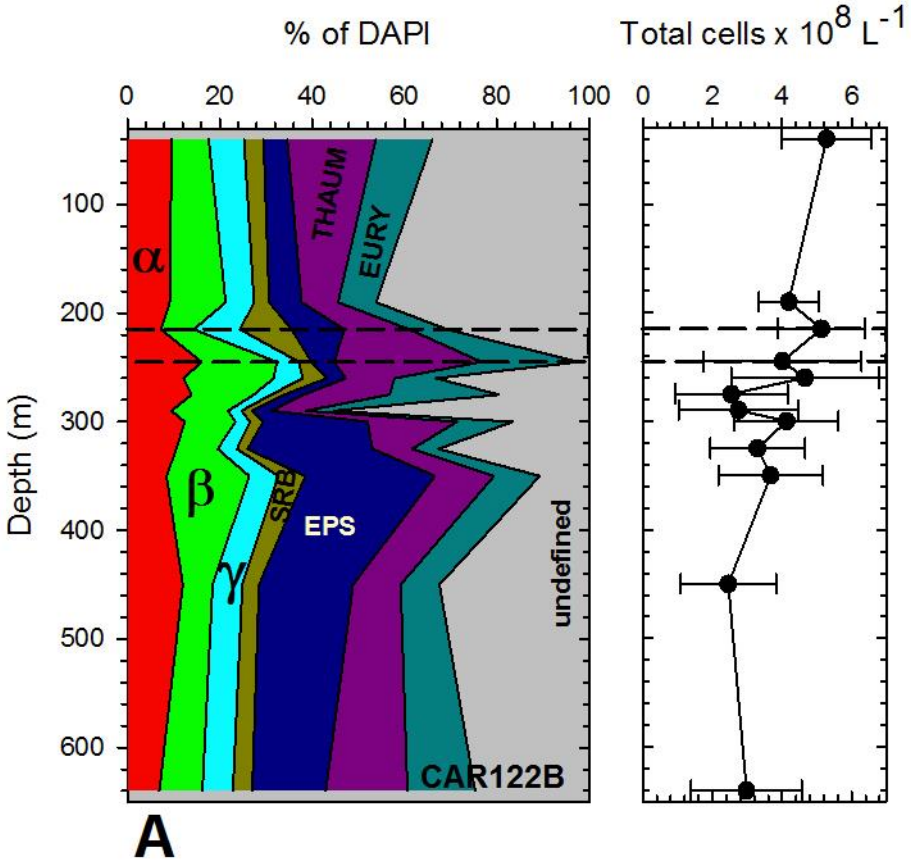
% of DAPI
Total cells x 10^8 L^-1
0
20
40
60
80
100
0
2
4
6
Depth (m)
100
200
300
400
500
600
α
β
γ
SRB
EPS
THAUM
EURY
undefined
CAR122B
A

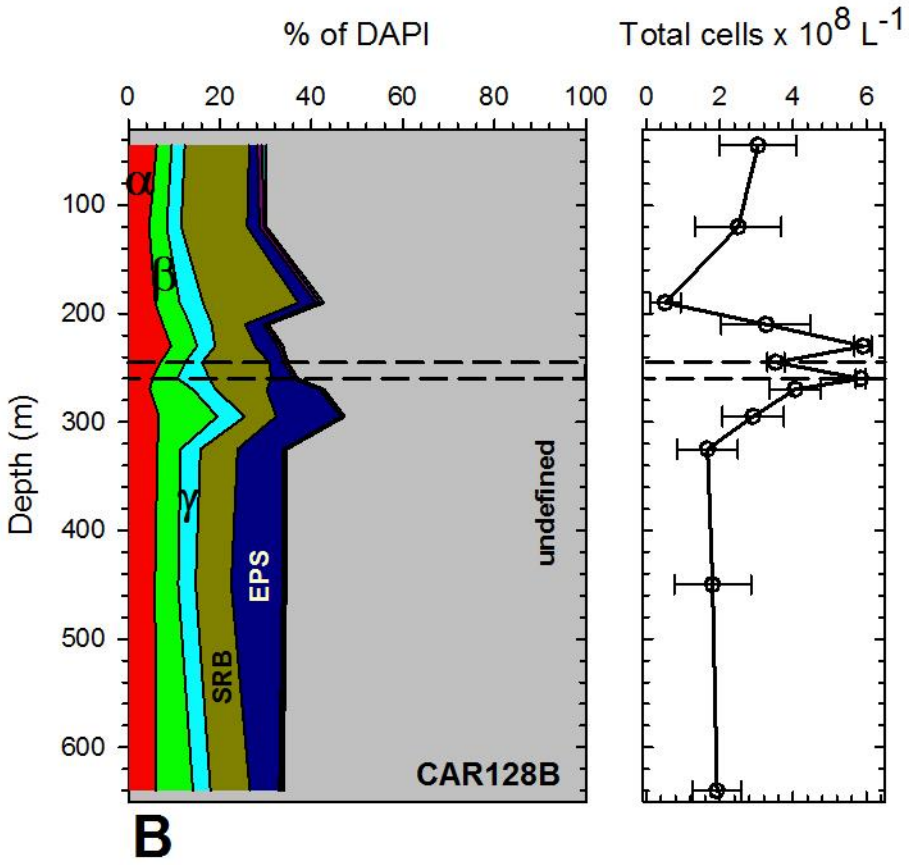
% of DAPI
Total cells x 10^8 L^-1
0
20
40
60
80
100
0
2
4
6
Depth (m)
100
200
300
400
500
600
α
β
γ
SRB
EPS
undefined
CAR128B
B

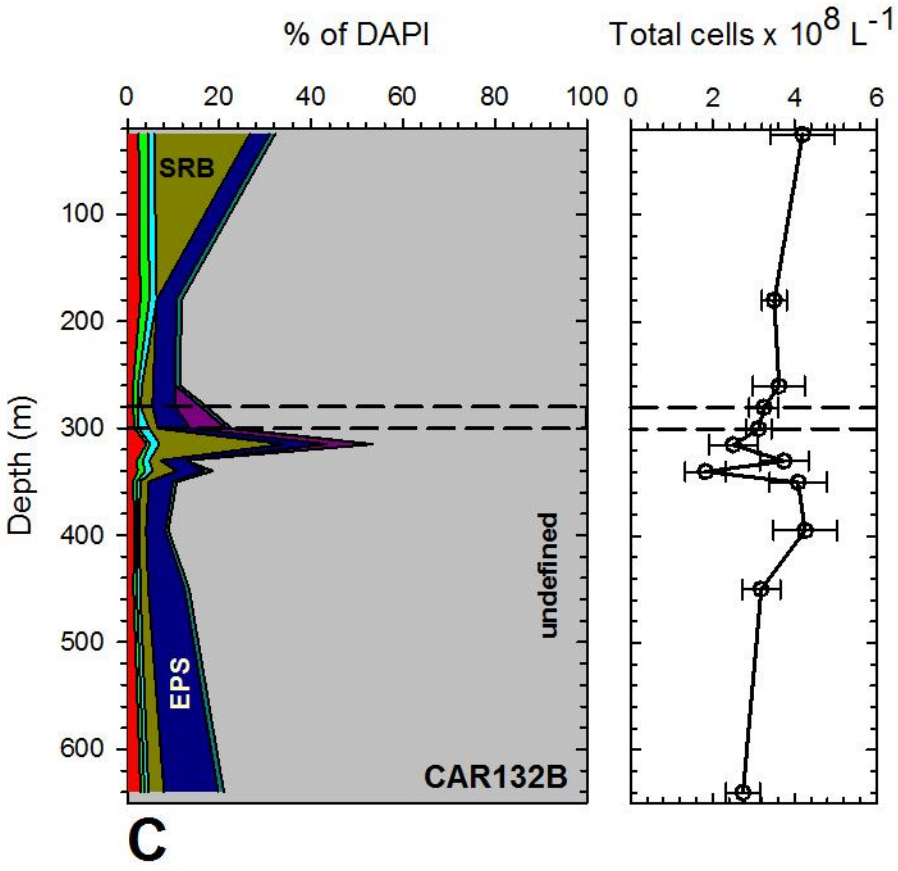

Figure 2.4. A-C. Vertical distributions of Bacteria and Archaea (left panel) and the total prokaryotic community (right panel) abundances at station B during three cruises. Abundances of clades are presented as percentages of the total prokaryotic community based on coincident DAPI-positive cell counts. Dotted lines depict upper and lower boundary of the suboxic layer ($O_2 < 2$ µM). Bacteria: α-proteobacteria, β-proteobacteria, γ-proteobacteria, ε-proteobacteria, sulfate-reducing bacteria (SRB) as representatives of δ-proteobacteria. Archaea: Thaumarchaeota and Euryarchaeota. Undefined fraction represents fraction of the prokaryotic community not captured by suite of selected probes. Error bars represent one standard deviation.

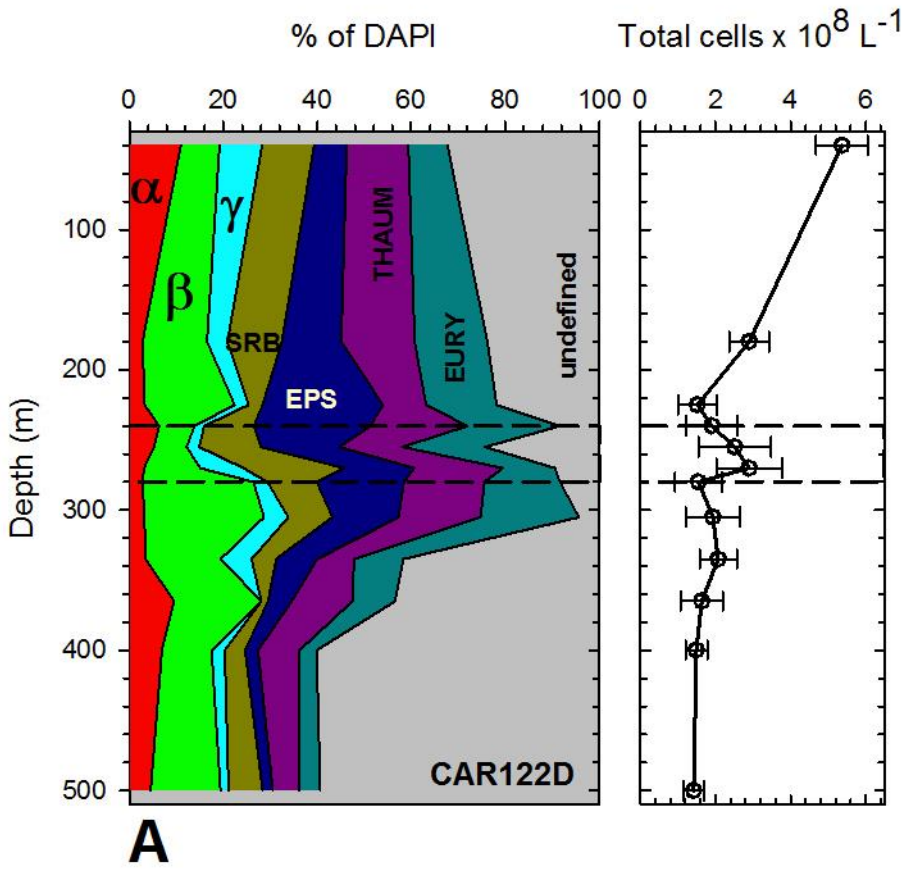
% of DAPI
Total cells x 10^8 L^-1
0
20
40
60
80
100
0
2
4
6
Depth (m)
100
200
300
400
500
α
β
γ
SRB
EPS
THAUM
EURY
undefined
CAR122D
A

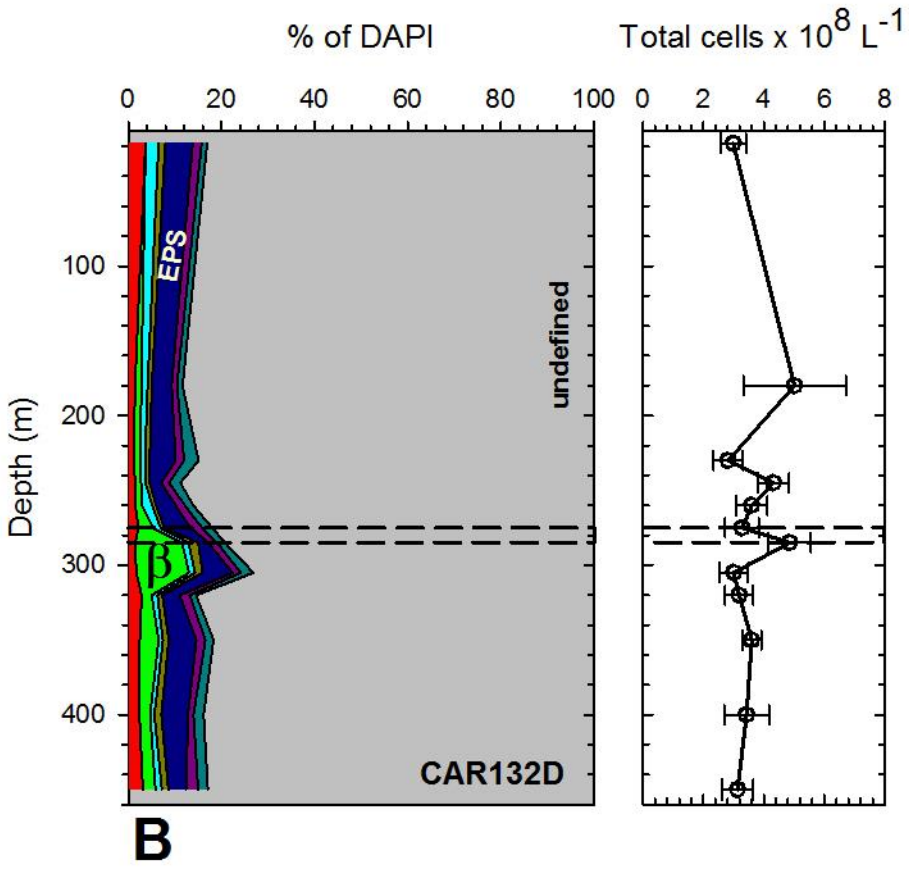

Figure 2.5. A-B. Vertical distributions of Bacteria and Archaea (left panel) and the total prokaryotic community (right panel) abundances at station D during two cruises. Abundances of clades are presented as percentages of the total prokaryotic community based on coincident DAPI-positive cell counts. Dotted lines depict upper and lower boundary of the suboxic layer (O_2 < 2 µM). Bacteria: α-proteobacteria, β-proteobacteria, γ-proteobacteria, ε-proteobacteria, sulfate-reducing bacteria (SRB) as representatives of δ-proteobacteria. Archaea: Thaumarchaeota and Euryarchaeota. Undefined fraction represents fraction of the prokaryotic community not captured by suite of selected probes. Error bars represent one standard deviation.

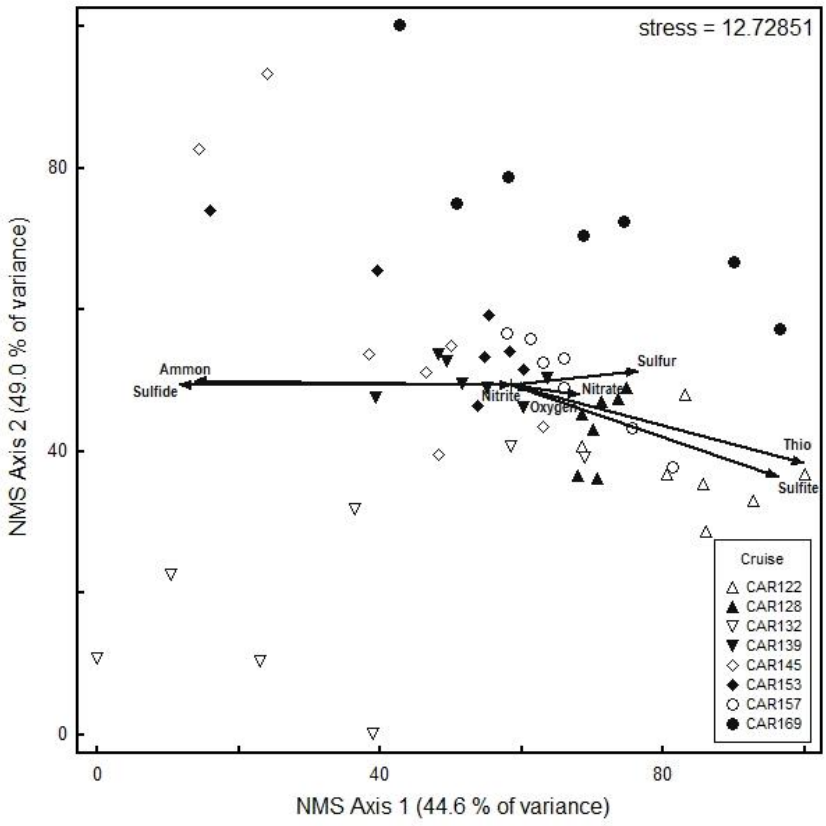

Figure 2.6. Non-parametric multidimensional scaling (NMS) ordination of all clades showing their distribution at seven depths within the redoxcline during each cruise at station A with a joint plot of environmental variables. Analysis performed on Bray-Curtis dissimilarities of transformed clades data.

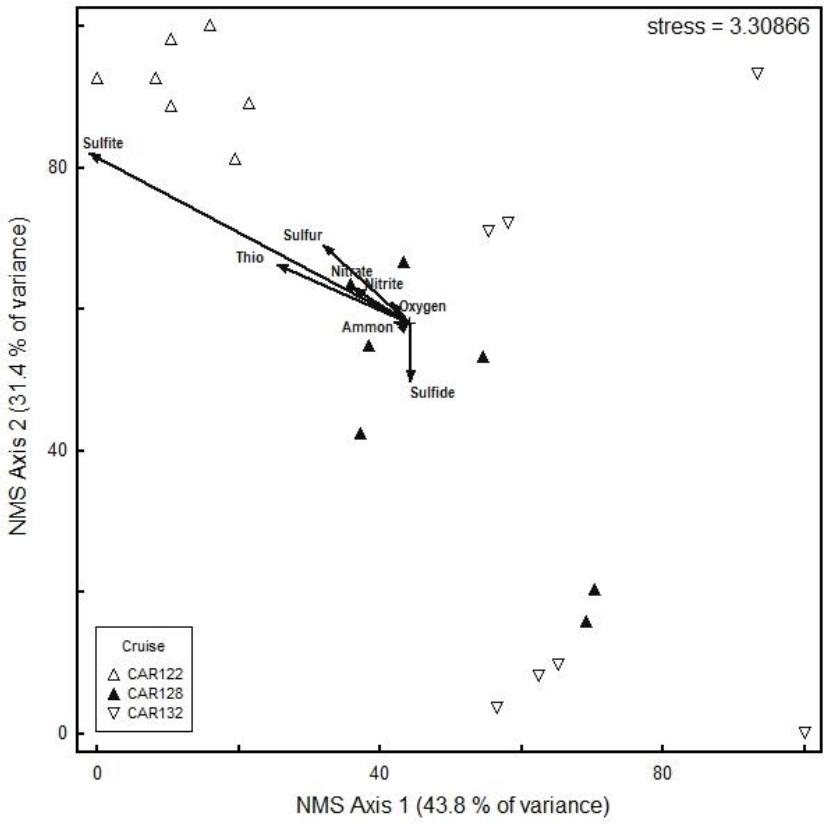

Figure 2.7. Non-parametric multidimensional scaling (NMS) ordination of all clades showing their distribution at seven depths during each cruise at station B. Analysis performed on Bray-Curtis dissimilarities of transformed clades data. Two axes with most variance for the 3-dimensional solution are presented with a join plot of the environmental variables.

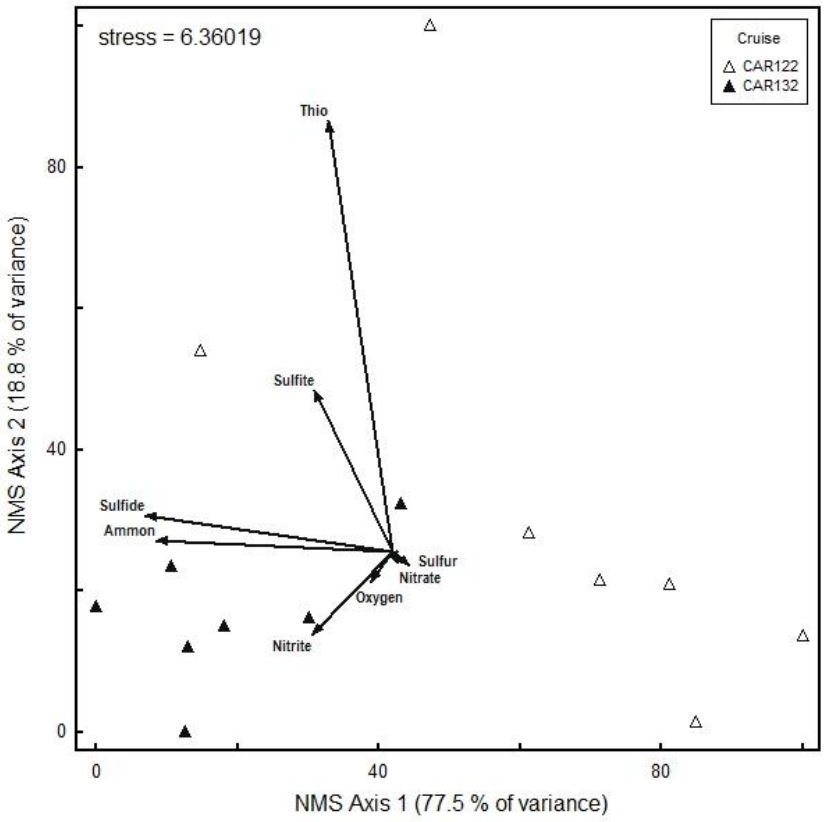

Figure 2.8. Non-parametric multidimensional scaling (NMS) ordination of all clades showing their distribution at seven depths during each cruise at station D with a joint plot of the environmental variables. Analysis performed on Bray-Curtis dissimilarities of transformed clades data.

Chapter 3

Top-down and bottom-up control of prokaryotic communities in the Cariaco Basin's redoxcline

1. Abstract

Effects of bacterivory and additions of selected reductants and oxidants on the total prokaryotic community and individual clades were investigated at two depths in the Cariaco's redoxcline during cruise CAR163 on Nov 5-6, 2009. At 250 m (upper boundary of the suboxic layer), abundance of the total prokaryotic community doubled in response to removal of grazers but did not respond to substrate additions indicating that grazing was the primary factor controlling prokaryotic abundance. At 260 m (depth of first appearance of sulfide), abundance of the total community did not increase in response to predator exclusion. However, the total community abundance increased after addition of H_2S/Mn(IV) or H_2S/NO_3^- in the absence of grazers indicating substrate or oxidant limitation. Among seven examined clades, α-proteobacteria were preferentially consumed by grazers in unamended control and in H_2S/Mn(IV) amended sample while removal of grazers resulted in ~ 60 % increase in abundance of this clade at 250 m. Abundances of γ-proteobacteria, β-proteobacteria and ε-proteobacteria increased by 30-40 % at 250 m and γ-proteobacteria and β-proteobacteria at 260 m in response to predator exclusion in unamended samples. Abundance of ε-proteobacteria increased in response to addition of H_2S/NO_3^- at both depths in the whole water and predator-excluded samples. Findings from this study indicate that protistan grazing can significantly affect the standing stock and composition of the prokaryotic community in the Cariaco's redoxcline. Further, enriching with selected substrates showed that releasing substrate limitation in the absence of grazers can significantly affect abundance of the total community and individual clades.

2. Introduction

Microbial communities are important components of pelagic food webs because they remineralize organic matter and thereby affect the cycling of carbon and inorganic nutrients (Pomeroy, 1974; Taylor, 1982; Azam et al., 1983). Mechanisms controlling standing stock of prokaryotes are of special importance because they affect the abundance, biomass and composition of prokaryotic communities (Thingstad and Lignell, 1997; Taylor, 1982; Sherr and Sherr, 2002). Among the most recognized mechanisms are bottom-up control of prokaryotic production by the availability of substrates such as organic matter and inorganic nutrients (Azam et al., 1983; Thingstad and Lignell, 1997; Thingstad, 2000) and top-down control of prokaryotic population size exerted by grazing activities mostly of heterotrophic protists (Taylor, 1982; Gasol, 1994; Sherr and Sherr, 2002). The size of prokaryotic communities can also be significantly affected by marine viruses and many studies have shown that mortality of prokaryotes due to viral lysis can be as high as due to grazing (Fuhrman and Noble, 1995; Fuhrman, 1999; Simek et al., 2001; Suttle, 2005). Previous study in the Cariaco showed that the vertical distributions of abundances of viral-like particles in the water column were very similar to those of prokaryotic cells indicating that viral-induced mortality can be an important factor controlling the bacterial standing stock as well (Taylor et al., 2003). However, the effects of viral lysis on the abundances of the total prokaryotic community and specific clades were outside the scope of this study. Numerous laboratory, mesocosm, and field studies have shown that the balance between controlling mechanisms depends mostly on the overall productivity of the investigated ecosystem and concluded that bottom-up control is more common in eutrophied waters while top-down control is more common in less eutrophic and oligotrophic waters (reviewed by Gasol, 1994; Gasol et al., 2002; Pernthaler, 2005). In marine pelagic waters, prokaryotes are subject to grazing mainly by heterotrophic phagotrophic flagellates generally ranging in size between 2 and 5 μm (Sherr and Sherr, 1987; McManus and Fuhrman, 1988; Pernthaler, 2005) and small heterotrophic ciliates of sizes < 20 μm (Sherr and Sherr, 1987; Epstein and Shiaris, 1992) . These phagotrophic grazers select their prey mainly based on size and physiological state, but other factors, such as motility of prey and chemical signatures have been shown to be important as well (Weisse, 2002; Pernthaler, 2005; Jurgens and Massana, 2008; Massana et al., 2009).

Mechanisms controlling prokaryotic communities are of special interest in the Cariaco Basin because of its unique biogeochemical settings and because of a general paucity of studies of such mechanisms in anoxic waters. Cariaco's waters are devoid of oxygen below depth of about 250 m but are characterized by an active microbial community with high chemoautotrophic activities which on occasions match or exceed those of primary producers (Taylor et al., 2001). Fluorescence in situ hybridization and studies of 16S and 18S rRNA gene sequences revealed diverse, dynamic, and distinct communities of Bacteria, Archaea, and protists occupying oxic, suboxic, and anoxic layers within the Cariaco Basin's redoxcline (Madrid et al., 2001; Stoeck et al., 2003; Lin et al., 2006, 2008; Edgcomb et al., 2011 a, b; Orsi et al., 2011). Elevated abundances of heterotrophic flagellates and ciliates coincide with peaks in prokaryotic activities and are usually observed in the vicinity of the oxic-anoxic interface (Taylor et al., 2001, 2006). Grazing impact on the total prokaryotic community and a few selected clades has been previously evaluated in the Cariaco Basin by Lin et al. (2007). Though substrate availability in the redoxcline has been shown to significantly influence the activities of the microbial communities, it is still not clear which electron donors and acceptors provide the most sustenance for the highly active microbes (Madrid et al., 2001; Taylor et al., 2001; Lin et al., 2007; Li et al., 2008). The goal of this study was to examine the effect of bacterivory on the size and composition of the prokaryotic community and the effect of additions of specific substrates on growth of the total community and selected clades at specific depths within the Cariaco's redoxcline.

3. Materials and methods

3.1. Grazer exclusion and amendment experiments

Replicate water samples were collected from two depths (250 m – upper boundary of the suboxic layer and 260 m – first appearance of sulfide) within the redoxcline for two types of treatments: whole water samples and filtered samples. Seawater samples were first withdrawn from Niskin bottles under N_2 pressure into 1 L glass dispensing bottles. Six replicate subsamples for whole water (unfiltered) treatments were withdrawn under N_2 pressure directly from the

dispensing bottle into 74 mL serum bottles. Then six replicate subsamples for predator-exclusion treatments were withdrawn under N_2 pressure from the same dispensing bottle into 74 mL serum bottles using an in-line polycarbonate filter (47 mm diameter, 2.0 µm pore size, GTTP type). Prefiltering through 2.0 µm polycarbonate filters was performed to exclude cells > 2 µm in size (bacterivorous grazers) but let most prokaryotes pass through. All subsamples were then sealed without headspace with butyl rubber septa. Two hundred milliliters of additional unfiltered seawater from the same depths were collected in replicate 50 mL Falcon tubes, preserved with 2 % borate-buffered formaldehyde (final concentration) and stored at 4°C for microscopy analysis in the lab.

Two replicate samples for each treatment were amended with combinations of 15 µM H_2S and 50 µM Mn(IV) (final concentration) or 15 µM H_2S and 50 µM NO_3^- (final concentration). Two replicate samples for each treatment without any additions served as unamended controls. All experimental samples were incubated immersed in seawater at 17 ± 2°C for 48 hours in the dark. After incubations, samples were preserved with 2 % borate-buffered formaldehyde (final concentration) and frozen overnight before further processing. After thawing, cells were captured on Millipore Isopore® Membrane filters (47 mm diameter, 0.2 µm pore size, GTTP type), rinsed with 10 mL of distilled water, dried, and stored in Petrislides® at -20˚C until further processing at Stony Brook University.

3.2. FISH and statistical analyses

All experimental samples were processed following standard oligo-FISH (for the domain Bacteria) and CARD-FISH (for Archaea) protocols as described in Pernthaler et al. (2001a) and Lin et al. (2006), respectively. Oligonucleotide probes and hybridization conditions employed in this study were as described in Chapter 2.

To assess the effect of prefiltration on the total prokaryotic community and grazer abundances, the following analyses were implemented. From the additional seawater samples collected in the field, 100 mL were filtered through black 0.8 µm polycarbonate membrane (25 mm diameter) for enumeration of grazers by staining with acridine orange and counting using epifluorescence microscopy at 630x total magnification. Another 100 mL were filtered through

2.0 µm polycarbonate filters (47 mm diameter) and stained with DAPI for enumeration of grazers and prokaryotes using epifluorescence microscopy at 630x and 1000x total magnification, respectively. The number of grazers captured on 2.0 µm filters was compared to the number of grazers captured on the 0.8 µm filters to determine what proportion of the total grazer cells escaped prefiltration and was present in filtered treatment samples. The number of prokaryotic cells on 2.0 µm filters was compared with the number of prokaryotic cells captured on 0.2 µm filters to determine what proportion of the total prokaryotic cells was retained on 2.0 µm filters.

FISH results at time of sampling (T_0) and after 48h incubations with added substrates in unfiltered and filtered subsamples were used to assess the changes in microbial community structure in response to grazing pressure, energy substrates and oxidants. Assuming exponential growth of microbes and substrate excess (non-limiting), first-order growth and loss rates (μ, d^{-1}), were calculated using the following equation:

$$\mu = \ln (N_1 / N_0) / (t),$$

where N_0 is the microbial abundance (cells L^{-1}) at the beginning of incubation, N_1 is the microbial abundance (cells L^{-1}) at the end of 48 h, and t is the time of incubation in days.

Removal rates (k, d^{-1}) by grazing for the total prokaryotic community and individual clades were calculated using the following equation:

$$k = \mu_f - \mu_w,$$

where μ_f is rate of change in filtered samples and μ_w is rate of change in whole water samples.

Differences between treatments in abundance and first-order growth and loss rates of the total prokaryotic community and specific clades were tested using a t-test at a significance level of $\alpha = 0.05$. All analyses were performed on duplicate samples using SigmaStat® version 3.5.

4. Results

4.1. Physico-chemical conditions in the redoxcline

Samples from discrete depths for measurements of O_2, H_2S, NO_3^-, total prokaryotic and flagellate abundances as well as microbial productivities were collected as part of semi-annual cruises of the CARIACO Ocean Time-Series study as described in Taylor et al. (2001) and Li et al. (2008). Results of these measurements are provided as background. During CAR163, oxygen concentrations decreased to below 2 µM at 250 m (upper boundary of the suboxic layer) while H_2S concentrations above 1 µM were detected at 260 m (lower boundary of the suboxic layer, depth of first appearance of sulfide). Nitrate concentrations decreased sharply to below 1 µM 10 m above the suboxic layer (at 240 m). Distinct peaks in chemoautotrophic productivity (between 5 and 9 µg C L^{-1} d^{-1}) were measured at the upper boundary of the suboxic layer (at 250 m) and 20 and 50 m below the oxic-anoxic interface (at 280 and 310 m, respectively). Heterotrophic productivity was much lower than chemoautotrophic production and reached a maximum of ~ 1 µg C L^{-1} d^{-1} at 240 m. A secondary peak in heterotrophic productivity at 270 m corresponded to a slight increase in oxygen concentration suggesting a recent intrusion of oxygenated water into the sulfidic zone and a sharp decline in chemoautotrophic productivity. Elevated flagellate cell numbers corresponded to elevated chemoautotrophic and heterotrophic productivities at 250 m (Fig. 3.1).

4.2. Methodological considerations

Prefiltration of seawater through a 2.0 µm polycarbonate filter using the in-line filtering system in the present study resulted in exclusion of at least 89 and 85 % of grazers at 250 and 260 m, respectively. The size of grazers was not determined in this study but Lin et al. (2007) estimated that the size of more than 93 % of grazers varied between 2 and 7 µm and only a small portion of grazers of sizes < 2 µm escaped prefiltration . Therefore, up to 15 % of initial grazers might have been present in the exclusion treatments. Prefiltration allowed passage of at least 85 and 83 % of total bacterial cells at 250 and 260 m, respectively. I note that the effect of prefiltration was not evaluated for individual clades.

4.3. Effects of predator exclusion and additions of energy substrates and oxidants on total prokaryotic community

Distinct responses of the total prokaryotic community were observed between whole water treatments and grazer-excluded treatments after 48 hr incubations. Net growth rates of the total community in unamended whole water sample were almost three times higher (1.6 d^{-1}) at 260 m than at 250 m (0.6 d^{-1}) and additions of H_2S/Mn(IV) and H_2S/NO_3^- significantly stimulated community growth only at 250 m (t-test, $p < 0.05$) (Figs. 3.2 and 3.3). In response to removal of grazers, community abundance increased 7-fold and growth rate doubled in unamended control at 250 m. In samples amended with H_2S/Mn(IV) and H_2S/NO_3^- abundance of the total community decreased by 30-40 % and net growth rates were 1.5-3 times lower than in unamended control in the absence of grazers (Fig. 3.2). At 260 m, community size increased significantly in samples amended with H_2S/Mn(IV) (30 %) and H_2S/NO_3^- (46 %) compared to unamended controls but only in the absence of grazers (t-test, $p < 0.05$) (Fig. 3.3). Removal rates by grazing were highest in unamended controls at 250 m (0.8 d^{-1}) and in samples amended with H_2S/NO_3^- at 260 m (0.1 d^{-1}) (Table 3.1).

4.4. Response of specific clades to predator exclusion and additions of energy substrates and oxidants

Variations in abundance of the seven clades examined in this study were more pronounced at 250 m than at 260 m. At 250 m, α-proteobacteria abundances significantly declined in unamended whole water (~ 8 %) and in whole water samples amended with H_2S/Mn(IV) (31 %) after 48 hr incubations, at rates of -0.1 and -0.6 d^{-1}, respectively (t-test, $p < 0.05$). Abundances of this clade increased by ~ 60 % when released from grazing pressure at rates of 0.4 d^{-1} in both, unamended control and sample amended with H_2S/Mn(IV) (Fig. 3.2). Addition of H_2S/NO_3^- stimulated growth of α-proteobacteria (15 % increase) in unfiltered samples but removal of grazers did not result in higher abundances of this clade (Fig. 3.2). At 260 m, growth rates of α-

proteobacteria increased in filtered samples by 36 and 50 % in H_2S/Mn(IV) and H_2S/NO_3^- amendments, respectively compared to the unamended control (Fig. 3.3). Removal rates of α-proteobacterial cells were highest in sample amended with H_2S/Mn(IV) (0.9 d^{-1}) and in unamended control (0.5 d^{-1}) at 250 m and lowest (-0.3 d^{-1}) in unamended control at 260 m (Table 3.1).

β-proteobacteria, γ-proteobacteria and ε-proteobacteria grew at similar rates (~ 0.3-0.4 d^{-1}) in unamended whole water samples and their abundances increased by about 10-30 % in response to removal of grazers (Figs. 3.2 and 3.3). At 250 m, addition of H_2S/Mn(IV) slightly stimulated growth of β-proteobacteria in whole water samples but not in filtered samples relative to unamended control. Addition of H_2S/NO_3^- stimulated growth of ε-proteobacteria in whole water and filtered samples (t-test, $p < 0.05$) compared to unamended controls. At 260 m, addition of H_2S/NO_3^- stimulated growth of ε-proteobacteria and β-proteobacteria in whole water sample, but only ε-proteobacteria in filtered sample (t-test, $p < 0.05$) (Fig. 3.3). Removal rates of β-proteobacteria were highest in unamended sample (0.2 d^{-1}) and lowest (-0.2 d^{-1}) in sample amended with H_2S/Mn(IV) at 250 m (Table 3.1). Removal rates of ε-proteobacteria were in general an order of magnitude lower than for other clades (Table 3.1). γ-proteobacteria were not stimulated by any additions in whole water or filtered samples and removal rates of their cells by grazing varied between 0.1 and 0.2 d^{-1} in most samples (Table 3.1).

Sulfate-reducing δ-proteobacteria (SRB), Thaumarchaeota and Euryarchaeota in general grew at rates 2-3 times higher (> 0.9 d^{-1}) than other clades in unamended controls and in samples amended with H_2S/Mn(IV) and H_2S/NO_3^-. SRB abundances were ~ 16 % higher in predator-excluded sample amended with H_2S/NO_3^- at 250 m compared to whole water sample amended with H_2S/NO_3^-. However, addition of H_2S/NO_3^- did not stimulate growth of SRB when compared to whole water and filtered water unamended controls at 250 m (Fig. 3.2). At 260 m, SRB abundances declined by 44 % in whole water sample amended with H_2S/Mn(IV) compared to unamended sample and increased 9.5-fold in response to predator removal (Fig. 3.3). In the remaining samples, abundances of SRB were maintained at high numbers, generally 2-3-fold higher than those of other clades in most samples, but removal rates of this clade were similar to those for β-proteobacteria and γ-proteobacteria (Table 3.1). Abundances of Thaumarchaeota increased in response to additions of H_2S/Mn(IV) and H_2S/NO_3^- at 250 m (14-15 %) and at 260 m (63 %) in whole water samples (t-test, $p < 0.05$). In the absence of grazers, Thaumarchaeota

grew faster in samples amended with H_2S/NO_3^- than in unamended controls at both depths and in sample amended with H_2S/Mn(IV) at 250 m (t-test, $p < 0.05$). Removal rates of thaumarchaeal cells were highest (0.3 d^{-1}) in unamended control at 260 m (Table 3.1). Euryarchaeota growth was stimulated only by addition of H_2S/Mn(IV) in filtered samples at 250 m (t-test, $p < 0.05$) (Fig. 3.2). Removal rates of euryarchaeal cells by grazing were highest (0.4 d^{-1}) in sample amended with H_2S/Mn(IV) at 250 m (Table 3.1).

5. Discussion

5.1. Impact of grazing on the total prokaryotic community and selected clades

Significant shifts in the total prokaryotic community and individual clades in response to grazers and added substrates were observed after a relatively short incubation time. Total community growth rates doubled in response to removal of grazers at 250 m while at 260 m that effect was not observed. Additions of H_2S/Mn(IV) and H_2S/NO_3^- did not stimulate community growth in the absence of grazers at 250 m. These findings suggest that at this depth prokaryotic community size was affected more by grazing than by substrate availability. Previous studies in the Cariaco showed that elevated abundances of bacterivorous grazers coincided with elevated prokaryotic activities but not necessarily their abundances (Taylor et al., 2001, 2006). Indeed, during CAR163, at 250 m, elevated abundances of grazers coincided with elevated heterotrophic and chemoautotrophic activities and these observations suggest active bacterivory.

It has been shown that bacterivory can depend more on the quality than the quantity of prey (Epstein and Shiaris, 1992). Bacterivorous grazers tend to feed selectively on prey of specific cell size and more importantly favor bacteria with high nucleic acid content (indicator of high metabolic activity) over slower growing, dormant, or dead cells (Massana et al., 2009). Such selective feeding behavior of grazers might explain preferential consumption of α-proteobacteria and possibly SRB in this study. Abundances of α-proteobacteria declined significantly in unamended samples and even more in those amended with H_2S/Mn(IV) in the presence of grazers, whereas, in the absence of grazers, their abundances increased by ~ 60 %. Abundances of SRB declined by > 40 % in whole water samples amended with H_2S/Mn(IV) and increased

more than 9-fold in response to predator exclusion at 260 m only. Abundances of other clades such as β-proteobacteria, ε-proteobacteria, and Euryarchaeota increased in the absence of grazers in unamended control as well but not as much as those of α-proteobacteria indicating that the former clades were less controlled by bacterivory possibly due to their slower growth which may have been limited by substrate availability. This conclusion is supported by the insignificant to small stimulation of ε-proteobacteria, β-proteobacteria, and γ-proteobacteria, in samples amended with H_2S/Mn(IV) or H_2S/NO_3^- in the absence of grazers. In addition to substrate limitation, slow growth of these prokaryotes might be a manifestation of a "deliberate" adaptive behavior of maintaining cell abundances below some threshold to avoid grazing. For example, a study of abundances and activities of four bacterial clades in the Delaware estuary showed that clades which contributed less than 15 % to the total community could experience reduced grazing and grow larger while more abundant clades regardless of cell sizes could be preferentially grazed (Cottrell and Kirchman, 2004).

Thaumarchaeota, Euryarchaeota and sulfate-reducing δ-proteobacteria usually have minority representation in the Cariaco community compared to other clades and their very high abundances in most incubated samples might indicate that these clades grow particularly well in confinement most probably by outcompeting other clades for substrates. Similar behavior for bacteria detectable at low abundances in situ but dominating in microcosms has been observed in other settings (Eilers et al., 2000; Schafer et al., 2000; Pernthaler et al., 2001b).

5.2. Impact of substrate availability and grazing pressure on carbon cycling

Protistan bacterivory is an important source of bacterial mortality in oxygenated aquatic environments and therefore can significantly alter the abundance, biomass and composition of microbial communities and indirectly affect export of organic carbon (Taylor, 1982; Sherr and Sherr, 2002; Pernthaler et al., 2005; Jurgens and Massana, 2008). Recent advances in high-throughput sequencing revealed relatively high diversity of protists in the anoxic Cariaco Basin (Edgcomb et al., 2011a, b; Orsi et al., 2011), Framvaren Fjord (Behnke et al., 2011) as well as in the seasonally anoxic Saanich Inlet (Orsi et al., 2012). However, the impact of protistan grazing on bacterial communities and carbon cycling in oxygen minimum zones and anoxic pelagic waters is very poorly known. Consistent with previous observations by Lin et al. (2007), results

from the present study indicate that bacterivory has a significant effect on abundances and composition of the prokaryotic community in the Cariaco's redoxcline. Findings from my study indicate that bacterivory was more pronounced at the depth where the highest heterotrophic and chemoautotrophic activities were measured. At 250 m, grazing had a significant impact on abundance of the total community and additions of H_2S/Mn(IV) or H_2S/NO_3^- did not stimulate accumulations of prokaryotes in the absence of grazers. At this depth, grazers preferentially fed on α-proteobacteria which have been shown to be heterotrophic in this system (Lin et al., 2007). Abundances of γ-proteobacteria and ε-proteobacteria, which have been shown to be dominant chemoautotrophs in other pelagic redoxclines (Glaubitz et al., 2009; Walsh et al., 2009; Zaikova et al., 2010; Grote et al., 2013), increased in response to predator exclusion but to a lesser degree than α-proteobacteria, and only growth of ε-proteobacteria was stimulated by ~ 10 % by additions of H_2S/NO_3^- (t-test, $p < 0.05$). This suggests that activities of grazers can to some extent regulate the community size and composition in the redoxcline by selective feeding on specific bacterial clades which in turn might affect the balance between heterotrophic and chemoautotrophic productivities. However, whether grazing or substrate availability affects heterotrophic clades more than chemoautotrophic clades in the Cariaco Basin remains to be evaluated in the future.

6. Conclusions

This study demonstrated responses of major bacterial and archaeal clades to predator removal as well as to additions of selected electron donors and acceptors. In general, changes in abundance of the total prokaryotic community were dominated by bacterivory at upper boundary of the suboxic layer (250 m) where highest prokaryotic activities were measured. Removal of grazers had the most significant effect on abundances of α-proteobacteria at that depth, but abundances of β-proteobacteria, γ-proteobacteria and ε-proteobacteria also increased in predator-excluded samples albeit much less than those of α-proteobacteria. Further, at depth of first appearance of sulfide (260 m) additions of H_2S/Mn(IV) and H_2S/NO_3^- significantly stimulated growth of the prokaryotic community in the absence of grazers indicating substrate or oxidant limitation. Thus, findings from this study indicate that the balance between bottom-up and top-

down controlling mechanisms affects the variations in size, composition and growth of the total prokaryotic community and even more specifically individual clades and can have a significant influence on cycling of carbon, sulfur, nitrogen, and metals in the Cariaco Basin's redoxcline.

Table 3.1. Removal rates (k, d^{-1}) by grazing for the total prokaryotic community (DAPI) and individual clades. Control - unamended samples, A1 - samples amended with 15 µM H_2S and 50 µM Mn(IV) (final concentration), A2 - samples amended with 15 µM H_2S and 50 µM NO_3^- (final concentration). ALF – α-proteobacteria, BET – β-proteobacteria, GAM – γ-proteobacteria, SRB - sulfate-reducing δ-proteobacteria, EPS - ε-proteobacteria, THAUM – Thaumarchaeota, EURY – Euryarchaeota.

Depth (m)	Sample	DAPI	ALF	BET	GAM	SRB	EPS	THAUM	EURY
250	Control	0.8	0.5	0.2	0.2	0.0	0.0	-0.1	0.1
250	A1	0.0	0.9	-0.2	0.0	-0.1	0.1	-0.1	0.4
250	A2	-0.7	-0.1	0.0	0.0	0.2	0.0	0.1	-0.1
260	Control	-0.9	-0.3	0.1	0.1	0.0	0.0	0.3	0.0
260	A1	-0.4	-0.1	0.0	0.1	1.1	0.0	-0.3	0.0
260	A2	0.1	0.0	-0.1	0.0	-0.1	0.0	0.0	-0.1

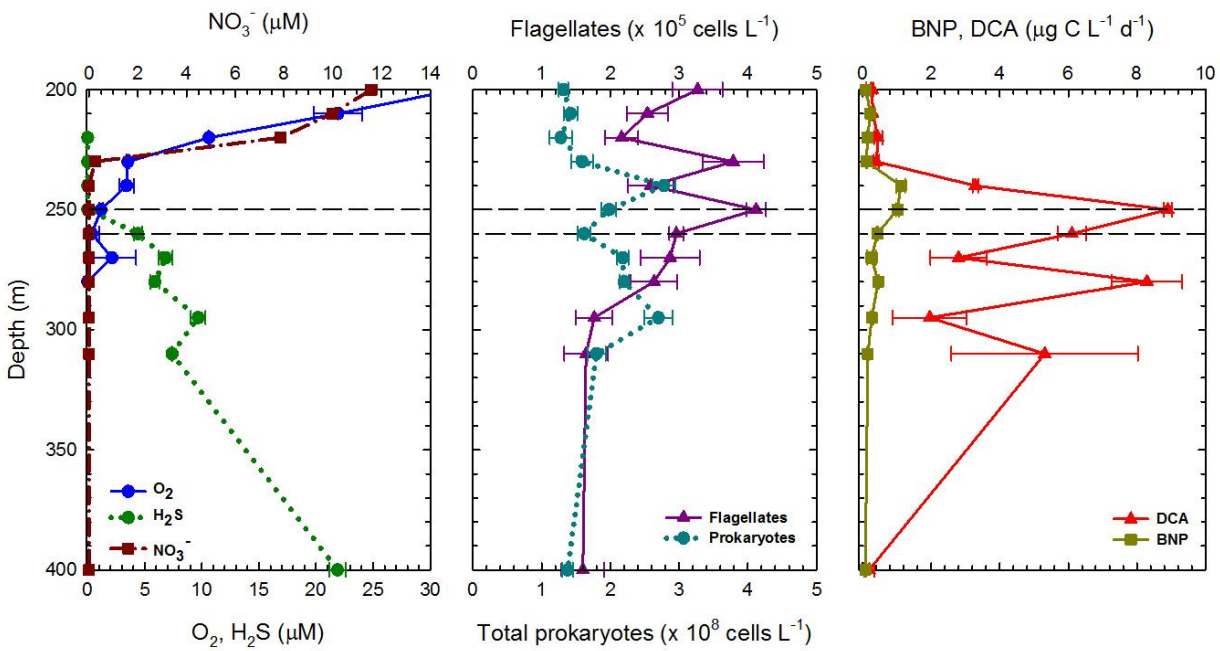

Figure 3.1. Vertical distributions of selected electron donors and acceptors, heterotrophic (BNP) and chemoautotrophic (DCA) productivities, abundance of total prokaryotic community and heterotrophic flagellates during cruise CAR163 (Nov. 5-6, 2009). The horizontal dashed lines represent the upper and lower boundary of the suboxic layer. Error bars represent one standard deviation. In some profiles standard deviation is too small to be visible. Standard deviation not available for nitrate. Data provided by G.T. Taylor, M.I. Scranton, Y. Astor, K. Fanning.

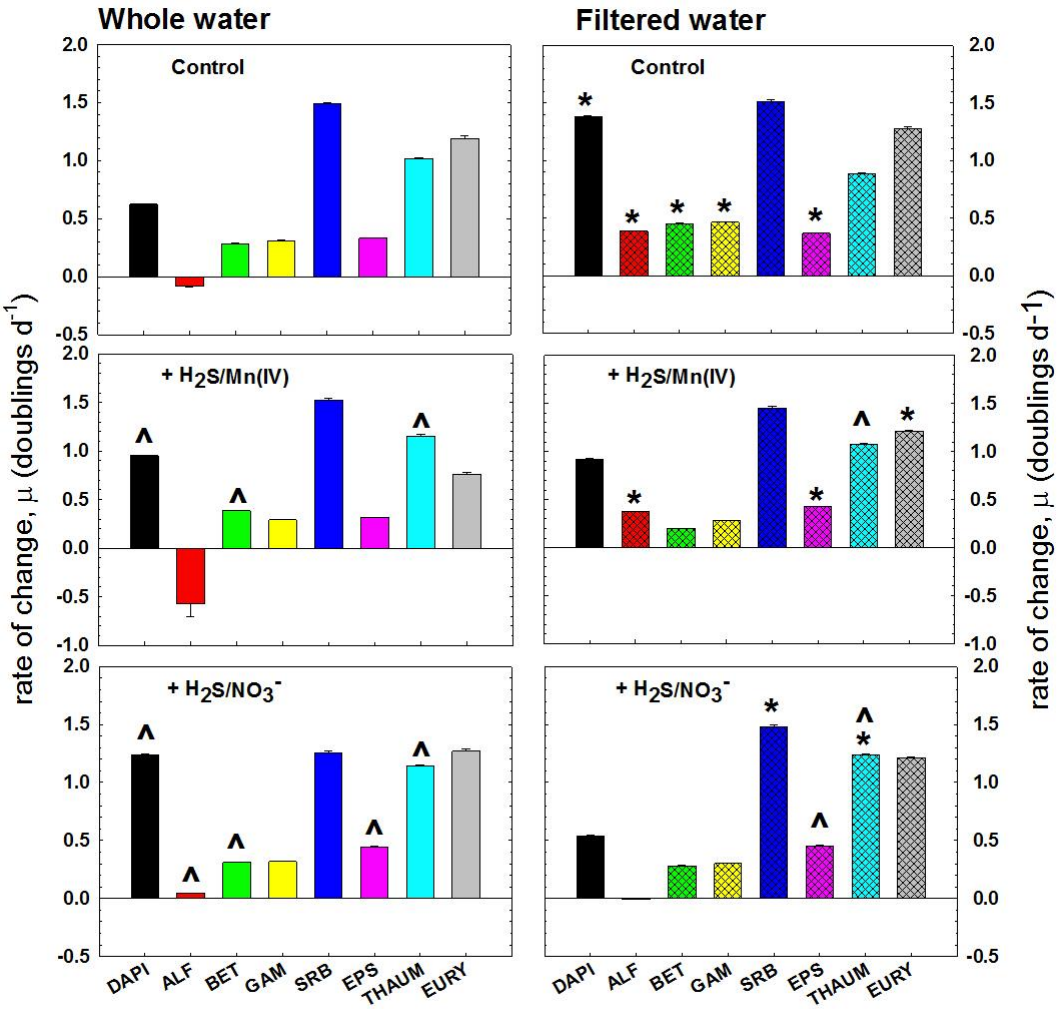

Figure 3.2. First order rates of change, μ (d^{-1}) in abundances of the total prokaryotic community (DAPI) and specific clades during CAR163 at 250 m in whole water treatments (left panels) and filtered water treatments (right panels) after 48 h incubations. Control - unamended samples, + H_2S/Mn(IV) - samples amended with 15 μM H_2S and 50 μM Mn(IV) (final concentration), + H_2S/NO_3^- - samples amended with 15 μM H_2S and 50 μM NO_3^- (final concentration). ALF – α-proteobacteria, BET – β-proteobacteria, GAM – γ-proteobacteria, SRB - sulfate-reducing δ-proteobacteria, EPS - ε-proteobacteria, THAUM – Thaumarchaeota, EURY – Euryarchaeota. Error bars represent standard error; ***** statistically significant increase between whole water and filtered water treatments; ^ statistically significant increase between unamended control and amended sample.

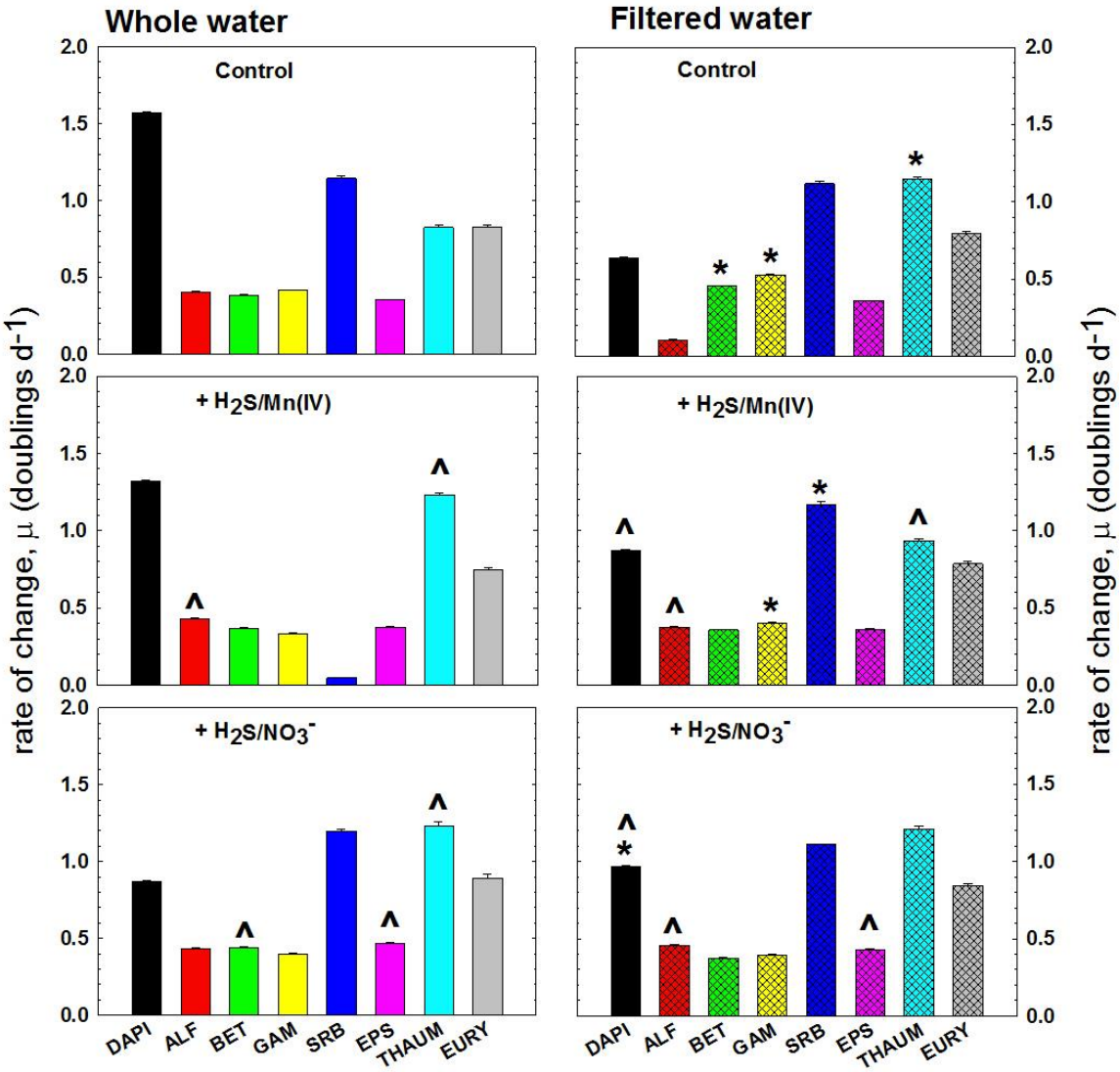

Figure 3.3. First order rates of change, μ (d^{-1}) in abundances of the total prokaryotic community (DAPI) and specific clades during CAR163 at 260 m in whole water treatments (left panels) and filtered water treatments (right panels) after 48 h incubations. Control - unamended samples, + H_2S/Mn(IV) - samples amended with 15 μM H_2S and 50 μM Mn(IV) (final concentration), + H_2S/NO_3^- - samples amended with 15 μM H_2S and 50 μM NO_3^- (final concentration). ALF – α-proteobacteria, BET – β-proteobacteria, GAM – γ-proteobacteria, SRB - sulfate-reducing δ-proteobacteria, EPS - ε-proteobacteria, THAUM – Thaumarchaeota, EURY – Euryarchaeota. Error bars represent standard error; ***** statistically significant increase between whole water and filtered water treatments; ^ statistically significant increase between unamended control and amended sample.

Chapter 4

Quantification of chemoautotrophs by microautoradiography combined with fluorescence in situ hybridization (MAR-FISH)

1. Abstract

Chemoautotrophic activities of major prokaryotic clades in the Cariaco Basin's redoxcline were investigated in May 2010 using microautoradiography combined with FISH (MAR-FISH). ^{14}C-bicarbonate assimilating prokaryotic cells accounted for up to 26 % of the total community in the three depths examined. Between 44 and 50 % of all γ-proteobacterial cells detected by FISH exhibited active uptake of ^{14}C-bicarbonate. To determine what energy substrates and oxidants fueled chemoautotrophic activities, duplicate samples were amended with combinations of H_2S/Fe(III) or $S_2O_3^{2-}$/NO_3^-. γ-proteobacteria, ε-proteobacteria and Thaumarchaeota assimilated ^{14}C-bicarbonate in incubations amended with H_2S/Fe(III) and accounted for ~ 14, 91 and 80 % of probe-positive cells detected by FISH, respectively. In incubations amended with $S_2O_3^{2-}$/NO_3^-, only active ε-proteobacteria were detected and accounted for up to 25 % of probe-positive cells detected by FISH. These findings indicate that the active chemoautotrophic community in the Cariaco's redoxcline appears to be confined to three clades. Provision of excess substrates showed that at least some of the active chemoautotrophs utilized H_2S and $S_2O_3^{2-}$ as reductants, and may have used NO_3^- and iron oxide as oxidants.

2. Introduction

The activity of chemoautotrophs is hypothesized to play an important role in biogeochemical cycles of carbon, sulfur, and nitrogen in many pelagic redoxclines, e.g., the Cariaco Basin (Taylor et al., 2001, 2006; Li et al, 2008), the Baltic Deeps (Labrenz et al., 2005; Grote et al., 2007), the Black Sea (Lam et al., 2007; Grote et al., 2008), the seasonally anoxic Saanich Inlet, a fjord (Walsh et al., 2009; Zaikova et al., 2010), and oxygen minimum zones off Chile and Peru (Canfield et al., 2010; Lam et al., 2009). Highest inorganic carbon fixation rates are usually measured below the oxic-anoxic interface in the Cariaco Basin, the Baltic Deeps, and the Black Sea (Taylor et al., 2001; Labrenz et al., 2005; Grote et al., 2008) and chemoautotrophic

production in the Cariaco's redoxcline can correspond to between 10 and 333 % of the primary production in the surface waters (Taylor et al., 2001). In the permanently anoxic Cariaco Basin, sulfide, intermediate sulfur species (sulfite, thiosulfate, and elemental sulfur), nitrate and metal oxides, such as manganese and iron, are implicated as the primary substrates and oxidants that fuel chemoautotrophic activity (Taylor et al., 2001).

Culture-independent studies of the Cariaco's prokaryotic communities by Madrid et al. (2001) and Lin et al. (2006) have revealed the prevalence of ε- and β-proteobacteria in the redoxcline at or near depths where chemoautotrophic productivity peaked. My FISH surveys of the prokaryotic community structure showed prevalence of ε- and β-proteobacteria in the redoxcline sampled in most of the investigated cruises (on average 15 and 10 % of the total community, respectively), but other clades, such as γ-proteobacteria and Thaumarchaeota were on occasion elevated as well (Chapter 2). Abundances of ε- and β-proteobacteria clades correlated with intermediate sulfur and nitrogen species, indicating the importance of these environmental variables in shaping the microbial community structure. Further, Li et al. (2008) found significant positive correlations between chemoautotrophic productivity and elemental sulfur concentrations in the Cariaco's redoxcline and hypothesized that the latter might be the end product of biological H_2S oxidation at the expense of Mn or Fe oxidants. Moreover, incubations amended with intermediate sulfur species stimulated chemoautotrophic productivity by 2 to > 100-fold depending on specific substrate and depth (Taylor et al., 2001, 2006).

Metabolically active cells can be identified using microautoradiography combined with FISH (MAR-FISH) (Lee et al., 1999; reviewed in Nielsen and Nielsen, 2005). This method has been successfully employed in ecophysiological studies of bacteria present in activated sludge in wastewater treatment plants (Daims et al., 2001; Nielsen et al., 2003), enrichment reactors (Ginige et al., 2004), the Delaware Estuary (Cottrell and Kirchman, 2004), as well as in diverse marine environments (Teira et al., 2004; Lin et al., 2007, Grote et al., 2008; Jost et al., 2008). In a previous Cariaco Basin study, MAR-FISH was successfully applied to enumerate heterotrophic clades assimilating ^{3}H-labeled leucine as a substrate (Lin et al., 2007). However, activity of specific chemoautotrophic clades has not been so far examined. Therefore, the goal of this study was to enumerate specific bacterial and archaeal clades that assimilate dissolved inorganic carbon (^{14}C-labeled bicarbonate).

3. Materials and Methods

3.1. Sample collection

During the CAR169 (May 6-7, 2010) cruise to the CARIACO Ocean Time-Series station, replicate water samples were collected from three discrete depths (300, 310, and 320 m) in the anoxic layer. Seawater was first withdrawn from Niskin bottles to 1 L dispensing glass bottle under N_2 pressure to avoid oxygenation. Then subsamples for experimentation were dispensed directly from the dispensing bottle into 42 mL glass stopper bottles under N_2 pressure and allowed to overflow for a few seconds. Duplicate samples were amended with 200 µl of ^{14}C-bicarbonate (pH 7.5, 20 µCi L^{-1} final concentration) and combinations of H_2S/Fe(III) (15 and 50 µM final concentration, respectively) or $S_2O_3^{2-}$/NO_3^- (50 µM final concentration each). Samples amended with ^{14}C-bicarbonate alone served as unamended controls. All samples were sealed without headspace and incubated for about 18 h immersed in seawater at 17 ± 2 ºC in the dark. Incubations were terminated by addition of 2% (final concentration) borate-buffered formaldehyde. Duplicate negative control samples were collected at one depth, amended with ^{14}C-bicarbonate and 2% buffered formaldehyde, and incubated along with the other samples. Following termination, all samples were transferred to 50 mL Falcon tubes and frozen at -20˚C overnight to minimize leakage and loss of radiotracer from active cells (Nielsen et al., 2003). After thawing, cells were captured on Millipore Isopore® Membrane filters (47 mm diameter, 0.2 µm pore size, GTTP type), rinsed with 10 mL of distilled water, dried, and stored in Petrislides® at -20˚C until further processing. Samples for evaluation of community structure (by FISH) at the time of sampling from the same depths were collected and processed as described in Chapter 2.

3.2. Fluorescence in situ hybridization

All samples were processed following standard oligo-FISH (for the domain Bacteria) or CARD-FISH (for Archaea) protocols as described in Pernthaler et al. (2001a) and Lin et al. (2006), respectively. Oligonucleotide probes and hybridization conditions employed in this study were as described in Chapter 2.

3.3. Microautoradiography

After hybridization, the autoradiographic procedure was performed on filter wedges as described in Carman (1993) and Lee et al. (1999). Briefly, radiographic emulsion (LM-1 Amersham) was liquefied at 43°C in a water bath for about 1 hour and then diluted with distilled water (1:1 vol/vol). In a photographic dark room, microscope slides were coated with the emulsion by dipping them in a Coplin jar. FISH-processed filter wedges were placed on the slides face down and the slides were placed on a cool metal block for about 30 minutes to allow the emulsion to gel. After an additional hour of drying, the slides were placed in a light-tight box with a desiccant and exposed for 14 days at 4°C before further processing. The exposure time required for a sufficient number of silver grains to develop was determined empirically using *Synechococcus bacillaris* culture grown with ^{14}C-bicarbonate (the same final concentration as for the experimental samples). Negative controls, consisting of T_0 killed cells, were examined for silver grain formation due to chemography (non-radioactive chemical compounds forming silver grains) as recommended by Nielsen et al. (2003). Negligible numbers of silvers grains (1-2 per field) were present in these controls.

After exposure, slides were placed in a developer solution (Kodak® Developer D-19) for 2 minutes, soaked in distilled water for 10 seconds, and fixed in a fixer solution (Kodak® Fixer Powder) for 6 minutes (Malmstrom et al., 2004). After a final soak/rinse with distilled water for 6 minutes, slides were dried for about 1 hour and placed in a box with a desiccant overnight at 4°C. Developed slides were then stained with DAPI (2 µg/mL solution) for 2 minutes, rinsed with distilled water and 80 % ethanol for 1 minute each, dipped in 1 % glycerol for 2 minutes and dried overnight in a box with a desiccant at 4°C. The outlines of each filter wedge on the slides were traced on the underside of slides with an indelible ink marker prior to their removal from the slides. Cover slips were mounted on slides using Citifluor® antifade solution.

3.4. Microscopic analyses

Autoradiographs were examined under bright-field illumination for silver grain clusters and under epifluorescent illumination for probe-positive (specific clade) and DAPI-stained (total

community) cells, both associated and not associated with the silver grains. At least two silver grains had to be associated with the DAPI or probe-positive cell to be considered active, although there is no consensus number considered to unequivocally identify active cells. Grote et al. (2008) and Teira et al. (2004) considered cells as active when associated with two or more silver grains while other researchers required four or more (Lee et al., 1999; Nielsen et al., 1999; Cottrell and Kirchman, 2004). Up to thirty fields from the same filter wedge were examined for probe-positive and DAPI-stained cells, respectively. The total prokaryotic community, five proteobacterial (α-, β-, γ-, ε-proteobacteria, and sulfate-reducing δ-proteobacteriabacteria (SRB)) and two archaeal (Thaumarchaeota and Euryarchaeota) clades were enumerated in the time zero, unamended, and amended samples. First order net rates of change (μ, d^{-1}) in abundances of the total prokaryotic community and each clade were calculated assuming exponential growth or loss using the following equation:

$\mu = (\ln (N_1/N_0)/t,$

where N_0 is the number of cells L^{-1} at the time of sampling, N_1 is the number of cells L^{-1} after 18 hours of incubation, and t is the duration of incubation in days.

During visual inspection of microautoradiography slides, I observed clusters comprised of tens to hundreds of silver grains. Number of these clusters varied from a couple to several per examined filter wedge. In the enumeration of DAPI-stained and probe-positive cells positive for silver grains, I only included those cells that were clearly separated from the clusters. Therefore, the proportions of active cells reported below are most likely underestimated.

4. Results

4.1. Environmental setting and microbial productivity

Samples from discrete depths for measurements of O_2, H_2S, $S_2O_3^{2-}$, and NO_3^- as well as heterotrophic and chemoautotrophic productivities were collected as part of the semi-annual cruises of the CARIACO Ocean Time-Series study as described in Taylor et al. (2001) and Li et al. (2008). Results of these measurements are provided here as background. During cruise CAR169, oxygen concentrations decreased to below 2 μM at a depth of 260 m which marked the upper boundary of the suboxic layer and sulfide concentrations increased to > 1 μM below 280

m (lower boundary of the suboxic layer). Thiosulfate concentrations increased from undetectable at 280 m to 4.4 µM at 340 m. Nitrate concentrations remained below 1 µM starting at 260 m. Chemoautotrophic production (measured as dark carbon assimilation, DCA) exhibited a broad peak between 280 and 300 m reaching maximum of 1.5 µM C d^{-1} L^{-1}10 m below the suboxic zone at 290 m, sharply declined at 310 m to 0.2 µM C d^{-1} L^{-1}, and another peak of 0.8 µM C d^{-1} L^{-1} was measured 40 m below the suboxic layer at 320 m. Heterotrophic productivity (BNP) reached a maximum of 0.4 µM C d^{-1} L^{-1} at the bottom of the suboxic zone at 280 m and decreased to barely detectable below 300 m (Fig. 4.1).

4.2. Responses of the total prokaryotic community and specific clades to energy substrate and oxidant amendments

To evaluate the response of anoxic microbial communities to selected substrates, I enumerated cell abundances of the total prokaryotes and specific clades at the time of sampling (T_0) and at the end of 18 h incubations in unamended and amended samples. Probe-positive cells of the seven selected clades were enumerated in all samples. In unamended samples, only γ-proteobacteria and SRB δ-proteobacteria abundances increased by the end of the incubations at least in one of the examined depths, while abundances of other clades declined at all three depths. In samples amended with H_2S/Fe(III) or $S_2O_3^{2-}$/NO_3^-, growth of each clade was stimulated in at least one of the three examined depths. However, only γ-proteobacteria, ε-proteobacteria, and Thaumarchaeota exhibited active uptake of ^{14}C-bicarbonate, and for that reason just these clades are discussed further.

Distinct changes in abundances of the total prokaryotes, γ-proteobacteria, ε-proteobacteria, and Thaumarchaeota were evident in unamended and amended samples after 18 h incubations. Abundances of the total community at the time of sampling at 300, 310, and 320 m were very similar (average 3.68 x 10^8 cells L^{-1}) and decreased significantly by 48-60 % in unamended samples amounting to net loss rates of between -0.87 to -1.21 d^{-1} (ANOVA, $p < 0.001$, $n = 3$) (Fig. 4.2). However, the community abundance increased in samples amended with H_2S/Fe(III), and cell concentrations were 25 to 59 % higher compared to unamended samples at the end of incubations (ANOVA, $p < 0.001$, $n = 3$). Even more pronounced increase in the abundance of the total community was observed in samples amended with $S_2O_3^{2-}$/NO_3^- compared to unamended

control. Specific growth rates of the total prokaryote community in samples amended with $S_2O_3^{2-}$/NO_3^- were 3-4 times higher than in those amended with H_2S/Fe(III) (Fig. 4.2).

Abundances of γ-proteobacteria significantly decreased at the two shallower depths during 18 h incubations in unamended samples (ANOVA, $p < 0.05$, $n = 3$), but more than doubled at 320 m. In the sample amended with H_2S/Fe(III) at all three depths γ-proteobacterial abundances increased and were as much as 63-fold higher than in unamended samples at 310 m. γ-proteobacterial cell numbers increased significantly in sample amended with S_2O_3/NO_3 compared to unamended control only at 300 m (ANOVA, $p < 0.001$, $n = 3$) (Fig. 4.2).

ε-proteobacterial cell numbers in unamended samples remained almost the same at 300 m during 18 h incubations, but significantly increased at the two other depths (ANOVA, $p < 0.05$, $n = 3$). At all depths, in samples amended with S_2O_3/NO_3 and H_2S/Fe(III), ε-proteobacteria abundances significantly increased compared to unamended controls and the net growth rates were higher in amendments with S_2O_3/NO_3 than in amendments with H_2S/Fe(III) (ANOVA, $p < 0.001$, $n = 3$) (Fig. 4.2).

Thaumarchaeal cell numbers significantly declined in unamended samples during 18 h incubations to less than 20 % of the initial cell abundances (ANOVA, $p < 0.001$, $n = 3$). However, in samples amended with S_2O_3/NO_3 and H_2S/Fe(III), thaumarchaeal cell abundances increased at 300 and 320 m compared to unamended samples (ANOVA, $p < 0.001$, $n = 3$), but not at 310 m (Fig. 4.2).

4.3. Chemoautotrophic activity of the total prokaryotic community and specific clades

Enumeration of active cells (silver grain positive) as a proportion of all detected cells revealed a notable contribution of chemoautotrophic microorganisms to the total prokaryotic community (DAPI-positive cells) at the examined depths. The ^{14}C-assimilating prokaryotes accounted for 12-26 % of the total community in unamended samples, and 17-26 % and 4-40 % in samples amended with H_2S/Fe(III) and $S_2O_3^{2-}$/NO_3^-, respectively (Fig. 4.3). Amendment with $S_2O_3^{2-}$/NO_3^- yielded ^{14}C-assimilating communities almost three-fold more abundant at 310 and 320 m compared to unamended samples, while amendment with H_2S/Fe(III) resulted in only slight increases in the ^{14}C-assimilating populations at the same depths. At 300 m, ^{14}C-assimilating communities were not stimulated by any of the additions (Fig. 4.4).

Among all investigated clades, ^{14}C-assimilating γ-proteobacteria accounted for 44 and 50 % of all γ-proteobacterial cells in unamended samples at 300 and 310 m, respectively, but active cells (silver grain positive) were not detected at 320 m (Fig. 4.5). In samples amended with H_2S/Fe(III) ^{14}C-assimilating γ-proteobacteria accounted for ~ 14 % of all γ-proteobacterial cells at 310 m and active cells were not detected at other depths. ^{14}C-assimilating ε-proteobacteria accounted for as much as 91 % and 25 % of all ε-proteobacterial cells in samples amended with H_2S/Fe(III) and $S_2O_3^{2-}$/NO_3^-, respectively (Fig. 4.5). ^{14}C-assimilating thaumarchael cells were detected only at 310 m in sample amended with H_2S/Fe(III) and accounted for 80 % of all thaumarchael cells (Fig. 4.5).

4.4. Contribution of specific clades to total inorganic carbon fixation

To estimate how much carbon specific clades fixed, I calculated the fraction of the total ^{14}C-assimilating prokaryotes represented by each ^{14}C-assimilating clade. If I assume equal uptake of ^{14}C-bicarbonate among cells associated with silver grains, γ-proteobacterial cells would have fixed between 4 and 6 % of the total carbon (^{14}C-assimilating DAPI-positive cells) in unamended samples and 6 % in samples amended with H_2S/Fe(III) (Fig. 4.6). ε-proteobacterial cells would have fixed between 6 and 11 % of the total carbon in samples amended with H_2S/Fe(III) and about 5 % in samples amended with $S_2O_3^{2-}$/NO_3^- (Fig. 4.6). Thaumarcheal cells would have fixed about 5 % of the total carbon only in samples amended with H_2S/Fe(III) at 310 m (Fig. 4.6). Chemoautotrophic activities of all three clades would have accounted for fixing about 21 % of the total carbon in samples amended with H_2S/Fe(III) at 310 m (Fig. 4.6).

5. Discussion

5.1. Identification of active chemoautotrophs and method evaluation

In this study, MAR-FISH provided insight into the ^{14}C-bicarbonate assimilating prokaryotic community of the Cariaco Basin's redoxcline. Analyses of the total community showed that between 12 and 26 % of the prokaryotes (depending on depth) were chemoautotrophic in unamended samples, similar to ranges reported for other marine

environments. For example, Kirchman et al. (2007) estimated that between 5 and 26 % (average 10 %) of all *Bacteria* and *Archaea* in the oxygenated waters of the western Arctic Ocean were chemoautotrophic depending on depth. In the Baltic Deeps and the Black Sea redoxclines, total ^{14}C-bicarbonate assimilating cells accounted for about 29 and 12 % of all cells, respectively (Grote et al., 2008).

Despite its high potential for detection of active microorganisms among members of an investigated community, application of MAR-FISH in this study produced disparities between numbers of active cells (silver grain positive) and their proportion of all probe-positive cells. ^{14}C-assimilating γ-proteobacteria accounted for up to 50 and 14 % of all γ-proteobacterial cells in unamended samples and in samples amended with H_2S/Fe(III), respectively. In samples amended with H_2S/Fe(III) and $S_2O_3^{2-}$/NO_3^-, ε-proteobacteria cell numbers increased ~2-3-fold and 3-9-fold compared to unamended samples, and active cells accounted for up to 91 and 25 % of all ε-proteobacterial cells, respectively. It was surprising that active ε-proteobacteria were not detected in unamended samples since the abundance of this clade is usually enhanced in the redoxcline and this clade is hypothesized to represent the most important chemoautotrophs of the prokaryotic community in this system (Madrid et al., 2001; Taylor et al., 2001; Lin et al., 2006). However, during the investigated cruise (CAR169) ε-proteobacteria cell numbers detected by FISH accounted for less than 5 % of the total prokaryotic community at the time of sampling and declined by > 90 % over 18 h incubations in unamended samples at all three depths. Large discrepancies between percentages of active (silver grain positive) and probe-positive cells have been observed by other researchers. For example, in a MAR-FISH study employed to specifically detect ^{14}C-assimilating ε-proteobacteria, between 22 and 35 % and between 39 and 91 % of all probe-positive ε-proteobacteria were not active (silver grain negative) in the Baltic Deeps and the Black Sea, respectively (Grote et al., 2008). In another example, Cottrell and Kirchman (2004) examined the Delaware estuary bacterial communities for uptake of ^{3}H-thymidine or ^{3}H-leucine and showed that the fraction of probe-positive bacterial cells assimilating the labeled substrates varied for three examined clades from undetectable to 50 %. Further, they showed that bacterial activity was not correlated with abundance (probe-positive cells). Therefore, detection of cells by FISH does not always imply that the cells are active since some cells might not assimilate offered substrate, some might be inactive, and some might be senescent and still maintain sufficient levels of ribosomal RNA for FISH detection (Amann et

al., 2001; Nielsen et al., 2003). Furthermore, activities of some microorganisms might be too low for single-cell detection by microautoradiography because the substrate uptake rate might not exceed a detection threshold and assimilation of the same substrate may vary among cells of the same population (Nielsen et al., 1999, 2003).

Very low contributions of active clades to the total inorganic carbon fixing community were observed at all depths examined. In unamended samples, active γ-proteobacteria accounted for 4-6 % of all active DAPI-positive cells. In samples amended with H_2S/Fe(III), active γ-proteobacteria, ε-proteobacteria, and Thaumarchaeota accounted for 21 % of all active DAPI-positive cells at 310 m, and in samples amended with $S_2O_3^{2-}$/NO_3^-, ε-proteobacteria accounted for 5 % of all active DAPI-positive cells. One of the reasons for such low contributions of active clades might be specificity of the applied FISH probes. There are no group-specific probes targeting 100 % of representatives, and the coverage of specific clades might range between 76 % for γ-proteobacteria (GAM42a probe) (Wagner et al., 2003; Amann et al., 2008) and 90 % for ε-proteobacteria (EPS682 probe) (http://www.arb-silva.de; accessed June 7, 2013). Therefore, some members of specific clades might have been missed with the probes applied in this study.

Another reason for discrepancies between active clades and the total active community might be the fact that I targeted members of selected clades of *Bacteria* (but all of *Archaea*) and unidentified (non-targeted) groups assimilated ^{14}C-bicarbonate. The majority of MAR-FISH studies of natural assemblages are confined to only a few clades and to my knowledge no other studies employed such a broad variety of group-specific probes as in this study. Therefore, it is not possible to unequivocally determine if the low contribution of all active clades is an isolated result or is a more general problem. However, in a MAR-CARD-FISH study of L-^{3}H-aspartic acid assimilating *Bacteria* (EUB338 probe) and *Archaea* (CREN537 plus EURY806) active *Bacteria* and *Archaea* accounted for as little as 25 and 50 % of total active cells (L-^{3}H-Asp-assimilating DAPI), respectively (estimated from Teira et al., 2004). Thus, even application of domain-level EUB338 probe showed high discrepancies between detection of active FISH-positive groups and the total active DAPI-positive community.

Another source of small proportions of active members of specific clades and their low contribution to the total active community might be the silver grain clusters I observed in the majority of the samples. Most cells associated with those clusters were difficult to enumerate because the cell fluorescence was very faint or only the edge of the cell was visible. Because of

high variability in the number of clusters per sample and the possibility that some cells may have been entirely covered with the silver grains, I excluded cells associated with clusters from enumeration. This exclusion likely resulted in underestimation of the active chemoautotrophic community. The silver grain density and distribution associated with cells might not only depend on cell-specific activity but also on cell size and shape as well as the exposure time during sample development (Nielsen et al., 2003). I used cultured *Synechococcus bacillaris* cells incubated with ^{14}C-bicarbonate to determine the optimal exposure time for my samples. However, for environmental samples comprised of mixed prokaryotic communities, the same exposure length as for cultured cells might have resulted in the saturation in the silver grains and essentially formation of indistinguishable clusters (Nielsen et al., 2003). In future MAR-FISH experiments, an additional sample could be collected solely for the purpose of a more appropriate determination of the optimal exposure time to minimize or eliminate the silver grains saturation in order to accurately enumerate active members of the prokaryotic community.

5.2. Significance of chemoautotrophic clades in total inorganic carbon assimilation

Inorganic carbon fixation by chemoautotrophic microorganisms in pelagic redoxclines accounts on average for 30 to 64 % of primary production (Taylor et al., 2001; Jost et al., 2008). Thus, it is essential to know who the chemoautotrophs are and what fraction of the total chemoautotrophic community they constitute in order to determine how important their activities are in cycling of inorganic carbon, nitrogen, and sulfur. Chemoautotrophs with thiotrophic metabolism at the expense of nitrate have been identified among γ-proteobacteria and ε-proteobacteria in diverse marine environments, such as deep-sea cold-seep sediments, hydrothermal vents, and oxygen-deficient pelagic zones (Li et al., 1999; Campbell et al., 2006, Canfield et al., 2010; Labrenz et al., 2013). These prokaryotes may account for a significant fraction of the total community in anoxic systems, but ε-proteobacteria are usually the dominant clade (Lin et al., 2006; Grote et al., 2008; this work) and in hydrothermal vent systems might represent more than 80 % of the total community (Nakagawa and Takai, 2008). In this study, chemoautotrophic γ-proteobacteria accounted for up to 50 % of all γ-proteobacterial cells, but never more than 6 % of all chemoautotrophic cells. Chemoautotrophic ε-proteobacteria in samples amended with H_2S/Fe(III) were almost twice as abundant as ^{14}C-assimilating γ-

proteobacteria. Further, chemoautotrophic ε-proteobacteria appeared to be more broadly distributed throughout the redoxcline than chemoautotrophic γ-proteobacteria. Such results suggest that even though distributions of these two clades slightly overlap, each probably occupies very distinct ecological niches in the Cariaco Basin. Genomic analyses of deep-sea chemoautotrophic γ-proteobacteria and ε-proteobacteria showed that these clades have different sulfur oxidation and inorganic carbon fixation pathways: γ-proteobacteria have a *Sox*-independent sulfur oxidation pathway and fix carbon via Calvin-Benson-Bassham cycle while ε-proteobacteria have *Sox*-dependent sulfur oxidation pathway and fix carbon via the reverse-tricarboxylic acid cycle (Nakagawa and Takai, 2008). Further, chemoautotrophic γ-proteobacteria are facultative aerobes or strict aerobes while chemoautotrophic ε-proteobacteria are strict anaerobes or facultative aerobes (Nakagawa and Takai, 2008).

To the best of my knowledge, anaerobic chemoautotrophic γ-proteobacteria capable of H_2S oxidation at the expense of Fe reduction are so far only found in acidic environments (Hedrich and Johnson, 2013; Osorio et al., 2013) and there are no known chemoautotrophic ε-proteobacteria capable of thiotrophic metabolism at the expense of iron oxides. However, detection of ^{14}C-assimilating γ-proteobacteria and ε-proteobacteria in samples amended with H_2S/Fe(III) suggests that yet unidentified representatives of these two clades might be important in inorganic carbon fixation in the Cariaco Basin and elsewhere as well. Whether the detection of ^{14}C-assimilating thaumarchaeal cells in this study points to a novel metabolism is too speculative based on only one sample and requires further investigation.

6. Conclusions

This study demonstrated for the first time that up to 26 % of the total prokaryotic community in the Cariaco's redoxcline was chemoautotrophic at selected depths. Further, γ-proteobacteria, ε-proteobacteria, and Thaumarchaeota were identified as chemoautotrophic clades in this system. Chemoautotrophic activities of these three clades indicate thiotrophic-based metabolism in which H_2S and $S_2O_3^{2-}$ can be utilized as energy substrates at the expense of NO_3^- or Fe(III).

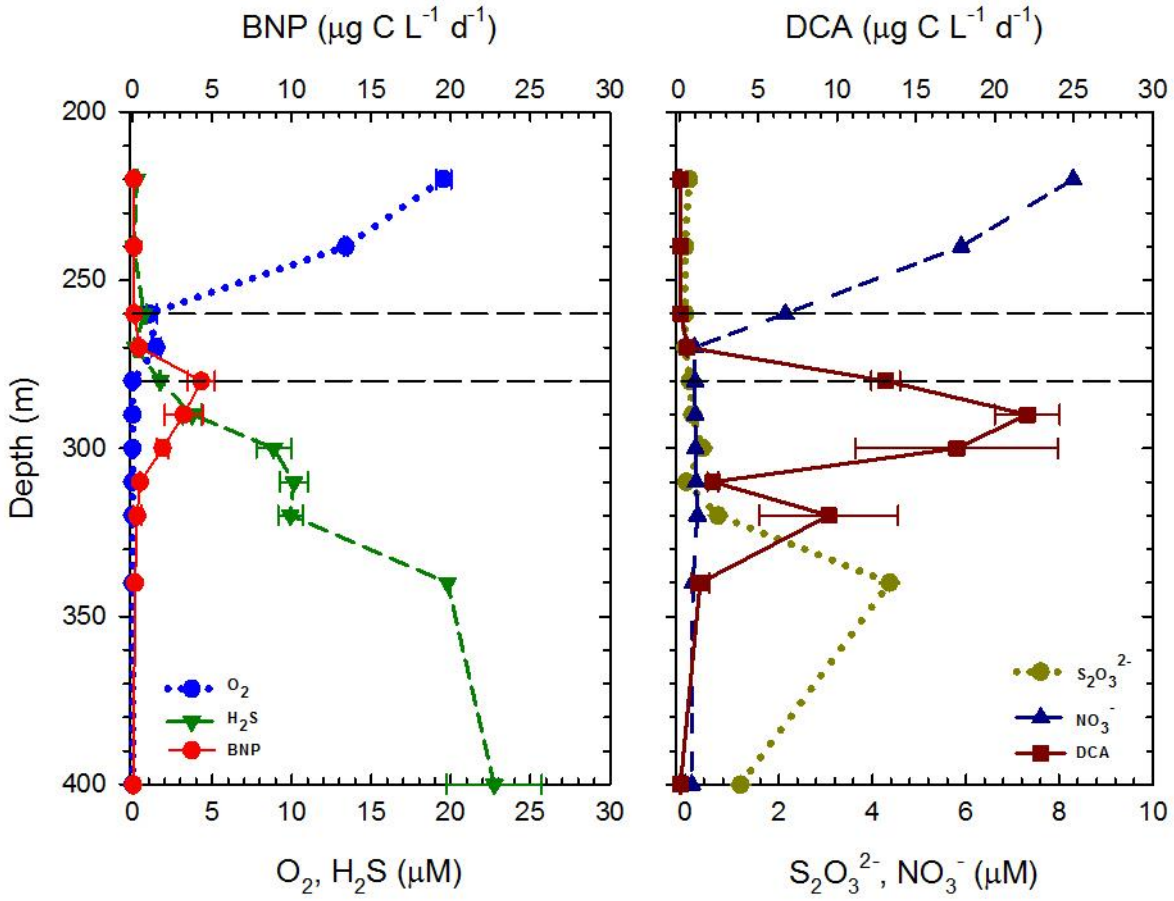

Figure 4.1. Vertical distributions of selected electron donors and acceptors, heterotrophic productivity (BNP) and chemoautotrophic productivity (DCA) during cruise CAR169 (May 6-7, 2010). The horizontal dashed lines represent the upper and lower boundary of the suboxic layer. Error bars represent standard error. Data provided by G.T. Taylor, Y. Astor, M. Scranton.

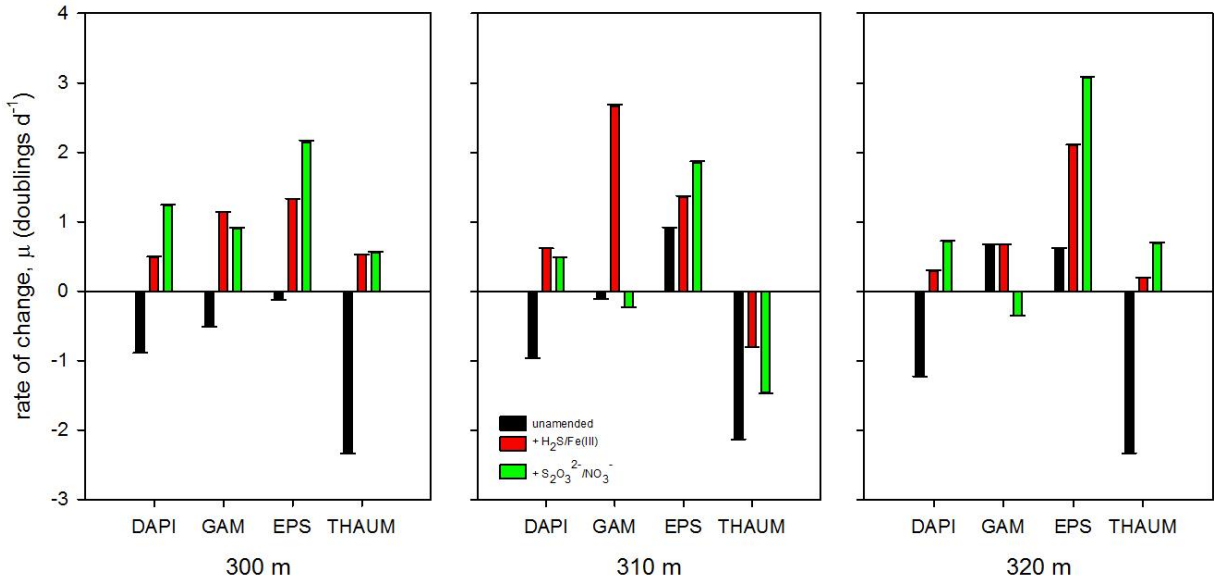

Figure 4.2. First order rates of change, μ (d^{-1}), in abundances of the total prokaryotic community (DAPI-positive cells) and selected clades (probe-positive cells). GAM: γ-proteobacteria, EPS: ε-proteobacteria, THAUM: Thaumarchaeota. Unamended sample - seawater only; amendment with H_2S/Fe(III) (15 and 50 μM final concentration, respectively); amendment with $S_2O_3^{2-}$/NO_3^- (50 μM final concentration each). Error bars represent standard error.

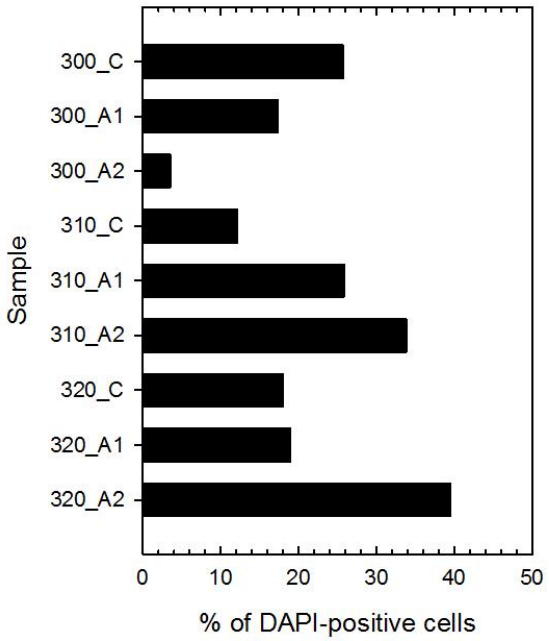

Figure 4.3. Total ^{14}C-assimilating prokaryotes as a fraction of all DAPI-positive cells after 18 h incubations. C: control, seawater amended with ^{14}C-bicarbonate only (20 µCi L^{-1}, ~2 µM final concentration); A1: ^{14}C-bicarbonate and H_2S/Fe(III) (15 and 50 µM final concentration, respectively); A2: ^{14}C-bicarbonate and $S_2O_3^{2-}$/NO_3^- (50 µM final concentration each).

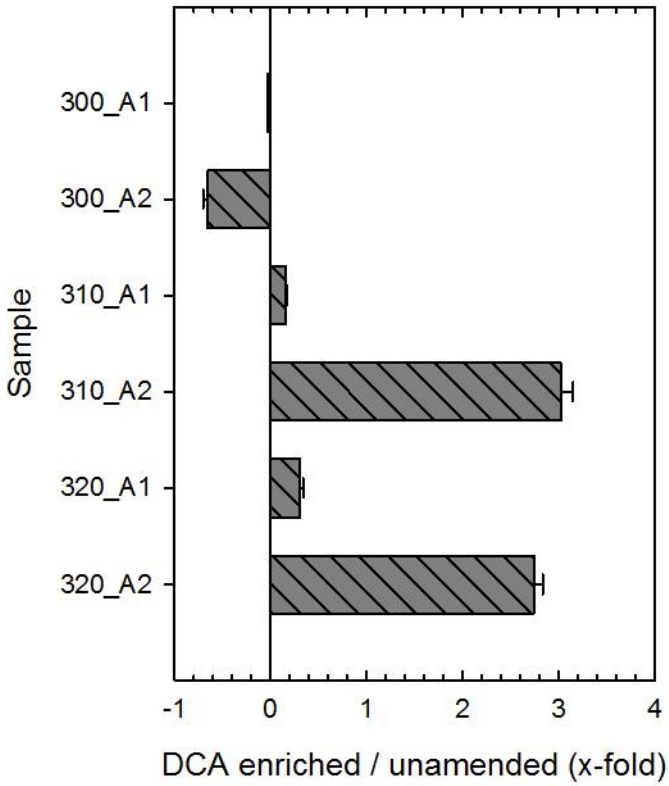

Figure 4.4. Effects of amendments on the total ^{14}C-assimilating prokaryotes (DAPI-stained) after 18 h incubations compared to unamended samples. A1: amendment with H_2S/Fe(III) (15 and 50 µM final concentration, respectively); A2: amendment with $S_2O_3^{2-}$/NO_3^- (50 µM final concentration each); DCA: dark carbon assimilation (chemoautotrophy). Error bars represent standard error.

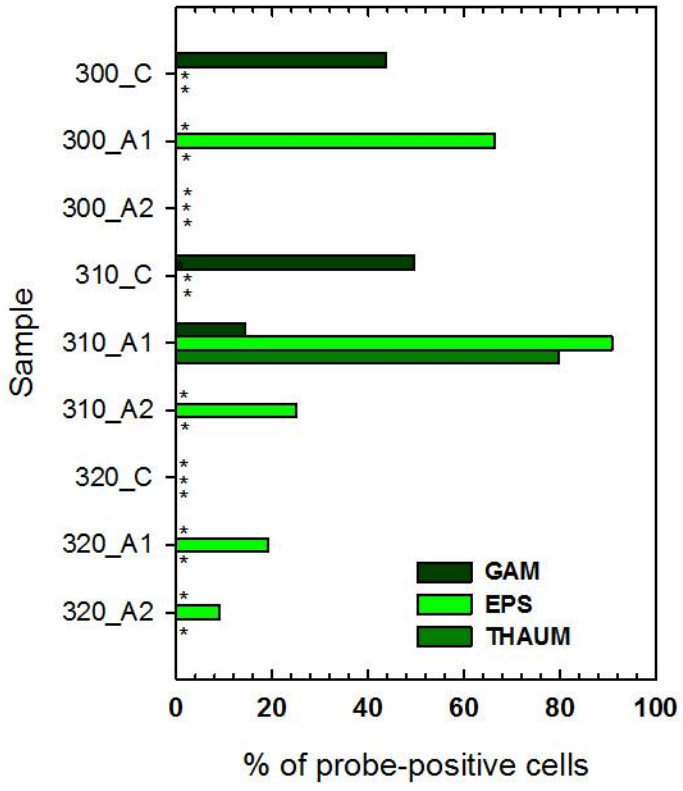

Figure 4.5. Specific ^{14}C-assimilating clades as fractions of probe-positive cells. C: control, seawater amended with ^{14}C-bicarbonate only (20 µCi L^{-1}, ~2 µM final concentration); A1: ^{14}C-bicarbonate and H_2S/Fe(III) (15 and 50 µM final concentration, respectively); A2: ^{14}C-bicarbonate and $S_2O_3^{2-}$/NO_3^- (50 µM final concentration each); *- ^{14}C-assimilating probe-positive cells not detected.

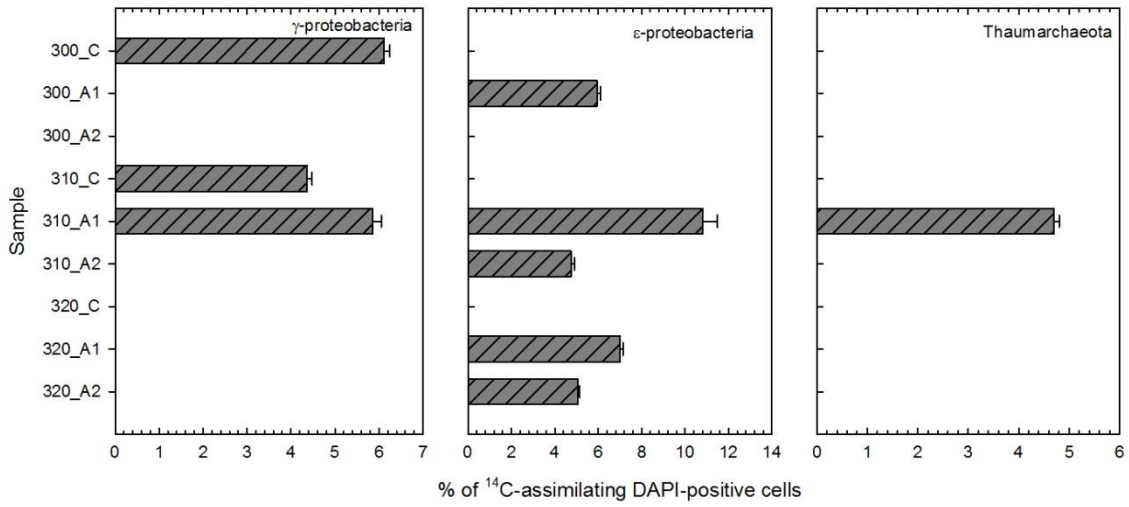

Figure 4.6. Specific ^{14}C-assimilating clades as fractions of total ^{14}C-assimilating prokaryotes. C: control, seawater amended with ^{14}C-bicarbonate only (20 µCi L^{-1}, ~2 µM final concentration); A1: ^{14}C-bicarbonate and H_2S/Fe(III) (15 and 50 µM final concentration, respectively); A2: ^{14}C-bicarbonate and $S_2O_3^{2-}$/NO_3^- (50 µM final concentration each).

Chapter 5

Identification of active chemoautotrophic bacteria by $^{13}C/^{15}N$-DNA stable isotope probing

1. Abstract

During cruises CAR163 (Nov 5-6, 2009) and CAR169 (May 6-7, 2010), $^{13}C/^{15}N$-DNA stable isotope probing was employed in combination with terminal restriction fragment length polymorphism (TRFLP), cloning and sequencing of bacterial 16S rRNA genes in order to identify active chemoautotrophs in the Cariaco Basin's redoxcline. Combinations of $S_2O_3^{2-}/NO_3^-$, H_2S/NO_3^-, H_2S/Fe(III), and H_2S/Mn(IV) were added as substrates together with the isotopes to determine what fuels chemoautotrophic activity. The majority (64 %) of all 16S rRNA gene sequences obtained from the labeled $^{13}C/^{15}N$-DNA fraction among all treatments were most closely related (93-99 % of identity) to two strains of ε-proteobacteria from genus *Sulfurovum*. In silico analysis of the highly similar ε-proteobacterial sequences allowed identification of unique terminal restriction fragments (TRFs) representative of ε-proteobacteria in each of three separate restriction enzyme digests. Prevalence of ε-proteobacterial TRFs in the $^{13}C/^{15}N$-DNA fraction indicates that this clade represents the dominant chemoautotrophs in the Cariaco's redoxcline community. TRFs representing chemoautotrophic ε-proteobacteria were detected in all treatments employed in this study suggesting that members of this clade use $S_2O_3^{2-}$ or H_2S as energy substrates, and NO_3^- and metal oxides as electron acceptors.

2. Introduction

High rates of dark inorganic carbon fixation are observed in aquatic systems where the transition zone between oxic and anoxic layers (redoxcline) displays strong chemical gradients in electron donors such as H_2, H_2S, NH_4^+, NO_2^- and electron acceptors such as O_2, NO_3^-, manganese and iron oxides, e.g., in the Cariaco Basin (Taylor et al., 2001), the Baltic Deeps (Labrenz et al., 2005), and the Black Sea (Yilmaz et al., 2006). In the Cariaco Basin, chemoautotrophy can rival photosynthetic productivity (Taylor et al., 2001), yet the identity of chemoautotrophic microbes and what drives their activity in this system are not fully understood.

Based on their prevalence in 16S rRNA gene libraries recovered from the redoxcline and high cell numbers detected by fluorescence in situ hybridization (FISH) (on average ~ 30 % of the total microbial community), ε-proteobacteria have been suggested to be important chemoautotrophs in the Cariaco Basin (Madrid et al., 2001; Lin et al., 2006). ε-proteobacteria are prevalent chemoautotrophic microorganisms in many marine environments where reduced sulfur is abundant, such as hydrothermal deep-sea vents (Campbell et al., 2001; Miroshnichenko et al., 2002; Takai et al. 2005; Inagaki et al., 2004), deep-sea cold seeps sediments (Inagaki et al., 2002; 2003), the Baltic Deeps (Grote et al., 2008; Glaubitz et al., 2009), and the Black Sea (Fuchsman et al., 2012). However, their ecological significance in cycling of carbon, sulfur, and nitrogen remains to be elucidated.

Identification of microbes active in natural environments is imperative to understanding their physiology and their ecological role, especially in cycling of carbon and other elements. Because the vast majority of microbes detected in situ do not have cultured representatives, their identification is cumbersome and a combination of different methods is required. One of the approaches that has received increasing attention is based on the use of substrates labeled with stable isotopes (^{13}C, ^{15}N) which can be incorporated by microorganisms into their DNA, RNA, and lipids (Boschker et al., 1998; Radajewski et al., 2000; Buckley et al., 2007; Neufeld et al., 2007a, 2007b). These isotope-labeled biomarkers can be separated from the unlabeled fraction using cesium chloride gradient ultracentrifugation for further analyses by fingerprinting, cloning, and sequencing of 16S rRNA or functional genes (reviewed in Dumont and Murrell, 2005). ^{13}C and ^{15}N-biomarker stable isotope probing (SIP) approaches have been successfully applied in studies of microbial communities in marine (Glaubitz et al., 2009; Redmond et al., 2010; Wakeham et al., 2010; Wawrik et al., 2012) and soil environments (Radajewski et al., 2003; Buckley et al., 2008), in activated sludge (Moreno et al., 2010), and bioreactors (Ginige et al., 2004).

In the present study of the Cariaco's redoxcline microbial community, $^{13}C/^{15}N$-DNA SIP was combined with fingerprinting by terminal restriction fragment length polymorphism (TRFLP), cloning, and sequencing of bacterial 16S rRNA genes in order to detect and identify active chemoautotrophs. Selected electron donors (H_2S and $S_2O_3^{2-}$) and electron acceptors (NO_3^-, Mn(IV), and Fe(III)) were provided in addition to ^{13}C and ^{15}N-labeled substrates to determine the identity of the chemoautotrophs stimulated by their presence.

3. Materials and Methods

3.1. ^{13}C and ^{15}N-DNA stable isotope probing

Water samples from two depths within the redoxcline were collected for DNA-SIP experimentation during seven cruises: CAR132 (Apr 11-13, 2007), CAR139 (Nov 30-Dec 1, 2007), CAR145 (May 6-7, 2008), CAR153 (Jan 19-20, 2009), CAR157 (May 16-17, 2009), CAR163 (Nov 5-6, 2009) and CAR169 (May 6-7, 2010). Time zero samples (~ 5 L) were withdrawn directly from Niskin bottles into sterile IV bags (Secure^{TM} EVA Compounder Bags, non-DEHP, latex free, 2000 mL, The Metrix Company) under N_2 pressure and avoiding aeration and immediately filtered through Millipore Durapore® Membrane filters (47 mm diameter, 0.2 µm pore size, GV type) and the filters were stored in cryovials at -40°C until further processing. Between two and four samples (depending on cruise) for incubations from each depth were withdrawn into one gallon (~ 4 L) acid-washed polycarbonate bottles (with silicone stoppers and polyethylene caps) and immediately amended with ^{13}C-bicarbonate and ^{14}N-ammonium (1.1 mM and 5 µM final concentrations, respectively). Between one and three samples (depending on cruise) were additionally amended with selected substrates (electron donors and acceptors). A summary of samples collected for DNA-SIP is presented in Table 5.1. All samples were incubated at ~ 17 ± 2°C (ambient water temperature) for 48 hours in the dark. Incubations were terminated by filtration through Millipore Durapore® Membrane filters (47 mm diameter, 0.2 µm pore size) and the filters were stored in cryovials at -20°C until further processing.

Concentrations of stable isotope-labeled substrates were chosen based on in situ concentrations of dissolved inorganic carbon (2.2 mM) and ammonium (5 µM) at comparable depths in the Cariaco Basin. ^{13}C-bicarbonate concentration was selected by making step-wise additions of $NaHCO_3$ to Cariaco seawater to determine a point at which pH changed by 0.1-0.2. To avoid a potential effect of pH change on the prokaryotic community, concentration of 1.1 mM was chosen because it was the highest value at which the pH did not change. Therefore, additions of 1.1 mM ^{13}C-bicarbonate would have resulted in an increase of the total DIC pool in the incubations by about one-third. Addition of 5 µM of ^{15}N-ammonium resulted in an increase of ammonium pool in the incubations by about 100 %. The actual percentage of incorporation of

each labeled substrate into the DNA of the investigated microorganisms was not determined in the present study.

3.2. DNA extraction and cesium chloride (CsCl) gradient centrifugation

Genomic DNA from filters collected during cruises CAR132-CAR157 was extracted using DNeasy Blood and Tissue kit (Qiagen®) following the manufacturer's instructions. Concentrations of extracted DNA were measured using PicoGreen (Invitrogen®) following the manufacturer's protocol. Because of lack or insufficient amount of environmental DNA extracted from filters collected during the above cruises, genomic DNA from filters collected during CAR163 and CAR169 was extracted using a modified phenol-chloroform method and results from only these two cruises are presented (Sakano and Kerkhof, 1998). Modifications included splitting filters into smaller pieces, five cycles of freezing with liquid nitrogen and thawing at 37°C in a water bath, and addition of approximately 3 µg of *Halobacterium salinarum* (Archaea) DNA (labeled with ^{12}C and ^{13}C, cells cultivated in Isogoro medium, Isotec, Miamisburg, OH) to 500 µL of extraction buffer in each sample to aid in recovery of small amounts of environmental genomic DNA. Concentrations of extracted DNA were measured using PicoGreen (Invitrogen®) following the manufacturer's protocol. Between 0.2 and 1.0 µg of genomic DNA (depending on sample) were added to CsCl gradients (0.54 g of CsCl in 500 µL or 0.8 g of CsCl in 750 µL of DEPC-treated water (Ambion®, Life Technologies) and 1 µL of 1 % ethidium bromide) and separated either in a TLA 120 rotor on a Beckman Optima ultracentrifuge at 77,000 rpm (~ 215,000 xg) or in a TLA120.2 rotor on a Beckman TL ultracentrifuge at 80,000 rpm (~250,000 xg) for 44-48 hours at 20°C. Top ($^{12}C/^{14}N$-DNA) and bottom ($^{13}C/^{15}N$-DNA) bands were visualized by UV illuminator and between 20 and 40 µL of gradient around each band were withdrawn with a pipette. The genomic DNA was dialyzed for 4 hours on a 25 mm diameter Millipore membrane (MF type, VS filter, mean pore size = 0.025 µm) floating in a Petri plate containing PCR grade water. The concentration of the cleaned genomic DNA was determined by PicoGreen.

3.3. Terminal restriction fragment length polymorphism (TRFLP)

To fingerprint ^{13}C and ^{15}N-labeled microorganisms, terminal restriction fragment length polymorphism of 16S rRNA genes was employed. Only bacterial 16S rRNA genes were amplified because archaeal DNA was used as a carrier to optimize separation of $^{13}C/^{15}N$-labeled environmental DNA. Bacterial 16S rRNA genes were amplified with primers 63F (Marchesi et al., 1998) and 778R (Marchesi et al., 1998, Rosch and Bothe, 2005). The forward primer was labeled with FAM (5[6]-carboxyfluorescein) dye on the 5' end (Integrated DNA Technologies, Inc). Three to five replicates of 50 µL PCR reactions included final concentrations of 1X PCR buffer, 1.5 mM $MgCl_2$, 200 µM dNTPs, 200 nM each primer, 2 units Paq5000 DNA polymerase (Agilent Technologies, Inc.), and between 2 and 5 ng of template DNA. PCR amplification was performed in a Stratagene Mx3000p real-time PCR system using an initial denaturation step of 95°C for 10 min and then 30 cycles of 95°C for 30 seconds, 55°C for 30 seconds, 72°C for 90 seconds, with a final extension at 72°C for 7 min. Amplification of archaeal 16S rRNA genes with the same bacterial 16S rRNA primers was attempted with *H. salinarium* genomic DNA confirming that no archaeal DNA was amplified from the extracted DNA. PCR products of expected size (755 base pairs) were visualized on a 1 % agarose gel stained with 1 % ethidium bromide and then the amplicons were purified using QIAquick PCR purification kit (Qiagen, Inc.) according to manufacturer's specifications. In samples with visible smearing, the PCR product was extracted directly from the gel using QIAEX II gel extraction kit (Qiagen, Inc.) following the manufacturer's specifications. Replicates of cleaned PCR product were pooled and quantified with PicoGreen. Thirty nanograms of the PCR product were digested with *Alu*I, *Hha*I, *Hinf*I, or *Rsa*I restriction endonucleases with corresponding buffers (New England Biolabs, MA) in separate 20 µL reactions at 37 °C for ~ 6 hours. Additional digestion of each reaction with mung bean nuclease (New England Biolabs, MA) was performed to remove any single-stranded DNA fragments which could result in formation of pseudo-TRFs in downstream analysis (Egert and Friedrich, 2003). After ethanol precipitation, the digested DNA was resuspended in 40 µL of Hi-Di formamide. Two replicate 10 µL subsamples were each combined with 0.5 µL of a MapMarker® Rox1000 size standard (23 discrete DNA fragments ranging in size from 50 to 1000 bp labeled with X-Rhodamine at 16 fmol/band/µl) (Bioventure, Inc.) and 9.5 µL of Hi-Di

formamide, and the fluorescently labeled DNA fragments were separated on an ABI 310 genetic analyzer (Applied Biosystems, Foster City, CA).

3.4. TRFLP data processing

Electropherograms were analyzed for fragment lengths between 50 and 760 base pairs (bp) with peak detection set to 25 arbitrary fluorescence units using Genescan® software. All peaks within a fingerprint were normalized to the total area of the peaks in that fingerprint and peaks with area below 1 % were excluded from further analysis. The area of each remaining peak was then recalculated. Peaks from replicate samples were manually aligned by size (in base pairs) and grouped within 1 base pair (Clement et al., 1998). Only peaks occurring in both replicates were included in further analysis. Terminal restriction fragment (TRF) richness (number of individual TRFs in a sample) was evaluated based on the presence or absence of peaks (Liu et al., 1997; Blackwood et al., 2003).

3.5. Cloning of PCR product and sequence analysis

To identify the predominant TRFs in $^{12}C/^{14}N$-DNA and $^{13}C/^{15}N$-DNA bands, bacterial 16S rRNA genes from each sample were amplified as described above (except 63F primer was not fluorescently labeled), cloned, and sequenced. Replicate PCR products visualized on a 1 % agarose gel stained with 1 % ethidium bromide were extracted directly from the gel, purified using QIAEX II gel extraction kit (Qiagen, Inc.) and quantified using PicoGreen. Two microliters of purified amplicons were ligated into the StrataClone blunt PCR cloning vector (Agilent Technologies, CA) and ligation products were transformed into *E. coli* StrataClone SoloPack competent cells according to the manufacturer's specifications. Positive and negative controls (included in the manufacturer's kit) were done in parallel to confirm successful transformation of the desired insert (PCR product). All transformants were collected for further analysis because of low yields of colonies. The plasmid DNA was extracted using Zyppy™ plasmid miniprep kit (Zymo Research, CA) according to manufacturer's specifications and additionally purified by ethanol precipitation. Clones were sequenced using the Sanger method with the universal reverse M13 primer by Genewiz, Inc., NJ, USA. Sequences of quality score

over 40 and contiguous read length over 500 were edited manually using FinchTV software v1.4 (Geospiza, Inc.) and trimmed to exclude low quality regions. The final 500 nucleotide-long sequences were analyzed for closest matches with Basic Local Alignment Search Tool (BLAST) using the National Center for Biotechnology Information (NCBI) highly similar bacterial 16S rRNA gene sequences. Chimeric sequences were identified with the DECIPHER program (Wright et al., 2012). To determine what TRF size each clone would produce, in silico digestions of closest matches to each sequence (with the same set of primers as used for PCR amplification) were performed with the computer program TRiFLe available at http://cegg.unige.ch/trifle/trifle.jnlp (Junier et al., 2008).

4. Results

4.1. Terminal restriction fragment length polymorphism analysis of 16S rRNA genes

A total of 20 CsCl gradient bands (11 top and 9 bottom) from both cruises were analyzed; seven samples were not processed either due to poor DNA extraction, lack of band separation in CsCl gradient, or unsuccessful PCR amplification. Totals of 95, 109, 86 and 90 different TRFs were observed across all bands as a result of *Alu*I, *Hha*I, *Hinf*I, and *Rsa*I digestion of DNA, respectively. Number of individual TRFs in each band (TRF richness) varied between zero and 26 depending on the sample and digest (Fig. 5.1). However, the average TRF richness was very similar across enzymes and varied only between 9.8 (*Rsa*I) and 11.7 (*Hinf*I).

4.2. Phylogenetic characterization of 16S rRNA gene sequences

Cloning of 16S rRNA genes was performed to obtain environmental sequences in order to identify microorganisms incorporating inorganic carbon and nitrogen into their DNA as well as those active when offered selected energy substrates and electron acceptors, and to assign phylogenetic identity to the TRFs. In total, 224 clones were retrieved; 121 clones were from eight top bands ($^{12}C/^{14}N$-DNA) and 103 clones were from 6 bottom bands ($^{13}C/^{15}N$-DNA). Sufficient quantities of plasmid DNA for sequencing of the inserts were obtained from 159 clones. One hundred thirty nine sequences were of good quality and 20 were of poor quality due

to no priming or early termination. Analysis of partial sequences (500 bp) of 16S rRNA genes resulted in identification of one as a chimera and 22 sequences as undecipherable (could not be identified as chimeras or good sequences). Consequently, 116 environmental 16S rRNA gene sequences were utilized in the final exploration of the closest matches to the sequences in the NCBI database and the results are summarized in Table 5.1. Among all classifiable sequences obtained in this study, 98 % (114 sequences) fell within three classes of *Proteobacteria*, one sequence belonged to *Actinobacteria* and one to *Firmicutes*.

In the top bands, 47 out of 60 sequences were most closely related to two strains of chemoautotrophic ε-proteobacteria from genus *Sulfurovum*. Three out of six γ-proteobacterial sequences were most closely related to genus *Neptuniibacter*, two sequences to genus *Alteromonas*, and one sequence to genus *Pseudoalteromonas*. Three out of four α-proteobacterial sequences were most closely related to genus *Roseovarius* and one to genus *Oceanicola*.

In the bottom bands, 26 out of 56 sequences were most similar to the same two strains of chemoautotrophic ε-proteobacteria from genus *Sulfurovum* as in the top bands. Among γ-proteobacterial sequences, one was closely related to genus *Neptuniibacter* and 17 were related to several representatives of genus *Pseudoalteromonas*. α-proteobacterial sequences were most closely related to four different genera: 10 sequences were most similar to *Roseovarius* and single sequences were related to *Phaeobacter*, *Shimia*, and *Oceanicola*.

4.3. Identification of bacterial TRFs

In silico analysis of partial bacterial 16S rRNA gene sequences generated in this study permitted identification of several TRFs allowing for 1-4 bp differences between observed and predicted TRF sizes (Kent et al., 2003). The TRFs identified based on the closest matches to bacterial 16S rRNA gene sequences in the NCBI database are summarized in Table 5.2. The size standard used in this study does not permit correct determination of TRF sizes below 50 bp, therefore peaks < 50 bp in length were excluded from my analysis. That exclusion significantly affected the identification of TRFs in *Alu*I fingerprints because many of the predicted TRFs fell below 50 bp. As a consequence, only one TRF was identified as γ-proteobacterial *Pseudoalteromonas* and two TRFs as α-proteobacterial *Rhodobacterales* in *Alu*I fingerprints, hence data from *Alu*I fingerprints are not discussed further.

In *Hha*I fingerprints, two TRFs were identified as ε-proteobacteria from genus *Sulfurovum*. Three TRFs were identified as γ-proteobacterial genus *Pseudoalteromonas* and two as genus *Alteromonas*. Two TRFs matched α-proteobacterial *Rhodobacteraceae* and one TRF matched *Actinobacteria*.

In *Hinf*I fingerprints, three TRFs matched ε-proteobacterial genus *Sulfurovum* and two TRFs were identified as α-proteobacterial *Rhodobacteraceae*. γ-proteobacterial genera *Pseudoalteromonas* and *Alteromonas* were represented by four and two TRFs, respectively. Single TRFs were identified as *Actinobacteria* and *Firmicutes*.

In *Rsa*I fingerprints, two TRFs were identified as ε-proteobacteria from genus *Sulfurovum.* γ-proteobacterial genera *Pseudoalteromonas, Alteromonas,*and *Neptuniibacter* were represented each by two different TRFs. α-proteobacterial *Rhodobacteraceae* were represented by two TRFs as well.

4.4. Dominant TRFs in $^{13}C/^{15}N$-DNA fractions

TRFLP of bacterial 16S rRNA genes was used to obtain fingerprints of microbial assemblages in order to compare the $^{12}C/^{14}N$-DNA (top) and $^{13}C/^{15}N$-DNA (bottom) bands. Fingerprints from treatments with just ^{13}C-bicarbonate and ^{15}N-ammonium (unamended control) are available for only one (CAR169 at 310 m) of four samples collected in this study for reasons described above. In that sample, putative ε-proteobacterial peaks appeared in the digests: T513, T295, and T420 ('T' stands for 'terminal' fragment) in the *Hha*I, *Hinf*I, and *Rsa*I fingerprints, respectively. Furthermore, they were highly enriched in the $^{13}C/^{15}N$ band and barely detectable in the $^{12}C/^{14}N$ band. An example of an *Rsa*I fingerprint for that sample is illustrated in Fig. 5.2. Peak T295 in the *Hinf*I fingerprint in the $^{13}C/^{15}N$ band of that sample also corresponded to the predicted TRF from *Pseudoalteromonas prydzensis*. However, three other peaks predicted for *P. prydzensis*, T335 and T336 in the *Hha*I and T535 in the *Rsa*I fingerprints, were absent in the $^{13}C/^{15}N$ band of that sample and did not co-occur in the majority of the remaining samples. Consequently, detection of all three peaks (T513, T295, and T420) predicted for ε-proteobacteria in the same $^{13}C/^{15}N$ band strongly implies that peak T295 in *Hinf*I fingerprints was produced by ε-proteobacteria, not *P. prydzensis,* and this approach was applied to analyses of all remaining *Hinf*I fingerprints.

The response of microorganisms to additions of H_2S/NO_3^-, H_2S/Mn(IV), $S_2O_3^{2-}/NO_3^-$, and H_2S/Fe(III) in addition to ^{13}C-bicarbonate and ^{15}N-ammonium was evaluated based on the presence or absence of enriched TRFs in the $^{13}C/^{15}N$ bands compared to the $^{12}C/^{14}N$ bands. For clarity, examples of fingerprints obtained from each treatment are illustrated in the figures for one depth and a selected enzyme (e.g., Fig. 5.3). During CAR169, ε-proteobacteria (T420, *Rsa*I fingerprint) were very abundant in the $^{13}C/^{15}N$ band of samples amended with $S_2O_3^{2-}/NO_3^-$ and absent in the $^{12}C/^{14}N$ band at 280 m (not shown) while at 310 m they were present in both bands (Fig. 5.3). Along with ε-proteobacteria (in the same fingerprint), two unidentified peaks T104 and T160 were fairly abundant in the $^{13}C/^{15}N$ band at 310 m (Fig. 5.3) but not at 280 m (not shown). In samples amended with H_2S/Fe(III), ε-proteobacterial peak T420 was accompanied by an unidentified peak T104 in the $^{13}C/^{15}N$ band at 280 m (Fig. 5.4) but not at 310 m (not shown). The unidentified peaks T104 and T160 were detected in the *Rsa*I fingerprints only during CAR169.

During CAR163, in the samples amended with H_2S/Mn(IV), ε-proteobacterial peak T513 (*Hha*I) was predominant in the $^{12}C/^{14}N$ bands at 250 and 260 m. In the $^{13}C/^{15}N$ bands at both depths, this peak was accompanied by two unidentified peaks T246 (*Hha*I) and T295 (*Hha*I) (Fig. 5.5). In the samples amended with H_2S/NO_3^- at 250 m, ε-proteobacterial peak T295 (*Hinf*I) and γ-proteobacterial *Pseudoalteromonas* peak T288 (*Hinf*I) were present in both bands, and an unidentified peak T187 (*Hinf*I) was also present in the $^{13}C/^{15}N$ band (Fig. 5.6). At 260 m, only ε-proteobacterial peak T295 and unidentified peak T187 were predominant in the $^{13}C/^{15}N$ band (not shown).

5. Discussion

5.1. Inferred chemoautotrophic activity of ε-proteobacteria

One of the long-standing mysteries in the study of Cariaco's prokaryotic community has been the identity of the dominant chemoautotrophs. ε-proteobacteria have been hypothesized to be one of the most important taxa in dark carbon fixation in the Cariaco Basin based on their numerical prevalence in FISH surveys of the redoxcline at depths where elevated chemoautotrophic production rates are measured (Taylor et al., 2001; Lin et al., 2006, 2008).

Therefore, $^{13}C/^{15}N$-based DNA-SIP was employed here to detect and identify metabolically active chemoautotrophic microorganisms in the Cariaco Basin's redoxcline. About 60 % of all recovered 16S rRNA gene sequences were classified as ε-proteobacteria from genus *Sulfurovum*. These sequences were most similar to genomes of two strains of facultative anaerobic, mesophilic ε-proteobacteria isolated from hydrothermal vent sites, *Sulfurovum* sp NBC37-1 strain NBC37-1 (94-99 % identity) and *Sulfurovum lithotrophicum* strain 42BKT (95-99 % identity) (Inagaki et al., 2004; Nakagawa et al., 2007). Three unique TRFs (T513, T295, T420) produced by digestion of ε-proteobacterial 16S rRNA genes with three different restriction enzymes were identified in the isotope-labeled DNA samples. In the sample amended with just ^{13}C-bicarbonate and ^{15}N-ammonium, each of these TRFs was abundant in the $^{13}C/^{15}N$-labeled DNA and barely detectable in the $^{12}C/^{14}N$-labeled DNA. Thus, these findings demonstrate chemoautotrophic production by members of the ε-proteobacteria clade and their prevalence in the community over the course of the experiment. Further, these results are consistent with findings from previous studies of the Cariaco Basin microbial community by 16S rRNA gene sequencing. While subsequent research suggested some PCR bias (Lin, 2006), Madrid et al. (2001) showed that ε-proteobacterial sequences were dominant in libraries obtained from the redoxcline at 320 m and anoxic layer at 500 m. These ε-proteobacteria were most closely related to ectosymbionts of shrimp and epibionts of polychaetes endemic to deep-sea hydrothermal vents. A recent study by Rodriguez-Mora et al. (2013) utilizing the Sanger sequencing of DNA obtained from denaturing gradient gel electrophoresis of 16S rRNA genes showed that the majority of the recovered ε-proteobacterial sequences were closely related to genus *Sulfurovum*.

Based on their distribution in the redoxcline and chemical potential, H_2S, S^0, SO_3^{2-} and $S_2O_3^{2-}$ have been proposed as the most likely electron donors and NO_3^-, iron and manganese oxides as electron acceptors to fuel the Cariaco's chemoautotrophs (Scranton et al., 2001; Taylor et al., 2001; Ho et al., 2004; Hayes et al., 2006; Percy et al., 2008; Li et al., 2008). Chemoautotrophs capable of H_2S and $S_2O_3^{2-}$ oxidation with NO_3^- as an electron acceptor have been previously isolated from the water column and sediments in the Cariaco Basin (Tuttle and Jannasch, 1973). Selected electron donors and acceptors, when provided in excess, stimulate the chemoautotrophic productivity (measured by ^{14}C-bicarbonate assimilation) usually several fold but stimulation of > 100 fold has been occasionally measured as well (Taylor et al., 2001, 2006). One of the goals of the present study was to determine which chemoautotrophs are fueled by

selected energy substrates and electron acceptors. During CAR169, at 310 m (30 m below the oxic-anoxic interface), only a few TRFs were detected in the $^{12}C/^{14}N$ band in the sample amended with just isotopes and only ε-proteobacteria were detected in the $^{13}C/^{15}N$ band. This suggests that the activities of the microorganisms were low or the community was represented by fewer taxa at this depth. In fact, at this depth, the chemoautotrophic productivity sharply declined suggesting substrate limitation (data from G.T. Taylor, not shown). Amendments with $S_2O_3^{2-}$ /NO_3^- stimulated the ^{14}C-bicarbonate assimilation 14-fold. Prevalence of ε-proteobacterial TRFs in the $^{13}C/^{15}N$-DNA in the presence of the same stimulants indicates that ε-proteobacteria utilized $S_2O_3^{2-}$ as an electron donor and NO_3^- as an electron acceptor. During CAR163, chemoautotrophic production exhibited maximum rates at 250 m (10 m above the oxic-anoxic interface), yet additions of H_2S/NO_3^- further stimulated inorganic carbon fixation (G.T. Taylor, unpublished). In the SIP experiment, ε-proteobacterial TRFs were again dominant in the $^{13}C/^{15}N$ bands with the same stimulants suggesting growth by H_2S oxidation at the expense of NO_3^-.

Cultured representatives of *Sulfurovum* to which the Cariaco ε-proteobacteria are highly similar, are able to use H_2, S^{2-}, S^0 and $S_2O_3^{2-}$ (*Sulfurovum* sp NBC37-1 strain NBC37-1) (Nakagawa et al., 2007) and S^0 and $S_2O_3^{2-}$ (*Sulfurovum lithotrophicum* strain 42BKT) (Inagaki et al., 2004) as electron donors. Both strains use oxygen (in micro-oxic conditions) or nitrate (in sub-oxic to anoxic conditions) as electron acceptors (Inagaki et al., 2004; Nakagawa et al., 2007). Recent study using stable isotope probing of ^{13}C-fatty acid methyl esters (FAMEs) revealed co-occurrence of high concentrations of mid-chain methoxy fatty acids derived from sulfur-utilizing bacteria with elevated abundances of ε-proteobacteria in the redoxcline implying thiotrophic metabolism of these bacteria in the Cariaco's redoxcline (Wakeham et al., 2010). These mid-chain methoxy fatty acids accounted for about 73 % of the total fatty acids in the redoxcline. Further, amendments with $S_2O_3^{2-}$ resulted in detection of even higher concentrations of mid-chain methoxy fatty acids (up to 80 % of the total fatty acids) suggesting that thiosulfate was utilized as an electron donor by thiotrophic bacteria in the Cariaco's redoxcline (Wakeham et al., 2010). Findings from the present study suggest that ε-proteobacteria are the primary metabolizers of reduced sulfur species at the expense of nitrate reduction.

To my knowledge, there is no study in which chemoautotrophic activity of ε-proteobacteria has been demonstrated in the presence of Fe(III) or Mn(IV) as electron acceptors. None of the ε-proteobacterial isolates from the hydrothermal vents is capable of that type of metabolism in

culture either (Inagaki et al., 2004). In the Cariaco Basin, previous amendment experiments with Fe(III) and Mn(IV) as electron donors demonstrated stimulation of the chemoautotrophic productivity below the oxic-anoxic interface (Taylor et al., 2001, 2006). During CAR169, in the samples amended with H_2S/Fe(III), predominantly ε-proteobacterial TRFs were detected in $^{13}C/^{15}N$-DNA at 280 and 310 m. In my MAR-FISH sample from 310 m, 90 % of all detected ε-proteobacterial cells exhibited active uptake of ^{14}C-bicarbonate when provided with excess H_2S/Fe(III) (Chapter 4). Furthermore, chemoautotrophic productivity was stimulated by additions of H_2S/Fe(III) 21-fold at 310 m (30 m below the interface) but only 1.5-fold at 280 m at the oxic-anoxic interface. In contrast, during CAR163 at 250 (10 m above the interface) and 260 m (the interface), the chemoautotrophic production in the samples amended with H_2S/Mn(IV) did not exceed rates measured in the unamended samples. In the SIP experiment, ε-proteobacterial TRFs were again abundant in the $^{13}C/^{15}N$-DNA indicating activity of these bacteria in the presence of H_2S/Mn(IV). MAR-FISH results are unfortunately unavailable for comparison with these samples. Measurements of iron and manganese oxide concentrations are also not available for these two cruises. Nonetheless, past measurements indicate accumulation of dissolved Mn and Fe below the oxic-anoxic interface (Ho et al., 2004) and the peaks in concentrations of dissolved Mn and Fe usually coincide with chemoautotrophic productivity peaks below the oxic-anoxic interface (Taylor et al., 2001). During CAR163, two peaks in the chemoautotrophic productivity were observed, one at 250 m in the suboxic zone and one at 280 m (20 m below the oxic-anoxic interface). Lack of stimulation of chemoautotrophic productivity by addition of H_2S/Mn(IV) at both depths during CAR163 and a very low stimulation with H_2S/Fe(III) at 280 m during CAR169 might then suggest that the metal oxides were not preferentially utilized by the chemoautotrophs but the enrichments in ε-proteobacterial TRFs in the $^{13}C/^{15}N$-DNA suggest that members of this clade exhibit potential for that type of metabolism.

5.2. Significance of ε-proteobacteria in carbon, sulfur, and nitrogen cycling

Marine mesophilic ε-proteobacteria are increasingly being recognized as an important group of microorganisms in pelagic redoxclines (Lin et al., 2006, 2008; Glaubitz et al., 2009, 2010; Grote et al., 2012; Fuchsman et al., 2012). Initially, this clade was thought to live only in

extreme habitats, such as hydrothermal vents or hot sulfur springs (reviewed in Campbell et al., 2006), but now it is fairly well documented that relatives of these extremophiles are common in mesophilic sulfidic habitats as well (Inagaki et al. 2003, 2004; Campbell et al., 2006; Grote et al., 2008; Glaubitz et al., 2009; Fuchsman et al., 2012). Estimates of ε-proteobacterial abundance by FISH show that this clade accounts for a considerable fraction of the total community, i.e. 20 % in the Black Sea and ~ 30 % in the Cariaco Basin (Lin et al., 2006). Further, MAR-CARD-FISH based measurements of ε-proteobacterial activities in the redoxcline revealed that ~ 70 % of all ε-proteobacterial cells in the Baltic Sea and nearly 100 % in the Black Sea were chemoautotrophic (Grote et al., 2008). The high abundance and activity of pelagic ε-proteobacteria in habitats where H_2S and NO_3^- concentrations overlap indicate that this clade might be important in the carbon cycle. For example, Lavik et al. (2009) showed that ε-proteobacteria (along with γ-proteobacteria) were responsible for removal of high concentrations of sulfide at the expense of NO_3^- in an upwelling event off Namibia. In the present study, ε-proteobacteria were the only identifiable clade present in the $^{13}C/^{15}N$-DNA fraction in a sample amended with just stable isotopes indicating the dominance of this clade in the chemoautotrophic community in the Cariaco Basin. Amendment with H_2S or $S_2O_3^{2-}$ as energy substrates and NO_3^- as an electron acceptor demonstrated similar activities of ε-proteobacteria in the $^{13}C/^{15}N$-DNA fraction indicating that this clade is important also in sulfur and nitrogen cycles in the Cariaco Basin. Identification of the dominant chemoautotrophs in this system will guide future efforts in isolation of these microorganisms and detailed study of their activities in situ.

5.3. Activity of chemoheterotrophic gammaproteobacteria and unidentified TRFs

Through the use of ^{13}C and ^{15}N-labeled substrates, stable isotope probing links the identity of metabolically active microorganisms to their function in the environment (Radajewski et al., 2000; Neufeld et al., 2007b). As with every method, however, there are some important factors that may limit the interpretation of the results. Among such factors, cross-feeding of the labeled substrate to other bacteria or higher trophic level organisms during prolonged incubations might be the most obvious (Neufeld et al., 2007b; Moreno et al., 2010). In the present study, 48 h incubation time was sufficient to detect presence of chemoautotrophic ε-proteobacteria and no other lineages (clades) exhibited similar dominance in the $^{13}C/^{15}N$-DNA fraction in samples

amended with only isotopes as illustrated in Fig. 5.3. Transfer of labeled substrate to bacterivorous grazers was beyond the scope of this study and my results suggest that the transfer of labeled substrates to other bacteria was not significant at least in unamended control (Fig. 5.3). The detection of chemoorganotrophic γ-proteobacteria and several unidentified TRFs in the samples amended with selected substrates suggests either direct incorporation of ^{13}C and/or ^{15}N into their DNA or some cross-feeding as discussed below.

Chemoorganotrophic *Pseudoalteromonas* γ-proteobacteria are obligate aerobes commonly found in marine environments (Gauthier et al., 1995; Bowman and McMeekin, 2005). These microbes use organic substrates as carbon and energy sources, most use NH_4^+ as nitrogen source and oxygen as a terminal electron acceptor but some species can reduce NO_3^- to NO_2^- (Gauthier et al., 1995; Bowman and McMeekin, 2005). In the present study, 16S rRNA gene sequences highly similar (97-99 % identity) to several *Pseudoalteromonas* species were numerically abundant (17 clones) in the $^{13}C/^{15}N$-DNA amended with H_2S and NO_3^- during CAR163 at 250 m but did not exhibit similar prevalence at other depths or amendments. Trace amounts of oxygen (< 2 µM) were measured at 250 m indicating that the Cariaco relatives of *Pseudoalteromonas* might be facultative aerobes or microaerophilic. *Pseudoalteromonas* sp. have been shown to readily dominate microbial communities in microcosms when provided with excess stimulants (Schafer et al., 2000; Eilers et al., 2000) although these microbes are rarely abundant in situ (Schafer et al., 2000). Many *Pseudoalteromonas* sp. produce unknown bioactive compounds in order to outcompete or impede growth of other microorganisms (Bowman, 2007). Thus, it is likely that in my study the detection of these prokaryotes in the $^{13}C/^{15}N$-DNA fraction resulted partially from their faster growth than other microorganisms, incorporation of ^{15}N-ammonium, and incorporation of carbon fixed by chemoautotrophs (labeled with ^{13}C) through cross-feeding.

The presence of unidentified peaks cannot be adequately explained. However, the most likely reason for their detection in the $^{13}C/^{15}N$-DNA fraction is either direct incorporation of labeled substrates or a combination of incorporation of ^{15}N-ammonium, and incorporation of carbon fixed by chemoautotrophs. For example, TRF T104 was barely detectable in the bottom band at 310 m in sample amended with just isotopes (Fig. 5.3) but enriched in samples amended with $S_2O_3^{2-}/NO_3^-$ and H_2S/Fe(III) (Figs. 5.4 and 5.5). This suggests that the microorganisms that produced TRF T104 are capable of using $S_2O_3^{2-}$ and H_2S as energy substrates, or NO_3^- and iron oxide as electron acceptors. Another unidentified TRF T160 was not enriched in the sample

amended with just isotopes at 310 m and was only detected in samples amended with $S_2O_3^{2-}$ /NO_3^-, suggesting thiotrophic metabolism of that organism at the expense of nitrate but needs to be confirmed. These two TRFs were only enriched with the above amendments during CAR169 and not during CAR163 where different stimulants were applied. This suggests that the specificity of the response to these stimulants was the likely reason for the detection of these unidentified microorganisms. Enrichments in unidentified TRFs unique to CAR163 were also observed, however reference samples with just isotopes are not available for comparison. Whether the bacteria that produced these peaks are chemoautotrophs or chemoorganotrophs cannot be fully determined since both can incorporate ^{15}N-ammonium into their DNA. Future SIP experiments with ^{13}C and ^{15}N in separate incubations should shed some light on the type of metabolism some microorganisms express in the amendments.

6. Conclusions

This study demonstrated for the first time that ε-proteobacteria related to the genus *Sulfurovum* represent chemoautotrophs in the Cariaco Basin's redoxcline. Further, detection of ε-proteobacteria in amendments with selected substrates suggests that members of this clade are capable of utilizing H_2S and $S_2O_3^{2-}$ as energy substrates, or NO_3^- and iron oxide (and possibly manganese oxide) as electron acceptors. The detection of unidentified microorganisms in the ^{13}C/^{15}N-DNA in samples amended with selected substrates suggests that other chemoautotrophs might also be important but remains for further investigation.

Table 5.1. Summary of DNA-SIP samples and substrates (electron donors and acceptors) used in experiments in addition to ^{13}C-bicarbonate/^{15}N-ammonium amendments.

Cruise	Depth (m)	Substrate	Final concentration (µM)
CAR132	320, 340	$S_2O_3^{2-}$	50
CAR139	240, 270	$S_2O_3^{2-}$ SO_3^{2-} S^0	50 50 50
CAR145	250, 280	$S_2O_3^{2-}$ S^0	50 50
CAR153	240, 275	$S_2O_3^{2-}$/Mn(IV) $S_2O_3^{2-}$/Fe(III)	50/50 50/50
CAR157	278, 300	$S_2O_3^{2-}$/Mn(IV) $S_2O_3^{2-}$/Fe(III)	50/50 50/50
CAR163	250, 260	H_2S/NO_3^- H_2S/Mn(IV)	15/50 15/50
CAR169	280, 310	$S_2O_3^{2-}/NO_3^-$ H_2S/Fe(III)	50/50 15/50

Table 5.2. Phylogenetic assignment of individual 16S rRNA gene cloned sequences obtained from $^{13}C/^{15}N$-DNA (bottom band) and $^{12}C/^{14}N$-DNA (top band) and results from in silico digestions of all sequences. Out of 139 clones sequenced, one was a chimera and 22 could not be identified as chimeras or good sequences. Only good sequences are presented here. (-) not observed because TRFs of sizes below 50 bp were excluded from analysis (see text for details), (N/A) not assigned, (*) applies only to *P. aliena*. In sample labeling number (e.g., 250) indicates sample collection depth, C - control ($^{13}C/^{15}N$ amendments only), H – H_2S, M – Mv(IV), F – Fe(III), N – NO_3^-, S – $S_2O_3^{2-}$, T- top band ($^{12}C/^{14}N$-DNA), B - bottom band ($^{13}C/^{15}N$-DNA).

Sample	**Clone #**	**Phylogenetic group**	**Nearest NCBI match (accession no.) / % identity**	**Predicted (observed) TRFs**			
				***Alu*I**	***Hha*I**	***Hinf*I**	***Rsa*I**
CAR163 250_HMT	1, 2, 5 ,10	ε-proteobacteria	*Sulfurovum* sp. NBC37-1 strain NBC37-1 (NR_074503.1)/97-98 % *Sulfurovum lithotrophicum* strain 42BKT (NR_024802.1)/97-98 %	39 (-)	511 (513) (514)	296 (295) (296)	420 (420) (421)
	11	α-proteobacteria	*Oceanicola marinus* strain AZ0-C (NR_043969.1)/95 %	213 (213) (214)	26 (-)	263 (261)	71 (N/A)
	18	γ-proteobacteria	*Neptuniibacter caesariensis* strain MED92 (NR_042749.1)/96 %	39 (-)	336 (335) (336)	84 (N/A)	754 (752) (756)
CAR163 250_HMB	20-23	ε-proteobacteria	*Sulfurovum* sp. NBC37-1 strain NBC37-1 (NR_074503.1)/97-99 % *Sulfurovum lithotrophicum* strain 42BKT (NR_024802.1)/97-99 %	39 (-)	511 (513) (514)	296 (295) (296)	420 (420) (421)
CAR163 250_HNT	28, 30	ε-proteobacteria	*Sulfurovum* sp. NBC37-1 strain NBC37-1 (NR_074503.1)/95, 97 % *Sulfurovum lithotrophicum* strain 42BKT (NR_024802.1)/95, 97 %	39 (-)	511 (513) (514)	296 (295) (296)	420 (420) (421)

Table 5.2. Continued.

Sample	Clone #	Phylogenetic group	Nearest NCBI match (accession no.) / % identity	Predicted (observed) TRFs			
				***Alu*I**	***Hha*I**	***Hinf*I**	***Rsa*I**
CAR163 250_HNB	32-41, 45-46, 48-49, 51, 56-57	γ-proteobacteria	*Pseudoalteromonas paragorgicola* strain KMM3548 (NR_025654.1)/98 % *Pseudoalteromonas tetraodonis* strain IAM14160 (NR_041787.1)/98 % *Pseudoalteromonas atlantica* strain IAM12927 (NR_026218.1)/98 % *Pseudoalteromonas agarivorans* strain KMM255 (NR_025509.1)/98 % *Pseudoalteromonas elyakovii* strain KMM162 (NR_028722.1)/98 % *Pseudoalteromonas nigrifaciens* strain NCIMB8614 (NR_026222.1)/97-99 % *Pseudoalteromonas haloplanktis* strain ATCC14393 (NR_044837.1)/97-99 % *Pseudoalteromonas aliena* strain KMM3562 (NR_025775.1)/97-99 %	39 (-) 40 (-) 199* (198)*	330 (332) 331 (332) 332 (332)	287 288 289 (287) (288) (290)	528 529 530 (530)

Table 5.2. Continued.

Sample	Clone #	Phylogenetic group	Nearest NCBI match (accession no.) / % identity	Predicted (observed) TRFs			
				***Alu*I**	***Hha*I**	***Hinf*I**	***Rsa*I**
CAR163 260_T0T	60, 62, 66, 73	ε-proteobacteria	*Sulfurovum* sp. NBC37-1 strain NBC37-1 (NR_074503.1)/95-97 % *Sulfurovum lithotrophicum* strain 42BKT (NR_024802.1)/95-97 %	39 (-)	511 (513) (514)	296 (295) (296)	420 (420) (421)
	71	ε-proteobacteria	*Sulfurovum* sp. NBC37-1 strain NBC37-1 (NR_074503.1)/94 %	39 (-)	511 (513) (514)	296 (295) (296)	420 (420) (421)
	58, 61	γ-proteobacteria	*Alteromonas macleodii* str.'Balearic Sea AD45' strain Balearic Sea AD45 (NR_074797.1)/97 % *Alteromonas macleodii* strain 107 (NR_037127.1)/97 %	39 (-)	172 (173) (174)	287 (287) (288)	748 (751)
	72	γ-proteobacteria	*Pseudoalteromonas prydzensis* strain MB8_11 (NR_044803.1)/98 %	40 (-)	338 (336)	295 (295) (296)	536 (535)
	67	Actinobacteria	*Iamia majanohamensis* strain NBRC102561 (NR_041634.1)/89 %	128 (N/A)	334 (335)	300 (300)	424 (N/A)

Table 5.2. Continued.

Sample	Clone #	Phylogenetic group	Nearest NCBI match (accession no.) / % identity	Predicted (observed) TRFs			
				***Alu*I**	***Hha*I**	***Hinf*I**	***Rsa*I**
CAR163 260_CT	77, 80, 91, 99	ε-proteobacteria	*Sulfurovum* sp. NBC37-1 strain NBC37-1 (NR_074503.1)/95-97 % *Sulfurovum lithotrophicum* strain 42BKT (NR_024802.1)/95-97 %	39 (-)	511 (513) (514)	296 (295) (296)	420 (420) (421)
	79, 93	α-proteobacteria	*Thalassobius mediterraneus* strain:CECT5383=XSM19 (NR_042377.1)/96,98 %	215 (213) (214)	25 (-)	263 (261)	699 (701) (702)
CAR163 260_HMT	102-104, 106-112, 114-124, 127, 130, 133-136	ε-proteobacteria	*Sulfurovum* sp. NBC37-1 strain NBC37-1 (NR_074503.1)/96-98 % *Sulfurovum lithotrophicum* strain 42BKT (NR_024802.1)/96-98 %	39 (-)	511 (513) (514)	296 (295) (296)	420 (420) (421)

Table 5.2. Continued.

Sample	Clone #	Phylogenetic group	Nearest NCBI match (accession no.) / % identity	Predicted (observed) TRFs			
				***Alu*I**	***Hha*I**	***Hinf*I**	***Rsa*I**
CAR163 260_HMB	137-138, 141-143, 145, 147-148	ε-proteobacteria	*Sulfurovum* sp. NBC37-1 strain NBC37-1 (NR_074503.1)/94-98 % *Sulfurovum lithotrophicum* strain 42BKT (NR_024802.1)/94-98 %	39 (-)	511 (513) (514)	296 (295) (296)	420 (420) (421)
	146	α-proteobacteria	*Thalassobius mediterraneus* strain: CECT5383=XSM19 (NR_042377.1)/97 %	215 (213) (214)	25 (-)	263 (261)	699 (701) (702)
CAR163 260_HNT	153	ε-proteobacteria	*Sulfurovum* sp. NBC37-1 strain NBC37-1 (NR_074503.1)/97 % *Sulfurovum lithotrophicum* strain 42BKT (NR_024802.1)/97 %	39 (-)	511 (513) (514)	296 (295) (296)	420 (420) (421)
	151	α-proteobacteria	*Thalassobius mediterraneus* strain: CECT5383=XSM19 (NR_042377.1)/97 %	215 (213) (214)	25 (-)	263 (261)	699 (701) (702)

Table 5.2. Continued.

Sample	Clone #	Phylogenetic group	Nearest NCBI match (accession no.) / % identity	Predicted (observed) TRFs			
				***Alu*I**	***Hha*I**	***Hinf*I**	***Rsa*I**
CAR163 260_HNB	160, 164, 167, 170-171	ε-proteobacteria	*Sulfurovum* sp. NBC37-1 strain NBC37-1 (NR_074503.1)/97 % *Sulfurovum lithotrophicum* strain 42BKT (NR_024802.1)/97 %	39 (-)	511 (513) (514)	296 (295) (296)	420 (420) (421)
	155, 159, 161-163, 169, 176	α-proteobacteria	*Thalassobius mediterraneus* strain:CECT5383=XSM19 (NR_042377.1)/96-97 %	215 (213) (214)	25 (-)	263 (261)	699 (701) (702)
	157, 168	α-proteobacteria	*Roseovarius crassostreae* (NR_041731.1)/97 %	215 (213) (214)	26 (-)	263 (261)	80 (N/A)
	174	α-proteobacteria	*Phaeobacter daeponesis* strain TF-218 (NR_044026.1)/96 %	215 (213) (214)	26 (-)	263 (261)	699 (701) (702)
	177	α-proteobacteria	*Shimia marina* strain CL-TA03 (NR_043300.1)/98 %	215 (213) (214)	26 (-)	263 (261)	73 (N/A)
	178	α-proteobacteria	*Oceanicola granulosus* strain HTCC2516 (NR_027572.1)/95 %	215 (213) (214)	306 (305) (306)	263 (261)	387 (N/A)
	156	Firmicutes	*Lysinibacillus sphaericus* strain C3-41 (NR_074883.1)/99 % *Lysinibacillus sphaericus* strain DSM28 (NR_042073.1)/99 % *Lysinibacillus fusiformis* strain DSM2898 (NR_042072.1)/99 %	39 (-)	207 (204)	303 (305)	423 (N/A)

Table 5.2. Continued.

Sample	Clone #	Phylogenetic group	Nearest NCBI match (accession no.) / % identity	Predicted (observed) TRFs			
				***Alu*I**	***Hha*I**	***Hinf*I**	***Rsa*I**
CAR169 280_SNT	192	ε-proteobacteria	*Sulfurovum* sp. NBC37-1 strain NBC37-1 (NR_074503.1)/94 % *Sulfurovum lithotrophicum* strain 42BKT (NR_024802.1)/94 %	39 (-)	511 (513) (514)	296 (295) (296)	420 (420) (421)
	186, 191	γ-proteobacteria	*Neptuniibacter caesariensis* strain MED92 (NR_042749.1)/97-98 %	39 (-)	336 (335) (336)	84 (N/A)	754 (752) (756)
CAR169 280_SNB	194-195, 198-199	ε-proteobacteria	*Sulfurovum* sp. NBC37-1 strain NBC37-1 (NR_074503.1)/93-97 % *Sulfurovum lithotrophicum* strain 42BKT (NR_024802.1)/93-97 %	39 (-)	511 (513) (514)	296 (295) (296)	420 (420) (421)
CAR169 310_CT	208, 210-211	ε-proteobacteria	*Sulfurovum* sp. NBC37-1 strain NBC37-1 (NR_074503.1)/95-97 % *Sulfurovum lithotrophicum* strain 42BKT (NR_024802.1)/95-97 %	39 (-)	511 (513) (514)	296 (295) (296)	420 (420) (421)
CAR169 310_HFB	216, 220-224	ε-proteobacteria	*Sulfurovum* sp. NBC37-1 strain NBC37-1 (NR_074503.1)/96-978 % *Sulfurovum lithotrophicum* strain 42BKT (NR_024802.1)/96-98 %	39 (-)	511 (513) (514)	296 (295) (296)	420 (420) (421)
	218	γ-proteobacteria	*Neptuniibacter caesariensis* strain MED92 (NR_042749.1)/97 %	39 (-)	336 (335) (336)	84 (N/A)	754 (752) (756)

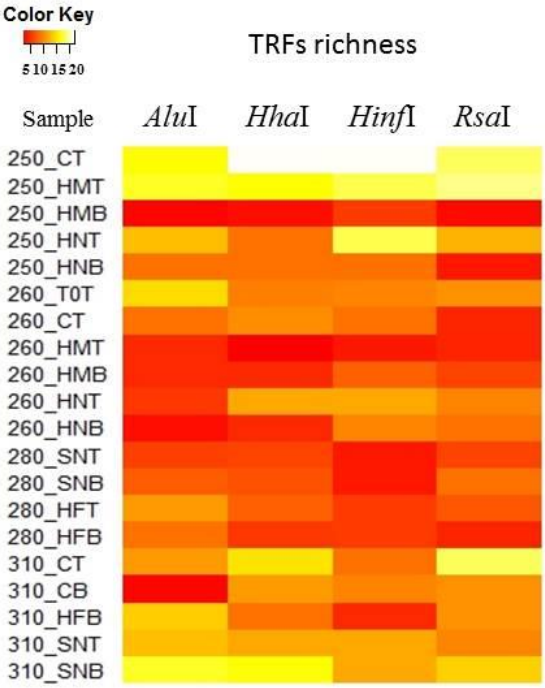

Sample	16S rRNA gene analysis No. of clones & phylogenetic affiliation	TRFLP & 16S rRNA
250_CT	N/A	
250_HMT	4 ε-proteobacteria, 1 α-proteobacteria, 1 γ-proteobacteria	X
250_HMB	4 ε-proteobacteria	X
250_HNT	2 ε-proteobacteria	X
250_HNB	17 γ-proteobacteria	X
260_T0T	5 ε-proteobacteria, 3 γ-proteobacteria, 1 Actinobacteria	X
260_CT	4 ε-proteobacteria, 2 α-proteobacteria	X
260_HMT	27 ε-proteobacteria	X
260_HMB	8 ε-proteobacteria, 1 α-proteobacteria	X
260_HNT	1 ε-proteobacteria, 1 α-proteobacteria	X
260_HNB	5 ε-proteobacteria, 12 α-proteobacteria, 1 Firmicutes	X
280_SNT	1 ε-proteobacteria, 2 α-proteobacteria	X
280_SNB	4 ε-proteobacteria	X
280_HFT	N/A	
280_HFB	N/A	
310_CT	3 ε-proteobacteria	X
310_CB	N/A	
310_HFB	6 ε-proteobacteria, 1 γ-proteobacteria	X
310_SNT	N/A	
310_SNB	N/A	

Figure 5.1. Heatmap representing TRF richness (number of peaks) in each sample from four restriction enzyme digestions and results of in silico 16S rRNA gene sequence analysis. 'X' in last column indicates samples for which both TRFLP and 16S rRNA sequencing data were obtained. N/A - not available, results not obtained because of poor DNA extraction, no separation in CsCl gradient, no PCR amplification, or bad quality 16S rRNA sequence. In sample labeling number indicates sample collection depth, C - control ($^{13}C/^{15}N$ amendments only), H – H_2S, M – Mv(IV), F – Fe(III), N – NO_3^-, S – $S_2O_3^{2-}$, T- top band ($^{12}C/^{14}N$-DNA), B - bottom band ($^{13}C/^{15}N$-DNA), T0 – time zero.

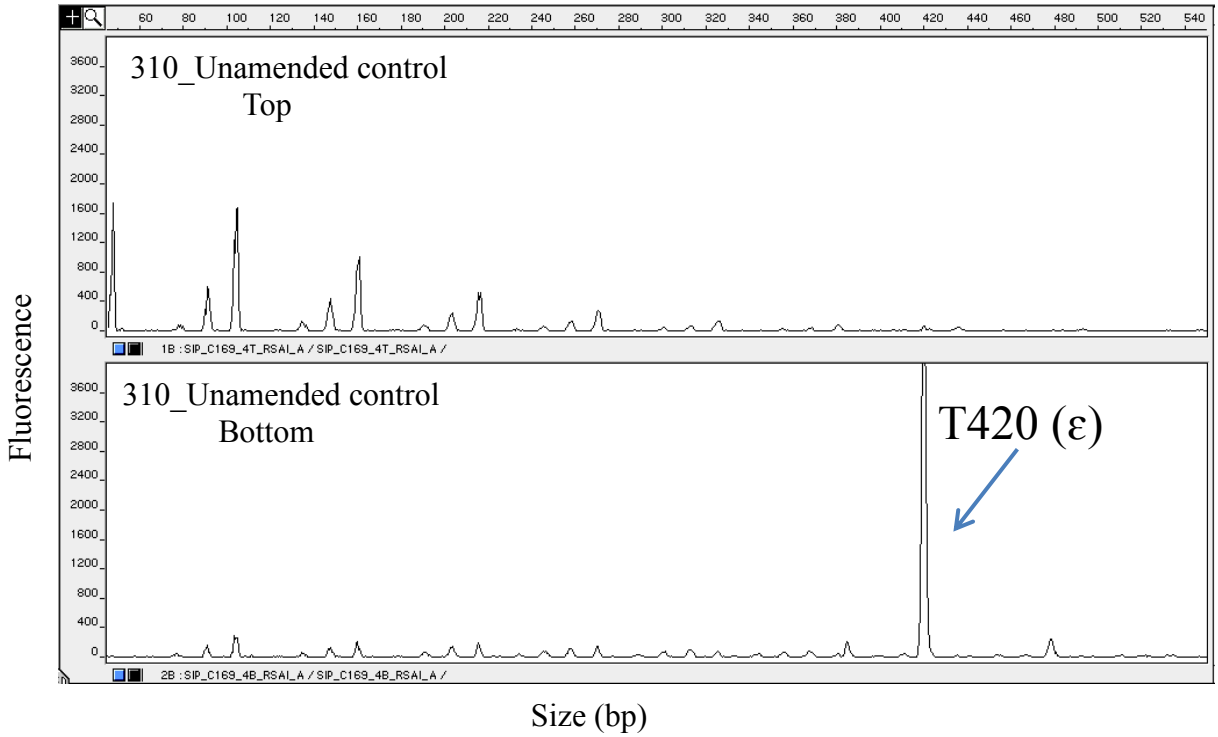

Figure 5.2. TRFLP fingerprints of $^{12}C/^{14}N$-DNA (upper panel) and $^{13}C/^{15}N$-DNA (lower panel) bands from unamended controls obtained after 48 h incubations of water from 310 m (CAR169) with ^{13}C-bicarbonate and ^{15}N-ammonium after digestion of amplified 16S rRNA genes with *Rsa*I endonuclease. (ε) ε-proteobacteria. Horizontal axis represents size of TRFs (in base pairs), vertical axis represents arbitrary fluorescence units.

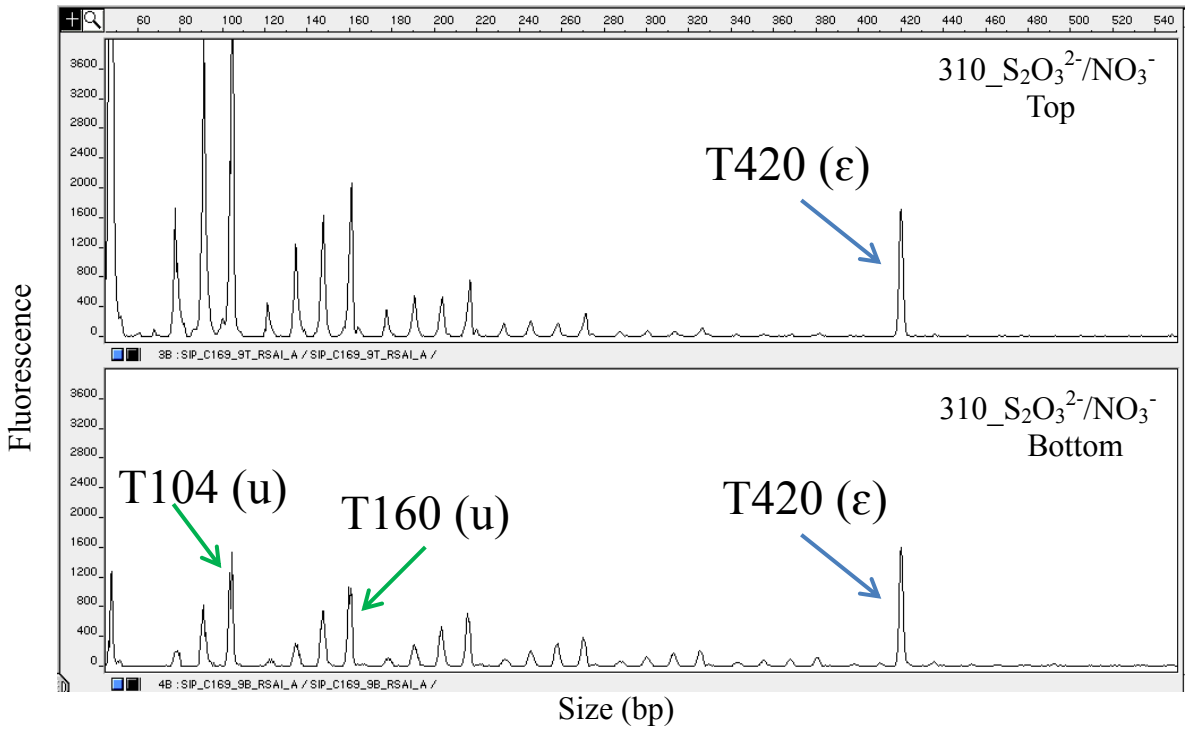

Figure 5.3. TRFLP fingerprints of $^{12}C/^{14}N$-DNA (upper panel) and $^{13}C/^{15}N$-DNA (lower panel) bands from samples amended with $S_2O_3^{2-}/NO_3^-$ obtained after 48 h incubations of water from 310 m (CAR169) with ^{13}C-bicarbonate and ^{15}N-ammonium after digestion of amplified 16S rRNA genes with *Rsa*I endonuclease. (ε) ε-proteobacteria, (u) unidentified. Horizontal axis represents size of TRFs (in base pairs), vertical axis represents arbitrary fluorescence units.

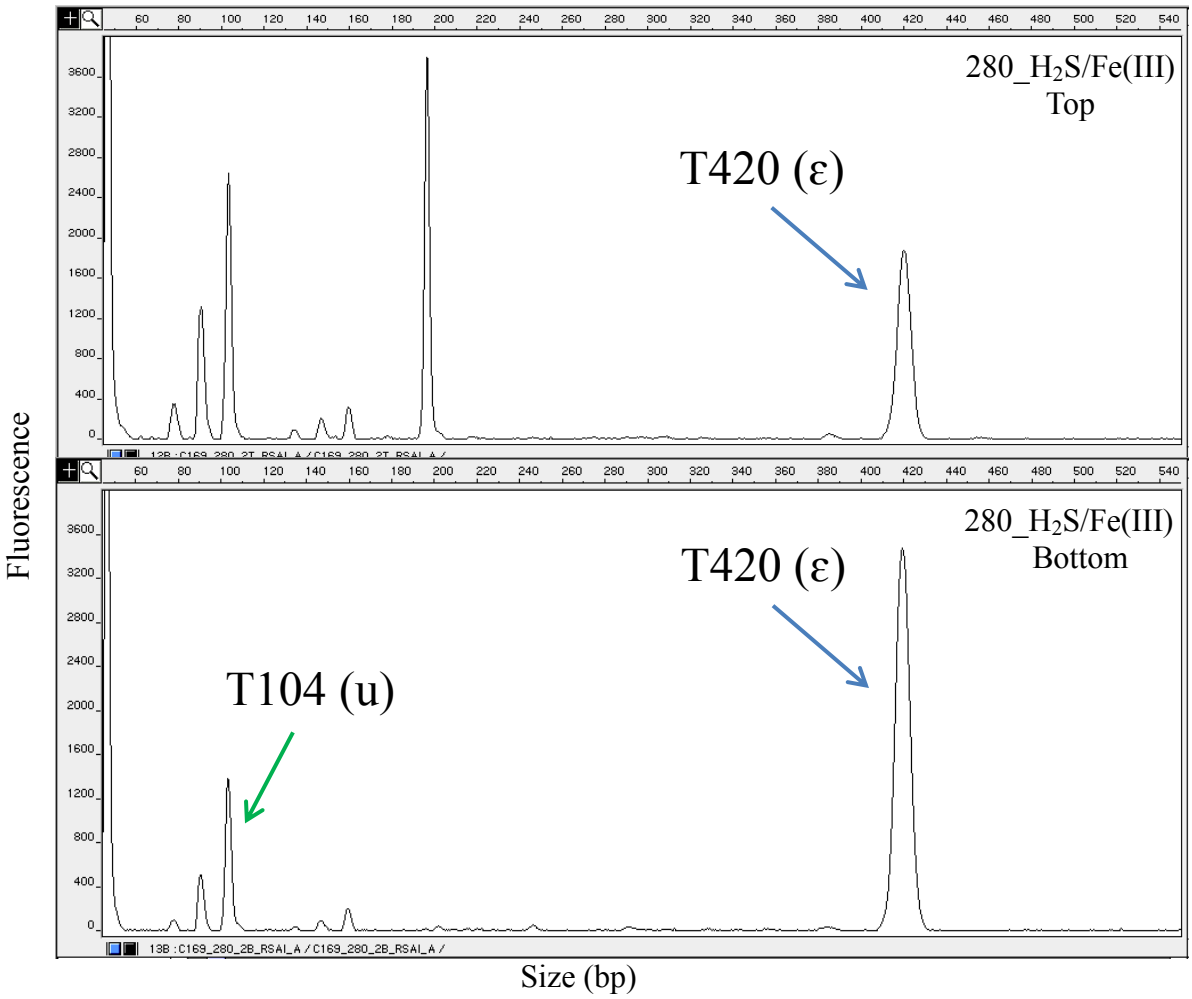

Figure 5.4. TRFLP fingerprints of $^{12}C/^{14}N$-DNA (upper panel) and $^{13}C/^{15}N$-DNA (lower panel) bands from samples amended with H_2S/Fe(III) obtained after 48 h incubations of water from 280 m (CAR169) with ^{13}C-bicarbonate and ^{15}N-ammonium after digestion of amplified 16S rRNA genes with *Rsa*I endonuclease. (ε) ε-proteobacteria, (u) unidentified. Horizontal axis represents size of TRFs (in base pairs), vertical axis represents arbitrary fluorescence units.

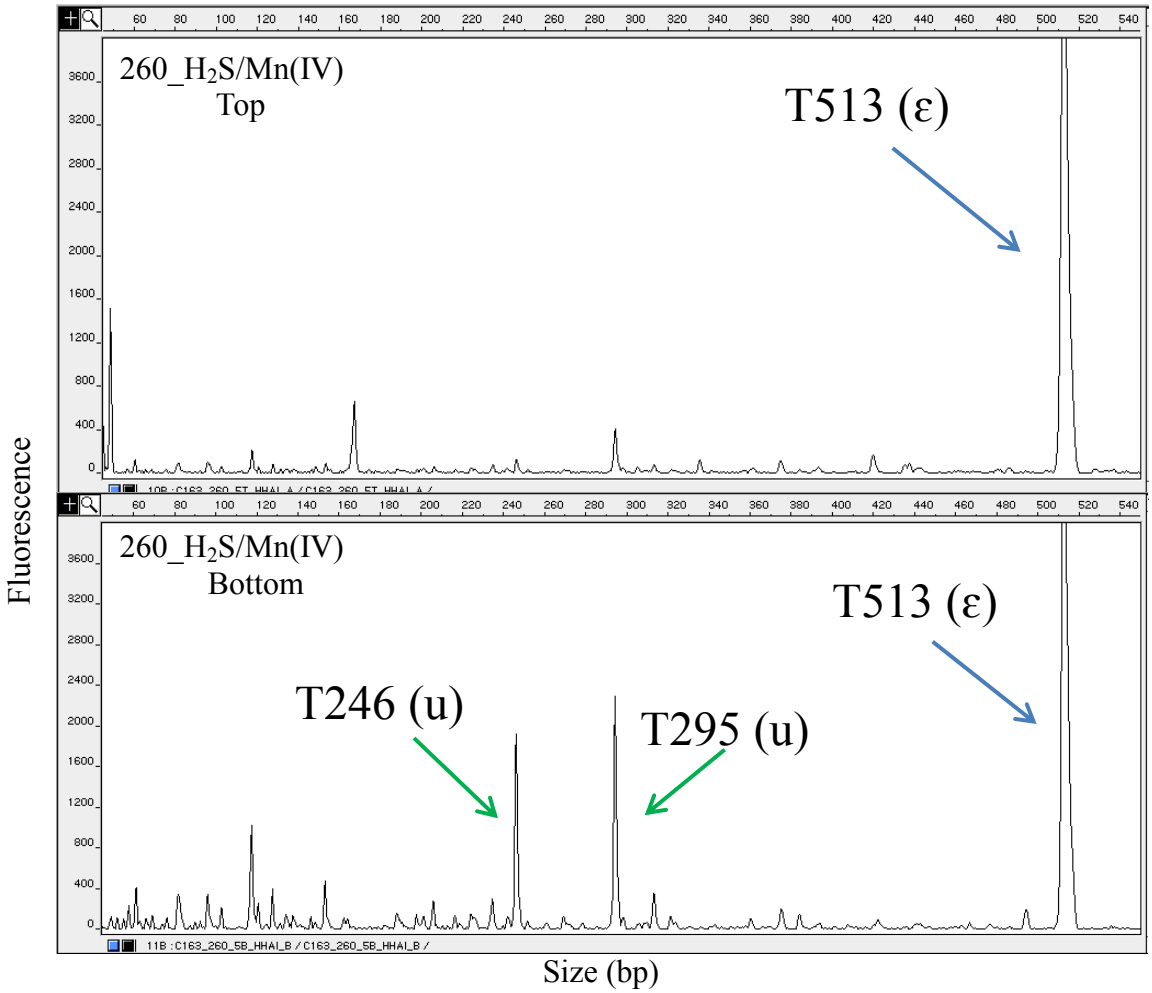

Figure 5.5. TRFLP fingerprints of $^{12}C/^{14}N$-DNA (upper panel) and $^{13}C/^{15}N$-DNA (lower panel) bands from samples amended with H_2S/Mn(IV) obtained after 48 h incubations of water from 260 m (CAR163) with ^{13}C-bicarbonate and ^{15}N-ammonium after digestion of amplified 16S rRNA genes with *Hha*I endonuclease. (ε) ε-proteobacteria, (u) unidentified. Horizontal axis represents size of TRFs (in base pairs), vertical axis represents arbitrary fluorescence units.

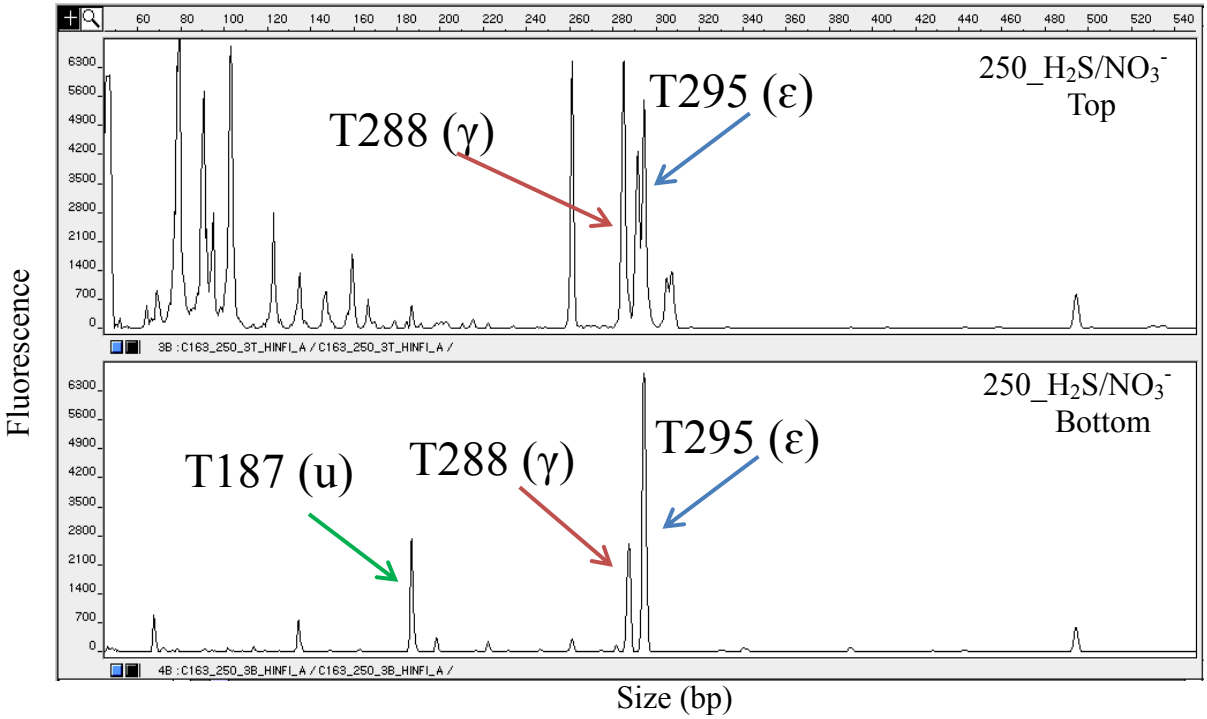

Figure 5.6. TRFLP fingerprints of $^{12}C/^{14}N$-DNA (upper panel) and $^{13}C/^{15}N$-DNA (lower panel) bands from samples amended with H_2S/NO_3^- obtained after 48 h incubations of water from 250 m (CAR163) with ^{13}C-bicarbonate and ^{15}N-ammonium after digestion of amplified 16S rRNA genes with *Hinf*I endonuclease. (ε) ε-proteobacteria, (γ) γ-proteobacteria, (u) unidentified. Horizontal axis represents size of TRFs (in base pairs), vertical axis represents arbitrary fluorescence units.

Chapter 6

Summary and Future Perspectives

Prokaryotic community abundances, distributions, and activities in relation to selected energy substrates and electron acceptors

In this work, I used a variety of molecular-based methods to study abundances, distributions, and activities of major proteobacterial and archaeal clades in the Cariaco Basin's redoxcline and to determine how these prokaryotes respond to selected electron donors and electron acceptors. I applied the FISH method to enumerate five major proteobacterial and two archaeal clades, and MAR-FISH with ^{14}C-bicarbonate and DNA SIP with ^{13}C/^{15}N as metabolic tracers in order to identify chemoautotrophic representatives of the prokaryotic community. Analyses of the prokaryotic community structure revealed prevalence of ε- and β-proteobacteria cells in the redoxcline while other bacterial clades (α-, γ-proteobacteria, and SRB δ-proteobacteria) were consistently less abundant, although occasional peaks in their cell numbers were observed. Archaeal clades Thaumarchaeota and Euryarchaeota were enriched in the redoxcline as well, although they were not as prevalent as bacterial clades.

ε-proteobacteria. ε-proteobacteria on average accounted for 15 % of the total prokaryotic community in the redoxcline (between 200 and 400 m) and peaks in abundance of this clade between 20-40 % of the total community were observed across the oxic-anoxic interface in most of the investigated cruises. Distributions of ε-proteobacteria covaried significantly with concentrations of sulfide, sulfite, thiosulfate, and ammonium. Distributions of thiosulfate and ammonium concentrations alone accounted for ~ 13-55 % and 8 % of variance in distributions of ε-proteobacteria, respectively. These results indicate that ε-proteobacteria are probably thiotrophic in the Cariaco Basin's redoxcline. Although concentrations of Mn and Fe substrates were not available for similar analysis, MAR-FISH results showed that up to 25 and 91 % of all ε-proteobacterial cells detected in the upper anoxic layer during CAR169 actively assimilated ^{14}C-bicarbonate in the presence of $S_2O_3^{2-}$/NO_3^- and H_2S/Fe(III), respectively. Additionally, abundances of ε-proteobacteria increased by 10-30 % in the presence of H_2S/NO_3^- or H_2S/Mn(IV) in the absence of bacterivorous grazers during CAR163 further suggesting that

these selected substrates are important in this clade's metabolism. Moreover, $^{13}C/^{15}N$-DNA SIP revealed that ε-proteobacteria related to the genus *Sulfurovum* were active chemoautotrophs in unamended samples and in samples amended with H_2S/Fe(III), H_2S/Mn(IV), H_2S/NO_3^-, and $S_2O_3^{2-}/NO_3^-$ suggesting that thiotrophic members of this clade are capable of using NO_3^- or metals as oxidants. Identification of these active chemoautotrophs should aid future efforts in isolation of these microorganisms in culture by designing more specific growth media and choosing the optimal growth conditions. Further, identification of ε-proteobacteria closely related to the genus *Sulfurovum* should aid in designing more specific oligonucleotide probes which can be applied to specifically target these chemoautotrophs and to quantify their abundances in situ more accurately than with the probe applied in my study. Moreover, newly designed FISH probes can be combined with microautoradiography to confirm the activity of identified ε-proteobacteria (full cycle rRNA approach) and additionally determine their metabolic activity in the presence of specific reductants and oxidants. Altogether, these results suggest that ε-proteobacteria found in the Cariaco Basin's redoxcline are represented by chemoautotrophs with thiotrophic metabolism coupled to NO_3^-, Fe(III), or Mn(IV) reduction.

γ-proteobacteria. γ-proteobacteria on average accounted for up to 5 % of the total prokaryotic community in the redoxcline and maximal contributions of this clade up to 18 % of the total community were observed across the oxic-anoxic interface in some cruises. Distributions of γ-proteobacteria covaried significantly with distributions of sulfide, sulfite, thiosulfate, nitrate, and nitrite. Distributions of sulfite and elemental sulfur alone accounted for ~ 21 and 20 % of variance in distributions of γ-proteobacteria, respectively, indicating that this clade might be represented by thiotrophic bacteria using NO_3^- as an oxidant and by nitrifying bacteria. In the MAR-FISH study, chemoautotrophic members of this clade accounted for up to 55 % of all γ-proteobacterial cells in unamended samples collected in the upper anoxic layer and for ~ 14 % of all γ-proteobacterial cells in a sample amended with H_2S/Fe(III). However, abundances of γ-proteobacteria did not increased in response to additions of H_2S/NO_3^- or H_2S/Mn(IV) in the absence of grazers during the investigated cruise nor could chemoautotrophic members of this clade be identified in the $^{13}C/^{15}N$-DNA SIP study. Either the combinations of substrates offered in the predator exclusion experiment were not limiting growth of this clade or these substrates are not the preferred electron donors and acceptors.

β-proteobacteria. β-proteobacteria on average accounted for 10 % of the total prokaryotic community in the redoxcline and peaks of about 20 % of the total community were observed in some cruises. Distributions of β-proteobacteria covaried significantly with concentrations of sulfide, sulfite, thiosulfate, elemental sulfur, ammonium, nitrate, and oxygen. Distributions of sulfite, thiosulfate, and ammonium accounted for up to 35, 15, and 36 % of variance in the distributions of this clade, respectively. Abundances of β-proteobacteria increased in response to grazers removal in the predator exclusion experiment but did not increase in response to additions of H_2S/NO_3^- or H_2S/Mn(IV) compared to unamended controls suggesting that this clade did not use NO_3^- and Mn(IV) as oxidants nor H_2S as substrate. These findings suggest that members of β-proteobacteria might be represented by nitrifiers and thiotrophs using sulfur substrates other than sulfide.

α-proteobacteria. α-proteobacteria on average accounted for up to 6 % of the total prokaryotic community in the redoxcline. Distributions of this clade covaried significantly with concentrations of sulfide, sulfite, and thiosulfate. Distributions of sulfide, sulfite, and thiosulfate accounted for ~ 11, up to 31 and up to 29 % of variance in the distributions of this clade, respectively. Additionally, distributions of α-proteobacteria significantly covaried with concentrations of ammonium. These findings suggest that members of this clade in the Cariaco Basin's redoxcline might be mainly represented by thiotrophs but some might be nitrate and nitrite reducers. Moreover, abundances of α-proteobacteria significantly declined in the presence of grazers and increased when released from grazing pressure indicating that this clade might be preferentially consumed by bacterivorous phagotrophs residing in the redoxcline.

Sulfate-reducing δ-proteobacteria. SRB on average accounted for 5-7 % of the total community in the redoxcline and distributions of this clade covaried with distributions of sulfide, thiosulfate, elemental sulfur, and nitrite but only distributions of elemental sulfur accounted for ~ 13 % of variance in the distributions of this clade. These results suggest that members of SRB found in the Cariaco Basin's redoxcline might be mostly represented by thiotrophic microorganisms.

Thaumarchaeota. Thaumarchaeota on average accounted for 4-8 % of the total prokaryotic community in the redoxcline and distributions of this clade covaried significantly with concentrations of sulfide, sulfite, thiosulfate, ammonium, and nitrite. Distributions of sulfide, thiosulfate, and elemental sulfur accounted for ~ 5, 7, and 29 % of variance in distributions of

this clade. Additionally, 80 % of all thaumarchaeal cells detected in the MAR-FISH study at one depth in the upper anoxic layer exhibited chemoautotrophic activity in the presence of H_2S/Fe(III). Moreover, abundances of Thaumarchaeota increased in response to additions of H_2S/NO_3^- or H_2S/Mn(IV) in the absence of grazers, indicating that these substrates are important in this clade's metabolism. Altogether, these findings suggest that members of Thaumarchaeota found in the Cariaco Basin's redoxcline have thiotrophic metabolism with possibly NO_3^-, Fe(III), or Mn(IV) as oxidants and some representatives might be nitrifying archaea.

Euryarchaeota. Euryarchaeota on average accounted for 4-8 % of the total prokaryotic community in the redoxcline depending on cruise and distributions of this clade covaried significantly with sulfide, elemental sulfur, and ammonium concentrations. Further, distributions of the above substrates and also sulfite accounted for ~ 16, 24, 28, and 17 % of variance in the distributions of this clade, respectively. Moreover, abundances of Euryarchaeota increased in response to addition of H_2S/Mn(IV) in the absence of grazers indicating that either sulfide alone was used as an energy substrate and/or the combination of sulfide and Mn oxide was used in the metabolic activity of this clade. These results suggest that members of Euryarchaeota found in the Cariaco Basin's redoxcline might be mostly represented by thiotrophic microorganisms. Based on the above findings, a modified conceptual model of major biogeochemical processes of carbon, sulfur, nitrogen, and metals cycles as well as major bacterial and archaeal clades whose representatives might be involved in these processes in the Cariaco Basin's redoxcline is illustrated in Fig. 6.1.

Methodological considerations

FISH is widely used for identification and enumeration of prokaryotic populations in many aquatic environments, but successful application of this method depends on several important factors discussed below (e.g., reviews by Amann et al., 1995; Amann and Fuchs, 2008). Organisms targeted with a specific rRNA probe have to be present in the environment in sufficient numbers at the time of sampling in order to be detected. Detection of specific groups might therefore depend on the volume of sample collected at specific depths but more importantly on the physiological state of target organisms (Amann et al., 1995; Amann and Fuchs, 2008). Small or slow growing cells can have low quantities of target rRNA and therefore

the signal intensity after hybridization can be low and hinder detection by epifluorescence microscopy. On the other hand, even large or fast growing cells can escape detection if their cell walls are not permeable enough for the probe to access the target site. And some live, but inactive, cells maintain sufficient amounts of rRNA for fluorescence detection (Amann et al., 1995).

Further, the relative contribution of specific clades to the total community is derived from its proportion to all DAPI-stained cells. DAPI staining is commonly used in enumeration of total prokaryotic cells, yet it does not discriminate between live, active or dead cells (Porter et al., 1995). Porter et al. (1995) reported that even up to 93 % of total DAPI-stained cells in an oligotrophic lake had membrane damage or lacked a nucleoid, indicating that a majority of the prokaryotic community was comprised of dead cells. Studies of marine bacterioplankton viability yielded variable results in which as little as 10 % or as much as 70 % of the total community was inactive (e.g., Zweifel and Hagstrom, 1995; Ouverney and Fuhrman, 1999).

Specificity of a probe applied to target microorganisms of interest is an important factor in detecting live cells by FISH. Probe specificity depends on its design which is based on the 16S or 23S rRNA sequences available for comparison in international databases, such as SILVA (http://www.arb-silva.de/). The number of sequences available for comparison in probe design increased rapidly over the last decade, yet many probes still target less than 90 % of specific groups and their coverage can be as low as 44 %, e.g., for *Planctomycetes* (Amann and Fuchs, 2008). Additionally, many of these probes hybridize with groups outside of the target group producing false-positive cell counts which might result in overestimation of some targeted populations. It is thus important to make every effort to design highly specific probes to more accurately assess contribution of specific organisms to the community. The fluctuations in each clade's contribution to the total community observed in the present study probably resulted from a combination of variations in cell abundances of the total prokaryotic community determined by DAPI staining, some limitations of the FISH method as well as temporal variations in the geochemistry of the Cariaco Basin's water column.

Since the vast majority of microorganisms detected in situ fail to grow in culture, their identification requires alternative approaches. During CAR169, when both MAR-FISH and DNA-SIP experiments were conducted, γ-proteobacteria accounted for 7 and 5 % of the total community while ε-proteobacteria accounted for 5 and 3 % of at 300 and 310 m, respectively. In

my MAR-FISH study with ^{14}C-bicarbonate as a metabolic tracer (Chapter 4), between 12 and 26 % of the total DAPI-stained community in unamended samples was chemoautotrophically active (silver grain positive cells). However, among all clades detected by FISH only γ-proteobacteria showed activity and these chemoautotrophs accounted for up to 50 % of all γ-proteobacteria probe-positive cells at two (300 and 310 m) out of the three investigated depths. ε-proteobacteria, which can account for a considerable fraction of the total community in the Cariaco Basin (Lin et al., 2006; this work) and in other pelagic redoxclines, such as in the Baltic Deeps and the Black Sea (Grote et al., 2008), were not detected as active in my MAR-FISH study in unamended samples despite concomitant detection of ε-proteobacteria probe-positive cells. To the contrary, ^{13}C/^{15}N-based DNA-stable isotope probing demonstrated that ε-proteobacteria related to the genus *Sulfurovum* were active chemoautotrophs in the Cariaco's redoxcline but no chemoautotrophic γ-proteobacteria were identified. Possible explanations for variations in detection and identification of active chemoautotrophs by MAR-FISH and DNA-SIP are discussed below.

Prominent differences between probe-positive, but inactive, cells have been observed by other researchers employing the MAR-FISH method in studies of prokaryotic activities and these discrepancies have been attributed to activities of prokaryotes below a detection threshold, inactivity at the time of sampling, or the cells were not using the substrate employed (Teira et al. 2004; Cottrell and Kirchman, 2004; Grote et al., 2008). Using MAR-FISH, Cottrell and Kirchman (2004) showed that the active prokaryotic community might vary between undetectable to 50 %. In my study, the initial contributions of γ-proteobacteria to the total prokaryotic community were only slightly higher than ε-proteobacteria (see above) but the incubation times for MAR-FISH and SIP were very different. Samples for MAR-FISH experiment were incubated for 18 hours while for SIP for 48 hours, which is ~ 2.5 times longer. Abundances of both clades decreased over the course of the MAR-FISH experiment indicating that cell growth was limited by substrate availability and/or that the prokaryotic assemblages were controlled by mortality. Therefore, the lack of detectable active ε-proteobacteria in the unamended samples in MAR-FISH might have been the result of too low abundance and probably too low activity of this clade compared to γ-proteobacteria for the detection by microautoradiography. Nielsen et al. (2000, 2003) showed that the level of metabolic activities varies between different prokaryotic assemblages and even between cells of the same population.

Although in the SIP experiment during CAR169 the active chemoautotrophic γ-proteobacteria could not be identified, there were several unidentified TRFs detected in the $^{13}C/^{15}N$-DNA fractions indicating that some unknown representatives of bacteria were chemoautotrophic. The lack of identifiable clones of chemoautotrophic γ-proteobacteria might, therefore, be the result of the PCR and cloning biases (Sambrook et al., 1989; Wintzingerode et al., 1997).

Discrepancies between different measurements add to the debate about what is actually important in assessments of the total community structure. Do we want to know the total number of cells or the number of cells that are alive and display activity when the right conditions arise? Many researchers suggest that reporting the number of active cells as fraction of viable cells instead of total DAPI-stained cells would be more informative in terms of the metabolic potential of different communities (e.g., Gasol et al., 1999; Karner and Fuhrman, 1997; Berman et al., 2001; Lebaron et al., 2001, 2002). Since active cells are responsible for cycling of carbon and other elements, it is imperative to know what fraction of the total live community they account for. Assessments of live versus dead cells have not been carried out in the Cariaco Basin. It would be worth investigating what the actual viable prokaryotic population is compared to the total cells detected by DAPI and what the spatial and temporal variations of the live community fraction are.

Since representatives of different groups can display similar metabolisms, it would be worth investigating how availability of different substrates and bacterivory affect specific functional groups, such as nitrate reducers, denitrifiers, and sulfur and ammonium oxidizers in addition to individual clades. This could be achieved by combining enumeration of specific clades by FISH with quantification of 16S rRNA and functional genes (e.g., *soxB, amoA, narG*) and comparison with measurements of prokaryotic metabolic rates, for example, by utilizing stable-isotope pairing technique in the presence and absence of grazers. Combination of these measurements (in the presence of grazers) has been successfully applied, e.g., in identification of nitrifying Thaumarchaeota and anammox bacteria in the Black Sea redoxcline (Lam et al., 2007).

In summary, this study showed that the prokaryotic community composition and distribution in the Cariaco Basin is highly variable and depends on the balance between bottom-up and top-down controlling mechanisms. These findings expand the understanding of the prokaryotic community structure in stratified marine pelagic environments depleted in oxygen and expand our knowledge about the dominant chemoautotrophs and their metabolic potential not only in the

Cariaco Basin but also in other marine pelagic redoxclines. My results show that methodological drawbacks can impose limitations on rigorous assessments of metabolic activities of some prokaryotic assemblages. More detailed studies are required to determine what can be improved in order to increase the confidence of results. On the other hand, despite these limitations, this work demonstrated for the first time that γ-proteobacteria and ε-proteobacteria represent active chemoautotrophic prokaryotes in the Cariaco Basin. Further, activities of these chemoautotrophs were detected when enriched with selected energy substrates and oxidants indicating potential for metabolic versatility not observed in other systems. These findings signify the importance of chemoautotrophic γ-proteobacteria and ε-proteobacteria in carbon, nitrogen and sulfur cycling in marine pelagic redoxclines.

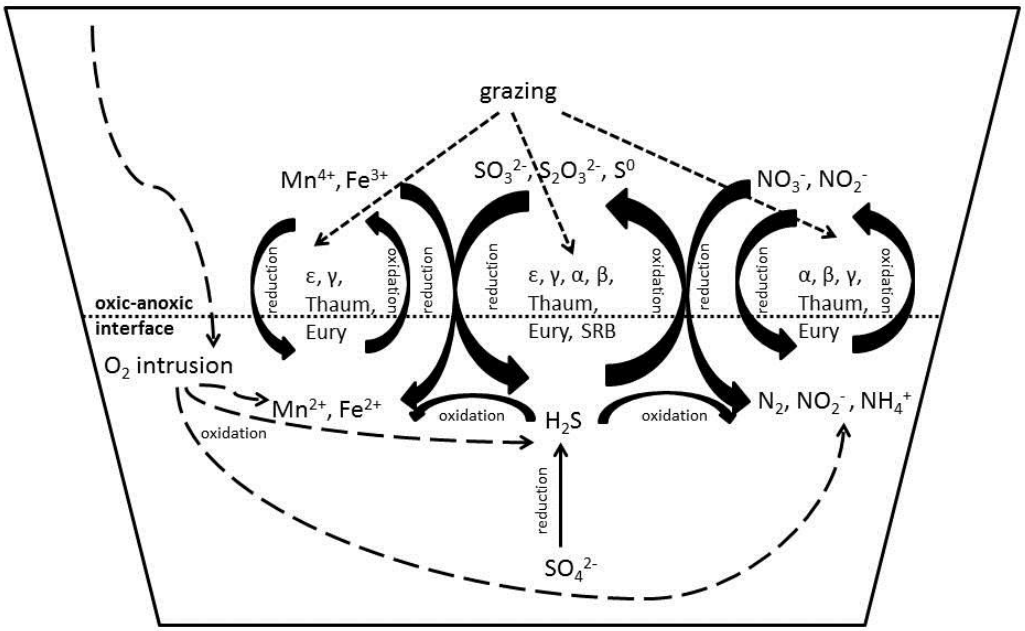

Figure 6.1. Schematic illustration of major biogeochemical processes in the Cariaco Basin's redoxcline with selected prokaryotic clades potentially involved in these processes. ε: ε-proteobacteria, γ: γ-proteobacteria, β: β-proteobacteria, α: α-proteobacteria, SRB: sulfate-reducing δ-proteobacteria, Thaum: Thaumarchaeota, Eury: Euryarchaeota.

References:

Aller, R.C. and Rude, P.D. 1988. Complete oxidation of solid phase sulfides by manganese and bacteria in anoxic marine sediments. Geochemica et Cosmochimica Acta 52(3): 751-795.

Amann, R. and Fuchs, B.M. 2008. Single-cell identification in microbial communities by improved fluorescence in situ hybridization techniques. Nature Rev. Microbiol. 6: 339-348.

Amann, R., Ludwig, W. and Schleifer, K-H. 1995. Phylogenetic identification and in situ detection of individual microbial cells without cultivation. Microbiol. Reviews 59(1): 143-169.

Amann, R. and Ludwig, W. 2000. Ribosomal RNA-targeted nucleic acid probes for studies in microbial ecology. FEMS Microbiol. Rev. 24: 555-565.

Amann, R., Fuchs, B.M. and Behrens, S. 2001. The identification of microorganisms by fluorescence in situ hybridization. Curr. Opin. Biotechnol. 12: 231-236.

Amann, R.I., Binder, B.J., Olson, R.J., Chisholm, S.W., Devereux, R. and Stahl, D.A. 1990. Combination of 16S rRNA-targeted oligonucleotide probes with flow cytometry for analyzing mixed microbial populations. Appl. Environ. Microbiol. 56: 1919-1925.

Amann, R.I., Snaidr, J., Wagner, M., Ludwig, W. and Schleifer, K. H. 1996. In situ visualization of high genetic diversity in a natural microbial community. J. Bacteriol. 178: 3496-3500.

Anderson, M.J. 2001. A new method for non-parametric multivariate analysis of variance. Austral Ecol. 26: 32-46.

Anderson, M.J. 2003. DISTLM *forward*: a FORTRAN computer program to calculate a distance-based multivariate analysis for a linear model using forward selection. Department of Statistics, University of Auckland, New Zealand.

Anderson, M.J. 2005. PERMANOVA: a FORTRAN computer program for permutational multivariate analysis of variance. Department of Statistics, University of Auckland, New Zealand.

Astor, Y., Muller-Karger, F. and Scranton, M.I. 2003. Seasonal and interannual variation in the hydrography of the Cariaco Basin: implications for basin ventilation. Cont. Shelf Res. 23: 125-144.

Azam, F.T, Fenchel, T., Field, J.G., Gray, J.S., Meyer-Reil, L.A., and Thingstad, T.F. 1983. The ecological role of water-column microbes in the sea. Mar. Ecol. Prog. Ser. 10: 257-263.

Bak, F. and Cypionka, H. 1987. A novel type of energy metabolism involving fermentation of inorganic compounds. Nature 326: 891-892.

Bak, F. and Pfennig, N. 1987. Chemolithotrophic growth of *Desulfovibrio sulfodismutans* sp. nov. by disproportionation of inorganic sulfur compounds. Archives of Microbiol. Vol. 147, no. 2, pp. 184-189.

Beller, H.R., Chain, P.S.G., Letain, T.E., Chakicherla, A., Larimer, F.W., Richardson, P.M., Coleman, M.A., Wood, A.P. and Kelly, D.P. 2006. The genome sequence of the obligately chemolithoautotrophic, facultatively anaerobic bacterium *Thiobacillus denitrificans.* J. Bacteriol. 188(4): 1473–1488.

Berger, W., Fischer, K., Lai, C. and Wu, G. 1988. Ocean carbon flux: Global maps of primary production and export production. *In* C. Agegian (ed.). Biogeochemical cycling and fluxes between the deep euphotic zone and other oceanic realms. NOAA National Undersea Research Program Report 88-1: 131-176.

Berman, T., Kaplan, B., Chava, S., Viner, Y., Sherr, B.F. and Sherr, E.B. 2001. Metabolically active bacteria in Lake Kinneret. Aquat. Microb. Ecol. 23: 213-224.

Bhowal, S. and Chakraborty, R. 2011. Five novel acid-tolerant oligotrophic thiosulfate-metabolizing chemolithotrophic acid mine drainage strains affiliated with the genus Burkholderia of Betaproteobacteria and identification of two novel soxB gene homologues. Res. Microbiol. 162(4): 436-45.

Black, D.E., Peterson, L.C, Overpeck, J.T, Kaplan, A., Evans, M.N and Kashgarian, M. 1999. Eight centuries of North Atlantic Ocean atmosphere variability. Science 286: 1709-1713.

Black, D.E., Thunell, R.C, Kaplan, A., Peterson, L.C., and Tappa, E.J. 2004. A 2000-year record of Caribbean and tropical North Atlantic hydrographic variability. Paleoceanogr. 19, PA2022, doi:10.1029/2003PA000982.

Blackwood, C.B., Marsh, T., Kim, S-H. and Paul, E.A. 2003. Terminal restriction fragment length polymorphism data analysis for quantitative comparison of microbial communities. Appl. Environ. Microbiol. 69(2): 926-932.

Boschker, H.T.S. and Middelburg, J.J. 2002. Stable isotopes and biomarkers in microbial ecology. FEMS Microbiol. Ecology 40: 85-95.

Boschker, H.T.S., Nold, S.C., Wellsbury, P., Bos, D., de Graaf, W., Pel, R., Parkes, R.J. and Cappenberg, T.E.. 1998. Direct linking of microbial populations to specific biogeochemical processes by ^{13}C-labelling of biomarkers. Nature 392: 801-805.

Bowman, J.P. and McMeekin, T.A. 2005. Genus XI. Pseudoalteromonas Gauthier, Gauthier and Christen 1995a, 759VP, In Bergey's Manual of Systematic Bacteriology, 2nd ed., Vol. 2 The Proteobacteria, Part B, The Gammaproteobacteria, DJ Brenner, NR Krieg, JT Staley, GM Garrity (ed), Springer, New York, pp. 467-478. ISBN 0-387-24144-2.

Bowman, J.P. 2007. Bioactive compound synthetic capacity and ecological significance of marine bacterial genus *Pseudoalteromonas*. Mar. Drugs 5: 220-241.

Brettar, I. and Rheinheimer, G. 1991. Denitrification in the Central Baltic: evidence for H_2S-oxidation as motor of denitrification at the oxic-anoxic interface. Mar. Ecol. Prog. Ser. 77: 157-169.

Brettar, I., Labrenz, M., Flavier, S., Bötel, J., Kuosa, H., Christen, R., and Höfle, M.G. 2006. Identification of a *Thiomicrospira denitrificans* -like epsilonproteobacterium as a catalyst for autotrophic denitrification in the central Baltic Sea. Appl. Environ. Microbiol. 72(2): 1364-1372.

Brochier-Armante, C., Boussau, B., Gribaldo, S., Forterre, P. 2008. Mesophilic crenarchaeota: proposal for a third archaeal phylum, the Thaumarchaeota. Nature Rev. Microbiol. 6: 245-252.

Bruckner, C.G., Mammitzsch, K., Jost, G., Wendt, J., Labrenz, M. and Jürgens, K. 2013. Chemolithoautotrophic denitrification of epsilonproteobacteria in marine pelagic redox gradients. Environ. Microbiol. 15(5): 1505-1513.

Buckley, D.H., Huangyutitham, V., Hsu, S.F., Nelson, T.A. 2007. Stable isotope probing with $^{15}N_2$ reveals novel non-cultivated diazotrophs in soil. Appl. Environ. Microbiol. 73: 3196-3204.

Buckley, D.H., Huangyutitham, V., Hsu, S.F., Nelson, T.A. 2008. $^{15}N_2$-DNA-stable isotope probing of diazotrophic methanotrophs in soil. Soil Biol. Biochem. 40: 1272-1283.

Burdige, D.J. 1993. The biogeochemistry of manganese and iron reduction in marine sediments. Earth Sci. Rev. 35(3): 249-284.

Burdige, D.J. and Nealson, K.H. 1986. Chemical and microbiological studies of sulfide-mediated manganese reduction. Geomicrobiol. J. 4: 361-387.

Cadisch, G., Espana, M., Causey, R., Richter, M., Shaw, E., Morgan, J.A.W., et al. 2005. Technical considerations for the use of ^{15}N-DNA stable-isotope probing for functional microbial activity in soils. Rapid Commun. Mass Spectrom. 19: 1424-1428.

Campbell, B.J. and Cary, S.C. 2004. Abundance of reverse tricaboxylic acid cycle genes in free-living microorganisms at deep-sea hydrothermal vents. Appl. Environ. Microbiol. 70(10): 6282-6289.

Campbell, B.J., Summers-Engel, A., Porter, M.L. and Takai, K. 2006. The versatile ε-proteobacteria: key players in sulphidic habitats. Nature Rev. 4: 458-468.

Campbell, B.J., Stein, J.L. and Cary, S.C. 2003. Evidence of chemolithoautotrophy in the bacterial community associated with *Alvinella pompejana*, a hydrothermal vent polychaete. Appl. Environ. Microbiol. 69: 5070-5078.

Campbell, B.J., Jeanthon, C., Kostka., J.E., Luther III, G.W. and Cary, S.C. 2001. Growth and phylogenethic properties of novel bacteria belonging to the Epsilon subdivision of the proteobacteria enriched from *Alvinella pompejana* and deep-sea hydrothermal vents. Appl. Environ. Microbiol. 67(10): 4566-4572.

Canfield, D.E., Stewart, F.J., Thamdrup, B., De Brabandere, L., Dalsgaard, T., Delong, E.F., Revsbech, N.P., Ulloa, O. 2010. A cryptic sulfur cycle in oxygen-minimum-zone waters off the Chilean coast. Science 330: 1375-1378.

Carman, K. 1993. Microautoradiographic detection of microbial activity. *In*: P.F. Kemp, B.F. Sherr, E.B. Sherr, and J.J. Cole (eds), Handbook of Methods in Aquatic Microbial Ecology, pp. 397-404. Lewis Publishers, London.

Cernadas Martin, S. 2012. Aerobic and anaerobic ammonia oxidizers in the Cariaco Basin: identification, quantification and community structure. Master Thesis. Stony Brook University. New York. USA.

Clement, B.G., Kehl, L.E., DeBord, K.L. and Kitts, Ch.L. 1998. Terminal restriction fragment patterns (TRFPs), a rapid, PCR-based method for the comparison of complex bacterial communities. J. Microbiol. Methods 31: 135-142.

Cline, J.D., 1969. Spectrophotometric determination of hydrogen sulfide in natural waters. Limnol. Oceanogr. 14: 454-458.

Cottrell, M.T., and Kirchman, D.L. 2004. Single-cell analysis of bacterial growth, cell size, and community structure in the Delaware estuary. Aquat. Microb. Ecol. 34: 139-149.

Crespo-Medina, M., Chatziefthimiou, A., Cruz-Matos, R., Pérez-Rodríguez, I., Barkay, T., Lutz, R.A., Starovoytov, V. and Vetriani, C. 2009. *Salinisphaera hydrothermalis* sp. nov., a mesophilic, halotolerant, facultatively autotrophic, thiosulfate-oxidizing gammaproteobacterium from deep-sea hydrothermal vents, and emended description of the genus *Salinisphaera*. Int. J. Syst. Evol. Microbiol. 59: 1497-503.

Cupples, A.M., Shaffer, E.A, Chee-Sanford, J.C. and Sims, G.K. 2006. DNA buoyant density shifts during ^{15}N-DNA stable isotope probing. Microbiol. Research doi: 10.1016/j.micres.2006.01.016.

Cypionka, H., Smock, A.M. and Böttcher, M.E. 1998. A combined pathway of sulfur compounds disproportionation in *Desulfovibrio desulfuricans.* FEMS Microbiol. Letters 166: 181-186.

Daims, H., Nielsen, J.L., Nielsen, P.H., Schleifer, K.-H., and Wagner, M. 2001. In situ characterization of *Nitrospira*-like nitrite-oxidizing bacteria active in wastewater treatment plants. Appl. Environ. Microbiol. 67: 5273-5284.

DeLong, E.F. 1992. Archaea in coastal marine environments. Proc. Natl. Acad. Sci. 89: 5685-5689.

Dumont, M.G. and Murrell, J.C. 2005. Stable isotope probing - linking microbial identity to function. Nat. Rev. Micro. 3: 499-504.

Edgcomb, V., Orsi, W., Bunge, J., Jeon, S., Christen, R., Leslin, C. et al. 2011a. Protistan microbial observatory in the Cariaco Basin, Caribbean. I. Pyrosequencing vs Sanger insights into species richness. ISME J 5: 1344-1356.

Edgcomb, V., Orsi, W., Taylor, G.T., Vdacny, P., Taylor, C., Suarez, P. et al. 2011b. Accessing marine protists from the anoxic Cariaco Basin. ISME J 5: 1237–1241.

Egert, M. and Friedrich, M.W. 2003. Formation of pseudo-terminal restriction fragments, a PCR-related bias affecting terminal restriction fragment length polymorphism analysis of microbial community structure. Appl. Environ. Microbiol. 69(5): 2555-2562.

Eilers, H., Pernthaler, J. and Amann, R. 2000. Succession of pelagic marine bacteria during enrichment: a close look on cultivation-induced shifts. Appl. Environ. Microbiol. 66: 4634–4640.

Epstein, S.S. and Shiaris, M.P. 1992. Size-selective grazing of coastal bacterioplankton by natural assemblages of pigmented flagellates, colorless flagellates, and ciliates. Microb. Ecol. 23(3): 211-225.

Fiala, G., Stetter, K.O., Jannasch, H.W., Langworthy, T.A. and Madon, J. 1986. *Staphylothermus marinus* sp. nov. represents a novel genus of extremely thermophilic submarine heterotrophic archaebacteria growing up to 98°C. *Syst. Appl. Microbiol*. 8: 106-113.

Finster, K., Liesack, W. and Thamdrup, B. 1998. Elemental sulfur and thiosulfate disproportionation by *Desulfocapsa sulfoexigens* sp. Nov., a new anaerobic bacterium isolated from marine surface sediment. Appl. Environ. Microbiol. 64(1): 119-125.

Fossing, H., Thode-Andersen, S. and Jorgensen, B.B. 1992. Sulfur isotope exchange between 35S-labeled inorganic compounds in anoxic marine sediments. Mar. Chem. 38: 117-132.

Friedrich, C.G., Quentmeier, A., Bardischewsky, F., Rother, D., Kraft, R., Kostka, S. and Prinz, H. 2000. Novel genes coding for lithotrophic sulfur oxidation of *Paracoccus pantotrophus* GB17. J. Bacteriol. 182(17): 4677-4687.

Fuchs G., Stupperich, E. and Eden, G. 1980. Autotrophic CO_2 fixation in *Chlorobium limicola* – evidence for the operation of a reductive tricarboxylic acid cycle in growing cells. Arch. Microbiol. 128: 64-71.

Fuchsman, C.A., Murray, J.W. and Staley, J.T. 2012. Stimulation of autotrophic denitrification by intrusions of the Bosporus Plume into the anoxic Black Sea. Front. Microbiol. 3: 1-14.

Fuhrman, J.A. 1999. Marine viruses and their biogeochemical and ecological effects. Nature 399: 541-548.

Fuhrman, J.A. and Noble, R.T. 1995. Viruses and protists cause a similar bacterial mortality in coastal seawater. Limnol. Oceanogr. 40: 1236-1242.

Gasol, J.M. 1994. A framework for the assessment of top-down vs bottom-up control of heterotrophic nanoflagellate abundance. Mar. Ecol. Prog. Ser. 113: 291-300.

Gasol, J.M., Zweifel, U.L., Peters, F., Fuhrman, J.A. and Hagstrom, A. 1999. Significance of size and nucleic acid content heterogeneity as measured by flow cytometry in natural planktonic bacteria. Appl. Environ. Microbiol. 65(10): 4475-4483.

Gasol, J.M., Pedros-Alio, C. and Vaque, D. 2002. Regulation of bacterial assemblages in oligotrophic plankton systems: results from experimental and empirical approaches. Antonie van Leeuwenhoek 81: 435-452.

Gauthier, G., Gauthier, M. and Christen, R. 1995. Phylogenetic analysis of the genera *Alteromonas, Shewanella,* and *Moritella* using genes coding for small-subunit rRNA sequences and division of the genus *Alteromonas* into two genera, *Alteromonas* (emended) and *Pseudoalteromonas* gen. nov., and proposal of twelve new species combinations. IJSEM 45(4): 755-461.

Ginige, M.P., Keller, J. and Blackall, L.L. 2005. Investigation of an acetate-fed denitrifying microbial community by stable-isotope probing, full-cycle rRNA analysis, and fluorescence in situ hybridization-microautoradiography. Appl. Environ. Microbiol. 71(12): 8683-8691.

Ginige, M.P., Hugenholtz,P., Daims, H., Wagner, M., Keller, J. and Blackall, L.L. 2004. Use of stable-isotope probing, full-cycle rRNA analysis, and fluorescence in situ hybridization-microautoradiography to study a methanol-fed denitrifying microbial community. Appl. Environ. Microbiol. 70(1): 588-596.

Glaubitz, S., Kießlich, K., Meeske, C., Labrenz, M. and Jürgens, K. 2013. SUP05 dominates the gammaproteobacterial sulfur oxidizer assemblages in pelagic redoxclines of the central Baltic and Black Seas. Appl. Environ. Microbiol. 79(8): 2767.

Glaubitz, S., Labrenz, M., Jost, G. and Jürgens, K. 2010. Diversity of active chemolithoautotrophic prokaryotes in the sulfidic zone of a Black Sea pelagic redoxcline as determined by rRNA-based stable isotope probing. FEMS Microbiol. Ecol. 74(1): 32-41.

Glaubitz, S., Lueders, T., Abraham, W-R., Jost, G., Jürgens, K. and Labrenz, M. 2009. ^{13}C-isotope analyses reveal that chemolithoautotrophic *Gamma*- and *Epsilonproteobacteria* feed a microbial food web in a pelagic redoxcline of the central Baltic Sea. Environ. Microbiol. 11(2): 326-337.

Goñi, M.A., Aceves, H.L., Thunell, R.C., Tappa, E., Black, D., Astor, Y., Varela, R. and Muller-Karger, F. 2003. Biogenic fluxes in the Cariaco Basin: a combined study of sinking particulates and underlying sediments. Deep Sea Research I 50: 781-807.

Gordon, L.I., Jennings, J.C. Jr., Ross, A.A. and Krest, J.M. 1993. A suggested Protocol For Continuous Flow Automated Analysis of Seawater Nutrients, *in*: WOCE Operations Manual. WHP office Report 90-1, WOCE report 77 No. 68/91, pp. 1-52.

Greene, E. A., Hubert, C., Nemati, M., Jenneman, G. E. and Voordouw, G. 2003. Nitrite reductase activity of sulphate-reducing bacteria prevents their inhibition by nitrate-reducing, sulphide-oxidizing bacteria. Environ. Microbiol. 5(7): 607-617.

Grote, J., Labrenz, M., Pfeiffer, B., Jost, G. and Jurgens, K. 2007. Quantitative distributions of *Epsilonproteobacteria* and a *Sulfurimonas* subgroup in pelagic redoxclines of the central Baltic Sea. Appl. Environ. Microbiol. 73: 7155-7161.

Grote, J., Schott., T., Bruckner, C.G., Glöckner, F.O., Jost, G., Teeling, H., Labrenz, M., and Jurgens, K. 2012. Genome and physiology of a model Epsilonproteobacterium responsible for sulfide detoxification in marine oxygen depletion zones. Proc. Natl. Acad. Sci. 109(2): 506-510.

Grote, J., Jost, G., Labrenz, M., Herndl, G.J. and Jurgens, K. 2008. *Epsilonproteobacteria* represent the major portion of chemoautotrophic bacteria in sulfidic waters of pelagic redoxclines of the Baltic and Black Seas. Appl. Environ. Microbiol. 74: 7546-7551.

Hayes, M.K, Taylor, G.T., Astor, Y. and Scranton, M.I. 2006. Vertical distributions of thiosulfate and sulfite in the Cariaco Basin. Limnol. Oceanogr. 51(1): 280-287.

Hedrich, S. and Johnson, D.B. 2013. *Acidithiobacillus ferridurans*, sp. nov.; 5 an acidophilic iron- , sulfur- and hydrogen-metabolizing 6 chemolithotrophic *Gammaproteobacterium.* Appl. Environ. Microbiol. doi:10.1099/ijs.0.049759-0

Ho, T.Y., Taylor, G.T., Astor, Y., Varela, R., Muller-Karger, F.E. and Scranton, M.I., 2004. Vertical and temporal variability of redox zonation in the water column of the Cariaco Basin: implications for organic carbon oxidation pathways. Mar. Chem. 86: 89-104.

Hobbie, J.E., Daley, R.J. and Jasper, S. 1977. Use of nucleopore filters for counting bacteria by fluorescence microscopy. Appl. Environ. Microbiol. 33: 1225-1228.

Holmen, K.J. and Rooth, C.G.H. 1990. Ventilation of the Cariaco Trench, a case of multiple source competition? Deep Sea Research Part A 37(2): 203-225.

Hugenholtz, P., Tyson, G.W. and Blackall, L.L. 2001. Design and evaluation of 16S rRNA-targeted oligonucleotide probes for fluorescence in situ hybridization. *In* M.Aquino de Muro and R. Rapley (ed.), Gene probes: principles and protocols. Humana Press, Totowa, N.J., pp. 29-42.

Hughen, A.K., Southon, J.R., Lehman, S.J. and Overpeck, J.T. 2000. Synchronous radiocarbon and climate shifts during the last Deglaciation. Science 290: 1951-1954.

Inagaki, F., Sakihama, Y., Inoue, A., Kato, C. and Horikoshi, K. 2002. Molecular phylogenetic analyses of reverse-transcribed bacterial rRNA obtained from deep-sea cold seep sediments. Environ. Microbiol. 4: 277-286.

Inagaki, F., Takai, K., Nealson, K. H. and Horikoshi, K. 2003. *Sulfurimonas autotrophica* gen. nov., sp. nov., a novel sulfur-oxidizing epsilon-proteobacterium isolated from hydrothermal sediments in the mid-Okinawa Trough. IJSEM 53: 1801-1805.

Inagaki, F., Takai, K., Nealson, K.H. and Horikoshi, K. 2004. *Sulfurovum lithotrophicum* gen. nov., sp. nov., a novel sulfur-oxidizing chemolithoautotroph within the e-Proteobacteria isolated from Okinawa Trough hydrothermal sediments. IJSEM 54: 1477-1482.

Ito, T., Nielsen, J.L., Okabe, S., Watanabe, Y. and Nielsen, P.H. 2002. Phylogenetic identification and substrate uptake patterns of sulfate-reducing bacteria inhabiting an oxic-anoxic sewer biofilm determined by combining microautoradiography and fluorescent in situ hybridization. Appl. Environ. Microbiol. 68(1): 356-364.

Jannasch, H.W. and Mottl, M.J. 1985. Geomicrobiology of deep-sea hydrothermal vents. Science 229: 717-725.

Jorgensen, B.B. 1990. A thiosulfate shunt in the sulfur cycle of marine sediments. Science 249: 152-154.

Jorgensen, B.B. and Nelson, D.C. 2004. Sulfide oxidation in marine sediments: geochemistry meets microbiology. *In* Sulfur Biochemistry. Past and Present. (ed) Amend J.P., K.J. Edwards, T.W. Lyons. Geological Society of America pp. 63-81.

Jorgensen, B.B. and Bak, F. 1991. Pathways and microbiology of thiosulfate transformations and sulfate reduction in marine sediment (Kattegat, Denmark). Appl. Environ. Microbiol. 57(3): 847-856.

Jost, G., Martens-Habbena, W., Pollehne, F., Schnetger, B. and Labrenz, M. 2010. Anaerobic sulfur oxidation in the absence of nitrate dominates microbial chemoautotrophy beneath the pelagic chemocline of the eastern Gotland Basin, Baltic Sea. FEMS Microbiol. Ecol. 71(2): 226-236.

Jost, G., Zubkov, M.V., Yakushev, E., Labrenz, M. and Jurgens, K.. 2008. High abundance and dark CO_2 fixation of chemolithoautotrophic prokaryotes in anoxic waters of the Baltic Sea. Limnol. Oceanogr. 53(1): 14-22.

Junier, P., Junier, T. and Witzel, K-P. 2008. TRiFLe, a program for in silico terminal restriction fragment length polymorphism analysis with user-defined sequence sets. Appl. Environ. Microbiol. 74(20): 6452-6456.

Jurgens, K. and Matz, C. 2002. Predation as a shaping force for the phenotypic and genotypic composition of planktonic bacteria. Antonie van Leeuwenhoek 81: 414-434.

Jurgens, K., Pernthaler, J., Schalla, S. and Amann, R. 1999. Morphological and compositional changes in a planktonic bacterial community in response to enhanced protozoan grazing. Appl. Environ. Microbiol. 65(3): 1241-1250.

Karner, M. and Fuhrman, J.A. 1997. Detremination of active marine bacterioplankton: a comparison of universal 16s rRNA probes, autoradiography and nucleoid staining. Appl. Environ. Microbiol. 63:1208-1213.

Kelly, D.P. and Wood, A.P. 2000. Confirmation of *Thiobacillus denitrificans* as a species of the genus *Thiobacillus*, in the *b*subclass of the *Proteobacteria*, with strain NCIMB 9548 as the type strain. IJSEM 50: 547–550.

Kent, A.D., Smith, D.J., Benson, B.J. and Triplett, E.W. 2003. Web-based phylogenetic assignment tool for analysis of terminal restriction fragment length polymorphism profiles of microbial communities. Appl. Environ. Microbiol. 69(11): 6768-6776.

Kirchman, D.L., Elifantz, H., Dittel, A.I., Malmstrom, R.R. and Cottrell, M.T. 2007. Standing stocks and activity of Archaea and Bacteria in the western Arctic Ocean. Limnol. Oceanogr., 52(2): 495-507.

Konneke, M., Bernhard, A.E., de la Torre, J.R., Walker, C.B., Waterbury, J.B. and Stahl, D.A. 2005. Isolation of an autotrophic ammonia-oxidizing marine archaeon. Nature 437: 543-546.

Kowalchuk, G.A. and Stephen, J.R. 2001. Ammonia-oxidizing bacteria: a model for molecular microbial ecology. Ann. Rev. Microbiol. 55(1): 485-529.

Kuypers, M.M.M., Sliekers, A.O., Lavik, G., Schmid, M., Jorgensen, B.B., Kuenen, J.G., Damste, J.S.S., Strous, M. and Jetten, M.S.M. 2003. Anaerobic ammonium oxidation by anammox bacteria in the Black Sea. Nature 422: 608-611.

La Cono, V., La Spada, G., Arcadi, E., Placenti, F., Smedile, F., Ruggeri, G., Michaud, L., Raffa, C., De Domenico, E., Sprovieri, M., Mazzola, S., Genovese, L., Giuliano, L., Slepak, V.Z. and Yakimov, M.M. 2013. Partaking of Archaea to biogeochemical cycling in oxygen-deficient zones of meromictic saline Lake Faro (Messina, Italy). Environ. Microbiol. 15(6): 1717-1733.

Labrenz, M., Jost, G., Pohl, Ch., Beckmann, S., Martens-Habbena, W. and Jurgens, K. 2005. Impact of different in vitro electron donor/acceptor conditions on potential chemolithoautotrophic communities from marine pelagic redoxclines. Appl. Environ. Microbiol. 71(11): 6664-6672.

Labrenz, M., Jost, G. and Jurgens, K. 2007. Distribution of abundant prokaryotic organisms in the water column of the central Baltic Sea with an oxic-anoxic interface. Aquat. Microb. Ecol. 46: 177-190.

Labrenz, M., Grote, J., Mammitzsch, K., Boschker, H.T.S., Laue, M., Jost, G., Glaubitz, S. and Jurgens, K. 2013. *Sulfurimonas gotlandica* sp. nov., a chemoautotrophic and psychrotolerant epsilonproteobacterium isolated from a pelagic Baltic Sea redoxcline, and an emended description of the genus *Sulfurimonas.* IJSEM doi:10.1099/ijs.0.048827-0.

Labrenz, M., Jost, G. and Jurgens, K. 2007. Distribution of abundant prokaryotic organisms in the water column of the central Baltic Sea with an oxic-anoxic interface. Aquat. Microb. Ecol. 46: 177-190.

Lam, P., Jensen, M.M., Lavik, G., McGinnis, D.F., Müller, B., Schubert, C.J., Amann, R., Thamdrup, B. and Kuypers, M.M.M. 2007. Linking crenarchaeal and bacterial nitrification to anammox in the Black Sea. Proc. Natl. Acad. Sci. 104(17): 7104-7109.

Lam, P., Lavik, G., Jensen, M.M., Van de Vossenberg, J., Schmid, M., Woebken, D., Gutiérrez, D., Amann, R., Jetten, M.S.M. and Kuypers, M.M.M. 2009. Revising the nitrogen cycle in the Peruvian oxygen minimum zone. Proc. Natl. Acad. Sci. 106(12): 4752-4757.

Lavik, G., Stührmann, T., Brüchert, V., Van der Plas, A., Mohrholz, V., Lam, P.,Mußmann, M., Fuchs, B. M., Amann, R., Lass, U. and Kuypers, M. M. M. 2009. Detoxification of sulphidic African shelf waters by blooming chemolithotrophs. Nature 457: 581-584.

Lebaron, P., Servais, P., Agouge, H., Courties, C. and Joux, F. 2001. Does the high nucleic acid content of individual bacterial cells allow us to discriminate between active cells and inactive cells in aquatic systems? Appl. Environ. Microbiol. 67(4): 1775-1782.

Lebaron, P., Servais, P., Baudoux, A-C., Bourrain, M., Courties, C. and Parthuisot, N. 2002. Variations of bacterial-specific activity with cell size and nnuclein acid content assessed by flow cytometry. Aquat. Microb. Ecol. 28: 131-140.

Lee, N., Nielsen, P.H., Andreasen, K.H., Juretschko, S., Nielsen, J.L., Schleifer, K-H. and Wagner, M. 1999. Combination of fluorescent in situ hybridization and microautoradiography-a new tool for structure-function analyses in microbial ecology. Appl. Environ. Microbiol. 65(3): 1289-1297.

Leuders, T., Wagner, B., Claus, P. and Friedrich, M.W. 2004a. stable isotope probing of rRNA and DNA reveals a dynamic methylotroph community and trophic interactions with fungi and protozoa in oxic rice field soil. Envir. Microbiol. 6(1): 60-72.

Leuders T., Manefield, M. and Friedrich, M.W. 2004b. Enhanced sensitivity of DNA- and rRNA-based stable isotope probing by fractionation and quantitative analysis of isopycnic centrifugation gradients. Envir. Microbiol. 6(1): 73-78.

Li, X., Taylor, G.T., Astor, Y. and Scranton, M.I. 2008. Relationship of sulfur speciation to hydrographic conditions and chemoautotrophic production in the Cariaco Basin. Mar. Chem. 112: 53-64.

Li, L., Kato, C. and Horikoshi, K. 1999. Microbial diversity in sediments collected from the deepest cold-seep area, the Japan Trench. Mar. Biotechnol. 1: 391-400.

Lin, X., Scranton, M.I., Varela, R., Chistoserdov, A.Y. and Taylor, G.T. 2007. Compositional responses of bacterial communities to redox gradients and grazing in the anoxic Cariaco Basin. Aquat. Microb. Ecol. 47: 57-72.

Lin, X. 2006. Bacterial population dynamics across the redox transition zone of the Cariaco Basin, Venezuela. Doctoral Dissertation. Stony Brook University. New York. USA.

Lin, X., Wakeham, S.G., Putnam, I.F., Astor, Y.M., Scranton, M.I., Chistoserdov, A.Y. and Taylor, G.T. 2006. Comparison of vertical distributions of prokaryotic assemblages in the anoxic Cariaco Basin and Black Sea by use of fluorescence in situ hybridization. Appl. Environ. Microbiol. 72(4): 2679-2690.

Lin, X., Scranton, M.I., Chistoserdov, A.Y., Varela, R. and Taylor, G.T. 2008. Spatiotemporal dynamics of bacterial populations in the anoxic Cariaco Basin. Limnol. Oceanogr. 53(1): 37-51.

Liu, W.T., Marsh, T.L., Cheng, H. and Forney, L.J. 1997. Characterization of microbial diversity by determining terminal restriction fragment length polymorphisms of genes encoding 16S rRNA. Appl. Environ. Microbiol. 63: 4516-4522.

Lorenzoni, L. 2005. The influence of local rivers on the eastern Cariaco Basin, Venezuela. M.Sc. Thesis. University of South Florida. Florida. USA.

Madrid, V. 2000. Characterization of the Bacterial communities in the anoxic zone of the Cariaco Basin. M.Sc. Thesis. SUNY Stony Brook. New York. USA.

Madrid, V.M., Taylor, G.T., Scranton, M.I. and Chistoserdov, A.Y. 2001. Phylogenetic diversity of bacterial populations in the anoxic zone of the Cariaco Basin. Appl. Environ. Microbiol. 67:1663-1674.

Malmstrom, R.R., Kiene, R.P., Cottrell, M.T., and Kirchman, D.L. 2004. Contribution of SAR11 Bacteria to Dissolved Dimethylsulfoniopropionate and Amino Acid Uptake in the North Atlantic Ocean. Appl. Environ. Microbiol. 70(7): 4129-4135.

Manefield, M., Whiteley, A.S., Ostle, N., Ineson, P. and Bailey, M.J. 2002a. Technical considerations for RNA-based stable isotope probing: an approach to associating microbial diversity with microbial community function. Rapid Commun. Mass Spectrom. 16: 2179-2183.

Manefield, M., Whiteley, A.S., Griffiths, R.I. and Bailey, M.J. 2002b. RNA stable isotoping probing, a novel means of linking microbial community function to phylogeny. Appl. Environ. Microbiol. 68(11): 5367-5373.

Manz, W., Amann, R., Ludwig, W., Wagner, M. and Schleifer, K.H. 1992. Phylogenetic oligodeoxynucleotide probes for the major subclasses of Proteobacteria: problems and solutions. Syst. Appl. Microbiol. 15: 593-600.

Marchesi, J., Sato, T., Weightman, A., Martin, T., Fry, J., Hiom, S., Dymock, D.and Wade, W. 1998. Design and evaluation of useful bacterium-specific PCR primers that amplify genes coding for bacterial 16S rRNA. Appl. Environ. Microbiol. 64: 795-799.

Marsh, T.L., Saxman, P., Cole, J. and Tiedje, J. 2000. Terminal restriction fragment length polymorphism analysis program, a web-based research tool for microbial community analysis. Appl. Environ. Microbiol. 66(8): 3616-3620.

Martin, J.H., Knauer, G.A., Karl, D.M. and Broenkow, W.W. 1987. VERTEX: carbon cycling in the northeast Pacific. Deep Sea Research Part A. 34(2): 267-285.

Massana, R., Unrein, F., Rodrıguez-Martinez, R., Forn, I., Lefort, T., Pinhassi, J. and Not, F. 2009. Grazing rates and functional diversity of uncultured heterotrophic flagellates. IJSME 3: 588-596.

McCune, B. and Mefford, M.J. 2006. PC-ORD. Multivariate Analysis of Ecological Data. Version 5.10. MjM Software, Gleneden Beach, Oregon, USA.

McManus, G.B., and Fuhrman, J.A. 1988. Control of marine bacterioplankton populations: Measurement and significance of grazing. Hydrobiologia 159: 51-62.

Miroshnichenko, M.L., Kostrikina, N.A., L'Haridon, S., Jeanthon, C., Hippe, H., Stackebrandt, E. and Bonch-Osmolovskaya, E.A. 2002. *Nautilia lithotrophica* gen. nov., sp nov., a thermophilic sulfur-reducing epsilon-proteobacterium isolated from a deep-sea hydrothermal vent. IJSEM 52: 1299-1304.

Moreno, A.M., Matz, C., Kjelleberg, S. and Manefield, M. 2010. Identification of ciliate grazers of autotrophic bacteria in ammonia-oxidizing activated sludge by RNA stable isotope probing. Appl. Environ. Microbiol. 76 (7): 2203-2211.

Mori, K., Suzuki, K-I., Urabe, T., Sugihara, M., Tanaka, K., Hamada, M. and Hanada, S. 2011. Thioprofundum hispidum sp. nov., an obligately chemolithoautotrophic sulfur-oxidizing gammaproteobacterium isolated from the hydrothermal field on Suiyo Seamount, and proposal of Thioalkalispiraceae fam. nov. in the order *Chromatiales.* IJSEM 61: 2412-2418.

Morris, I., Glover, H.E., Kaplan, W.A., Kelly, D.P. and Weightman, A.L. 1985. Microbial activity in the Cariaco Trench. Microbios. 42: 133-144.

Muller-Karger, F., Varela, R., Thunell, R., Astor, Y., Zhang, H., Luerssen, R. and Hu, Ch. 2004. Processes of coastal upwelling and carbon flux in the Cariaco Basin. Deep Sea Res. II 51: 927-943.

Nakagawa, S. and Takai, K. 2008. Deep-sea vent chemoautotrophs: diversity, biochemistry and ecological significance. FEMS Microbiol. Ecol. 65: 1-14.

Nakagawa, S., Takaki, Y., Shimamura, S., Reysenbach, A-L., Takai, K. and Horikoshi, K. 2007. Deep-sea vent ε-proteobacterial genomes provide insights into emergence of pathogens. PNAS 104(29): 12146-12150.

Nealson, K.H., Myers, C.R. and Wimpee, B.B. 1991. Isolation and identification of manganese-reducing bacteria and estimates of microbial Mn(IV)-reducing potential in the Black Sea. Deep Sea Res. 38, Suppl.2: S907-S920.

Neef, A., 1997. Anwendung der in situ Einzelzell-Identifizierung von Bakterien zur Populationsanalyse in komplexen mikrobiellen Biozönosen. Doctoral thesis (Technische Universität München).

Nelson, D.C. and Jannasch, H.W. 1983. Chemoautotrophic growth of marine *Beggiatoa* in sulfide-gradient cultures. Arch. Microbiol. 136: 262-269.

Neufeld, J.D., Vohra, J., Dumont, M.G., Lueders, T., Manefield, M., Friedrich, M.W. and Murrell, J.C. 2007a. DNA stable-isotope probing. Nature Protocols 2(4): 860-866.

Neufeld, J.D., Dumont, M.G., Vohra, J. and Murrell, J.C. 2007b. Methodological considerations for the use of stable isotope probing in microbial ecology. Microb. Ecol. 53: 435-442.

Nielsen J.L. and Nielsen, P.H. 2005. Advances in microscopy: microautoradiography of single cells. *In* J.R. Leadbetter (Ed): Methods of Enzymology. Academic Press, San Diego. 397: 237-256.

Nielsen, J.L., Anderson, K., Lee, N. and Wagner, M. 1999. Use of microautoradiography and fluorescent in situ hybridization for characterization of microbial activity in activated sludge. Wat. Sci. Tech. 39(1): 1-9.

Nielsen, J.L., Christensen, D., Kloppenborg, M., and Nielsen, P.H. 2003. Quantification of cell-specific substrate uptake by probe-defined bacteria under in situ conditions by microautoradiography and fluorescence in situ hybridization. Environ. Microbiol. 5: 202-211.

Orsi, W., Edgcomb, V.P., Jeon, S.O., Leslin, C., Bunge, J., Taylor, G.T., Varela, R. and Epstein, S. 2011. Protistan microbial observatory in the Cariaco Basin, Caribbean. II. Habitat specialization. ISME J. 5**:** 1357-1373.

Orsi, W., Song, Y.C., Hallam, S. and Edgcomb, V. 2012. Effect of oxygen minimum zone formation on communities of marine protists. ISME J. 6: 1586-1601.

Osorio, H., Mangold, S., Denis, Y., Nancucheo, I., Esparza, M., Johnson, D.B., Bonnefoy, V., Dopson, M. and Holmes, D.S. 2013. Anaerobic sulfur metabolism coupled to dissimilatory iron reduction in the extremophile *Acidithiobacillus ferrooxidans.* Appl. Environ. Microbiol. 79(7): 2172-2181.

Ouverney, C.C. and Fuhrman, J.A. 1999. Combined microautoradiography-16s rRNA probe techniques for determination of radioisotope uptake by specific microbial cell types in situ. Appl. Environ. Microbiol. 65: 1746-1752.

Ouverney, C.C. and Fuhrman, J.A. 2000. Marine planktonic Archaea take up amino acids. Appl. Environ. Microbiol. 66(11): 4829-4833.

Pace, M., Knauer, G., Karl, D. and Martin, J. 1987. Primary production, new production and vertical flux in the eastern Pacific Ocean. Nature 325: 803-804.

Percy, D., Li, X.N., Taylor, G.T., Astor, Y. and Scranton, M.I. 2008. Controls on iron, manganese and intermediate oxidation state sulfur compounds in the Cariaco Basin. Mar. Chem. 111: 47-62.

Pernthaler, A., Preston, Ch. M., Pernthaler, J., DeLong, E.F. and Amann, R. 2002. Comparison of fluorescently labeled oligonucleotide and polynucleotide probes for the detection of pelagic marine Bacteria and Archaea. Appl. Environ. Microbiol. 68(2): 661-667.

Pernthaler, J. 2005. Predation on prokaryotes in the water column and its ecological implications. Nat. Rev. Microbiol. 3 (7): 537-546.

Pernthaler, J., Glockner, F.O., Schonhuber, W. and Amann, R. 2001a. Fluorescence in situ hybridization with rRNA-targeted oligonucleotide probes. *In* J. Paul (ed.) Methods in Microbiology: Marine Microbiology., vol. 30. Academic Press Ltd, London.

Pernthaler, A., Pernthaler, J., Eilers, H. and Amann, R. 2001b. Growth patterns of two marine isolates: adaptations to substrate patchiness? Appl. Environ. Microbiol. 67(9): 4077-4083.

Perry, K.A., Kostka, J.E., Luther III, G.W., Nealson, K.H. 1993. Mediation of sulfur speciation by a Black Sea facultative anaerobe. Science 259: 801-803.

Podlaska, A., Wakeham, S.G., Fanning, K.A. and Taylor, G.T. 2012. Microbial community structure and productivity in the oxygen minimum zone of the eastern tropical North Pacific. Deep Sea Res. I 66: 77-89.

Porter, J., Diaper, J., Edwards, C. and Pickup, R. 1995. Direct measurements of natural planktonic bacterial community viability by flow cytometry. Appl. Environ. Microbiol. 61: 2783-2786.

Radajewski, S., Ineson, P., Parekh, N.R. and Murrell, J.C. 2000. Stable-isotope probing as a tool in microbial ecology. Nature 403: 646-649.

Radajewski, S., McDonald, I.R. and Murrell, J.C. 2003. Stable-isotope probing of nucleic acids: a window to the function of uncultured microorganisms. Curr. Opin. Biotechnol. 14: 296-302.

Redmond, M.C., Valentine, D.L. and Sessions, A.L. 2010. Identification of novel methane-, ethane-, and propane-oxidizing bacteria at marine hydrocarbon seeps by stable isotope probing. Appl. Environ. Microbiol. 76(19): 6412-6422.

Richards, F.A. 1975. The Cariaco Basin (Trench). Oceanogr. Mar. Bio. Ann. Rev. 13:11-67.

Rodriguez Mora, M.J. 2012. Bacterial communities in the Cariaco Basin redox transition zone and their role in sulfur and metal cycles. Doctoral dissertation. University of Louisiana. Lafayette. Luisiana. USA.

Rodriguez-Mora, M.J., Scranton, M.I., Taylor, G.T. and Chistoserdov, A.Y. 2013. Bacterial community composition in a large marine anoxic basin: a Cariaco Basin time-series survey. FEMS Microbiol. Ecol. 84: 625-639.

Rogers, S.W., Moorman, T.B. and Ong, S.K. 2007. Fluorescent in situ hybridization and microautoradiography applied to ecophysiology in soil. Soil Sci. Soc. Am. J. 71: 620-631.

Rösch, Ch. and Bothe, H. 2005. Improved assessment of denitrifying, N2-fixing, and total-community Bacteria by terminal restriction fragment length polymorphism analysis using multiple restriction enzymes. Appl. Environ. Microbiol. 71(4): 2026-2035.

Sakano, Y. and Kerkhof, L. 1998. Assessment of changes in microbial community structure during operation of an ammonia biofilter with molecular tools. Appl. Environ. Microbiol. 64(12): 4877-4882.

Sambrook, J., Fritch, E.F. and Maniatis, T. 1989. Molecular cloning: a laboratory manual. Cold Spring Harbor Laboratory. Cold Spring Harbor, NY. 2nd edition.

Schafer, H., Servais, P. and Muyzer, G. 2000. Successional changes in the genetic diversity of a marine assemblage during confinement. Arch. Microbiol. 173: 138–145.

Scott, K.M., Sievert, S.M., Abril, F.N., Ball, L.A., Barrett, C.J., et al. 2006. The genome of deep-sea vent chemolithoautotroph *Thiomicrospira crunogena* XCL-2. PLoS Biol. 4(12): e383.

Scranton, M.I. Sayles, F.L., Bacon, M.P. and Brewer, P.G. 1987. Temporal changes in the hydrography and chemistry of the Cariaco Trench. Deep Sea Res. Part A 34(5-6): 945-963.

Scranton, M.I., Astor, Y., Bohrer, R., Ho, T-Y. and Muller-Karger, F. 2001. Controls on temporal variability of the geochemistry of the deep Cariaco Basin. Deep Sea Res. I 48: 1605-1625.

Scranton, M.I., McIntyre, M., Astor, Y., Taylor, G.T., Muller-Karger, F., and Fanning, K. 2006. Temporal variability in the nutrient chemistry of the Cariaco Basin. Past and Present Water Column Anoxia. Nato Science Series IV; Earth and Environmental Sciences 64:139-160.

Sherr, E.B. and Sherr, B.F. 1987. High rates of consumption of bacteria by pelagic ciliates. Nature 325: 710-711. doi:10.1038/325710a0

Sherr, E.B. and Sherr, B.F. 2002. Significance of predation by protists in aquatic microbial food webs. Antonie van Leeuwenhoek 81: 293-308.

Simek, K., Pernthaler, J., Weinbauer, M.G., Hornak, K., Dolan, J.R., Nedona, J., Masin, M. and Amann, R. 2001. Changes in bacterial community composition and dynamics and viral mortality rates associated with enhanced flagellate grazing in a mesoeutrophic reservoir. Appl. Environ. Microbiol. 67(6): 2723-2733.

Siyambalapitiya, N. and Blackall, L.L. 2004. Discrepancies in the widely applied GAM42a flourescence in situ hybridisation probe for Gammaproteobacteria. FEMS Microbiol. Lett. 242: 367-373.

Sorokin, D.Y. 2003. Oxidation of inorganic sulfur compounds by obligately organotrophic bacteria. Microbiology 72(6): 641-653.

Stevens, H. and Ulloa, O. 2008. Bacterial diversity in the oxygen minimum zone of the eastern tropical South Pacific. Environ. Microbiol. 10(5): 1244-1259.

Stoeck, T., Taylor, G.T. and Epstein, S.S. 2003. Novel eukaryotes from the permanently anoxic Cariaco Basin (Caribbean Sea). Appl. Environ. Microbiol. 69(9): 5656-5663.

Strauss, H. 2006. Anoxia through time. *In*: Neretin L. (ed) Past and Present Water Column Anoxia. Springer, Dordrecht, Netherlands, pp. 3-19.

Sunamura, M., Higashi, Y., Miyako, C., Ishibashi, J-I. and Maruyama, A. 2004. Two *Bacteria* phylotypes are predominant in the Suiyo seamount hydrothermal plume. Appl. Environ. Microbiol. 70(2): 1190-1198.

Suttle, C. A. 2005. Viruses in the sea. Nature 437: 356-361.

Swan, B.K and Valentine, D.L. 2009. Diversity of Archaea. *In*: Encyclopedia of Life Sciences (ELS). John Wiley & Sons, Ltd: Chichester. DOI: 10.1002/9780470015902.a0000444.pub2.

Takai, K., Campbell, B.J., Cary, S.C., Suzuki, M., et al. 2005. Enzymatic and genetic characterization of carbon and energy metabolisms by deep-sea hydrothermal chemolithoautotrophicisolates of *Epsilonproteobacteria.* Appl. Environ. Microbiol. 71(11): 7310-7320.

Takai, K., Miyazaki, M., Hirayama, H., Nakagawa, S., Querellou, J., and Godfroy, A. 2009. Isolation and physiological characterization of two novel, piezophilic, thermophilic chemolithoautotrophs from a deep sea hydrothermal vent chimney. Environ. Microbiol. 11: 1983-1997.

Taylor, G. T. 1982. The role of pelagic heterotrophic protozoa in nutrient cycling: A review. Annales Inst. Oceanogr. (Paris) 58 (Suppl.): 227-241.

Taylor, G.T., Muller-Karger, F.E., Thunell, R.C., Scranton, M.I., Astor, Y., Varela, R., Troccoli Ghinagliae, L., Lorenzoni, L., Fanning, K. A., Hameed, S. and Doherty, O. 2012. Ecosystem responses in the southern Caribbean Sea to global climate change. Proc. Natl. Acad. Sci. 109(47): 19315-19320.

Taylor, G.T., Hein, C. and Iabichella, M. 2003. Temporal variations in viral distributions in the anoxic Cariaco Basin. Aquat. Microb. Ecol. 30(2): 103-116.

Taylor, G.T., Iabichella, M., Varela, R., Muller-Karger, F., Lin, X. and Scranton, M.I. 2006. Microbial ecology of the Cariaco Basin's redoxcline: the U.S.-Venezuela CARIACO times series program. Pp. 473-499. *In*: L.N. Neretin (ed), Past and Present Water Column Anoxia, Springer, Netherlands.

Taylor, G.T., Scranton, M.I., Iabichella, M., Ho, T.Y., Thunell, R.C. and Varela, R. 2001. Chemoautotrophy in the redox transition zone of the Cariaco Basin: a significant source of midwater organic carbon production. Limn. Oceanogr. 46: 148-163.

Teira, E., Reinthaler, T., Pernthaler, A., Pernthaler, J. and Herndl, G.J. 2004. Combining catalyzed reporter deposition-fluorescence in situ hybridization and microautoradiography to detect substrate utilization by Bacteria and Archaea in the deep ocean. Appl. Environ. Microbiol. 70: 4411-4414.

Thamdrup, B., Finster, K., Würgler Hansen, J. and Bak, F. 1993. Bacterial disproportionation of elemental sulfur coupled to chemical reduction of iron or manganese. Appl. Environ. Microbiol. 59(1): 101-108.

Thingstad, T.F. 2000. Control of bacterial growth in idealized food webs. *In* D.L. Kirchman (ed.), Microbial Ecology of the Oceans, 1st edn. Wiley-Liss, pp. 229-260.

Thingstad, T.F. and Lignell, R. 1997. Theoretical models for the control of bacterial growth rate, abundance, diversity and carbon demand. Aquat. Microb. Ecol. 13: 19-27.

Thunell, R.C., Varela, R., Llano, M., Collister, J., Muller-Karger, F. and Bohrer, R. 2000. Organic carbon fluxes, degradation, and accumulation in an anoxic basin: sediment trap results from the Cariaco basin. Limnol. Oceanogr. 45(2): 300-308.

Tuttle, J.H. and Jannasch, H.W. 1972. Occurrence and types of *Thiobacillus*-like bacteria in the sea. *Limnol. Oceanogr.* 17:532–543.

Tuttle, J.H. and Jannasch, H.W. 1973. Sulfide and thiosulfateoxidizing bacteria in anoxic marine basins. Mar. Biol. 20: 64–70.

Tuttle, J.H. and Jannasch, H.W. 1977. Thiosulfate stimulation of microbial dark assimilation of carbon dioxide in shallow marine waters. Microbial ecology 4: 9-25.

Tuttle, J.H. and Jannasch, H.W. 1979. Microbial dark assimilation of CO2 in the Cariaco trench. Limnol. Oceanogr. 24(4): 746-753.

Urios, L., Michotey, V., Intertaglia, L., Lesongeur, F. and Lebaron, P. 2008. *Nisaea denitrificans* gen. nov., sp. nov. and *Nisaea nitritireducens* sp. nov., two novel members of the class *Alphaproteobacteria* from the Mediterranean Sea. IJSEM 58: 2336-2341.

Vairavamurthy, A. and Mopper, K. 1990. Determination of sulfite and thiosulfate in aqueous samples including anoxic seawater by liquid chromatography after derivatization with 2, 2′-dithiobis (5-nitropyridine). Environ. Sci. Technol. 24: 333-337.

Vésteinsdóttir, H., Reynisdóttir, D. B. and Orlygsson, J. 2011. Thiomonas islandica sp. nov., a moderately thermophilic, hydrogen- and sulfur-oxidizing betaproteobacterium isolated from a hot spring. IJSEM 61: 132-7.

Vetriani, C., Tran, H.V., Kerkhof, L.J. 2003. Fingerprinting microbial assemblages from the oxic/anoxic chemocline of the Black Sea. Appl. Environ. Microbiol. 69: 6481-6488.

Wagner, M., Horn, M. and Daims, H. 2003. Fluorescence in situ hybridization for the identification and characterization of prokaryotes. Curr. Opin. Microbiol. 6: 302-309.

Wakeham, S.G., Turich, C., Schubotz, F., et al. 2012. Biomarkers, chemistry and microbiology show chemoautotrophy in a multilayer chemocline in the Cariaco Basin. Deep Sea Res. I. 63: 133-156.

Wakeham, S.G., Turich, C., Taylor, G.T., Podlaska, A., Scranton, M.I., Li, X.N., Varela, R. and Astor, Y. 2010. Mid-chain mehtoxylated fatty acids within the chemocline of the Cariaco Basin: a chemoautotrophic source? Org. Geochem. 41: 498-512.

Wallner, G., Amann, R. and Beisker, W. 1993. Optimizing fluorescent in situ hybridization with rRNA-targeted oligonucleotide probes for flow cytometric identification of microorganisms. Cytometry. 14: 136-143.

Walsh, D.A., Zaikova, E., Howes, C.G., Song, Y.C., Wright, J.J., Tringe, S.G., Tortell, P.D. and Hallam, S.J. 2009. Metagenome of a versatile chemolithoautotroph from expanding oceanic dead zones. Science 236: 578-582.

Wawrik, B., Boling, W.B., Van Nostrand, J.D., Xie, J., Zhou, J. and Bronk, D.A. 2012. Assimilatory nitrate utilization by bacteria on the West Florida Shelf as determined by stable isotope probing and functional microarray analysis. FEMS Microbiol. Ecol. 79: 400-411.

Weisse, T. 2002. The significance of inter- and intraspecific variation in bacterivorous and herbivorous protists. Antonie van Leeuwenhoek 81: 327-341.

Widdel, F. 1988. Microbiology and ecology of sulfate- and sulfur-reducing bacteria. *In*: Zehnder A.J.B. (Ed) Biology of anaerobic microorganisms. Pp. 469-585. John Wiley & Sons, New York.

Wintzingerode, F.V., Gobel, U.B. and Stackebrandt, E. 1997. Determination of microbial diversity in environmental samples: pitfalls of PCR-based rRNA analysis. FEMS Microbiol. Rev. 21**:** 213-229.

Woebken, D., Fuchs, B.M., Kuypers, M.M. and Amann, R. 2007. Potential interactions of particle-associated anammox bacteria with bacterial and archaeal partners in the Namibian upwelling system. Appl. Environ. Microbiol. 73(14): 4648-4657.

Wright, E.S., Yilmaz, L.S. and Noguera, D.R. 2012. DECIPHER, a search-based approach to chimera identification for 16S rRNA sequences. Appl. Environ. Microbiol. 78(3): 717-725.

Wuchter, C., Abbas, B., Coolen, M.J.C., Herfort, L., van Bleijswijk, J., Timmers, P., Strous, M., Teira, E., Herndl, G.J., Middelburg, J.J., Schouten, S. and Sinninghe Damste, J.S. 2006. Archaeal nitrification in the ocean. Proc. Natl. Acad. Sci. 103:12317-12322.

Wuchter, C., Schouten, S., Boschker, H. T.S. and Sinninghe Damsté, J. S. 2003. Bicarbonate uptake by marine Crenarchaeota. FEMS Microbiol. Let. 219: 203-207. doi: 10.1016/S0378-1097(03)00060-0.

Yamamoto, M., Nakagawa, S., Shimamura, S., Takai, K. and Horikoshi, K. 2010. Molecular characterization of inorganic sulfur-compound metabolism in the deep-sea epsilonproteobacterium *Sulfurovum* sp. NBC37-1. Environ. Microbiol. 12: 1144-1153.

Yilmaz, A., Coban-Yildiz, Y., Telli-Karakoc, F. and Bologa, A. 2006. Surface and mid-water sources of organic carbon by photoautotrophic and chemoautotrophic production in the Black Sea. Deep Sea Res. II 53: 1988-2004.

Zaikova, E., Walsh, D.A., Stilwell, C.P., Mohn, W.W., Tortell, P.D. and Hallam, S.J. 2010. Microbial community dynamics in a seasonally anoxic fjord: Saanich Inlet, British Columbia. Environ. Microbiol. 12: 172-191.

Zillig, W., Gierl, A., Schreiber, G., Wunderl, S., Janekovic, D., Stetter, K.O. and Klenk, H-P. 1983. The archaebacterium *Thermofilum pendens* represents, a novel genus of the thermophilic, anaerobic sulfur respiring *Thermoproteales***.** *Syst. Appl. Microbiol.* 4: 79-87.

Zillig, W., Holz, I., Janekovic, D., Klenk, H-P., Imsel, E., Trent, J., Wunderl, S., Forjaz, V.H., Coutinho, R. and Ferreira, T. 1990. Hyperthermus butylicus, a hyperthermophilic sulfur-reducing archaebacterium that ferments peptides. J. Bacteriol. 172: 3959-3965.

Zopfi, J., Ferdelman, T.G. and Fossing, H. 2004. Distribution and fate of sulfur intermediates-sulfite, tetrathionate, thiosulfate, and elemental sulfur-in marine sediments. *In*: Amend J.P., Edwards K.J., Lyons T.W. (ed.). Sulfur biogeochemistry- past and present, Boulder, Colorado. Geological Society of America Special Paper, vol. 379, pp.97-116.

Zweifel, U. L., and Hagstrom, A. 1995. Total counts of marine bacteria include a large fraction of non-nucleoid-containing bacteria (ghosts). Appl. Environ. Microbiol. 61: 2180-2185.

Appendix A

Fluxes of potential energy substrates and oxidants in the Cariaco Basin's redoxcline

Net (downward and upward) fluxes of nutrients, reductants, and oxidants at seven depths within the Cariaco's redoxcline were used in permutational multivariate multiple regression analyses (PERMANOVA) as described in Chapter 2 to determine their effects on bacterial and archaeal clade distributions at three stations (Fig. A1, A2, A3). The fluxes were calculated using Fick's first law of diffusion flux assuming a steady state and ignoring any lateral advection as described in Li et al. (2008). The following equation represents Fick's first law of diffusion:

$$J\ [\text{mmol m}^{-2}\ \text{d}^{-1}] = -\ K_z\ (\Delta C/\Delta Z),$$

where J is the vertical flux (downward or upward), K_z is the diffusion coefficient, $\Delta C/\Delta Z$ is the concentration gradient. Further,

$$K_z\ [\text{m}^2\ \text{d}^{-1}] = a_0\ (1/N^2)^{1/2},$$

where a_0 is the input of energy; 0.0004 $\text{cm}^2\ \text{s}^{-2}$ ($4\text{x}10^{-8}\ \text{m}^2\ \text{s}^{-2}$) for the Cariaco Basin (Li et al., 2008),

$$N = \{(-g/\rho)\ (\delta\rho/\delta z)\}^{1/2},$$

where g is the gravity constant, ρ is density at given depth, $\delta\rho/\delta z$ is the water density gradient over a specific depth interval.

PERMANOVA analysis showed no significant multivariate interaction between any tested environmental fluxes nor between the fluxes and clade distributions at station A ($p > 0.05$, $n = 56$) and station D ($p > 0.05$, $n= 14$). At station B, there was a significant multivariate interaction between environmental fluxes ($p < 0.05$, $n = 21$), and overall clade distribution was significantly affected by ammonium and nitrite fluxes ($p < 0.05$, $n = 21$). However, analyses of individual clade distributions and their interactions with fluxes showed that only distribution of SRB was

significantly affected by nitrite and oxygen fluxes ($p < 0.05$, $n = 21$) and distribution of Thaumarchaeota was significantly affected by thiosulfate and ammonium fluxes ($p < 0.05$, $n = 21$). Despite significant multivariate interactions between clade distribution and fluxes at station B, multivariate DISTLM_*forward* analyses showed that none of the fluxes explained significant proportion of the variation in clade distribution ($p > 0.05$, $n = 21$). Since the fluxes explained less of the variability in clade distributions, simple concentrations of all nutrients, reductants, and oxidants were used in all statistical analyses.

References:

Li X., G.T. Taylor, Y. Astor, M.I. Scranton. 2008. Relationship of sulfur speciation to hydrographic conditions and chemoautotrophic production in the Cariaco Basin. Mar. Chem. 112: 53-64.

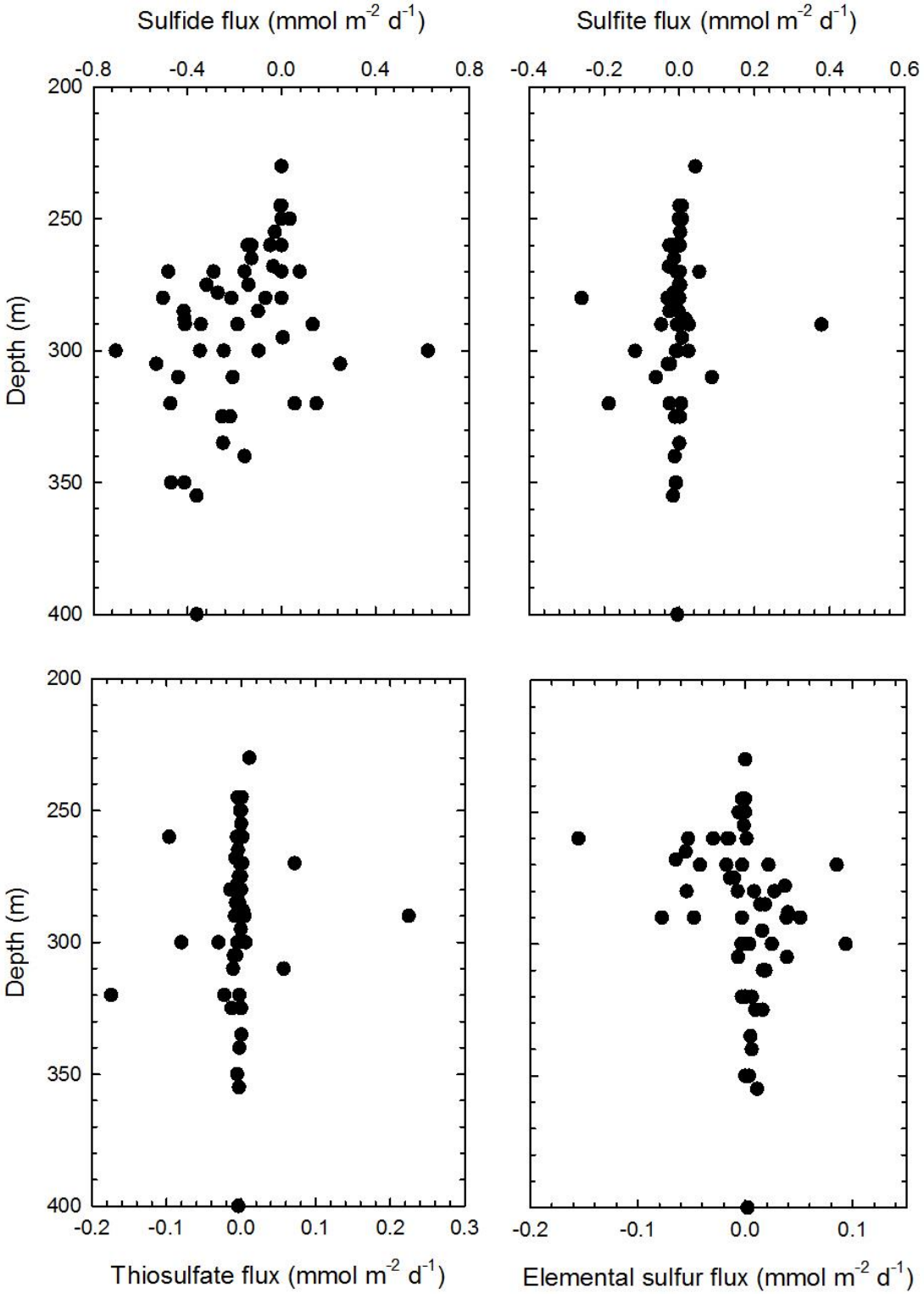
Sulfide flux (mmol m-2 d-1)
Sulfite flux (mmol m-2 d-1)
Depth (m)
Thiosulfate flux (mmol m-2 d-1)
Elemental sulfur flux (mmol m-2 d-1)

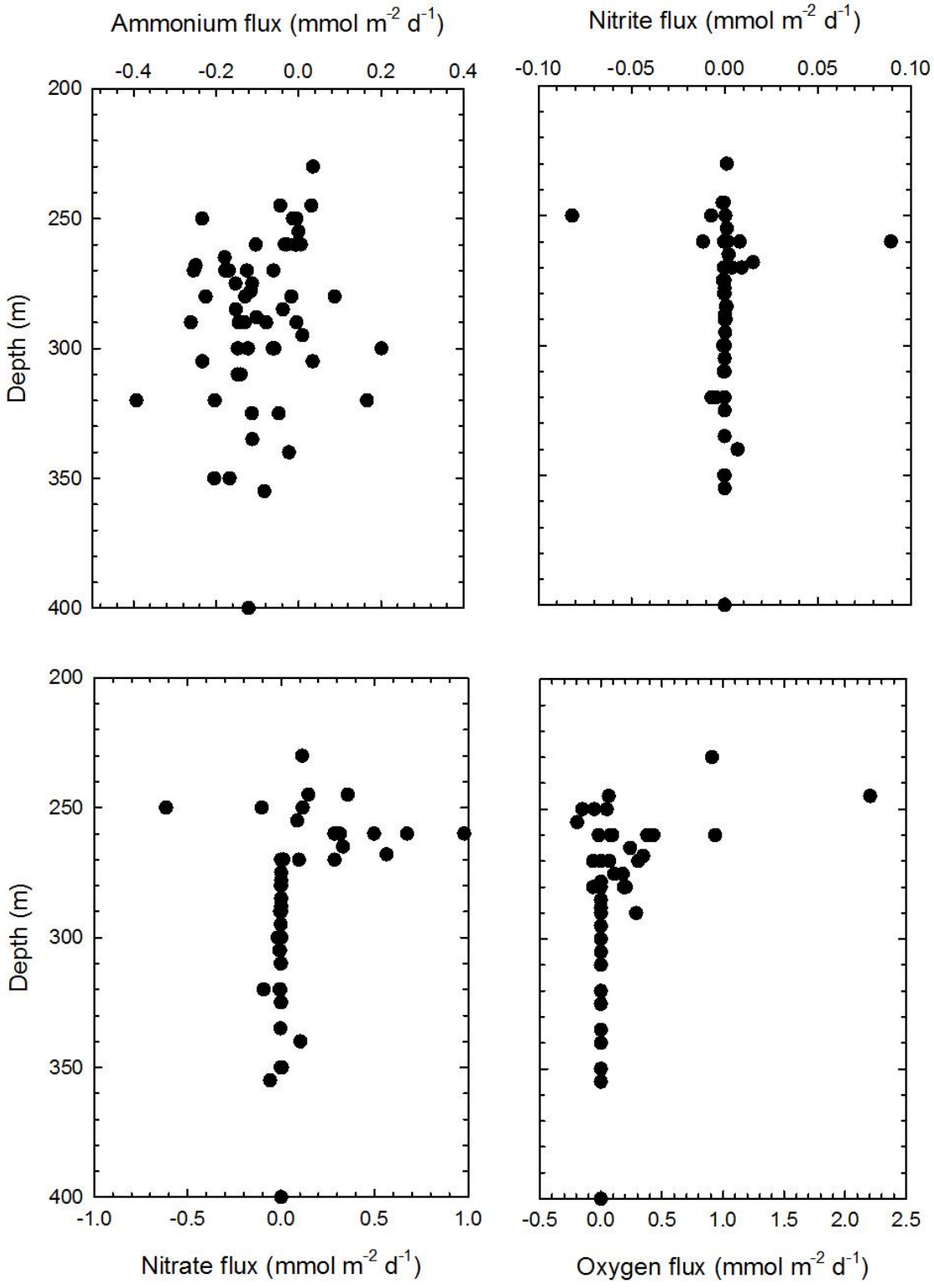

Figure A1. Net fluxes at specific depths within the redoxcline at station A (combined cruises CAR122, CAR128, CAR132, CAR139, CAR145, CAR153, CAR157, CAR169). Note x-axes have different scales.

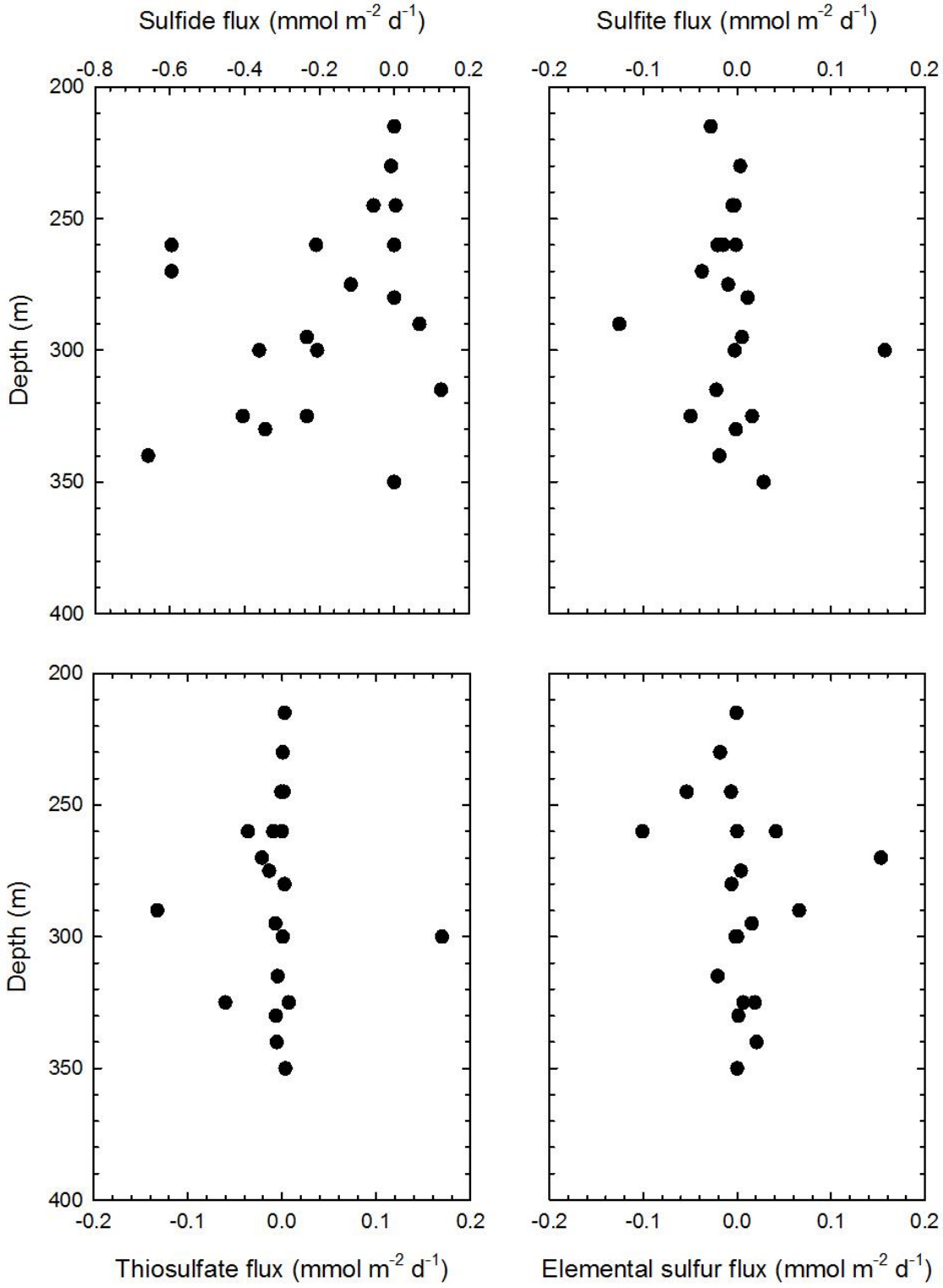
Sulfide flux (mmol m-2 d-1)
Sulfite flux (mmol m-2 d-1)
Depth (m)
Depth (m)
Thiosulfate flux (mmol m-2 d-1)
Elemental sulfur flux (mmol m-2 d-1)
-0.8
-0.6
-0.4
-0.2
0.0
0.2
-0.2
-0.1
0.0
0.1
0.2
200
250
300
350
400

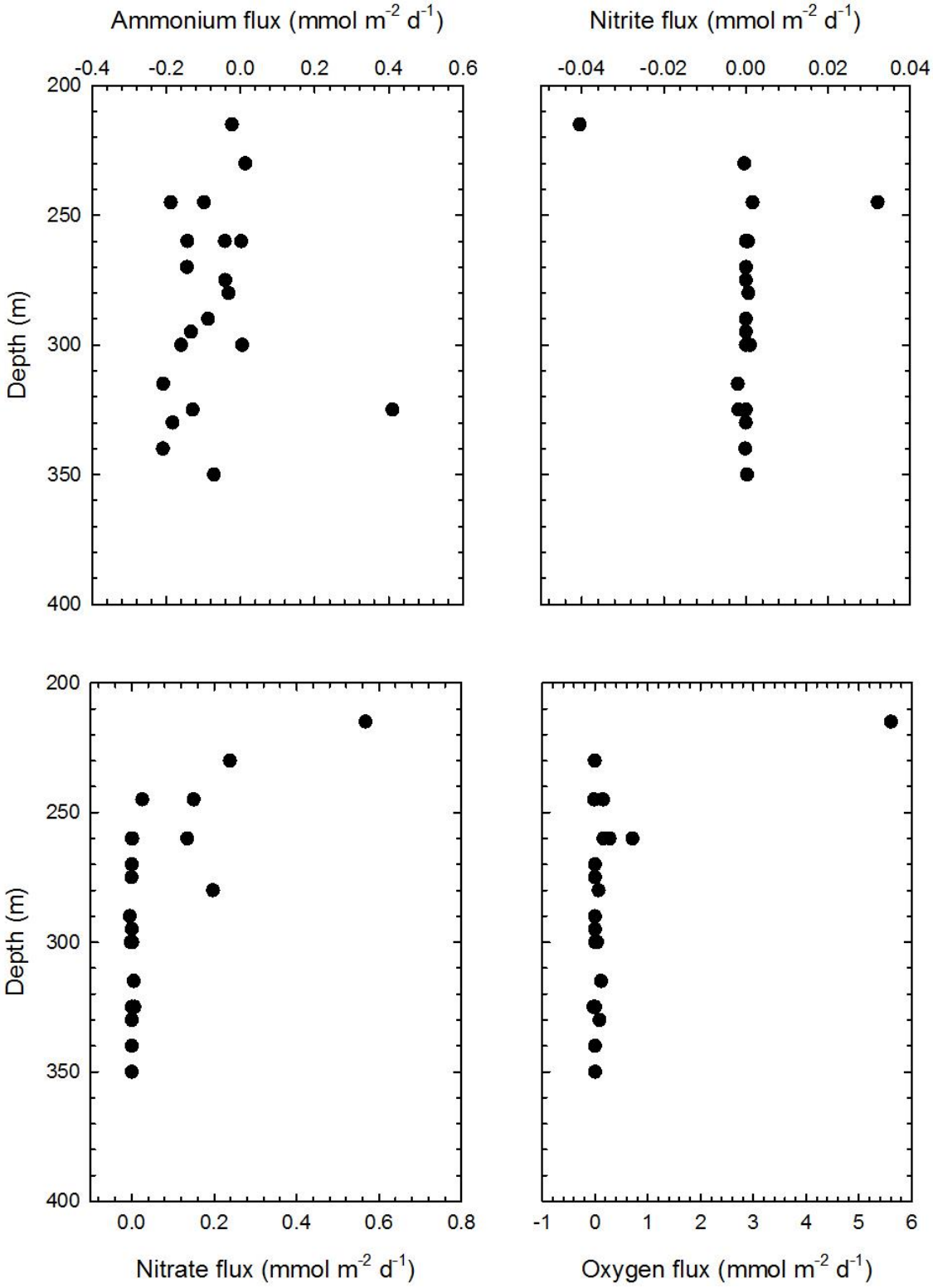

Figure A2. Net fluxes at specific depths within the redoxcline at station B (combined cruises CAAR122, CAR128, and CAR132). Notes x-axes have different scales.

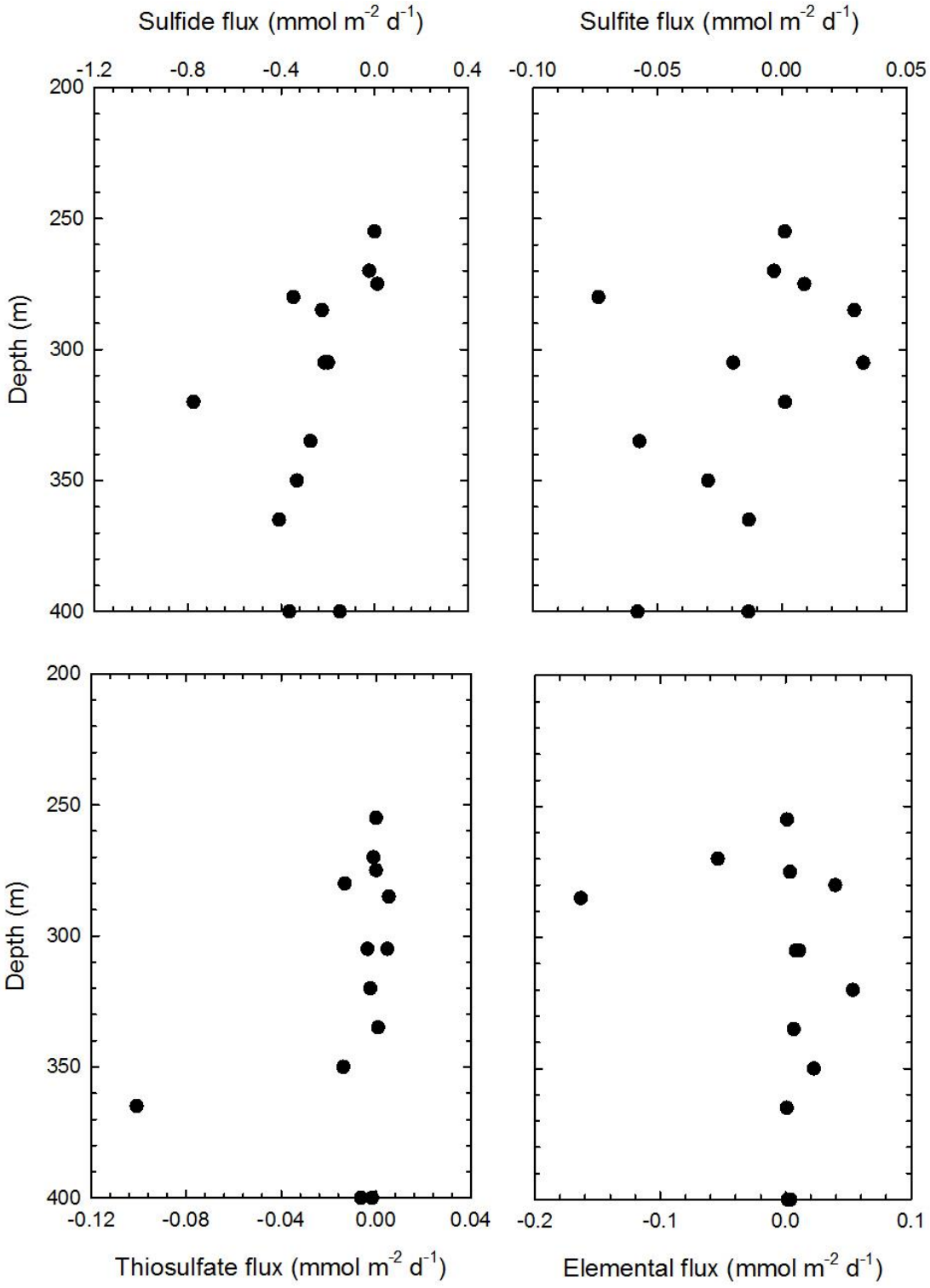
Sulfide flux (mmol m-2 d-1)
Sulfite flux (mmol m-2 d-1)
Depth (m)
Thiosulfate flux (mmol m-2 d-1)
Elemental flux (mmol m-2 d-1)

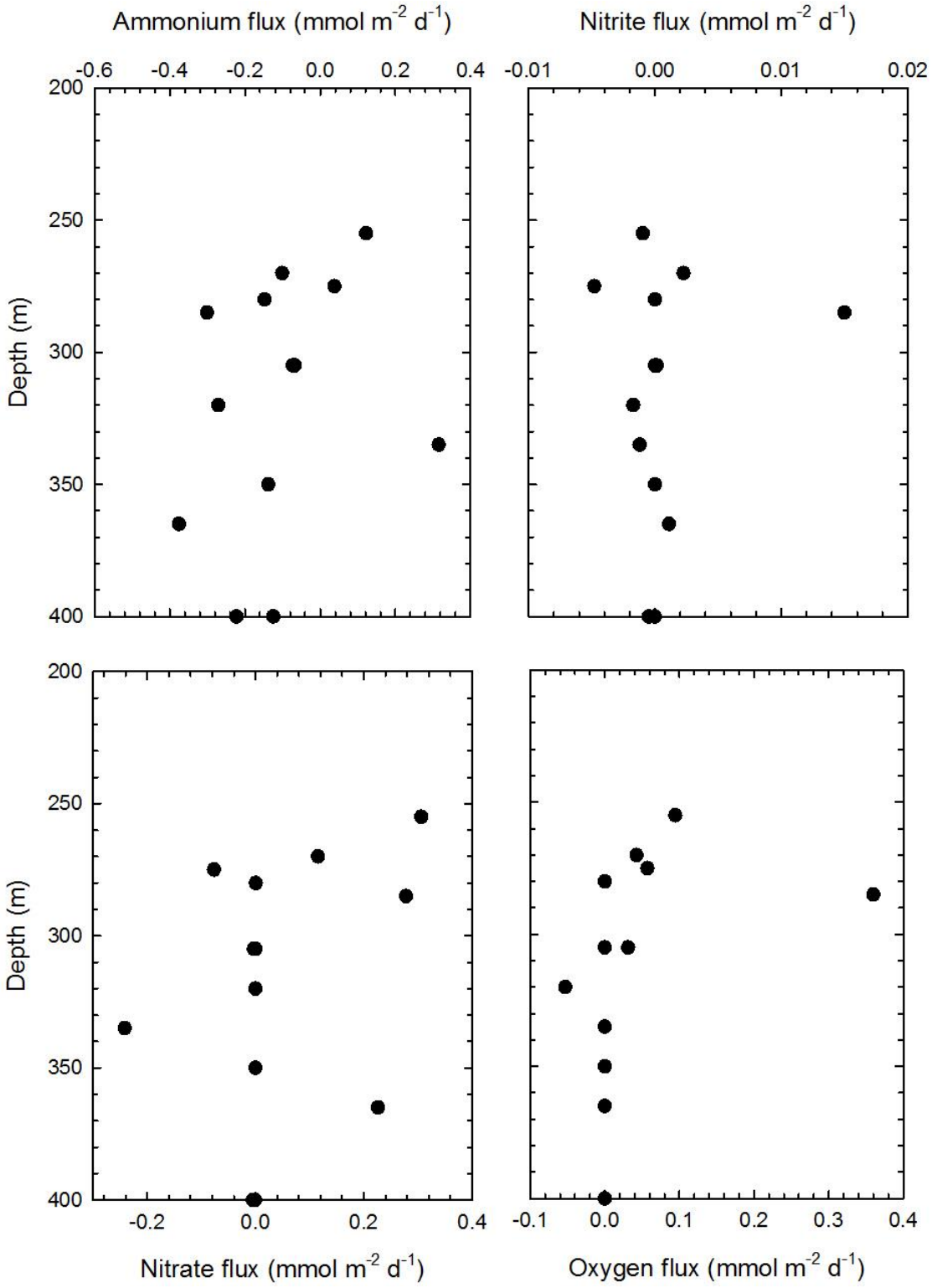

Figure A3. Net fluxes at specific depths within the redoxcline at station D (combined cruises CAR122 and CAR132). Note x-axes have different scales.

Appendix B

Cell concentrations of individual bacterial and archaeal clades and total prokaryotic community in the water column

Table B.1. Cell concentrations of individual bacterial and archaeal clades and total prokaryotic community in the water column at station A during nine cruises. Individual clade cell concentration units: x 10^7 L^{-1}; total community cell concentration units: x 10^8 L^{-1}. ALF – α-proteobacteria, BET – β-proteobacteria, GAM – γ-proteobacteria, SRB – sulfate-reducing δ-proteobacteria, EPS – ε-proteobacteria, THAUM – Thaumarchaeota, EURY – Euryarchaeota, DAPI – total prokaryotic community, SE – standard error.

CAR122A

Depth (m)	ALF	SE	BET	SE	GAM	SE	SRB	SE	EPS	SE	THAUM	SE	EURY	SE	DAPI	SE
45	1.73	0.13	4.51	0.20	1.18	0.05	2.42	0.14	3.85	0.10	1.01	0.15	2.23	0.32	5.05	0.53
100	1.30	0.18	3.18	0.24	1.30	0.14	1.27	0.08	6.77	0.27	6.37	0.30	5.63	0.45	4.64	0.30
200	1.75	0.15	5.02	0.26	2.89	0.04	0.00	0.07	9.26	0.28	0.00	0.06	0.00	0.09	3.46	0.40
215	1.51	0.08	3.54	0.11	1.22	0.04	0.64	0.05	4.47	0.16	3.42	0.19	0.96	0.11	4.42	0.23
230	3.68	0.19	3.05	0.19	2.66	0.04	0.54	0.04	6.20	0.25	0.09	0.05	1.25	0.19	4.84	0.27
245	2.60	0.15	9.34	0.22	2.94	0.06	1.24	0.06	15.58	0.41	7.83	0.24	10.61	0.82	5.17	1.17
260	3.44	0.23	7.21	0.37	3.44	0.13	0.35	0.05	27.76	0.58	4.18	0.30	11.55	0.78	5.26	0.88
270	3.60	0.30	8.59	0.21	2.24	0.14	1.13	0.10	18.75	0.33	4.78	0.21	2.24	0.15	5.17	0.86
280	4.71	0.17	5.30	0.14	5.43	0.07	4.29	0.09	17.47	0.35	9.72	0.27	1.85	0.09	3.35	0.38
290	1.49	0.06	4.68	0.08	1.41	0.02	3.92	0.05	4.50	0.13	1.49	0.06	0.92	0.04	3.34	0.61
300	2.80	0.15	5.79	0.15	1.84	0.04	2.48	0.06	8.27	0.15	2.06	0.17	4.32	0.16	3.64	0.21
310	1.00	0.14	8.00	0.22	1.38	0.06	1.56	0.10	12.06	0.46	1.98	0.23	6.19	0.46	3.65	0.23
320	6.82	0.23	5.97	0.17	2.23	0.07	3.46	0.21	19.73	0.33	0.72	0.12	4.39	0.19	5.05	0.71
350	1.61	0.13	4.03	0.16	2.16	0.10	0.27	0.07	10.64	0.39	0.62	0.17	4.14	0.17	4.97	0.30
400	4.92	0.14	2.08	0.11	1.16	0.05	0.38	0.04	8.78	0.27	2.27	0.10	3.81	0.15	4.11	0.14
500	1.37	0.07	1.92	0.09	2.03	0.04	0.31	0.05	6.96	0.20	1.09	0.09	4.55	0.08	3.41	0.20
900	7.94	0.21	7.94	0.26	2.33	0.05	0.72	0.06	5.89	0.32	0.00	0.09	0.00	0.09	3.29	0.23
1300	2.82	0.10	2.19	0.10	1.12	0.04	1.49	0.11	3.61	0.15	3.77	0.12	4.05	0.14	3.85	0.15

Table B.1. Continued.

CAR128A

Depth (m)	ALF	SE	BET	SE	GAM	SE	SRB	SE	EPS	SE	THAUM	SE	EURY	SE	DAPI	SE
45	0.80	0.03	4.58	0.10	0.49	0.03	0.53	0.03	2.40	0.09	3.32	0.08	1.26	0.03	3.98	0.48
100	0.57	0.03	3.72	0.06	0.64	0.03	0.17	0.02	2.62	0.04	2.91	0.04	0.53	0.02	3.86	0.57
150	1.60	0.04	4.68	0.09	0.47	0.02	0.57	0.03	4.41	0.07	1.98	0.05	0.85	0.02	3.76	0.39
190	1.00	0.04	5.67	0.09	0.46	0.03	1.16	0.07	2.12	0.07	1.08	0.04	0.73	0.02	4.39	0.33
205	0.90	0.03	3.83	0.06	0.37	0.02	0.44	0.03	1.45	0.04	2.33	0.03	1.59	0.03	3.81	0.27
220	0.82	0.03	4.91	0.05	0.37	0.03	0.48	0.03	1.72	0.05	2.36	0.06	0.75	0.04	3.97	0.24
235	0.68	0.02	7.81	0.13	0.29	0.01	0.68	0.03	0.81	0.03	2.75	0.06	0.75	0.02	3.39	0.26
245	0.21	0.02	4.52	0.08	0.56	0.02	0.67	0.02	1.67	0.02	1.36	0.03	1.99	0.04	3.53	0.15
255	0.46	0.05	9.76	0.11	0.82	0.03	0.78	0.05	1.77	0.08	1.85	0.06	1.26	0.05	4.26	0.13
265	0.35	0.03	5.34	0.11	0.28	0.03	1.02	0.04	1.59	0.04	2.08	0.06	0.91	0.04	4.16	0.12
275	0.54	0.03	3.55	0.06	0.40	0.02	0.62	0.02	4.51	0.11	2.03	0.03	2.28	0.06	3.79	0.92
285	0.52	0.04	4.05	0.08	1.73	0.05	0.70	0.04	4.12	0.15	2.03	0.07	0.85	0.03	4.24	0.70
295	0.22	0.02	5.76	0.11	0.43	0.05	0.76	0.05	7.75	0.08	1.27	0.03	2.71	0.03	3.98	0.70
325	0.24	0.03	3.32	0.07	0.35	0.02	0.87	0.04	4.23	0.09	3.50	0.11	3.04	0.04	4.29	0.15
400	0.22	0.03	3.93	0.08	0.34	0.03	0.71	0.03	3.81	0.13	1.19	0.03	1.07	0.03	4.05	0.99
500	0.45	0.03	3.37	0.06	0.37	0.03	0.72	0.03	5.49	0.14	0.83	0.06	2.80	0.09	3.99	0.46
900	0.09	0.02	3.33	0.12	0.28	0.02	0.44	0.03	1.57	0.07	0.96	0.04	0.57	0.03	4.26	0.54
1300	0.03	0.02	4.57	0.13	0.17	0.03	0.61	0.03	4.81	0.14	0.84	0.03	0.54	0.04	4.28	0.31

Table B.1. Continued.

CAR132A

Depth (m)	ALF	SE	BET	SE	GAM	SE	SRB	SE	EPS	SE	THAUM	SE	EURY	SE	DAPI	SE
40	7.61	0.13	3.58	0.14	0.62	0.07	1.75	0.06	9.93	0.14	0.72	0.05	0.47	0.05	3.65	0.33
100	3.82	0.07	1.92	0.06	0.95	0.04	2.04	0.06	6.10	0.13	0.71	0.03	0.47	0.04	3.56	0.20
150	2.38	0.07	2.73	0.11	1.73	0.09	0.95	0.03	13.66	0.28	0.63	0.03	0.53	0.05	3.68	0.32
200	2.07	0.05	1.48	0.06	0.99	0.03	0.81	0.03	6.92	0.17	0.59	0.03	0.59	0.04	3.52	0.30
230	1.33	0.03	1.53	0.07	0.73	0.03	3.70	0.08	6.41	0.12	2.72	0.05	0.48	0.04	3.00	0.50
240	1.15	0.04	7.34	0.09	1.33	0.05	4.13	0.18	10.40	0.22	2.10	0.06	0.68	0.03	2.85	0.31
250	1.89	0.05	5.90	0.10	2.45	0.07	3.84	0.10	13.09	0.31	0.61	0.05	0.66	0.05	3.21	0.51
260	1.15	0.05	5.91	0.08	1.89	0.05	4.90	0.09	11.77	0.17	0.41	0.04	0.57	0.06	3.47	0.40
270	1.12	0.05	2.79	0.11	1.44	0.07	4.00	0.08	8.39	0.30	1.82	0.05	1.55	0.08	3.65	0.31
280	1.09	0.08	3.74	0.09	0.79	0.04	3.00	0.10	5.34	0.13	1.57	0.06	0.22	0.06	3.81	0.46
290	0.00	0.00	1.53	0.06	0.49	0.06	1.97	0.09	7.22	0.28	0.00	0.00	1.27	0.06	3.77	0.85
305	0.00	0.00	1.58	0.07	0.18	0.04	2.23	0.07	5.56	0.12	5.72	0.10	0.00	0.00	3.49	0.28
320	0.00	0.00	4.37	0.15	3.75	0.07	5.01	0.10	8.88	0.28	0.15	0.05	0.00	0.03	3.47	0.21
340	0.00	0.00	1.56	0.06	0.58	0.04	4.59	0.11	4.46	0.22	0.00	0.04	0.00	0.00	3.32	0.28
400	0.49	0.07	0.93	0.04	2.44	0.07	6.28	0.12	5.57	0.17	0.14	0.05	0.00	0.00	3.52	0.21
500	0.52	0.07	1.11	0.06	1.69	0.05	4.40	0.06	5.75	0.10	0.65	0.04	0.00	0.03	3.36	0.21
900	0.72	0.03	1.00	0.05	1.67	0.03	4.11	0.09	6.75	0.16	6.91	0.11	0.13	0.02	2.97	0.19
1300	0.19	0.04	0.90	0.06	0.80	0.04	4.33	0.08	8.94	0.25	0.33	0.04	0.09	0.04	3.42	0.21

Table B.1. Continued.

CAR139A

Depth (m)	ALF	SE	BET	SE	GAM	SE	SRB	SE	EPS	SE	THAUM	SE	EURY	SE	DAPI	SE
30	4.53	1.92	5.20	1.47	1.15	0.51	8.21	0.41	7.80	0.55	1.97	0.09	2.94	0.10	4.96	0.18
100	4.76	0.87	4.08	0.39	1.40	0.27	1.40	0.42	6.62	0.16	1.32	0.03	1.77	0.03	3.00	0.30
150	3.31	0.36	3.38	0.51	2.16	0.34	2.24	0.66	6.63	0.09	1.24	0.02	0.24	0.03	2.97	0.16
205	1.44	0.27	2.06	0.35	0.83	0.18	1.14	0.39	2.70	0.07	0.76	0.03	0.32	0.01	3.44	0.16
220	1.19	0.33	1.67	0.28	0.43	0.28	0.96	0.46	2.50	0.15	0.91	0.05	0.56	0.02	4.75	0.16
230	1.09	0.21	2.62	0.30	0.42	0.21	0.77	0.32	3.31	0.28	0.71	0.03	0.16	0.03	4.22	0.21
240	1.21	0.35	2.32	0.53	0.80	0.25	0.73	0.36	4.84	0.25	0.80	0.03	0.21	0.02	4.88	0.31
250	0.95	0.39	3.00	0.85	0.79	0.42	0.41	0.21	4.75	0.26	0.28	0.03	1.14	0.09	5.18	0.18
260	0.60	0.19	1.80	0.55	0.35	0.22	1.11	0.48	3.97	0.19	0.89	0.04	1.51	0.06	4.33	0.16
270	0.56	0.20	2.56	0.39	0.30	0.20	0.72	0.33	4.64	0.29	0.54	0.03	0.35	0.03	4.57	0.30
285	0.46	0.19	2.31	0.92	0.69	0.38	0.56	0.28	4.07	0.21	0.24	0.04	0.32	0.03	5.00	0.34
300	0.31	0.16	2.03	0.77	0.56	0.19	0.46	0.18	3.45	0.08	0.46	0.02	0.28	0.03	3.87	0.18
335	0.30	0.13	1.71	0.48	0.55	0.11	1.85	0.61	3.37	0.09	0.16	0.02	0.20	0.02	3.29	0.19
355	0.68	0.20	1.57	0.35	0.50	0.17	1.75	0.71	2.34	0.12	0.32	0.01	0.95	0.02	4.05	0.34
400	0.44	0.12	1.26	0.17	1.74	0.21	1.43	0.50	4.18	0.10	3.61	0.04	0.58	0.02	3.51	0.43
500	0.20	0.12	1.17	0.32	0.58	0.12	1.24	0.42	3.21	0.06	0.55	0.03	1.00	0.01	3.42	0.26
900	0.24	0.12	1.77	0.36	0.77	0.17	0.84	0.30	3.02	0.08	0.30	0.02	0.37	0.02	3.55	0.25
1300	0.14	0.10	1.95	0.43	1.99	0.44	1.53	0.47	2.64	0.05	0.63	0.01	0.51	0.02	3.09	0.20

Table B.1. Continued.

CAR145A

Depth (m)	ALF	SE	BET	SE	GAM	SE	SRB	SE	EPS	SE	THAUM	SE	EURY	SE	DAPI	SE
30	10.18	0.33	5.51	0.15	5.57	0.18	4.61	0.17	1.07	0.39	0.96	0.31	0.18	0.06	3.28	0.48
100	0.69	0.16	3.89	0.08	2.50	0.06	3.48	0.09	0.53	0.13	0.47	0.11	0.18	0.04	2.34	0.14
150	0.30	0.08	1.55	0.05	2.31	0.06	1.14	0.04	0.42	0.13	0.24	0.07	0.08	0.02	2.74	0.31
200	0.12	0.03	0.07	0.01	0.10	0.02	0.59	0.01	0.37	0.09	0.29	0.06	0.05	0.01	2.18	0.22
220	0.51	0.09	0.28	0.05	2.16	0.04	1.71	0.04	0.53	0.00	0.28	0.05	0.13	0.02	1.69	0.16
230	0.05	0.01	0.07	0.02	0.35	0.01	0.43	0.01	1.10	0.02	0.05	0.01	0.03	0.01	2.43	0.20
240	0.36	0.07	0.81	0.15	2.12	0.04	6.13	0.11	7.19	0.11	0.25	0.05	0.57	0.11	1.87	0.15
250	1.02	0.19	1.23	0.23	3.52	0.07	5.87	0.10	10.21	0.23	0.33	0.06	0.37	0.07	1.88	0.15
260	1.34	0.26	3.73	0.73	0.62	0.12	0.70	0.14	30.67	0.70	0.63	0.12	0.74	0.14	1.98	0.01
270	0.62	0.10	0.82	0.14	0.62	0.10	0.50	0.08	17.58	0.28	0.43	0.07	0.49	0.08	1.67	0.01
280	0.37	0.06	0.77	0.14	0.35	0.06	0.39	0.07	13.65	0.23	0.37	0.07	0.36	0.06	1.76	0.01
290	0.56	0.07	0.78	0.09	0.71	0.09	0.54	0.07	3.33	0.17	0.46	0.06	0.39	0.05	1.22	0.09
300	0.11	0.04	0.32	0.11	0.10	0.04	0.19	0.07	0.45	0.08	0.09	0.03	0.29	0.10	3.51	0.23
350	0.52	0.13	0.40	0.10	0.16	0.04	0.08	0.02	0.15	0.04	0.08	0.02	0.16	0.04	2.47	0.18
400	0.22	0.04	0.21	0.04	0.09	0.02	0.08	0.01	0.11	0.02	0.08	0.01	0.10	0.02	1.77	0.13
500	0.17	0.02	0.16	0.02	0.08	0.01	0.07	0.01	0.30	0.04	0.07	0.01	0.08	0.01	1.43	0.12
900	0.08	0.01	0.12	0.01	0.06	0.00	0.06	0.00	0.21	0.02	0.06	0.00	0.06	0.01	0.83	0.12
1300	0.11	0.01	0.14	0.01	0.06	0.01	0.06	0.01	0.34	0.03	0.06	0.01	0.08	0.01	1.01	0.10

Table B.1. Continued.

CAR153A

Depth (m)	ALF	SE	BET	SE	GAM	SE	SRB	SE	EPS	SE	THAUM	SE	EURY	SE	DAPI	SE
30	0.55	0.19	0.98	0.34	0.74	0.26	0.68	0.24	8.72	0.31	0.55	0.19	0.97	0.34	3.50	0.14
50	0.82	0.05	0.74	0.04	0.47	0.03	0.51	0.03	0.64	0.04	0.67	0.04	1.36	0.80	0.59	0.06
100	0.48	0.02	0.95	0.05	0.74	0.04	1.20	0.06	0.48	0.02	0.72	0.03	0.41	0.02	0.48	0.08
150	0.23	0.01	0.44	0.02	0.36	0.01	0.94	0.04	0.22	0.01	0.23	0.01	0.22	0.01	0.40	0.05
200	0.19	0.01	0.40	0.02	0.37	0.02	0.63	0.03	0.26	0.01	0.22	0.01	0.20	0.01	0.48	0.06
220	0.44	0.04	0.41	0.03	0.50	0.04	1.18	0.10	0.25	0.02	0.38	0.03	0.23	0.02	0.81	0.09
240	0.67	0.05	0.96	0.08	0.93	0.07	1.29	0.10	7.89	0.62	1.11	0.09	0.48	0.04	0.79	0.06
250	0.71	0.05	1.21	0.08	0.94	0.07	1.66	0.12	6.87	0.48	0.63	0.04	0.45	0.03	0.70	0.08
260	1.03	0.06	0.39	0.02	0.91	0.05	0.75	0.04	1.46	0.08	0.50	0.03	0.50	0.03	0.57	0.07
275	0.91	0.05	0.51	0.03	1.04	0.06	1.35	0.07	1.87	0.10	0.64	0.03	0.63	0.03	0.53	0.05
290	0.71	0.03	0.54	0.03	0.70	0.03	1.37	0.07	2.07	0.10	0.53	0.03	0.67	0.03	0.48	0.03
305	1.87	0.09	0.51	0.02	0.77	0.04	1.40	0.07	2.72	0.13	0.63	0.03	0.76	0.04	0.47	0.04
325	0.52	0.06	0.14	0.02	0.23	0.03	0.43	0.05	0.58	0.07	0.09	0.01	0.12	0.01	1.16	0.13
350	0.91	0.07	0.91	0.08	0.32	0.03	0.58	0.05	0.78	0.06	0.20	0.02	0.16	0.01	0.83	0.07
400	0.85	0.07	0.56	0.04	0.44	0.04	0.62	0.05	0.81	0.06	0.35	0.03	0.19	0.01	0.80	0.08
500	1.15	0.05	0.82	0.04	0.47	0.02	0.86	0.04	3.00	0.14	0.29	0.01	0.24	0.01	0.48	0.09
900	0.92	0.04	0.76	0.03	0.61	0.03	0.83	0.04	2.39	0.10	0.31	0.01	0.30	0.01	0.43	0.13
1300	0.61	0.04	0.78	0.05	0.77	0.05	0.64	0.04	2.47	0.15	0.26	0.02	0.32	0.02	0.59	0.07

Table B.1. Continued.

CAR157A

Depth (m)	ALF	SE	BET	SE	GAM	SE	SRB	SE	EPS	SE	THAUM	SE	EURY	SE	DAPI	SE
29	4.21	0.47	4.60	0.51	4.60	0.51	5.35	0.59	5.91	0.64	2.04	0.21	1.16	0.12	1.00	0.18
100	1.19	0.15	1.45	0.17	1.67	0.20	0.78	0.10	1.54	0.18	0.46	0.05	0.64	0.07	1.08	0.12
150	1.51	0.19	1.23	0.16	1.51	0.19	1.45	0.18	1.32	0.17	0.63	0.07	0.46	0.05	1.15	0.29
200	1.23	0.17	1.31	0.18	1.32	0.18	1.81	0.24	1.70	0.22	0.59	0.07	0.92	0.11	1.24	0.21
250	1.96	0.24	1.37	0.17	1.47	0.18	1.61	0.20	1.52	0.19	1.00	0.11	0.44	0.05	1.11	0.29
260	3.02	0.33	2.08	0.23	2.43	0.27	2.31	0.26	2.48	0.27	1.05	0.10	1.67	0.17	0.99	0.13
268	4.56	0.39	4.54	0.39	2.98	0.26	3.49	0.30	3.45	0.30	2.61	0.20	1.88	0.15	0.78	0.11
278	1.79	0.20	2.02	0.22	1.47	0.17	1.47	0.17	2.38	0.26	0.97	0.10	0.63	0.06	1.00	0.18
288	1.81	0.20	1.16	0.13	1.66	0.18	1.26	0.14	1.62	0.18	0.62	0.06	0.76	0.08	1.01	0.16
300	1.54	0.17	1.53	0.17	1.24	0.14	1.38	0.15	1.63	0.18	0.89	0.09	0.44	0.04	1.00	0.25
310	0.96	0.12	1.12	0.14	1.19	0.15	1.08	0.13	1.07	0.13	1.39	0.15	0.35	0.04	1.05	0.16
320	0.96	0.10	1.01	0.11	1.05	0.11	1.10	0.12	1.09	0.11	0.44	0.04	0.54	0.05	0.96	0.17
330	0.65	0.07	0.68	0.07	0.77	0.08	0.64	0.07	0.65	0.07	0.22	0.02	0.29	0.03	0.94	0.08
350	0.78	0.08	0.61	0.06	0.80	0.08	0.62	0.06	0.66	0.07	0.29	0.03	0.26	0.02	0.91	0.10
400	0.50	0.05	0.40	0.04	0.50	0.05	0.35	0.04	0.44	0.04	0.15	0.01	0.15	0.01	0.88	0.10
500	0.48	0.05	0.43	0.04	0.50	0.05	0.35	0.04	0.44	0.05	0.14	0.01	0.13	0.01	0.95	0.13
900	0.43	0.04	0.43	0.04	0.50	0.05	0.33	0.03	0.49	0.05	0.13	0.01	0.14	0.01	0.95	0.14
1300	0.53	0.06	0.72	0.08	0.57	0.06	0.35	0.04	0.53	0.06	0.18	0.02	0.16	0.02	1.04	0.13

Table B.1. Continued.

CAR163A

Depth (m)	ALF	SE	BET	SE	GAM	SE	SRB	SE	EPS	SE	THAUM	SE	EURY	SE	DAPI	SE
55	1.21	0.19	1.26	0.20	1.25	0.20	1.35	0.21	1.18	0.19	1.40	0.22	0.34	0.05	1.57	0.13
100	0.37	0.09	0.38	0.10	0.51	0.13	0.39	0.10	0.34	0.09	0.39	0.10	0.17	0.04	2.58	0.21
150	0.56	0.10	0.41	0.07	0.83	0.15	0.49	0.09	0.60	0.11	0.09	0.02	0.12	0.02	1.81	0.16
200	0.64	0.10	0.55	0.08	0.79	0.12	0.05	0.01	0.69	0.10	0.15	0.02	0.14	0.02	1.52	0.16
210	0.63	0.13	0.42	0.08	0.70	0.14	0.52	0.10	0.45	0.09	0.27	0.05	0.11	0.02	2.02	0.14
220	0.68	0.14	0.45	0.09	0.58	0.12	0.07	0.02	0.41	0.08	0.27	0.05	0.13	0.03	2.04	0.21
230	0.84	0.12	0.27	0.04	1.30	0.19	0.07	0.01	0.87	0.13	0.36	0.05	0.34	0.05	1.45	0.13
240	2.77	0.21	3.42	0.26	4.08	0.31	0.17	0.01	2.67	0.21	1.24	0.10	0.63	0.05	0.77	0.08
250	2.06	0.15	2.33	0.17	2.33	0.17	0.18	0.01	2.26	0.17	0.55	0.04	0.42	0.03	0.75	0.07
260	2.24	0.14	1.94	0.12	2.26	0.14	0.27	0.02	2.03	0.13	0.59	0.04	0.77	0.05	0.62	0.06
270	3.64	0.24	2.79	0.18	2.86	0.19	2.78	0.18	2.77	0.18	0.90	0.06	1.12	0.07	0.66	0.09
280	4.22	0.24	3.91	0.23	3.86	0.22	3.11	0.18	4.19	0.24	0.93	0.05	0.69	0.04	0.58	0.06
295	1.68	0.22	1.59	0.21	1.73	0.23	0.35	0.05	1.51	0.20	0.39	0.05	0.39	0.05	1.31	0.15
310	1.72	0.15	1.95	0.17	2.03	0.17	0.41	0.03	1.71	0.15	0.34	0.03	0.72	0.06	0.85	0.10
400	1.44	0.10	1.84	0.13	1.60	0.11	1.04	0.07	1.56	0.11	0.54	0.04	0.86	0.06	0.68	0.08
500	2.03	0.15	1.85	0.14	1.66	0.12	0.25	0.02	1.90	0.14	0.91	0.07	0.51	0.04	0.74	0.13
900	1.35	0.07	1.80	0.10	1.85	0.10	0.11	0.01	1.74	0.10	0.27	0.02	0.53	0.03	0.55	0.44
1300	1.50	0.09	1.64	0.10	2.04	0.12	0.14	0.01	1.63	0.10	1.32	0.08	0.40	0.02	0.61	0.07

Table B.1. Continued.

CAR169A

Depth (m)	ALF	SE	BET	SE	GAM	SE	SRB	SE	EPS	SE	THAUM	SE	EURY	SE	DAPI	SE
30	0.80	0.14	0.83	0.10	2.34	0.33	0.02	0.02	0.33	0.05	0.95	0.10	0.01	0.00	9.68	0.73
50	0.57	0.06	0.46	0.06	1.01	0.52	0.01	0.01	0.31	0.05	0.74	0.07	0.98	0.06	6.96	0.68
100	1.84	0.61	1.04	0.35	0.97	0.05	0.09	0.03	1.00	0.05	3.81	0.13	2.81	0.11	3.30	0.34
200	1.27	0.53	1.39	0.58	2.23	0.14	0.06	0.02	1.14	0.46	3.46	0.25	4.50	0.26	4.12	0.40
220	2.03	0.59	2.88	0.82	2.94	0.12	0.13	0.04	2.63	0.53	0.33	0.01	0.00	0.00	2.79	0.23
240	2.13	0.43	3.13	0.62	1.16	0.60	0.14	0.03	4.73	0.83	0.46	0.01	0.26	0.01	1.94	0.11
260	1.09	0.47	2.36	0.98	1.44	0.74	0.05	0.02	1.15	0.33	0.18	0.00	0.50	0.43	4.09	0.41
270	1.52	0.48	3.00	0.93	1.05	0.54	0.11	0.03	1.80	0.49	0.39	0.01	0.04	0.00	3.06	0.14
280	1.87	0.85	4.18	0.50	1.75	0.90	0.07	0.03	2.93	0.86	0.26	0.01	12.52	0.53	4.40	0.17
290	0.90	0.11	1.64	0.20	1.28	0.66	0.05	0.02	0.97	0.04	0.10	0.00	0.17	0.02	5.24	0.15
300	0.71	0.25	1.66	0.57	1.35	0.70	0.03	0.01	0.90	0.02	0.73	0.14	5.38	0.41	3.40	0.15
310	0.16	0.07	0.40	0.05	0.38	0.01	0.01	0.00	0.26	0.01	0.25	0.01	0.21	0.00	3.99	0.26
320	0.49	0.19	1.00	0.37	0.82	0.05	0.06	0.02	0.65	0.02	0.29	0.02	0.33	0.00	3.65	0.32
340	1.21	0.43	1.32	0.47	1.94	0.08	0.07	0.02	0.95	0.03	0.64	0.02	0.01	0.00	3.48	0.13
400	0.92	0.22	0.90	0.22	1.32	0.68	0.02	0.01	0.66	0.02	0.55	0.01	0.04	0.00	2.34	0.08
500	0.51	0.11	0.56	0.11	0.49	0.03	0.02	0.00	0.29	0.01	0.18	0.05	0.01	0.00	1.99	0.09
900	0.24	0.06	0.22	0.06	0.42	0.02	0.01	0.00	0.44	0.01	0.15	0.01	0.00	0.00	2.41	0.23
1300	0.43	0.11	0.40	0.10	0.47	0.02	0.04	0.01	0.46	0.01	0.25	0.02	0.01	0.00	2.43	0.08

Table B.2. Cell concentrations of individual bacterial and archaeal clades and total prokaryotic community in the water column at station B during three cruises. Individual clade cell concentration units: x 10^7 L^{-1}; total community cell concentration units: x 10^8 L^{-1}. ALF – α-proteobacteria, BET – β-proteobacteria, GAM – γ-proteobacteria, SRB – sulfate-reducing δ-proteobacteria, EPS – ε-proteobacteria, THAUM – Thaumarchaeota, EURY – Euryarchaeota, DAPI – total prokaryotic community, SE – standard error, ND – not detected.

CAR122B

Depth (m)	ALF	SE	BET	SE	GAM	SE	SRB	SE	EPS	SE	THAUM	SE	EURY	SE	DAPI	SE
40	5.06	0.14	4.24	0.27	4.02	0.36	2.25	0.11	2.69	0.14	10.12	0.33	6.50	0.21	3.70	0.24
190	3.85	0.17	5.08	0.35	2.57	0.19	1.38	0.06	2.95	0.13	3.31	0.15	3.46	0.14	4.58	0.19
215	3.71	0.26	3.66	0.23	5.14	0.27	5.73	0.37	5.85	0.14	7.23	0.38	4.21	0.14	4.48	0.16
245	6.45	0.24	6.52	0.99	1.92	0.27	1.09	0.10	1.99	0.16	12.76	0.35	8.42	0.45	5.49	0.28
260	5.65	0.17	9.09	0.68	2.94	0.37	2.47	0.15	1.84	0.11	4.96	0.21	4.17	0.30	4.62	0.25
275	3.52	0.14	3.44	0.27	0.95	0.19	0.73	0.05	1.08	0.05	4.70	0.33	6.05	0.47	4.95	0.16
290	2.64	0.14	3.36	0.41	0.80	0.36	0.59	0.05	1.20	0.08	2.02	0.15	1.68	0.12	6.11	0.24
300	5.10	0.17	4.54	0.59	1.31	0.23	1.18	0.09	9.36	0.71	7.97	0.29	4.99	0.21	5.01	0.16
325	3.50	0.25	2.94	0.24	1.37	0.33	0.75	0.07	8.91	0.31	2.81	0.18	1.89	0.09	5.22	0.26
350	3.10	0.08	6.59	0.12	2.31	0.31	2.15	0.09	10.32	0.41	4.68	0.09	3.65	0.08	2.39	0.20
450	2.94	0.07	1.59	0.04	1.59	0.19	0.88	0.04	5.01	0.26	2.53	0.05	2.06	0.04	2.16	0.14
640	2.06	0.04	2.77	0.08	1.97	0.11	1.26	0.04	4.74	0.28	5.26	0.14	4.37	0.07	1.73	0.13

Table B.2. Continued.

CAR128B

Depth (m)	ALF	SE	BET	SE	GAM	SE	SRB	SE	EPS	SE	THAUM	SE	EURY	SE	DAPI	SE
45	1.88	0.11	1.00	0.09	0.88	0.05	4.28	0.11	0.54	0.22	0.30	0.16	0.30	0.05	4.10	0.29
120	1.14	0.07	0.96	0.04	0.79	0.05	3.61	0.08	0.67	0.14	0.24	0.10	0.14	0.09	2.96	0.26
190	0.30	0.01	0.28	0.01	0.26	0.01	1.08	0.02	0.19	0.03	0.05	0.02	0.04	0.02	1.93	0.15
210	2.47	0.11	1.93	0.08	1.54	0.07	2.39	0.06	1.29	0.22	0.22	0.10	0.17	0.07	2.18	0.12
230	5.51	0.20	3.37	0.10	2.30	0.10	5.21	0.15	2.85	0.50	0.39	0.15	0.39	0.11	2.00	0.36
245	2.50	0.14	1.87	0.09	1.31	0.06	5.21	0.21	1.09	0.24	0.22	0.12	0.12	0.06	2.93	0.25
260	3.08	0.10	3.22	0.10	4.06	0.17	7.92	0.17	2.73	0.06	0.41	0.17	0.31	0.12	2.16	0.26
270	1.91	0.10	3.82	0.11	2.01	0.08	4.52	0.10	4.67	0.07	0.26	0.09	0.20	0.07	2.09	0.15
295	1.94	0.06	3.70	0.08	1.75	0.06	1.99	0.05	4.08	0.05	0.15	0.08	0.13	0.05	1.54	0.17
325	1.06	0.05	0.85	0.03	0.72	0.04	1.35	0.03	1.65	0.03	0.06	0.03	0.10	0.04	2.04	0.11
450	1.05	0.04	0.91	0.04	0.68	0.03	1.41	0.02	2.00	0.05	0.08	0.05	0.08	0.03	2.05	0.12
640	1.17	0.06	1.54	0.05	0.75	0.03	1.65	0.03	1.24	0.03	0.08	0.03	0.10	0.04	1.88	0.13

Table B.2. Continued.

CAR132B

Depth (m)	ALF	SE	BET	SE	GAM	SE	SRB	SE	EPS	SE	THAUM	SE	EURY	SE	DAPI	SE
25	1.03	0.02	0.85	0.02	0.57	0.02	8.73	0.26	1.82	0.04	ND	ND	0.52	0.01	2.15	0.15
180	0.98	0.02	0.70	0.01	0.57	0.01	0.00	0.00	1.48	0.04	ND	ND	0.42	0.11	1.65	0.12
260	0.47	0.01	0.37	0.01	0.32	0.01	0.87	0.02	1.78	0.04	ND	ND	0.34	0.07	1.71	0.15
280	0.41	0.01	0.29	0.00	0.23	0.00	0.85	0.02	1.61	0.04	1.79	0.01	0.43	0.11	1.69	0.17
300	0.49	0.01	0.29	0.00	0.71	0.01	0.58	0.02	2.21	0.03	2.42	0.00	0.36	0.08	1.60	0.18
315	1.05	0.01	0.21	0.00	0.50	0.00	6.81	0.08	2.28	0.05	2.54	0.00	ND	ND	1.28	0.84
330	0.78	0.01	0.47	0.01	0.56	0.01	0.89	0.01	2.08	0.04	ND	ND	ND	ND	1.78	0.16
340	0.41	0.00	0.30	0.00	0.31	0.00	0.94	0.01	1.07	0.05	ND	ND	0.36	0.05	0.93	0.10
350	0.53	0.02	0.28	0.01	0.34	0.01	0.78	0.01	2.14	0.10	ND	ND	0.32	0.08	2.04	0.15
395	0.64	0.02	0.28	0.01	0.22	0.01	0.61	0.01	1.79	0.07	ND	ND	0.28	0.08	2.13	0.13
450	0.42	0.01	0.23	0.01	0.24	0.01	0.56	0.01	2.52	0.04	ND	ND	0.32	0.07	1.60	0.15
640	0.79	0.01	0.23	0.01	0.24	0.00	0.93	0.01	3.22	0.04	ND	ND	0.34	0.07	1.50	0.11

Table B.3. Cell concentrations of individual bacterial and archaeal clades and total prokaryotic community in the water column at station D during two cruises. Individual clade cell concentration units: x 10^7 L^{-1}; total community cell concentration units: x 10^8 L^{-1}. ALF – α-proteobacteria, BET – β-proteobacteria, GAM – γ-proteobacteria, SRB – sulfate-reducing δ-proteobacteria, EPS – ε-proteobacteria, THAUM – Thaumarchaeota, EURY – Euryarchaeota, DAPI – total prokaryotic community, SE – standard error.

CAR122D

Depth (m)	ALF	SE	BET	SE	GAM	SE	SRB	SE	EPS	SE	THAUM	SE	EURY	SE	DAPI	SE
40	5.88	0.38	4.41	0.18	4.87	0.29	5.95	0.62	3.71	0.25	7.04	0.23	4.48	0.21	3.59	0.20
180	0.81	0.17	3.98	0.11	1.25	0.06	3.36	0.54	3.67	0.15	4.52	0.22	4.48	0.26	3.35	0.28
225	0.49	0.06	2.91	0.03	0.45	0.03	0.45	0.04	3.90	0.15	1.39	0.06	2.29	0.13	3.51	0.18
240	1.20	0.14	1.43	0.04	0.39	0.03	2.02	0.09	4.72	0.18	3.93	0.14	3.74	0.10	3.03	0.16
255	1.32	0.16	1.75	0.04	0.66	0.08	3.30	0.15	4.19	0.13	3.38	0.07	4.43	0.27	3.35	0.14
270	0.91	0.21	3.45	0.07	2.68	0.11	6.22	0.31	4.31	0.24	5.45	0.33	3.22	0.21	3.30	0.13
280	0.43	0.06	3.66	0.04	0.45	0.03	1.63	0.10	2.87	0.20	2.65	0.14	2.49	0.13	3.35	0.12
305	0.61	0.07	4.91	0.06	1.01	0.06	1.80	0.06	2.72	0.08	3.38	0.06	4.04	0.14	2.28	0.13
335	0.72	0.08	3.30	0.06	1.36	0.38	1.09	0.06	1.81	0.08	1.63	0.07	2.17	0.15	2.37	0.18
365	1.55	0.10	3.03	0.03	0.00	0.00	0.23	0.05	0.82	0.07	2.11	0.05	1.48	0.11	2.56	0.22
400	1.03	0.04	1.58	0.03	0.41	0.04	0.65	0.05	0.41	0.03	1.32	0.04	0.54	0.05	2.98	0.18
500	0.64	0.04	2.11	0.05	0.24	0.02	1.03	0.07	0.31	0.02	0.79	0.03	0.64	0.03	3.34	0.16

Table B.3. Continued.

CAR132D

Depth (m)	ALF	SE	BET	SE	GAM	SE	SRB	SE	EPS	SE	THAUM	SE	EURY	SE	DAPI	SE
18	1.10	0.02	ND	ND	0.84	0.02	0.44	0.01	1.76	0.06	0.57	0.14	0.35	0.09	2.46	0.85
180	0.71	0.01	0.69	0.02	0.67	0.02	0.47	0.01	2.13	0.08	0.58	0.15	0.58	0.15	2.55	0.85
230	0.33	0.01	0.40	0.01	0.28	0.01	0.30	0.01	1.57	0.05	0.51	0.11	0.87	0.19	2.20	0.81
245	0.63	0.02	0.56	0.01	0.38	0.01	0.42	0.01	1.06	0.03	0.73	0.17	1.06	0.24	2.30	0.73
260	0.55	0.01	0.51	0.01	0.79	0.02	0.30	0.01	1.52	0.04	0.71	0.14	0.64	0.12	1.91	0.73
275	0.71	0.02	1.02	0.01	0.53	0.01	0.26	0.00	1.87	0.05	0.79	0.14	0.73	0.12	1.71	0.83
285	0.71	0.02	4.90	0.10	0.66	0.02	1.02	0.02	1.02	0.04	0.94	0.23	0.82	0.20	2.41	0.83
305	0.52	0.01	3.39	0.05	0.40	0.01	0.49	0.01	1.94	0.04	0.52	0.11	0.81	0.17	2.06	0.89
320	0.91	0.02	0.69	0.01	0.40	0.01	0.33	0.01	1.19	0.02	0.69	0.11	0.44	0.07	1.58	0.93
350	0.89	0.02	1.45	0.02	0.35	0.01	0.44	0.01	2.13	0.06	0.71	0.13	0.62	0.12	1.85	0.97
400	0.82	0.02	0.78	0.01	0.32	0.01	0.52	0.01	1.95	0.04	0.41	0.09	0.75	0.17	2.20	0.85
450	0.98	0.02	0.85	0.01	0.43	0.01	0.44	0.01	1.20	0.02	0.80	0.12	0.66	0.10	1.52	0.63